

**Faculty of Science and Engineering**  
**Department of Civil Engineering**

Dynamic Fatigue Assessment of Fixed Offshore Platforms

**Azin Azarhoushang**

This thesis is presented for the Degree of  
Doctor of Philosophy  
of  
Curtin University

February 2017

# Declaration

This thesis contains no material which has been accepted for the award of any other degree or diploma in any university.

To the best of my knowledge and belief this thesis contains no material previously published by any other person except where due acknowledgement has been made.

The following publications have resulted from the work carried out for this degree.

## **Peer reviewed conference papers:**

*Azin Azarhoushang and Hamid Nikraz*  
Curtin University of Technology  
Perth, Australia

### **Nonlinear Water-Structure Interaction of Fixed Offshore Platform in Extreme Storm**

*Proceedings of the Twentieth (2010) International Offshore and Polar Engineering Conference  
Beijing, China, June 20-25, 2010  
Copyright © 2010 by The International Society of Offshore and Polar Engineers (ISOPE)  
ISBN 978-1-880653-77-7 (Set); ISSN 1098-6189 (Set); www.isope.org*

*Azin Azarhoushang and Hamid Nikraz*  
Curtin University of Technology  
Perth, Australia

### **Dynamic Fatigue Assessment of Fixed Offshore Platform**

*Proceedings of the Twenty-second (2012) International Offshore and Polar Engineering Conference  
Rhodes, Greece, June 17-22, 2012  
Copyright © 2012 by The International Society of Offshore and Polar Engineers (ISOPE)  
ISBN 978-1-880653-94-4 (Set); ISSN 1098-6189 (Set); www.isope.org*

Signature:

Date: 18/02/2017

# Abstract

In this thesis a practical method for dynamic fatigue assessment of jacket-type offshore structures is investigated using existing experience and the procedures available within the industry. Fatigue is a primary mode of failure for steel structures that are subjected to dynamic loads. For offshore structures the most significant dynamic loads are those induced by wave action. Since wave loads on offshore platforms varied with time they produce dynamic effects on structures.

Estimating the fatigue damage for offshore structures is a complicated problem, requiring accurate dynamic analysis of the structure. The spectral approach to fatigue analysis is an attempt to account for the random nature of a confused sea in a rational manner. The nonlinear structural behaviour incorporated using methods based on equivalent linearization and frequency domain expansions. Frequency domain-spectral techniques are used to generate statistical measures of random structural response via the combination of structural transfer functions with an appropriate wave spectrum, to produce response spectra. Statistical measures of random response are quantified by the evaluation of spectral moments. Care must be taken to ensure that the full response of the structure is determined.

The method is most appropriate when there is a linear relationship between wave height and the wave-induced loads, and the structural response to these loads is linear. Frequency domain-spectral analysis must linearly approximate  $P-\delta$  and foundation effects and are not able to directly capture the nonlinear wave loading due to the requirement for problem linearization. However, the numerical efficiency and ability to provide a realistic representation of the response process, makes this technique a very practical assessment tool for accurate fatigue assessments of fixed Jacket type offshore platforms.

An accurate procedure for the random vibration computation of structure is developed using frequency domain techniques. Adaptations to the basic method have been developed to account for various non-linearity. To illustrate the aforementioned methodology, a jacket type offshore platform in the Persian Gulf has been selected and the practical use of the method in the design of fixed jacket type offshore platforms is recommended.

# Acknowledgements

It is with the sincerest gratitude that I acknowledge the attention and guidance that my supervisor, Professor Hamid Nikraz, has given to this work. His brilliance, patience, and generally good nature have provided inspiration and motivation that shall guide me for many years. His friendship and support will be always cherished.

I dedicate this dissertation to my loved ones for their inspiration throughout my academic endeavours and making all this possible.

# Table of Contents

Declaration.....	ii
Abstract.....	iii
Acknowledgements.....	iv
Table of Contents.....	v
List of Figures.....	vii
List of Tables.....	x
Chapter 1            Introduction.....	1
1.1    Objectives.....	4
1.2    Background.....	5
1.3    Significance.....	6
1.4    Methods of analysis.....	7
1.5    Research Method.....	9
1.6    Solution techniques.....	13
Chapter 2            Literature review.....	21
2.1    Environmental conditions.....	22
2.2    Determination of wave forces.....	23
2.3    Forcing frequency and resonance effects.....	24
2.4    Applicability of wave theories.....	26
2.5    Wave action on offshore structure.....	26
2.6    Hydrodynamic loading.....	32
2.7    Hydrodynamic analysis.....	33
2.8    Global and local level approach.....	34
2.9    Probabilistic versus deterministic methods.....	35
2.10    Fatigue environment characterization.....	36
Chapter 3            Analysis.....	38
3.1    Model definition.....	39
3.2    The basics of random process.....	52
3.3    The applicability of the spectral method.....	68
3.4    Uncertainty in the process.....	69
3.5    Wave selection for transfer function.....	70
3.6    Calibration Method.....	79
3.7    Dynamic Analysis.....	128

Chapter 4	Discussion .....	144
4.1	Outline of the procedure .....	145
4.2	Results .....	152
Chapter 5	Conclusion .....	157
5.1	Summary.....	158
5.2	Recommendation.....	160
<b>References</b>	.....	<b>161</b>
Appendix A	Input Files .....	163
A.1	SACS Model.....	164
A.2	Fatigue .....	216
A.3	Wave response .....	219
A.4	Transfer function.....	222
A.5	Response function.....	225
A.6	Deterministic base shear range .....	232
A.7	Pile-stub generation .....	235
A.8	Dynamic characteristics .....	243
Appendix B	Fatigue analysis results .....	246

# List of Figures

Figure 1-1 General view of SACS structural model .....	2
Figure 1-2 Selection of Frequencies for Detailed Analyses.....	10
Figure 2-1 Resonance effects.....	25
Figure 2-2 Regions of Applicability of Wave Theory (API, 2007) .....	27
Figure 2-3 Typical long term cumulative distribution of stress ranges.....	37
Figure 3-1 General View of SACS Structural Model .....	40
Figure 3-2 Face Row A.....	41
Figure 3-3 Face Row B .....	42
Figure 3-4 Face Row 1.....	43
Figure 3-5 Face Row 2.....	44
Figure 3-6 Plan at -41.285 .....	45
Figure 3-7 Plan at -25.3 .....	46
Figure 3-8 Plan at -9.0 .....	47
Figure 3-9 Plan at 5.0.....	48
Figure 3-10 Probability density function $p(x)$ for a random process .....	53
Figure 3-11 First-order probability density for a normal (or Gaussian) process .....	53
Figure 3-12 Probability density function .....	54
Figure 3-13 Typical second-order or joint probability density function $p(x, y)$ .....	54
Figure 3-14 Autocorrelation function $R_x(\tau)$ of a stationary random process $x(t)$ .....	55
Figure 3-15 spectral density curve for zero mean stationary process when $\tau=0$ .....	55
Figure 3-16 Narrow band process.....	56
Figure 3-17 broad band process.....	56
Figure 3-18 Cross-correlation function $R_{xy}(\tau)$ of stationary processes $x(t)$ & $y(t)$ .....	57
Figure 3-19 Excitation and response parameters of a linear system.....	57
Figure 3-20 Frequency response characteristics for a simple system.....	58
Figure 3-21 impulse response function.....	59
Figure 3-22 Unit impulse response function.....	59
Figure 3-23 Arbitrary input $x(t)$ .....	60
Figure 3-24 Broad band noise transmission through resonant system.....	62
Figure 3-25 stationary, Gaussian, narrow band process .....	62
Figure 3-26 Narrow band process.....	63
Figure 3-27 Probability of crossing $y=a$ .....	64
Figure 3-28 Identification of peaks in the band $y = a$ to $y = a + da$ .....	65
Figure 3-29 Rayleigh distribution of peaks for a Gaussian narrow band process.....	66

Figure 3-30 irregularities in a narrow band process.....	66
Figure 3-31 Spectrum Analyser .....	67
Figure 3-32 Frequency grid selection .....	71
Figure 3-33 Leg spacing at Jacket work point (m) .....	72
Figure 3-34 Initial and Final frequency grid comparison at $0^\circ$ .....	75
Figure 3-35 Initial and Final frequency grid comparison at $45^\circ$ .....	76
Figure 3-36 Initial and Final frequency grid comparison at $90^\circ$ .....	77
Figure 3-37 Frequency grid distribution .....	78
Figure 3-38 Fatigue life comparison (years).....	90
Figure 3-39 Static Transfer Function ( $0^\circ, 1/25$ ).....	102
Figure 3-40 Static Transfer Function ( $0^\circ, 1/20$ ).....	103
Figure 3-41 Static Transfer Function ( $0^\circ, 1/15$ ).....	104
Figure 3-42 Static Transfer Function ( $45^\circ, 1/25$ ).....	105
Figure 3-43 Static Transfer Function ( $45^\circ, 1/20$ ).....	106
Figure 3-44 Static Transfer Function ( $45^\circ, 1/15$ ).....	107
Figure 3-45 Static Transfer Function ( $90^\circ, 1/25$ ).....	108
Figure 3-46 Static Transfer Function ( $90^\circ, 1/20$ ).....	109
Figure 3-47 Static Transfer Function ( $90^\circ, 1/15$ ).....	110
Figure 3-48 Dynamic Transfer Function ( $0^\circ, 1/16$ ) .....	111
Figure 3-49 Dynamic Transfer Function ( $45^\circ, 1/16$ ) .....	112
Figure 3-50 Dynamic Transfer Function ( $90^\circ, 1/16$ ) .....	113
Figure 3-51 Dynamic Transfer Function ( $135^\circ, 1/16$ ) .....	114
Figure 3-52 Dynamic Transfer Function ( $180^\circ, 1/16$ ) .....	115
Figure 3-53 Dynamic Transfer Function ( $225^\circ, 1/16$ ) .....	116
Figure 3-54 Dynamic Transfer Function ( $270^\circ, 1/16$ ) .....	117
Figure 3-55 Dynamic Transfer Function ( $315^\circ, 1/16$ ) .....	118
Figure 3-56 Response function ( $0^\circ, 1/15$ ).....	119
Figure 3-57 Response function ( $45^\circ, 1/15$ ).....	120
Figure 3-58 Response function ( $90^\circ, 1/15$ ).....	121
Figure 3-59 Response function ( $0^\circ, 1/20$ ).....	122
Figure 3-60 Response function ( $45^\circ, 1/20$ ).....	123
Figure 3-61 Response function ( $90^\circ, 1/20$ ).....	124
Figure 3-62 Response function ( $0^\circ, 1/25$ ).....	125
Figure 3-63 Response function ( $45^\circ, 1/25$ ).....	126
Figure 3-64 Response function ( $90^\circ, 1/25$ ).....	127
Figure 3-65 Deflected mode shape 1 .....	134
Figure 3-66 Deflected mode shape 2 .....	135



Figure 3-67 Deflected mode shape 3 .....	136
Figure 3-68 Deflected mode shape 4 .....	137
Figure 3-69 Deflected mode shape 5 .....	138
Figure 3-70 Deflected mode shape 6 .....	139
Figure 3-71 Deflected mode shape 7 .....	140
Figure 3-72 Deflected mode shape 8 .....	141
Figure 3-73 Deflected mode shape 9 .....	142
Figure 3-74 Deflected mode shape 10 .....	143
Figure 4-1 Tubular intersection (1 crown, 2 saddle).....	151
Figure 4-2 Face A joint numbers .....	156

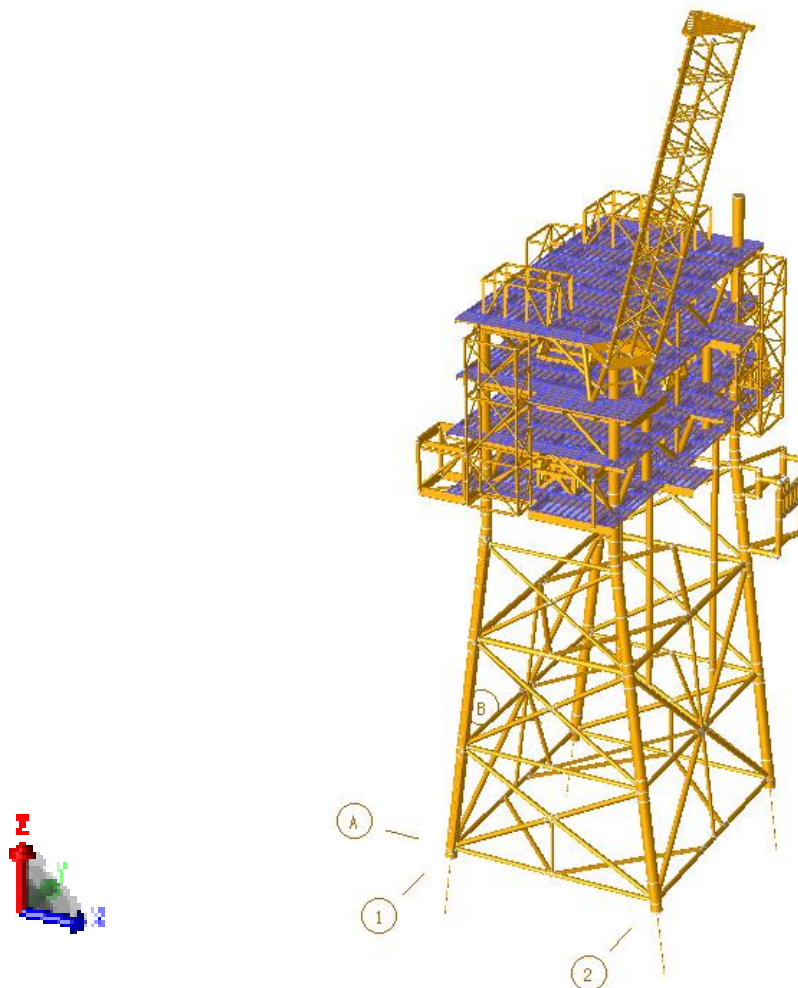
# List of Tables

Table 1-1 Platform General Data .....	3
Table 1-2 Directional wave scatter diagram – 0 degrees .....	9
Table 1-3 Frequencies and generalized mass .....	10
Table 3-1 Platform General Data .....	49
Table 3-2 First three modes of the structure .....	73
Table 3-3 Along Row A and B (d =18m) .....	73
Table 3-4 Along Row 1 and 2 (d = 36m).....	73
Table 3-5 Along diagonal (d = 40.25).....	73
Table 3-6 Enhanced Frequency Grid .....	74
Table 3-7 Directional wave scatter diagram (0 degree) .....	79
Table 3-8 Directional wave scatter diagram (45 degree) .....	79
Table 3-9 Directional wave scatter diagram (90 degree) .....	79
Table 3-10 Average Weighing factors ( $W_j$ ).....	80
Table 3-11 Fatigue centroid .....	81
Table 3-12 Shifted fatigue centroid .....	81
Table 3-13 RMS base shear (kN).....	82
Table 3-14 MPM VALUES .....	84
Table 3-15 Spectral base shear.....	85
Table 3-16 Deterministic base shear range .....	85
Table 3-17 Enhanced drag coefficient .....	89
Table 3-18 Enhanced mass coefficient .....	89
Table 3-19 Weighing factor (steepness 1/25, 0°).....	91
Table 3-20 Weighing factor (steepness 1/20, 0°).....	92
Table 3-21 Weighing factor (steepness 1/15, 0°).....	93
Table 3-22 Weighing factor (steepness 1/25, 45°).....	94
Table 3-23 Weighing factor (steepness 1/20, 45°).....	95
Table 3-24 Weighing factor (steepness 1/15, 45°).....	96
Table 3-25 Weighing factor (steepness 1/25, 90°).....	97
Table 3-26 Weighing factor (steepness 1/20, 90°).....	98
Table 3-27 Weighing factor (steepness 1/15, 90°).....	99
Table 3-28 Fatigue damage (0 degree) .....	100
Table 3-29 Fatigue damage (45 degree) .....	100
Table 3-30 Fatigue damage (90 degree) .....	100
Table 3-31 Weighted fatigue damage (0 degree).....	101

Table 3-32 Weighted fatigue damage (45 degree).....	101
Table 3-33 Weighted fatigue damage (90 degree).....	101
Table 3-34 Weight and centre of gravity summary .....	131
Table 3-35 Frequencies and generalized mass.....	132
Table 3-36 Maximum deflection for modes .....	132
Table 3-37 Mass participation factor based on retained DoF .....	133
Table 3-38 Mass participation factor based on expanded DoF.....	133
Table 4-1 Fatigue life of selected joints for different case studies .....	155
Table 4-2 Fatigue life comparison to calibrated case.....	155

# Chapter 1 Introduction

Fixed offshore platforms including steel jacket, concrete caisson, floating steel and even floating concrete are economically feasible for installation in water depths up to about 520 m. The Persian Gulf region is one of the important energy zones in the world with numerous oil and gas fields and offshore structures to extract the valuable energy resources. These offshore structures are mainly fixed jacket type platforms, which are cost effective since the maximum installation depths of jackets are 70 m (Asgarian, 2009). The primary structural components of jacket type offshore structures include topside, jacket and pile foundations. The most common used offshore structure is a jacket structure, which comprises a prefabricated steel support structure (jacket) extended from the sea bed, connected with piles at the sea bed to some height above the water surface level and a steel deck (topside) on the top of the jacket. A general view of the structural model including the jacket and topside is shown in Figure 1-1.



**Figure 1-1 General view of SACS structural model**

The Platform description and environmental data is tabulated in Table 1-1.

**Table 1-1 Platform General Data**

Jacket dimension at mudline (EL -41.3 m)	30.15 (m)×36 (m)
Jacket dimension at work point (EL 7.3 m)	18 (m)×36 (m)
Upper Deck dimension at EL 35.5 m	41.2 (m)×23.2 (m)
Lower Deck dimension at EL 13.3 m	51.6 (m)×23.2 (m)
Topside Operating Weight	1140 (MT)
Water Depth	42.72 m

Fatigue is a primary mode of failure causing degradation in the long-term integrity of offshore structures. Fatigue damage accumulation experienced by an offshore structure is mainly caused by dynamic effects of small and medium sized ocean waves that are inertia dominated. Dynamic effects are clearly important in the determination of a platform's ultimate strength and cyclic degradation behaviour. For dynamically sensitive structures, the effects of dynamics and structural response become more important. In this regard, the structure must be adequately modelled to obtain realistic results for fatigue performance.

The elements contributing to dynamic effects are mostly excitation frequency, natural frequency, effective mass and stiffness of structure and the overall damping. Modal analysis is carried out to identify the eigen-frequencies and mode shapes as essential factors contributing to structural dynamic response magnifications due to excitation loads.

A structure's dynamic behaviour is significantly affected by the soil characteristics and the pile–soil interaction. The actual structure will be less stiff than estimated from a linear analysis because of displacement dependent effects. This will tend to increase the deflection of the structure, thereby reducing its effective stiffness (ABS, 2004). Finite deflection of the pile (the P- $\delta$  effect) is accounted for by using the equivalent pile stub based on pile–soil–structure interaction, which depends on pile head forces, pile stiffness, etc. The pile is represented by a beam column on a nonlinear elastic foundation and the finite difference solution method is used to solve the pile model. The structure resting on the piles is represented as a linear elastic model.

The random nature of the wave loading can be captured in the frequency domain spectral method using a wave spectrum and a structural transfer function, which is based on the linear concept. A sufficient number of suitably spaced frequencies are selected so that the transfer functions are adequately defined over the relevant frequency range where response is expected. In this manner, the peak wave spectrum period is properly mapped and the response effects of interest, including responses around structural resonances, wave load cancellation or enhancement points, are depicted.

The method is most applicable when there is a definable relation between wave height and stress ranges at the connections. This could be best implemented for a stationary process where the excitation is the elevation of the sea's surface at a point and the response of interest is the hot spot stress ranges. These assumptions are most applicable for low to moderate sea-states. Since these are the sea-states of interest in fatigue studies, these assumptions can reasonably be accepted. The basic method is improved to capture various non linearities. An enhanced frequency domain spectral technique is further developed as the relevant response process and the suitability of the method is investigated as a practical assessment tool.

## 1.1 Objectives

This PhD thesis has advanced the practice of fatigue assessment of offshore structures in frequency domain by accounting for non-linear system responses with due consideration of the system vibration characteristics and employing a rigorous calibration process. The applicability of the proposed approach is demonstrated in detail by applying the aforementioned methodology to a fixed jacket type offshore platform in the Persian Gulf.

The PhD researcher has had the opportunity to work in numerous FEED (Front End Engineering Design) and detail design projects comprising of fixed jacket type offshore platforms. Initially, a literature review of the industry experience and existing knowledge is conducted to identify recent important advances in dynamic fatigue assessment of fixed offshore platforms. Furthermore, the most appropriate design methods that meet functionality, safety and economical aspects of structural design for fatigue damage are investigated.

In this thesis dynamic fatigue damage of fixed offshore platforms in low to moderate sea-states is investigated with appropriate dynamic tools. Moreover, it is demonstrated how to develop an effective procedure to maintain fatigue life of fixed jacket type offshore platforms that are

subjected to hostile marine environments. In dynamic fatigue assessment a wave scatter diagram is used to represent the long-term statistics of the sea-state.

Actual wave steepness is determined using a suitable calibration process based on matching of global response parameters. The calibration determines a wave steepness value that matches the spectrally calculated response to a deterministically calculated response. The effect of wave frequency on wave loading and structural response is accounted for by using transfer functions for evaluating the response in each random sea-state. The emphasis is made on a procedure, which can be fit through existing design codes of practice. Finally, some recommendations will be made for future development work.

## 1.2 Background

Offshore platforms are one of the most important structures in exploration and production of oil and natural gas. Since its inception sixty years ago, the offshore structures industry has been growing at a fast rate. The literature on fixed offshore structures is huge. The failure of structure may occur due to the fatigue of the structure in the low to moderate sea-states as well as extreme response to the severest sea (Kim, 2008). Due to large investment that offshore platforms represent and the catastrophic consequences of their failure, safe, efficient and economical platform design approach is of prime importance.

Fatigue has become an important consideration both at the design stage and during maintenance for structural integrity assessment procedures. For reliable design of offshore platforms care should be taken on dynamic behaviour of jacket type offshore platforms to environmental loads. Dynamic analysis of offshore platforms can be performed for extreme loads (Azarhoushang, 2010a) or for long term effects (fatigue degradation), which is the subject of this research study. Dynamic effects are clearly important in the determination of platform ultimate pushover strength incorporating inertia and resonance effects, strain rate effects on yield stress and soil properties, and cyclic degradation behaviour (Frieze, 1997).

In addition to using a dynamic analysis, it is essential to use a stochastically defined sea-state in place of a single design wave. Such an analysis is essential in designing against the first excursion failure and an adequate fatigue life. The stochastic approach based on frequency domain spectral analysis or random time domain simulations enables the random nature of environment to be reflected. This approach leads to a more realistic solution and usually results in reduced design loads, which allow lighter and more efficient structures (Iraninejad, 1988).



The methodology used here is a frequency domain analysis using spectral density functions and the transfer function approach to model the response spectrum. This approach is useful to handle nonlinear effects when the wave statistics of random sea are not changing (due to existence of short periods in fatigue loading environment) and water surface elevation can be properly described by wave power spectra.

The most commonly used offshore platform is the jacket-type structure, which comprises of three main parts, namely the jacket itself, the deck and the piled foundation. The jacket consists of steel frames that extend to the mud line and are then supported by piles. Most steel offshore support structures are three-dimensional frames fabricated from tubular steel members. Fatigue life is one of the major concerns for offshore platforms since the utilization of tubular members gives rise to significantly high stress concentrations in the joints. In some cases, fatigue cracking has led to member severance, resulting in a consequent reduction of overall structural integrity.

The characteristics of fatigue loading on offshore structures such as fixed jacket type offshore platforms are dependent on environmental conditions and structural features. Environmental load assumptions introduce major sources of uncertainty in the design process. Despite of the engineering complexities and uncertainties, the optimum design of a structure with random response constraints is investigated in the this thesis.

### 1.3 Significance

Fatigue is a significant hazard causing degradation in the long-term integrity of offshore structures. The weld toes at tubular intersections are particularly vulnerable to fatigue failure in offshore structures due to the high local stress concentrations. The fatigue behaviour of welded tubular joints has been the focus of several major international research programs. Due to the large investment that offshore platforms require and the catastrophic consequences of their failure, reliable fatigue assessment procedures are required at the design stage. Owing to the variations in the controlling parameters, the results of the analyses are subject to uncertainties.

A comparative research is carried out to ensure the safe and reliable operation of such structures. This comparison is useful in developing methods to predefined levels of accuracy. Failing to properly incorporate dynamic effects will result in an incorrect evaluation of fatigue life. It can be clearly seen that calculated fatigue life is significantly higher than reality when

calibration is not undertaken (refer to Appendix B). This suggests the need to reconsider the models that have been deemed to be trustworthy so far.

The dynamic components of fatigue loading are unlikely to govern the bulk of the steel in the structure, provided the effects of flexibility are considered from an early stage in concept development. A relatively low weight growth can be achieved from a strong awareness of dynamic response effects and careful attention to the interaction between platform dynamic characteristics, wave loading and dynamic response. These experiences demonstrate the importance of a reliable assessment of dynamic response and the need to incorporate these effects at a very early stage in design development.

Methods to reflect the nonlinear stochastic dynamic behaviour in the frequency domain are assumed to provide the most accurate result and preserved as a point of reference to estimate the accuracy of simplified methods, which are all based on some kind of linearization theory. The research outcomes will hopefully supplement previous knowledge on fatigue assessment for dynamically responding structures subjected to random non-linear wave loading. Considering the significance of fatigue failure, extensive attention is granted to the development of guidance on safe prediction of fatigue performance with good awareness of the parameters influencing the dynamic response of the structure.

## 1.4 Methods of analysis

Fatigue is the process of damage accumulation initiated by material yielding due to sliding of atomic layers under cyclic stresses that develop into plastic deformation causing long term degradation to the integrity of offshore platforms.

The integrity of these structures is maintained in two stages. The first is the design stage, which is the main focus of the research program and discussed further in detail. The second stage is monitoring with underwater non-destructive inspections such as ultrasound, X-ray or eddy current. These measurement techniques could provide a robust and sensitive means for early detection and tracking of fatigue damage at an early stage. This will facilitate the maintenance scheduling to improve safety and reduce operating costs (Hillis, 2011). If any crack is discovered in service, crack growth analysis using techniques such as fracture mechanics will be carried out to assess the severity of the condition and to plan possible remedial actions.

Methods of analysis are probably the more reliable part of the design process. Methods are required that take into account the effect of randomness in structural properties and relate the

frequency content of the random seas to the fundamental natural mode of the structure (Ko, 1988).

Three notable methods of fatigue assessment at design stage are the simplified method, the spectral method and the deterministic method. The simplified method can be classified as an indirect fatigue assessment method and is often used for fatigue screening tools to identify fatigue sensitive areas of the structure. If the structural detail does not meet the requirement of simplified methods, it can be assessed with more rigorous techniques (ABS, 2010).

Spectral-based fatigue assessment is referred to as a direct method because it generates results in terms of fatigue life. This method is based on the stress range transfer function, which relates the hot spot stress and wave frequency for unit wave height. The hot spot stress (or strain) method has become the most commonly used approach for fatigue design of circular hollow section (CHS) connections. The accuracy of calculated long-term stress distributions depends mainly on the accuracy of the stress transfer functions that are cornerstones of a probabilistic analysis (Vugts, 1978). Spectral analysis is the most comprehensive analysis procedure, which takes account of the random nature of wave environment and is suitable for dynamically responding structures. This procedure should be used for the final verification of all structures unless they are located in areas that are known to have benign fatigue climates where dynamic effects can be ignored.

Deterministic method of fatigue assessment is a simplified version of the spectral method (ABS, 2010). It uses a series of periodic waves with different heights and periods to evaluate structural response, but does not reflect the true frequency content of the wave conditions. Deterministic method is highly sensitive to discrete deterministic wave selection to properly represent the fatigue environment. This procedure may be used for screening during initial design phases or for final verification of the design of structures in shallow and medium water depths where dynamic effects can be neglected.

Simplified method uses the most simplified representation of the long term wave climate and the associated loading. A single periodic wave is used to estimate the long term stress statistics from the long term wave height statistics. This method requires the least computational effort of the three. It is appropriate for screening during initial design phases or for final verification of the design of structures in very benign fatigue environments.

## 1.5 Research Method

For the purpose of fatigue assessment, an analytical representation of the structure (refer to Figure 1-1) is considered with the loadings and restraints using SACS software (refer to SACS input files in Appendix A). The primary structural components of jacket type offshore structures include deck, jacket and piled foundations. The piles and surrounding soil layers are replaced with equivalent elements called pile stub that have identical pile–soil lateral characteristics.

Considering natural variability in real sea waves, a probabilistic approach to define the wave environment and its resulting stresses is preferable to deterministic methods (refer to Section 1.4), which is followed in this research study. The effect of loading direction is considered with 45 degree intervals. Since the natural period of the structure (refer to Table 1-3) is in the range where there is sufficient wave energy (refer to Table 1-2) to excite significant dynamic response, the dynamic structural response needs to be considered in the fatigue analysis (Johansen, 2003).

In order to generate the peaks and valleys of the transfer function accurately, natural frequencies should be included with addition of at least three closely spaced frequencies on each side of the primary and secondary modes of the structure. For the wave response analysis, the initial frequency grid is modified in the vicinity of the first natural period. The revised frequency grid adequately describes the frequencies of the platform, cancellation and enhancement effects as well as the peak and valley period of the transfer function curve (refer to Figure 1-2).

**Table 1-2 Directional wave scatter diagram – 0 degrees**

4.25								1		
3.75								1		
3.25							1	1		
2.75							5	1		
2.25						6	34			
1.75				1	165	39	1			
1.25			1	246	394	1				
0.75			705	1141	54					
0.25		1	100	1262	167					
$H_s$ $T_p$	0.5	1.5	2.5	3.5	4.5	5.5	6.5	7.5	8.5	9.5

**Table 1-3 Frequencies and generalized mass**

MODE	FREQ. (CPS)	GEN. MASS	EIGENVALUE	PERIOD (SECS)
1	0.297	5.78E+03	2.88E-01	3.37
2	0.526	4.99E+03	9.17E-02	1.90
3	0.728	3.81E+03	4.78E-02	1.37
4	1.479	1.26E+02	1.16E-02	0.68
5	1.547	4.55E+02	1.06E-02	0.65
6	1.645	2.61E+03	9.36E-03	0.61
7	2.037	2.58E+03	6.10E-03	0.49
8	2.434	8.12E+03	4.28E-03	0.41
9	2.658	3.43E+03	3.59E-03	0.38
10	2.690	5.61E+03	3.50E-03	0.37

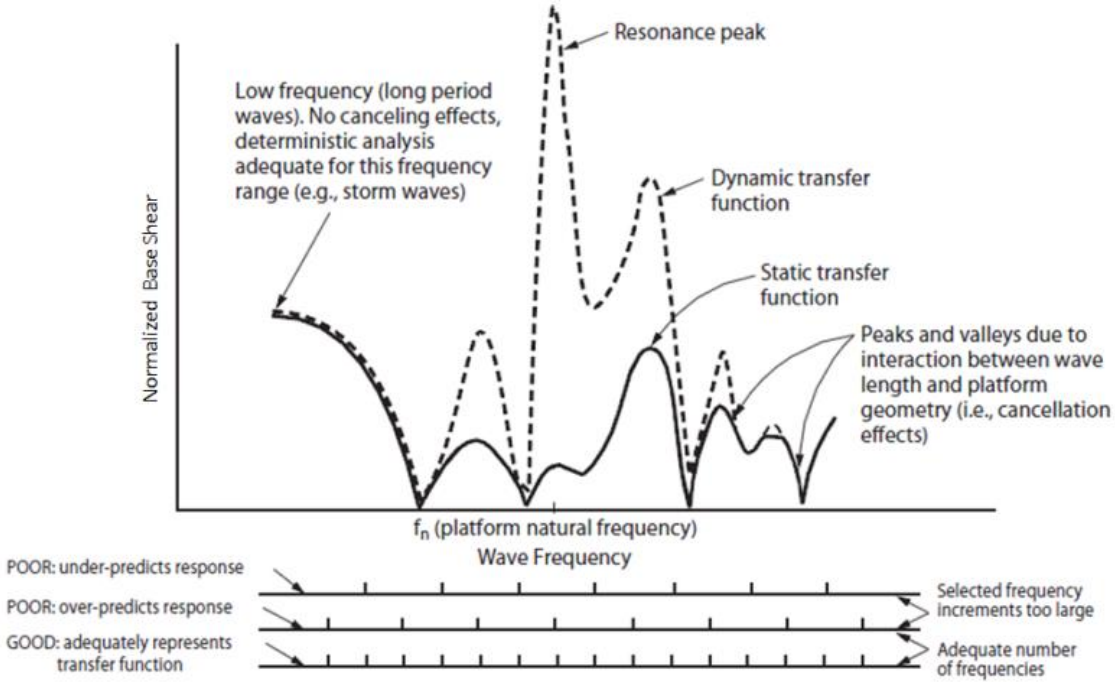


**Figure 1-2 Selection of Frequencies for Detailed Analyses**

The selected frequency grid includes the relevant frequency range where response is expected. The peak wave spectrum period is carefully mapped. If the dynamic amplification of the structural response is significant, special attention must be paid to the high frequency cut-off point (Vugts, 1978). Proximity of a structure resonant frequency with a wave load cancellation frequency can lead to the suppression of dynamic response effects. For this reason, a high frequency cut-off should be considered, so wave cancellation effects do not occur at higher frequencies.

The aim of the fatigue assessment method is to establish a good balance between complexity and accuracy in the prediction of the fatigue strength. Spectral analysis techniques account for the random nature of the wave environment. Since the method is based on some kind of linearization principle, it does not directly reflect response nonlinearity. However, for the determination of transfer functions in engineering applications, the linearity demand can be somewhat relaxed by an appropriate selection of the wave height input (ISO19902, 2007).

Alternatively, the stress transfer functions may be determined by performing global stress analyses in the time domain by stepping a full wave cycle past the structure. For drag dominated structures where nonlinear effects are more severe, time domain techniques are superior to other techniques. A realistic representation of the response process could be obtained by random time domain methods. Since time domain simulations are very time consuming, it is desirable to develop simple methods for fatigue analysis, especially during the initial design stages.

The frequency domain-spectral technique is superior to other techniques in parametric studies. The main advantages are numerical efficiency and realistic representation of the response process. It is also regarded as a very practical tool for site specific assessments of offshore platforms with a clear perception of the factors affecting the response at initial phase of the analysis.

However, these methods still require some theoretical development to reflect the free surface effects (Leira, 1990). In this regard an empirical modification near the free surface (Wheeler stretching) or an improved linearization method that includes inundation effects can improve fatigue assessment.

The heights of the regular waves used in the determination of the transfer functions shall be selected in a suitable manner to allow an appropriate level of non-linear (drag) action due to waves in the linearized calculations. This is achieved by calibrating the wave steepness, which matches the spectrally calculated range of applied wave action to the quasi-static calculated

range of applied wave action for the structure. For this purpose, the sea-state at the centre of the fatigue damage scatter diagram that makes the most contribution to the fatigue damage is used.

Constant wave steepness is considered to develop the transfer function. The constant-transfer function method will not only be sufficiently accurate but will also save time. However, this allots unrealistically large wave heights at low wave frequencies. Therefore, the wave heights at large wave lengths (low wave frequencies) are limited to a wave height corresponding to the one year return period as a maximum. A minimum wave height is also limited to 0.3 m (API, 2007).

To incorporate the structure's dynamic characteristics, fatigue assessment is carried out with dynamic approach in the research method. This will require the use of "Wave Response" module of SACS to generate the wave loading. The procedure to run a static fatigue analysis for cyclic wave forces is the same except that "Sea-state" module of SACS program is required to generate the wave loading.

Since the dynamic module in SACS uses the linear theory (i.e. modal superposition), linear foundation super elements are automatically created at each pile-head by the "PSI" module of SACS. Pile stubs of appropriate stiffness are modelled as equivalent linear foundation for evaluation of fatigue damage.

The dynamic analysis of a platform subjected to the design wave is normally performed for steady state conditions since it would be illogical to assume that the sea was at rest before waves arrived with their maximum amplitudes (Ko, 1988). A steady state structural response can be developed when the transient effects are negligible due to damping. For linear systems the response for a steady state harmonic excitation can be easily obtained in a closed form.

For spectral analyses, the loading specified to develop a transfer function is not the actual loading (fatigue environment) that causes fatigue damage, but it is rather the one that is determined by using the calibrated wave steepness value. The resulting wave heights should further be compared to the elevations of plan framing levels near the water surface, to ensure that no discontinuities in the applied wave action are likely to occur. Where appropriate, some final adjustment should be made (ISO19902, 2007).

The structural response under random loading is certainly a random process. Statistical definition of the random response could be obtained from spectral moments. Since the fatigue damage is a non-ageing effect process that means the load sequence interaction is negligible,

the spectral parameters of a stress power spectrum can be used to obtain the equivalent stress range. Fatigue damage is calculated by Miner's rule based on the assumption that it is only dependent on the current stress states. Therefore, the total damage due to a single sea-state is the linear summation of the fractional damages caused by individual stress ranges (Kam, 1990).

## 1.6 Solution techniques

Fixed jacket type offshore platforms are mainly fabricated from tubular steel members to satisfy the requirements of low drag coefficient, high buoyancy and high strength to weight ratio. However, utilization of these members generates high stress concentrations that are of major concern in fatigue life of offshore platforms (Jia, 2008).

The fatigue damage prediction may be principally performed using two techniques; namely the S–N approach and fracture mechanics (Shabakhty, 2011). The S–N method and the S–N curves are associated to a nominal stress approach, which relates a constant stress range,  $S$ , to the number of stress cycles,  $N$ , leading to the failure. The S–N curve is essentially obtained from empirical fatigue experiments. The nominal stress range for the location where the fatigue assessment is being conducted may need to be modified to account for local conditions that affect the local stress at that location. The ratio of the local to nominal stress is the definition of the Stress Concentration Factor (SCF). according to Miner's rule, fatigue assessment due to variable actions is normally based on the hypothesis of a linear accumulation of fatigue damage under constant amplitude stress ranges.

The second approach is based on fracture mechanics techniques, which describe the propagation of crack and its growth due to time-varying (tensile) stresses. Acknowledging the dominance of the S–N approach, fracture mechanics principles are best suited in situations where the normal S–N fatigue assessment procedures are inappropriate. For example, fracture mechanics has specific application in ancillary or supporting studies to develop an inspection plan followed by remedial actions (Kam, 1990).

This thesis presents a fixed jacket type offshore structure platform model for the prediction of fatigue degradation under hydrodynamic forces induced by wave action with due consideration of dynamic effects. The solution procedure is extended to a stochastic analysis in frequency domain dynamic response of fixed jacket offshore structures.

An analytical solution of fatigue analysis can be obtained through statistical analysis based on the assumption that the stress response of the structure is stationary, Gaussian, and narrow



band. However, the presence of the second peak per zero crossing due to local irregularities in a narrow band process causes the stress power spectra to become broad band, which means the spectral density covers a broad band of frequencies. Analysis of a broad band process requires a cycle counting algorithm in the time domain whereas the analytical solution is hardly utilised in this case.

Although time domain techniques are the most accurate in determination of stress power spectra, they are costly and time consuming. Simple methods for fatigue analysis can be developed if a proper balance between computational accuracy and physical realities can be achieved (Zienkiewicz et al., 1978). In this regard, it is desirable to simplify the statistical modelling based on the assumption that the load sequence can be ignored. This implies, for equal number of cycles, the equivalent (constant amplitude) stress range creates the same fatigue damage as the sequence of variable stress ranges that it replaces. The equivalent stress range can be obtained from the spectral parameters of a stress power spectrum (Chow, 1991). The concept works well for fatigue assessment even if the assumptions are not fully satisfied.

Frequency domain analysis is best suited for systems in random wave environments. The description retains the random nature as well as the frequency content of a real sea which means that it is able to realistically model the effect of wave frequency on applied wave actions and structural response. The response spectrum and its short term statistics is obtained using wave spectrum and the transfer function. In this approach water surface elevation is described by using a wave power spectra to account for nonlinear effects. The transfer function gives the steady state response of a system to a sine wave input and the dynamic characteristics of the system can be defined by measuring the transfer function over the entire frequency range.

Frequency domain analysis is usually applied in analyses of more moderate environmental conditions where wave statistics of the random sea is not altered (Etube, 1999). The main advantage of this method is that the computations are relatively simple and efficient compared to time domain analysis methods. For a motion analysis in the frequency domain, wave response analysis is performed for 55 frequencies (refer to Section 03.5), which is more than the 30 that is required by the codes (DNV, 2010).

Airy wave theory is used for low to moderate seas since the effect of drag forces on the local stress range is small. Linearization yields satisfactory results for structures that are exposed to small waves where nonlinear effects are negligible due to presence of inertia rather than drag dominated loading.

The significant wave height ( $H_s$ ) and peak period ( $T_p$ ) of a random sea-state should be specified for stochastic linearization to evaluate the linearized force vector. The linearization matrix could be obtained by minimizing the expected mean square error, considering the response to be Gaussian. The analysis is then performed by transforming the equilibrium equation into the frequency domain (Leira, 1990).

Methods reflecting free surface effects are expected to improve fatigue analysis. As an alternative this can be achieved by applying reasonable wave steepness, so the transfer functions automatically include the free surface effects (Vugts, 1978). For the determination of transfer function, the linearity demand can be relaxed to account for nonlinear (drag) wave loading by an appropriate selection of the wave height input.

The drag component of the hydrodynamic actions on the structure is also affected with the presence of a current. In addition to modifying the variable part of the wave action, this will cause a non-zero mean loading. However, for fatigue analysis the only concern is the range of applied action, which is much less affected than the peak action at the crest or the trough. Therefore, current forces can be ignored in fatigue analysis.

Marine growth affects platform added mass, member drag diameter and drag coefficient (API, 2007). This will increase the local and global wave loading on the structure and affects fatigue life of members. Both the drag and inertia term in Morison's equation should be increased to take the account of marine growth. The drag coefficient should additionally reflect the effect of roughness due to marine growth.

A marine growth profile is specified based on the thickness and roughness expected at the platform's site over the service life of the platform. The effect of marine growth on the hydrodynamic behaviour of members is included by increasing the member diameter in addition to adjusted drag and inertia coefficients.

The effect of nonlinearity depends on the amount that the structure is drag dominated (Skjong, 1991). Wave loading is nonlinear with wave height due to the drag term in the Morison wave load equation and free surface effects. In contrast, low to moderate seas are mainly inertial and require accurate assessment of the inertia coefficient for fatigue calculations (Vugts, 1978).

If the inertia forces are quite important, then dynamic analysis should be carried out either in frequency domain in which case transient effects will be neglected or in time domain in which case transient effects may be considered as well as non-linearity (Brebbia and Walker, 1979).

The influence of dynamic response on the long-term local stress range history is determined by using spectral analysis and a frequency domain dynamic solution.

The wave response method does not need any drag linearization (HSE, 2000). The type of wave theory depends on the procedure adopted. Since the hydrodynamic forces are essentially nonlinear, an iterative approach is employed. This precludes the requirement of performing a time history integration in a deterministic procedure on the assumption that an infinite train of a repeatable wave form has passed the structure with steady state response.

In the random approach, the repeatable wave is a wave train with the wave statistics model of the input wave spectrum or the surface profile input by the user. Therefore, the actual wave specified in the Sea-state input file is not critical if an accurate representation of the wetted surface is provided.

A sufficient number of steps (20 crest positions) are used to ensure that adequate member load segmentation occurs. The wave step yielding the highest degree of member segmentation and the greatest submerged length for each member is used by the program.

“*Sea-state*” module of SACS is used to calculate the hydrodynamic properties of each member and the wave kinematics are calculated by the “*Wave Response*” module. The wave elevation is modelled as a linear random superposition of regular wave components using information from the wave spectrum.

The effect of the structural motion on the relative water particle velocities can be accounted with an iterative approach to correct any nonlinearities. The distributed member forces are computed using Morrison’s equation for each wave crest position. The equivalent joint forces are determined using static equilibrium and multiplied by the modal eigenvectors to obtain the modal generalized forces.

The generalized force is decomposed into various Fourier components to obtain the modal response. The structural motion at any point is then determined by summing the responses from all modes. As a result, the relative fluid velocity and a new set of member forces can be determined.

The generalized forces for current iteration are compared with the specified tolerance unless the maximum number of iterations is reached. The modal static values are obtained from the first iteration for one full cycle of the wave on the structure at rest position. The modal dynamic values are obtained from the iterative solution including the dynamic amplification factors.

Wave kinematics for every iteration can be recalculated to take account of structural displacement when using a relative velocity formulation. Since the displacements of the structure in the fatigue environment are usually very small to cause any significant loss of accuracy, wave kinematics from the first iteration can be used for all subsequent iterations.

Furthermore, relative velocity formulation of the Morison equation causes additional hydrodynamic damping that will reduce the wave loading. This phenomena does not occur for small structural displacements, which is the case for fatigue environment (ISO19902, 2007). Hence, the use of relative velocity formulation is ignored in the fatigue analysis.

Energy dissipation due to damping may have a profound effect on the structural response. If the forcing frequency is close to the natural frequency of the system, and the system is lightly damped, huge vibration amplitudes may occur. This phenomenon is known as resonance. The physical sources of damping are difficult to determine and to quantify with any certainty. A total damping value of 2% of critical damping is considered as the viscous damping coefficient that accounts for all sources of damping, including structural, foundation and hydrodynamic effects (ISO19902, 2007).

Most dynamic analyses of offshore platforms apply modal analysis techniques since they are efficient and reliable methods for calculating global structural responses. However, pure modal techniques are not accurate for local responses due to numerical inaccuracies involved in high frequency modes. In fatigue analysis the effects of both local and global dynamic responses are important to represent all significant dynamic responses in an accurate and efficient manner. Furthermore, fatigue analysis requires a very large number of modes to represent the local (quasi-static) member deformations accurately.

The modal acceleration method overcomes these aspects by superimposing dynamic responses onto a full static solution. This method allows for stress recovery with sufficient number of modes, so all dynamic and static responses are accurately included in the solution with computational efficiency. In any case, a modal analysis should also be performed to obtain natural frequencies and mode shapes of the structure to verify the dynamic behaviour of the structure.

Natural frequencies and mode shapes of the structure are obtained by using sufficient number of modes to verify that the dynamic behaviour of the model is realistic. The position of the platform natural frequency is reviewed to verify that it does not fall in the valley of the transfer function. A realistic range of natural frequency values should be considered, based on lower and upper bound values for the platform mass and stiffness.

Global transfer function plots are generated to verify that the specified waves are sufficient to accurately define the transfer function used in a spectral fatigue analysis. In order to accurately generate the peaks and valleys of the transfer function, a group of waves with frequencies around the primary and secondary modes of the structure are selected.

The mass matrix may be generated based on the lumped or consistent mass approach. Mass matrix created in the consistent approach includes off-diagonal coupling terms since the mass is distributed along the element. When including effects of fluid added or virtual mass acting normal but not tangential to the element, the element mass is not the same in all three directions; hence, a consistent mass approach is preferred.

Using a lumped (or diagonal) mass matrix for the structure's global response has a significant computational advantage in solving dynamic equations of equilibrium. However, local response of individual components shall be examined using a consistent mass model (ISO19902, 2007).

Dynamic characteristics (mode shapes and frequencies) of a structure are obtained by using the “*Dynpac*” module of SACS. Since linear theory (i.e. modal superposition) is used in dynamic analysis, non-linear foundations must be represented by the equivalent linear foundation model (pile stub). The PSI module is used to generate an equivalent foundation stiffness matrix for dynamic analysis using the centre of fatigue damage sea-state. The “*Pile*” module is used to determine length, properties and offsets for equivalent pile stub element based on pile head forces obtained from PSI analysis.

A Guyan reduction is performed to reduce the structural stiffness and mass matrices. The eigenvalues/eigenvectors for the master degrees of freedom are first extracted and then expanded to obtain the results for the reduced degrees of freedom.

Failing to account for the higher frequency harmonics in the wave force that are due to its non-linearity may cause potential errors in frequency domain analyses. However, for most frequency domain methods, equations of motion are solved by using linearized drag and inertia components, in which case higher terms are dropped for mathematical simplification.

The higher order terms in the dynamic analysis occur due to drag term, higher order wave theory and variable submergence of elements near the water surface (inundation or free surface effects). The basis for all simplified methods is linearization of the force vector in the matrix equilibrium equation and depend on the linearization procedure plus the load level.

Since high frequency modes react statically, the structural inertia load, which includes dynamic amplification can be mainly obtained from the low frequency modes. Likewise, hydrodynamic loading including the effects of structural motion is not affected by local structural motion, which is defined in the high frequency modes. Therefore, a direct solution technique can be used to represent the total loading on the structure.

In the direct solution technique the total loading on the structure is represented by equivalent static loading, which includes the inertia loads and the applied hydrodynamic forces. The inertia load is determined from the low frequency structural modes. The effect of structural motion is accounted for by the applied hydrodynamic forces. These equivalent static loads may then be directly solved to obtain stresses.

Equivalent static loading is obtained to generate the transfer function required in a spectral fatigue analysis. The solution files created include nominal stresses that are to be used by transfer functions. The wave data is specified in a sea-state input file based on the peaks and valleys of the global transfer function plots. A single pass analysis is to be performed (i.e. no iterations), which means that no relative velocity or acceleration will be included.

An equivalent static load case representing static and inertia loads was created for each of the 20 crest position of each wave. The wave is stepped through the structure using an 18-degree increment for 20 crest positions for a total of 360 degrees (one full wave cycle). A common solution file includes nominal stresses to create the transfer function. The same number of modes is to be considered in both Wave Response and Dynpac input files.

In “Wave Response” module the stress can be retrieved using either the equivalent static load method, an enhanced modal acceleration method or a modal acceleration method. However, the equivalent static load method is the recommended procedure for stress recovery.

A short term condition (stationary situation) of the sea, which lasts for a standard period of three hours is known as *sea-state*. Response statistics for each random sea-state is evaluated using hot spot stress transfer functions to incorporate the effect of wave frequency. Transfer functions are obtained as the response of the structure to a series of harmonic waves with a sufficient number of suitably spaced frequencies. A wave spectrum is used as the theoretical model of the sea-state to reflect the actual wave conditions at a particular time and location.

The long term model provides the most logical approach to design, especially concerning fatigue problems. Long term wave climate at a particular location is always empirical and cannot be defined by theoretical models since it is not stationary. The long term stress

distributions over the lifetime of the structure are obtained from probabilistic methods using statistical measures of the stress history. The stress transfer functions are the cornerstones of a probabilistic analysis, affecting the accuracy of calculated long term stress distributions (Vugts, 1978).

The wave statistics model consists of zero up-crossing periods,  $T_z$ , significant wave heights,  $H_s$ , and their probability of occurrence to define the sea-state conditions during a long term period. The statistics of the original random process are assumed Gaussian, so they can be theoretically described. These assumptions are most applicable for low to moderate sea-states, which are the sea-states of interest in fatigue studies and create confused short-crested sea conditions (ABS, 2010).

The wave scatter diagram is used to represent the long term wave environment at a location during a year and is based on several years of site specific data to ensure realistic representation of the wave climate. This diagram specifies the probability density function of the joint occurrence of sea-state parameters, including significant wave height, a representative period and the mean wave direction. The method uses the wave spectrum to represent the range of wave frequencies existing in a random sea-state.

The long term fatigue calculation is based on the response spectrum, S-N curves and the scatter diagram where Rayleigh probability distribution function of the stress ranges is valid for narrow banded processes. Local stresses at connection discontinuities “*hot spot stresses*” are calculated using nominal stresses and stress concentration factors. Long term statistics of hot spot stresses is derived by accumulation of local hot spot stresses resulting from the variable loads.

S-N curves are used to define the fatigue characteristics of a material subjected to repeated cycles of stress with constant magnitude. The S-N curve delivers the number of cycles required to produce failure for a given magnitude of stress. Stress concentration factors are based on the level of detail in the model (Johansen, 2003) and determined based on the joint geometry and connection classification. Usage factors describe the rate of fatigue damage using Miner’s law.

For fatigue calculations, the calibration process is conducted on Morison equation parameters, including drag coefficient, inertia coefficient and the wave steepness (Vugts, 1978). The application of probabilistic techniques to a fatigue analysis of offshore structures is discussed further in detail using the calibration process.

## Chapter 2 Literature review



Literature review is conducted to identify the most appropriate design method and its significance meeting functionality, safety and economical aspects. Initially, the nature of the excitation forces with their effects on offshore structures are investigated in fatigue environment. Then, characterization of the fatigue environment is discussed with the objective of retaining the random nature as well as the frequency content of a real sea using spectral methods.

## 2.1 Environmental conditions

The performance and survival of offshore structures are mostly affected by environmental conditions including wave and wind action, currents and soil characteristics at the site. Long term deployment of offshore platforms necessitates proper consideration of fatigue both at the design stage and during maintenance for structural integrity assessment procedures. Fatigue loading on offshore structures is based on the wave loading regime, structural features and environmental conditions. Waves account for most of the structural loading and, as they are time dependent, produce dynamic effects that tend to increase the stresses and affect the long-term behaviour of the system. Wave-induced dynamic forces are one of the most significant forces leading to fatigue of offshore tubular structures. Furthermore, a structure's dynamic behaviour is significantly affected by the soil characteristics and the pile–soil interaction.

Estimating the fatigue damage of offshore structures is a complicated problem. When a structure is subjected to a long and complex random loading, power spectra representing different states of the load history are usually obtained from the structural dynamic analysis. The analysis usually relies on simple linear wave theories that assume sea elevations are stationary, Gaussian process and linearity of structure behaviour. The response of offshore structures to wave loading is of fundamental importance in the analysis.

If the stress response of structures can be assumed to be stationary, Gaussian, and narrow band, an analytical solution of fatigue analysis can be obtained through statistical analysis (Chow, 1991). However, if a narrow banded assumption is not valid, a correction factor is applied and the total fatigue damage is calculated through their weighted linear summation using Miner's rule (ABS, 2010).

## 2.2 Determination of wave forces

Determining the wave forces on a structure is difficult due to the nonlinear effects of water structure interaction (Azarhoushang, 2010b). Wave kinematics should be obtained by using the information on sea surface elevation and wave theory. This implies the calculation of the fluid velocities and accelerations in an undisturbed wave field with ideal inviscid fluid. Furthermore, hydrodynamic forces on a structure are derived by applying Morison's equation or the potential theory (Brebba and Walker, 1979).

Hydrodynamic loading on large volume elements is governed by the potential theory; however, Morison's equation governs in the case of slender structural elements because these types of elements do not influence the flow field significantly. The two main lateral wave forces on offshore structures are the drag and inertia forces that are induced as water passes the individual members. The nonlinear quadratic drag term is proportional to the square of the fluid velocity and the linear inertia term is proportional to the acceleration of the fluid.

Morison's equation is empirical and was originally developed for vertical, rigid cylinders. It was then extended to the relative Morison equation for flexible structures to incorporate the nonlinearity in the drag term (drag damping). This extension incorporates non-linear effects of water particle velocity relative to the moving structure. Morison's formulation, which is used in the present study, remains the most commonly utilized method of relating water particle kinematics to hydrodynamic loading on the structure.

The higher order terms in the dynamic analysis occur not only because of the velocity-squared term but also due to higher order wave theory and variable submergence of elements near the water surface. The influence of the higher order term is negligible in low to moderate seas, which is the case of fatigue wave environments. In contrast, an accurate assessment of the inertial coefficient is of prime importance since fatigue environments are mainly inertial (Vugts, 1978).

Linearization is essential for most frequency domain methods and can be achieved by using a constant wave steepness (ratio of wave height to wave length) when selecting wave heights for the transfer function. This will provide a simple relationship between the wave height and the frequency; however, the wave heights selected should introduce a suitable level of nonlinear drag term (HSE, 2000).

The linear force vector can be evaluated by stochastic linearization, defining the significant wave height ( $H_s$ ) and peak period ( $T_p$ ) of a random sea-state. Assuming the response to be

Gaussian, the linear matrix is derived by minimizing the expected mean square error and the analysis is performed by transforming the equilibrium equation into the frequency domain (Leira, 1990).

Spectral analysis is a powerful method to capture the random nature of the environmental loads; however, it is based on some kind of linearization. The characteristics of the excitation can be modified by the response of the system. In other words, a system's response may approximate to Gaussian if it is a narrow band response derived from a broad band excitation. Hence, even though the excitation is non-Gaussian, the linearized spectral response is a Gaussian process. This will enable frequency domain techniques to capture nonlinear drag wave loading and free surface inundation effects. Enhanced frequency-domain linearization methods can be expected to be very practical tools for fatigue assessment since the response process could be realistically presented (Greeves, 1996).

Following the above, the wave heights used for determining the transfer functions must be selected in a suitable manner, so an appropriate level of non-linear (drag) wave loading is introduced. Constant wave steepness is commonly used for this, which provides a simple relationship between the wave height and frequency. Typical values of steepness are in the range 1:15 to 1:25. The actual value should be determined using a suitable calibration process for the actual structure and environment as described in this research study. The calibration procedure is developed using the Morison equation with adjusted parameters to suit the spectral analysis (Vugts, 1978). The drag coefficient, inertia coefficient and wave height are the variables that are calibrated for a given wave theory to produce similar force levels as conventional methods.

## 2.3 Forcing frequency and resonance effects

The structure's natural period and the wave spectrum's dominant period have a great influence on the dynamic response. The closer these two values are, the larger the response will be. Therefore, it must be ensured that the frequency of applied periodic loading will not coincide with a modal frequency to avoid resonance and large oscillations. Furthermore, to avoid unrealistic suppression of dynamic effects, the influence of global wave load cancellation should be investigated when structural natural period coincides with the cancellation point (Greeves, 1996).

For low forcing frequencies the response is mostly controlled by stiffness and tends toward the static response. The coincidence of forcing period ( $T$ ) and natural period ( $T_n$ ) is termed resonance (i.e.,  $T_n/T$  is equal to 1.0). At this stage, the elastic and inertia forces are equal, so the motion continues if there are no excitation and damping. Subsequently, the structural response is greater than the static response depending on the damping ratio. As a result, the accuracy of a quasi-static analysis reduces and a dynamic analysis is essential for calculating the response in this regime. The structure reflects the waves entirely at the higher forcing frequencies and reversals are so rapid that inertia dominates (DNV, 2010).

The intensity of dynamic response is highly related to the natural period of an offshore structure. The first and second vibratory modes are usually lateral displacements at the deck level (surge and sway) out of which the higher mode is related to the less stiff direction of the structure. The third vibratory mode is usually a torsional mode. The ratio of dynamic response to static response is referred to as the *Dynamic Amplification Factor* (DAF). As shown in Figure 2-1 for the single-degree-of-freedom (SDOF) approach, DAF can be underestimated if the wave period is further away from the natural period (ABS, 2004).

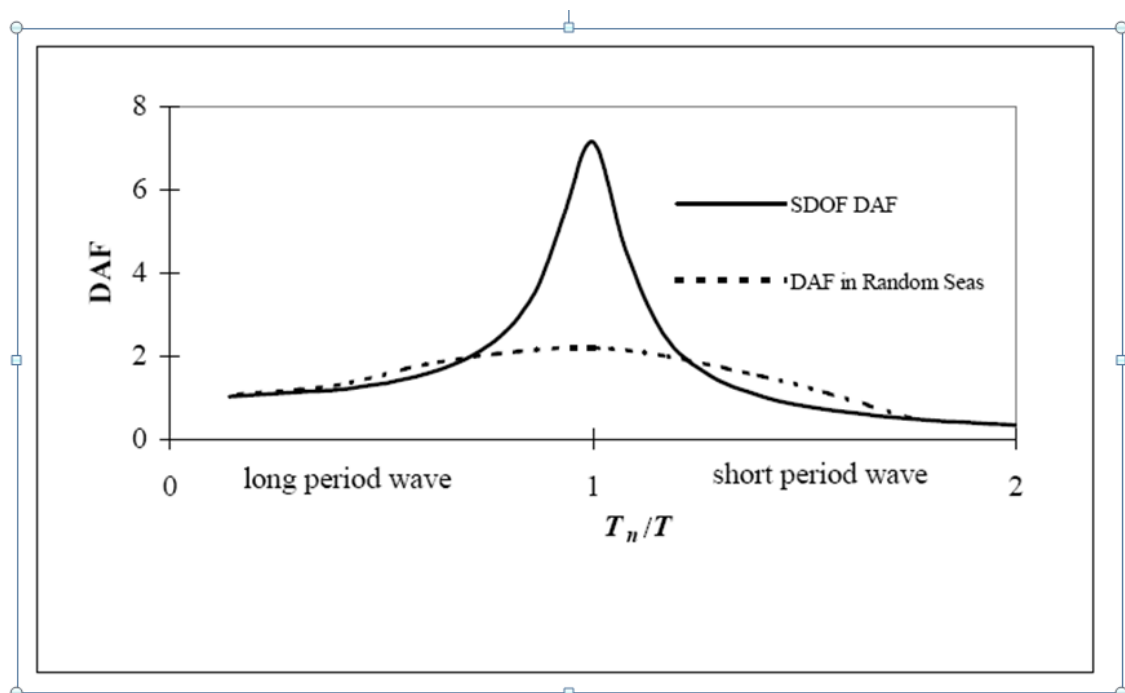


Figure 2-1 Resonance effects

## 2.4 Applicability of wave theories

Wave theories are classified as *small amplitude* or *finite amplitude* wave theories based on their formulas and boundary conditions at the surface of the wave (Ko, 1988). However, they all have symmetric crest and propagate without changing form. The small amplitude wave theory is referred to as linear wave theory and is often used in practice due to its simplicity. Since the motions are relatively small, higher order terms of wave amplitude are neglected to allow the linearization of the free surface boundary condition. Conversely, large or finite amplitude wave theories retain higher order terms, which applies to non-linear wave theories. For most applications where the ratio of water depth to wave length is not small, non-linear free surface effects in diffraction mechanics are generally negligible (Zienkiewicz et al., 1978).

Different wave theories may be applicable for the different wave height and period combinations used in the analysis. The applicability regions of wave theories are shown in Figure 2-2.

Fatigue damage calculation for offshore structures usually relies on simplifying assumptions on wave loads and the structural behaviour. As a common practice, simple linear wave theories are used where the sea elevations are assumed to be stationary, Gaussian process and the structure behaviour is assumed to be linear (Gupta, 2007). In this regard linear (Airy) wave theory is preferred in spectral analysis and normally could be used for all ratios of water depth to wave length (DNV, 2011). However, the linearity demand can be somewhat relaxed for the determination of transfer functions by an appropriate selection of the wave height input and suitable linearization of the results (ISO19902, 2007).

## 2.5 Wave action on offshore structure

Ocean based structures are mostly influenced by actions producing variable loads like waves and combinations of waves with other variable actions. If the loads are variable with time, they could excite dynamic response in the structure and intensify the fatigue stresses. This will cause degradation of structure due to cyclic wave loading, which leads to fatigue cracking and possible widespread fatigue. The static loads can be ignored in fatigue analysis. However, they must be considered in evaluating spring stiffness used to simulate piles. Since the pile load-deflection curve is nonlinear, appropriate spring stiffness for the low load levels associated with fatigue waves should be considered. Fatigue life of members and joints near the mud line are mostly affected with the boundary conditions of the model used to simulate the piled structure.

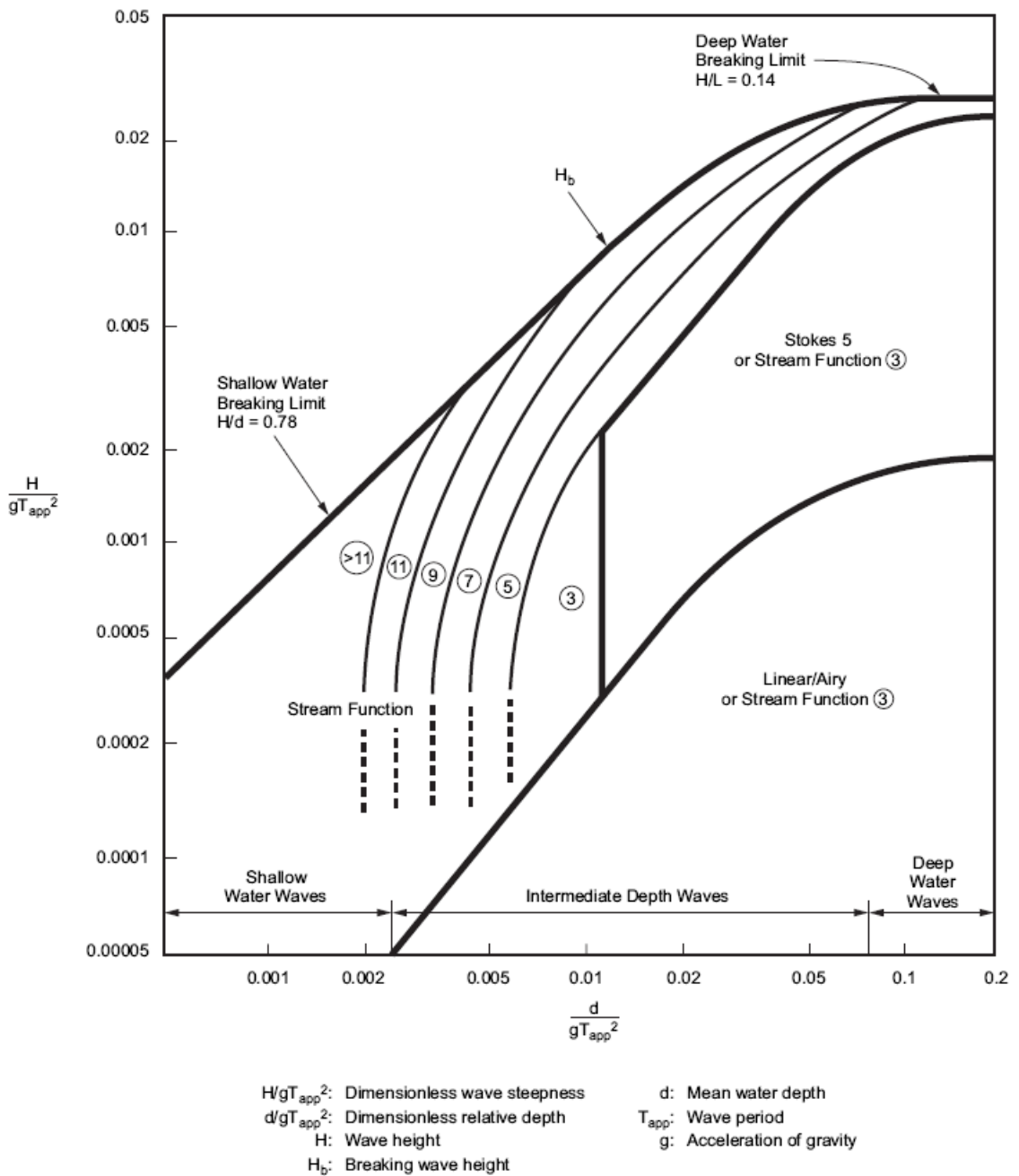


**Figure 2-2 Regions of Applicability of Wave Theory (API, 2007)**

Fatigue is known as a major mode of failure in marine structures, which respond dynamically to random wave and wind loading (Wirsching, 1987). Natural period of the offshore structure, shape and pick period of the wave spectrum, system damping and global wave load cancellation effects are considered as parameters influencing dynamic response. Where the first natural periods are in a range with significant wave energy to excite significant dynamic response, the dynamic structural response needs to be considered in the fatigue analysis. For

normal structure configurations and typical wave climates, dynamic response to waves can be ignored if the platform fundamental modes have periods that are less than 2.5 seconds.

In “quasi-static” method, dynamic effects into structural analysis is considered using a DAF for each global response parameter (e.g., base shear or overturning moment). DAF is the ratio of extreme dynamic response to the same response when dynamics is discounted. The hydrodynamic damping due to low waves is very small. Dynamic amplification increases in low damping systems when the period of the forcing function (the wave period) is close to the natural period of the structure and results in a fatigue-sensitive structure (Kinra, 1979).

The presence of higher harmonic components make the dynamic analysis more complicated, even for a regular wave in a frequency content of the wave forces on a structure caused by nonlinearity of the drag force, random nature of the wave, and structural or foundation nonlinearity.

Structural redundancy of a jacket type platform is low and a member failure in these structures cause immediate reduction of strength, which may result in catastrophic collapse of the structure (Golafshani, 2009). This will necessitate proper analysis technology to accurately account wave action on offshore structures. Steady state response of the structure to regular wave could be considered by methods based on mode superposition without the requirement for linearization. This will reduce the overall resonance effects predicted by the SDOF method due to the presence of higher harmonics. This method could be further extended for random seas using frequency domain methods provided that nonlinear effects such as P-delta, foundation stiffness, etc. are included in the method through suitable linearization.

Service loading of offshore platforms is mainly due to wave and wind action with variable amplitude and frequency content. The stochastic wave model accounts for the actual distribution of wave energy over the entire frequency range, which is the only method to simulate sea irregularity. The wave energy spectrum is characterized by the significant wave height ( $H_s$ ) and average zero-up-crossing period ( $T_z$ ) to represent a sea-state and is regarded as an extent of total energy distribution in a specific sea-state. For fully developed sea-states the Pierson Moskowitz wave spectrum is used, while for sea-states that are still developing, a Jonswap wave spectrum is preferred. The probability of occurrence of a particular sea-state is specified in a wave scatter diagram by  $H_s$  and  $T_z$ , which represents a composite of all wave directions and influences the stresses experienced. The stress spectrum is calculated by multiplying the wave spectrum by the square of the transfer function (Vugts, 1978).

The frequency domain method is well suited for systems exposed to random wave environments with moderate environmental conditions since the random response spectrum can be computed directly from the transfer function and the wave spectrum. The main advantage of this method is that the computations are relatively simple and efficient compared to time domain analysis methods. Long term effects should be specified for fatigue analysis to complete the definition of wave climate. For this purpose, the probabilistic description of the sea is defined by the wave scatter diagram that gives the probability of the joint occurrence of a particular  $H_s$  and  $T_z$ . The wave spectrum can be used to simulate the wave elevation as a linear random superposition of regular wave components.

Fatigue in offshore structures is regarded as a high cycle low stress incident. The response of a structure in moderate sea-states is of prime concern in fatigue damage considerations. In contrast, severe storms with return periods above 1 year are irrelevant since fatigue damage is mainly due to cycles with low stress ranges. Hence, linearization is deemed to be acceptable. This will meet the requirement of spectral methods using transfer functions. If nonlinear effects exist, the ratio of response amplitude will no longer be proportional to wave amplitude and the transfer functions will depend on the wave amplitudes that are selected. In this case, suitable linearization is required to avoid ambiguous results.

However, there is uncertainty involved in the stress transfer functions due to actual wave loads on the structure, linearization of the wave loading, and local stress concentration factors (Vugts, 1978). The structural response of an offshore platform could be non-Gaussian after inclusion of nonlinear drag force and free surface effects in the wave kinematics calculations, even though the waves considered are linear and statistically Gaussian. An empirical modification around the free surface may be considered to account for free surface effects (Wheeler stretching).

Wave loads are variable loads acting on the structure and have the main contribution to fatigue damage. The annual variability of sea-states, spreading of wave energies around a dominant mean wave direction and wave directions relative to the structure are considered to be the basic components of the wave environment (Vugts, 1978). These elements should be selected such that the resultant forces and moments can be obtained precisely. Variable local stresses are derived from wave force calculations and affect fatigue life estimates.

The annual variability of sea-states can be defined by *RMS* (Root Mean Square) wave elevation, the mean period and the spectral width for the various sea-states at the structure's location. Hence, the wave environment can be described adequately. The first two parameters



are defined by a wave scatter diagram that gives the probability of the simultaneous existence of a particular significant wave height and zero crossing period. There is uncertainty involved in the spectral width, since in transforming from the time domain to the frequency domain we are forced to employ selective filters, which automatically reduce the effective bandwidth and therefore reduce the statistical reliability of the results obtained (Newland, 2012).

The spectral width reflects the irregularity of the sea. For infinitely narrow spectrum, the statistical distribution of all wave crests is given by a Rayleigh distribution of the peaks. The distribution function is more complex for broad spectral widths. Stress response is obtained using a user specified wave spectrum from site measurements or standard forms of the spectrum. The wave spectrum shape should represent distribution of wave energy with wave frequency in each sea-state. It is important to simulate the correct frequency content of a typical wave loading because crack growth of the structural steels in tubular joints is dependent of frequency content. Wave power spectra can be generally classified into two characteristic forms (Kam, 1992). These are related to either the fetch-limited, developing sea conditions without swell (e.g. JONSWAP spectra) or the fully developed seas (e.g. Pierson-Moskowitz spectra).

Furthermore, the long term wave climate description is determined using a wave scatter diagram by two parameters; the significant wave height ( $H_s$ ) and the associated zero crossing period ( $T_z$ ). Both of these parameters appreciably influence the stresses that are experienced. A wave scatter diagram specifies the probability of occurrence of waves coming from specific directions, which enables the cumulative effect of all of the wave conditions occurring throughout the platform life to be determined. Directional wave scatter diagrams that indicate individual sea-state probabilities for a number of mean approach directions are the most comprehensive form in which this information can be presented.

Wave loads on slender members (drag dominated structures) should be calculated using Morison's equation. A wide range of wave heights and periods are contributing to fatigue analysis. The majority of these are much lower and shorter than the design wave height and period for the strength analysis. The inertia term in Morison's equation is therefore much more important in fatigue analyses than for the strength analysis in an extreme storm condition, up to the point where the inertia term can become dominant over the drag term and the fatigue damage accumulation experienced is mainly caused by inertia dominated wave loadings (Jia, 2008). Consequently, due to small and medium sized waves, more member segments are required to properly define the distributed loading in fatigue analysis compared to extreme storm analysis.

The use of the relative Morison equation with its 'drag' damping reduces the response at resonance due to additional hydrodynamic damping from drag forces. For small structural displacements, which is the case in fatigue loading conditions, this additional damping is not observed in measurements; therefore, relative velocity formulation is not used in fatigue analysis (Frieze, 1997).

The drag forces due to joint contribution of wave and current cannot be calculated as a linear combination of their individual effects because of their nonlinearity. Therefore, the drag force is calculated for the resulting velocity of current velocity plus liquid particle velocity in the waves (DNV, 2011). However, for fatigue assessment, it is not the absolute value of the stress that matters but it is rather the stress range. Sensitivity analyses have shown that the influence of currents on the range of the calculated stress variations and hence on the fatigue damage accumulation in the structure is small and can be ignored.

Wave conditions in random sea-states are known to be short crested; i.e. the component waves are spread over a range of directions centred on the mean direction. An appropriate spreading function (e.g. cosine squared) may be used in conjunction with the wave spectrum to account for the effect of wave spreading on structural responses. However, experience shows that the effect of wave spreading is not significant in fatigue analysis and can be ignored.

In addition to wave environment, marine growth affects platform dynamics and fatigue life of members with increased local and global wave loading. Marine growth is a surface coat on marine structures that is formed by plants, animals and bacteria during the first few years after platform installation. Therefore, for new designs the maximum marine growth thickness determined for the site should be used for the fatigue analysis. However, marine growth profile could be considered to be the average thickness instead if the results are conservative (API, 2007). Marine growth increases hydrodynamic action, weight and added mass, which may influence hydrodynamic instability as a result of vortex shedding and possible corrosion effects. The effect of marine growth is accounted for by using an effective diameter for submerged elements in conjunction with adjusted drag and inertia coefficients for fouled members.

For dynamic analyses the foundation stiffness can have a large effect on the natural periods of the structure. A sensitivity of the theoretical period should be investigated to verify that it does not fall in a valley of the transfer function. Fatigue sensitive members, especially in the base of the structure, should be investigated with the upper and lower bound foundation stiffness values. The stiffness values should reflect the foundation deflections and rotations in the

fatigue environment. For this purpose, the centre of fatigue damaged sea-state representing the wave conditions that contribute significantly to fatigue damage is used to develop the equivalent linear representations of the foundation stiffness.

The effect of wave action on appurtenances including conductors, caissons, risers, J-tubes, boat landings, fenders, launch rails, pile guides, pile sleeve assemblies, etc. are considered in their correct location and with their appropriate connection details to realistically transfer any loads on them to the structure. Miscellaneous attachments such as anodes also attract hydrodynamic actions. However, wave actions on anodes are distributed on the submerged structure and may be considered with an increase in the drag and/or inertia coefficients in the Morison equation (ISO19902, 2007).

Wave actions increase lateral loading and overturning moments of the structure, which can result in failure or possible collapse. Failure of primary structural members due to wave inundation mostly occurs in jacket-type platforms that have been designed to less stringent deck elevation requirements in shallow waters. The main causes of failure need to be addressed by reviewing current air-gap (the gap between the highest crest elevation for the design return period and the underside of the lowest deck level) standards that determine deck heights, as well as site assessment standards (Cruz, 2008).

There is no direct wave action on the topside structures supported by conventional jacket substructures provided that the air-gap requirement is met. However, for structures subjected to significant dynamic response (e.g. the elements span from the water surface to the deck without intermediate supports, like jacket structures with un-braced portal arrangements facilitating float over installation) cyclic wave loads on the substructure may introduce mass inertia forces in the deck, which result in significant fatigue loading of the topside structure. At this condition, fatigue of the topside structure should be performed for the combined substructure and topside system.

## 2.6 Hydrodynamic loading

Hydrodynamic loading on offshore structures are primarily composed of drag and inertia loading. Drag loading is caused by vortices generated in the flow as it passes the members and is more significant for tubular components of small diameter in waves of large height ( $D/H < 0.1$ ). Drag force is proportional to incident velocity squared and simply due to flow separation in viscose fluid (discounting the vortex shedding effects).

Inertia loads are caused by the pressure gradient and the local interaction of the structural member in an accelerating fluid and are most significant for structural components of large sectional dimensions ( $0.5 < D/H < 1.0$ ). The inertia force, which is independent of any viscosity is composed of two parts; added inertia due to virtual mass of the member in motion and distortion of the streamlines around the stationary member.

Diffraction loading is a type of inertia loading that occurs when a structure modifies the wave pattern and is only significant when the sectional dimensions are greater than 0.2 of the wave length ( $D/\lambda > 0.2$ ). The diffraction effect will be important for calculation of the air gap to the deck, wave loading on closely adjacent structures and drag loading on the towers and exposed conductors and risers of a gravity platform (Wilson, 2003).

Slam/slap loading is a local inertia force that occurs as a horizontal/vertical member passes through the water surface with a fluctuating buoyancy force due to the periodic immersion of the member. Since the force is applied impulsively, the dynamic response of the structure is of importance. It is recommended to allow for a pressure of 1 MPa on surfaces liable to slam or slap in exposed waters (Barltrop, 1991). Local inertia effects will be neglected when determining the global structure forces.

All slender members shall be investigated for the possibility of in-line and/or cross-flow vibrations due to vortex shedding resulting from the flow of water or air past the member, as appropriate. Vortex induced vibrations (VIV) causing drag amplification is considered for the global behaviour of the member (DNV, 2010).

## 2.7 Hydrodynamic analysis

Information on sea surface elevation in conjunction with a wave theory is used to compute the water particle kinematics. Furthermore, for a member with dimensions such that its presence does not significantly disturb the incident wave field, the in-line component of hydrodynamic loading is commonly evaluated by Morison's equation comprising of a nonlinear quadratic drag term that is proportional to the square of the fluid velocity and a linear inertia term that is proportional to the acceleration of the fluid.

This empirical equation was originally developed for vertical, rigid cylinders. Morison's formulation was later extended to include relative velocities term for flexible structures. If the structure moves, then the relative velocity modifies the drag force and can result in hydrodynamic damping. Relative acceleration results in a force that is similar to the inertia force, which can be most conveniently analysed by using the concept of an added mass of

water that is constrained to move with the structure or member. The non-linearity introduced by the drag force equation causes considerable problems in dynamic analysis. However, the higher order terms in the dynamic analysis occur not only because of the velocity-squared term but also due to higher order wave theory, variation in wetted leg length due to inundation effects, etc.

Despite the concerns raised, Morison's formulation, which is used in the present study, remains the most commonly utilized method of relating water particle kinematics to hydrodynamic loading on the structure. However, linearized drag and inertia components are used for most frequency domain methods. This will simplify the kinematic wave equation by dropping the high order terms, which will then be used in structural dynamic analysis (Greeves, 1996).

## 2.8 Global and local level approach

Fatigue damage is a highly localised phenomenon affected by local details in the structure. However, both the global loading on the structure and the local loading on individual members contribute to fatigue damage. In this regard a calibration process is developed, which is based on matching of global response parameters that are representative of the predominant fatigue loading. In certain situations, the structural design and assessment practices are based on component level whereas in certain other situations, a global level approach is necessitated (Rajasankar, 2003). All of these features must be correctly represented in the design process.

The hydrodynamic load comprises of in-line forces (i.e. forces in the wave and current direction) as well as transverse forces (i.e. forces normal to the wave and current direction). Transverse forces are neglected in the global analysis; however, they may cause vortex induced vibrations of individual legs, which has to be investigated as local checking.

Both type of the above forces have nonlinear interaction with fixed jacket type offshore platforms with slender elements. The in-line forces are the most important and are modelled by the extended Morison equation. In extreme wave situations, the quadratic drag term of this equation is the dominating term, which leads to a further increase of the extreme forces with severe consequences for the dynamic response (Karunakaran, 1995). However, the experienced fatigue damage accumulation is mainly caused by inertia dominated wave loadings due to small and medium sized waves.

Modal analysis techniques offer an efficient and reliable method for global structural response. A lumped mass model in modal analysis is adequate to be used in global structural response. If the mass of the structure is lumped at the nodal points, only the translational degrees of freedom is associated with mass. If a lumped parameter model is used, both for mass and loading, all rotational degrees of freedom, except at the base point may be eliminated by simple static condensation without introducing additional constraints on the model. This reduced model is a realistic proposition for even quite extensive parametric studies. However, it does not always adequately predict local dynamic response.

For fatigue analysis, we should accurately represent the local (quasi-static) member deformations. In this regard local responses shall be examined using a very large number of modes and consistent mass model. Disregarding three-dimensional effects (free surface), the added mass can be taken as being equal to the mass of the water displaced by the cylinder. It is found that the effects of the free surface will generally reduce the added mass and thus tend to increase the natural frequency of the structure.

## 2.9 Probabilistic versus deterministic methods

Frequency domain analysis is carried out by either deterministic or probabilistic methods. The deterministic approach is based on the height exceedance diagram while the probabilistic approach is based on the spectral curves of wave height (Brebbia and Walker, 1979). When the structural natural periods and the wave periods with significant energy are well spaced (i.e. when the structure does not respond at its natural period) a quasi-static behaviour is expected and the deterministic method of analysis is usually appropriate. This quasi static behaviour permits the dynamic amplification factor to be calculated by simply considering the dominant waves in the sea (Bartrop, 1991). However, it is recommended to account for the randomness of the loading and resulting responses.

Determination of local stress history depends on whether the fatigue design approach is deterministic or probabilistic. In a deterministic analysis, the total number of stress variations is the same for all points of the structure and equal to the total number of individual waves. In reality the number of stress variations changes from one point to another in the structure and neither of them is equal to the number of waves. This necessitates a probabilistic approach to reflect these properties in a random wave environment (Vugts, 1978).

In the deterministic approach, fatigue wave environment is defined using periodic (regular) waves, within which neither the random nature nor the frequency content of real waves are

reflected. Hence, the deterministic procedure, which produces a deterministic short-term distribution of the stress range for each sea-state is not suitable for dynamically sensitive structures. However, this approach is recommended for fatigue assessment of structures that are not fatigue sensitive, as well as during the initial design phases for screening purpose only (ISO19902, 2007).

To retain the random nature as well as the frequency content of a real sea, spectral methods should be used in the probabilistic approach. In the spectral analysis method, a sea-state (the short-term wave environment) is represented by a wave frequency spectrum to allow a probabilistic determination of the stress range (short-term distribution) for each sea-state and at each location of interest in the structure. This procedure is appropriate for final fatigue assessment, especially for dynamically responding structures. The disadvantage is the requirement for linearization of the hydrodynamic drag action, wave inundation effects and foundation behaviour in global analysis, by which the nominal stresses are determined.

Since environmental loads are random in nature and many of the fatigue design factors are subject to considerable variability, the probabilistic approach seems particularly relevant with no reliable link to the deterministic methods. Only the variable part of the local stresses is considered in the probabilistic approach, where both the magnitudes and the number of cycles of the long term stress response are affected (Wirsching, 1980).

## 2.10 Fatigue environment characterization

It is important to distinguish between the short-term and long-term descriptions in characterizing the fatigue environment. In the short-term description, the sea-state is considered stationary over a short time period and the variation of the short term statistics over a longer time scale (e.g. over the life time of the structure) is considered as long-term description in fatigue analysis (Iraninejad, 1988).

A short term sea-state is characterized by a significant wave height and a zero up-crossing period. For dynamic wave analysis, the structure is analysed for a range of frequencies at unit wave amplitude to obtain the structural transfer function. The transfer function is combined with the wave spectrum to evaluate the response spectrum. The statistical properties of the response can be found by standard spectral analysis techniques (HSE, 2000). For a zero-mean Gaussian process, extreme values are evaluated with a Rayleigh distribution of the peaks.

Statistical modelling under random loading is simplified by a linear damage accumulation assumption. This assumption simply states that the stress cycle interaction effect in the load history is negligible and therefore the fatigue damage due to a variable amplitude stress history can be evaluated as the linear summation of the damages caused by individual cycles. Therefore, the equivalent stress range can be determined by the probability density of stress peaks of equation (Chow, 1991). Short term statistics are weighted by the product of the probabilities of occurrence of the sea-state and the wave approach direction. Then Long-term statistics are obtained by accumulating the weighted short-term statistics over all sea-states in the scatter diagram and over all wave approach directions. From the cumulative distribution, the number of occurrences in discrete stress range blocks are calculated and used as input for the fatigue damage calculation. An example of a long term cumulative distribution of hot spot stress ranges and its subdivision into stress range blocks is shown in Figure 2-3. Fatigue calculations are based on the assumption that a single-slope or bi-linear SN-curve is used (Johansen, 2003).

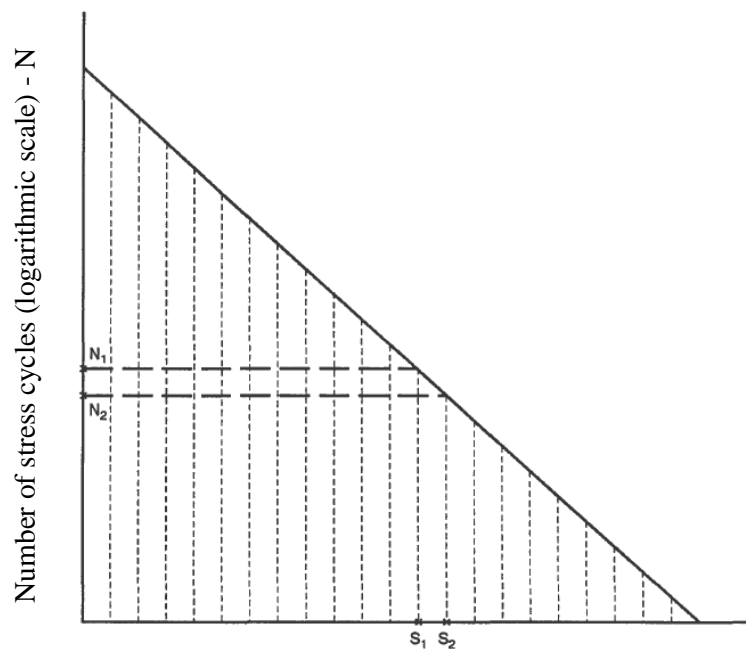


**Figure 2-3 Typical long term cumulative distribution of stress ranges**



## Chapter 3 Analysis

In this chapter an analytical solution of the fatigue assessment is presented through statistical analysis which suits a random process. The methodology used here is a frequency domain analysis using spectral density functions and the transfer function approach to model the response spectrum. This approach is useful to handle nonlinear effects while the wave statistics of random sea is not changing due to existence of short periods in fatigue loading environment and water surface elevation can be properly described by wave power spectra.

The realistic distribution of wave energy over the relevant frequency range is suitably accounted for using spectral analysis. The structural model is considered in sufficient detail and the applicability of analysis method to dynamically responding structures under random nonlinear wave loading demonstrated as a relevant response tool.

### 3.1 Model definition

SACS software is used to model the linear and nonlinear behaviour of the system. A jacket type offshore platform model is developed for dynamic fatigue assessment. The structural model is considered with an appropriate three dimensional distribution of the structure's stiffness including the topside, the jacket and its foundation to reflect all relevant characteristics of the structure as shown in Figure 3-1. The plan and elevation views of the jacket structure is presented in Figure 3-2 to Figure 3-9.

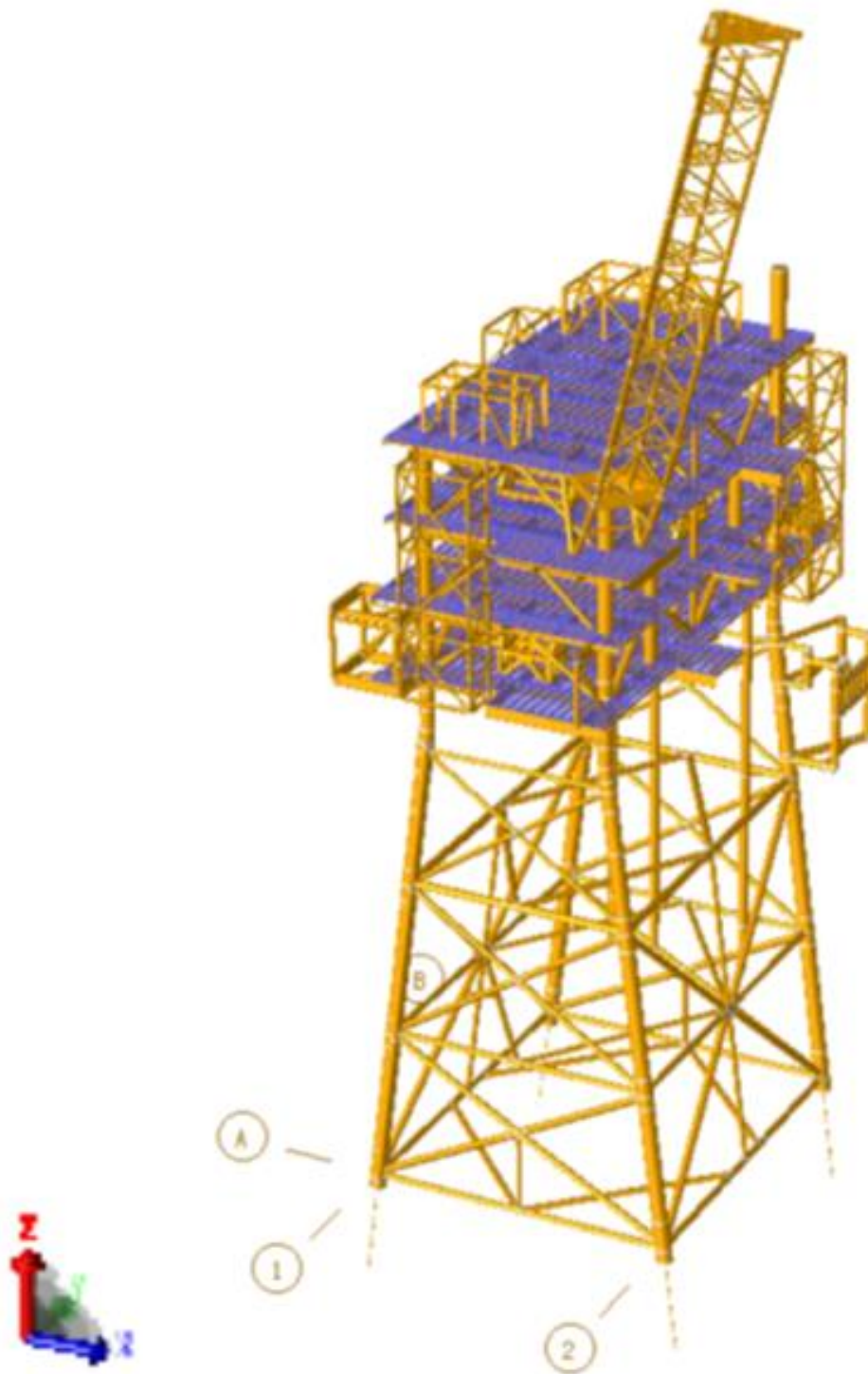


**Figure 3-1 General View of SACS Structural Model**

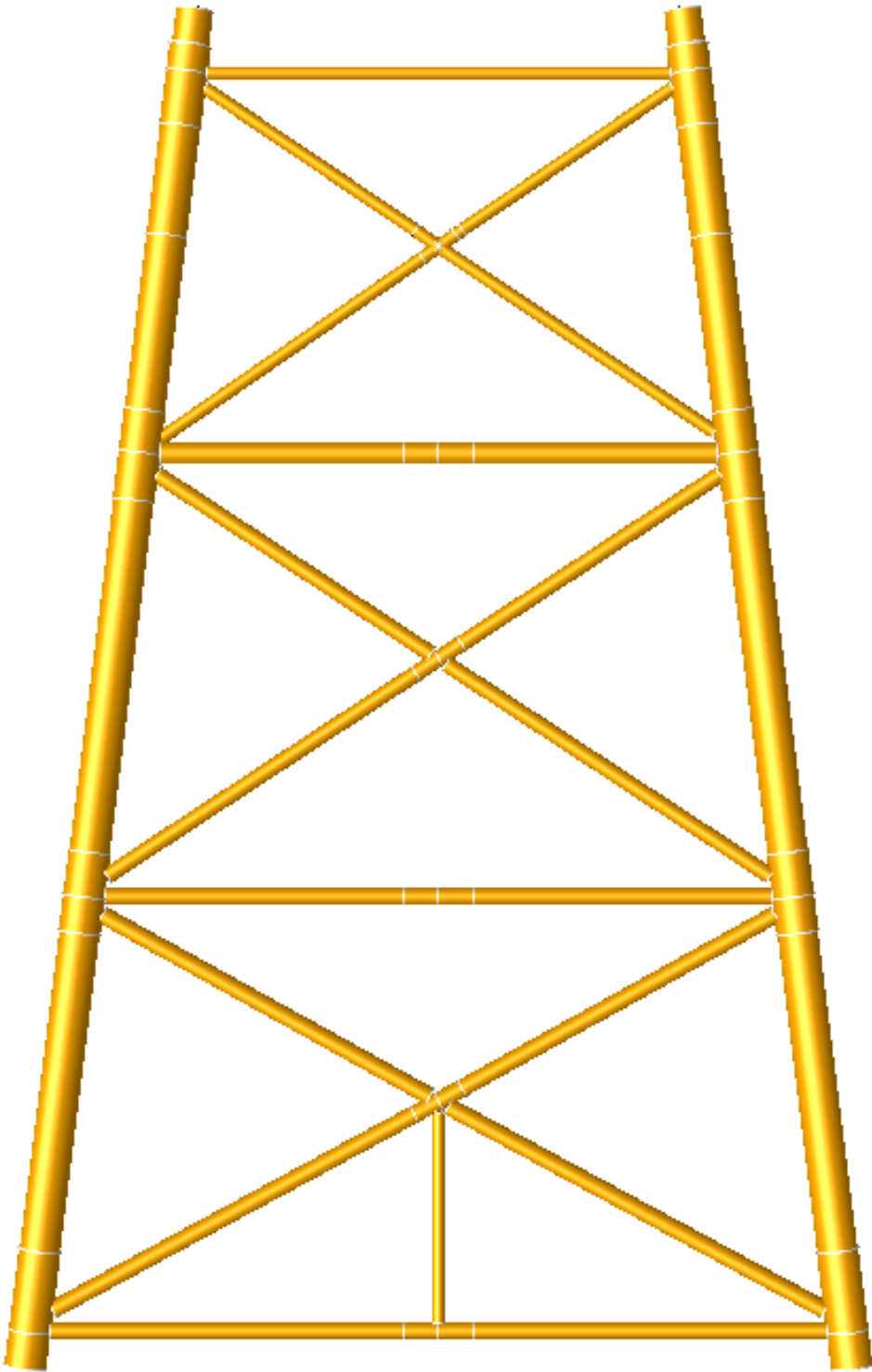


**Figure 3-2 Face Row A**

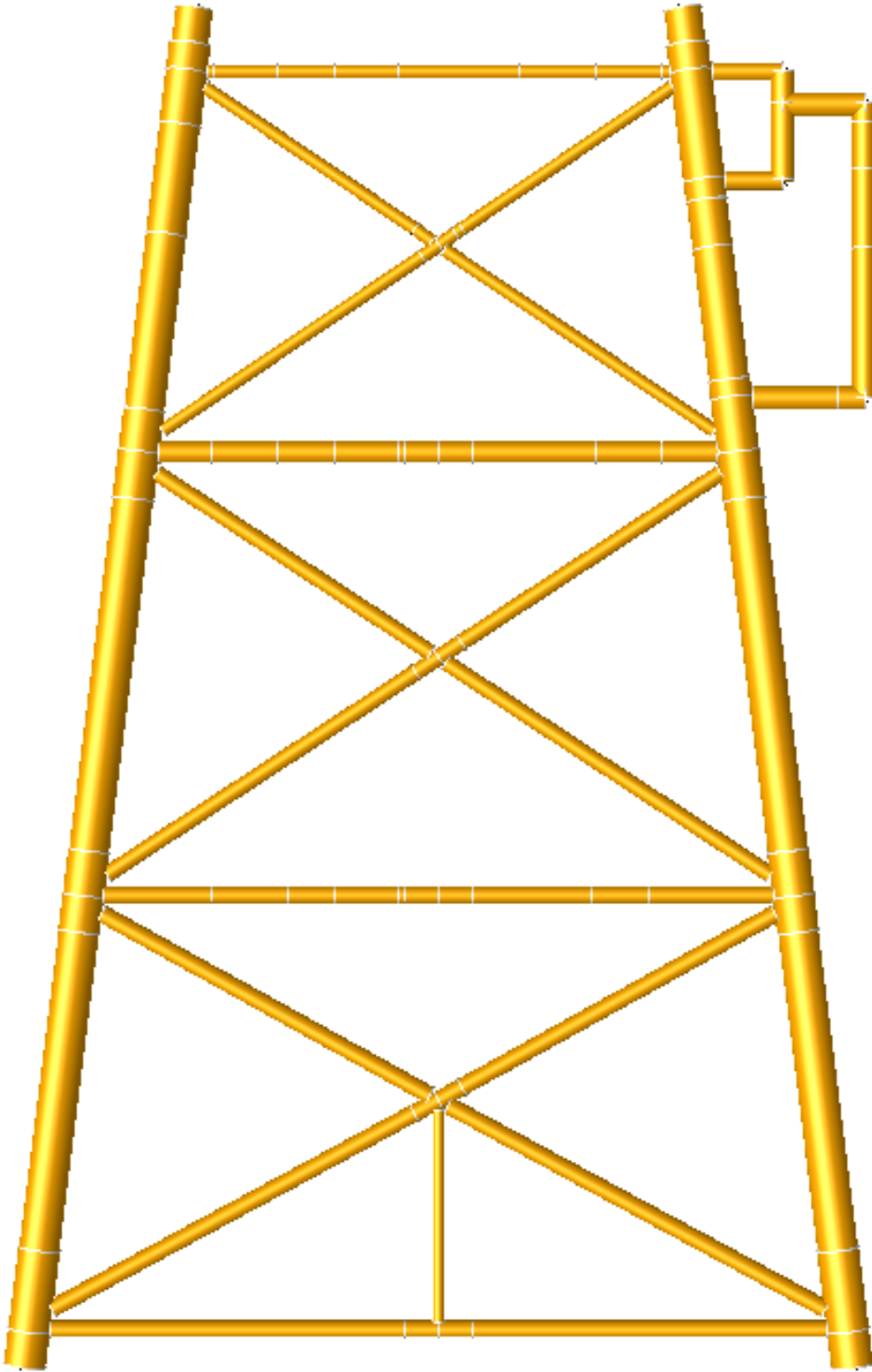


**Figure 3-3 Face Row B**

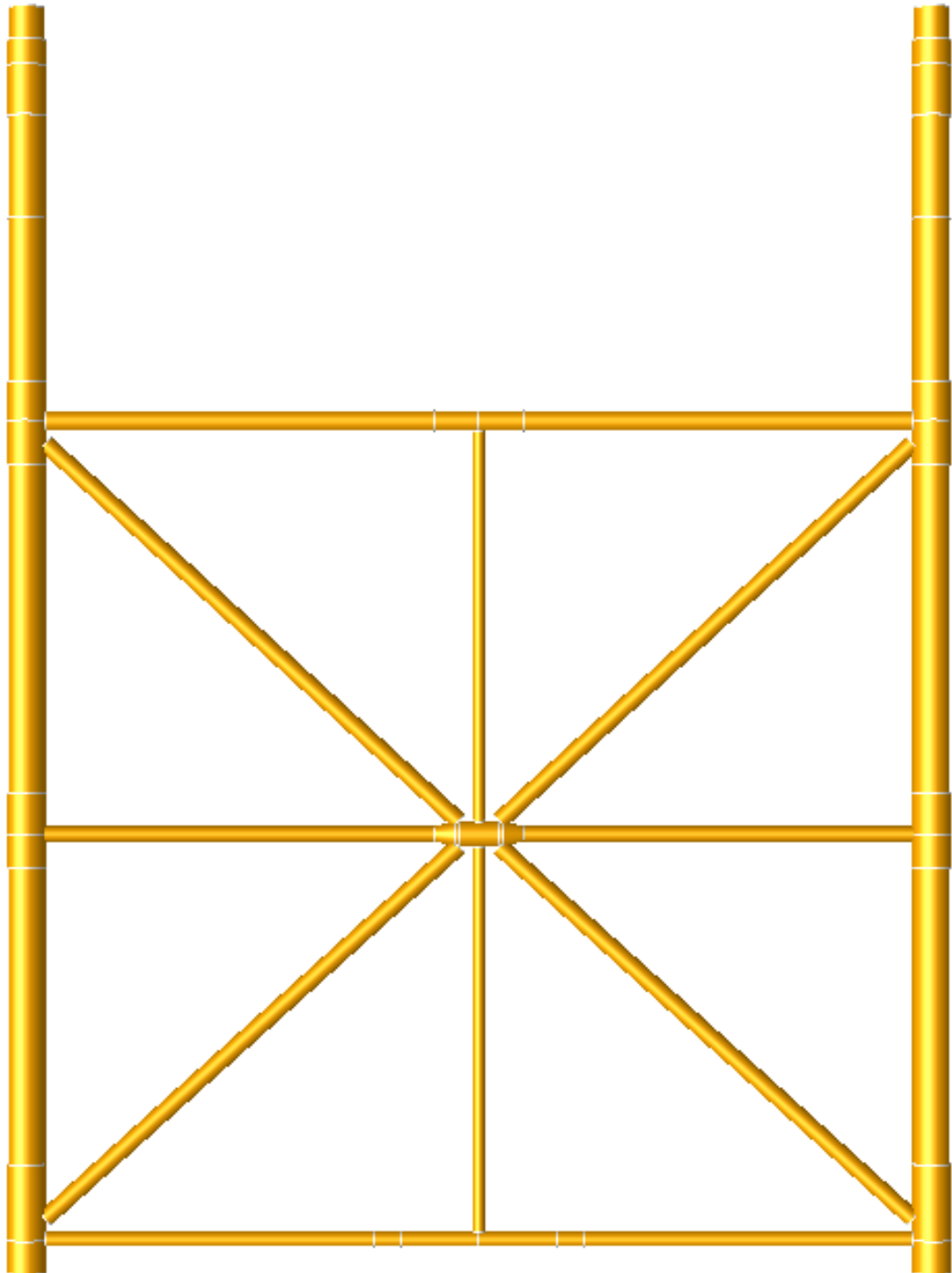


**Figure 3-4 Face Row 1**

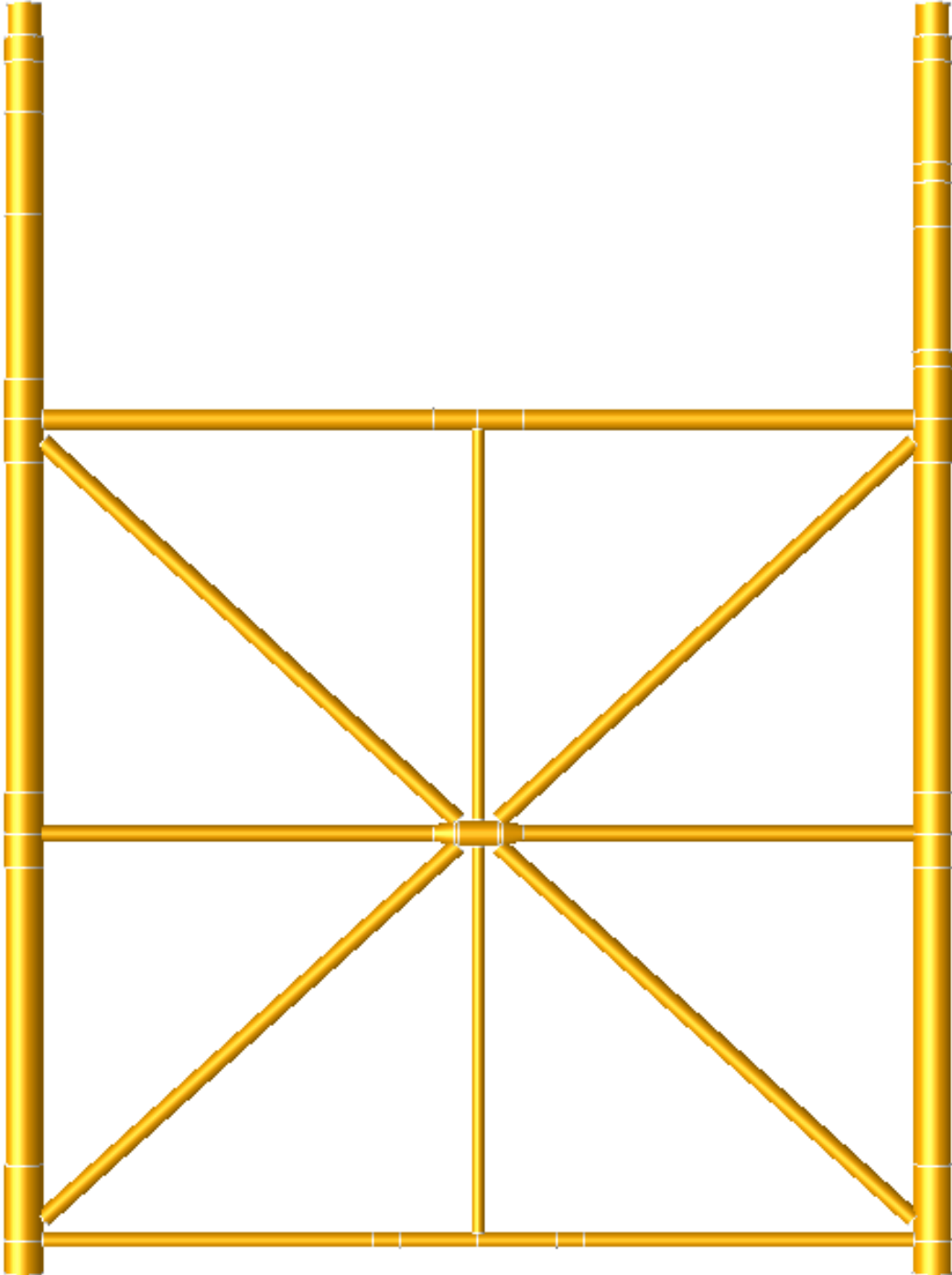
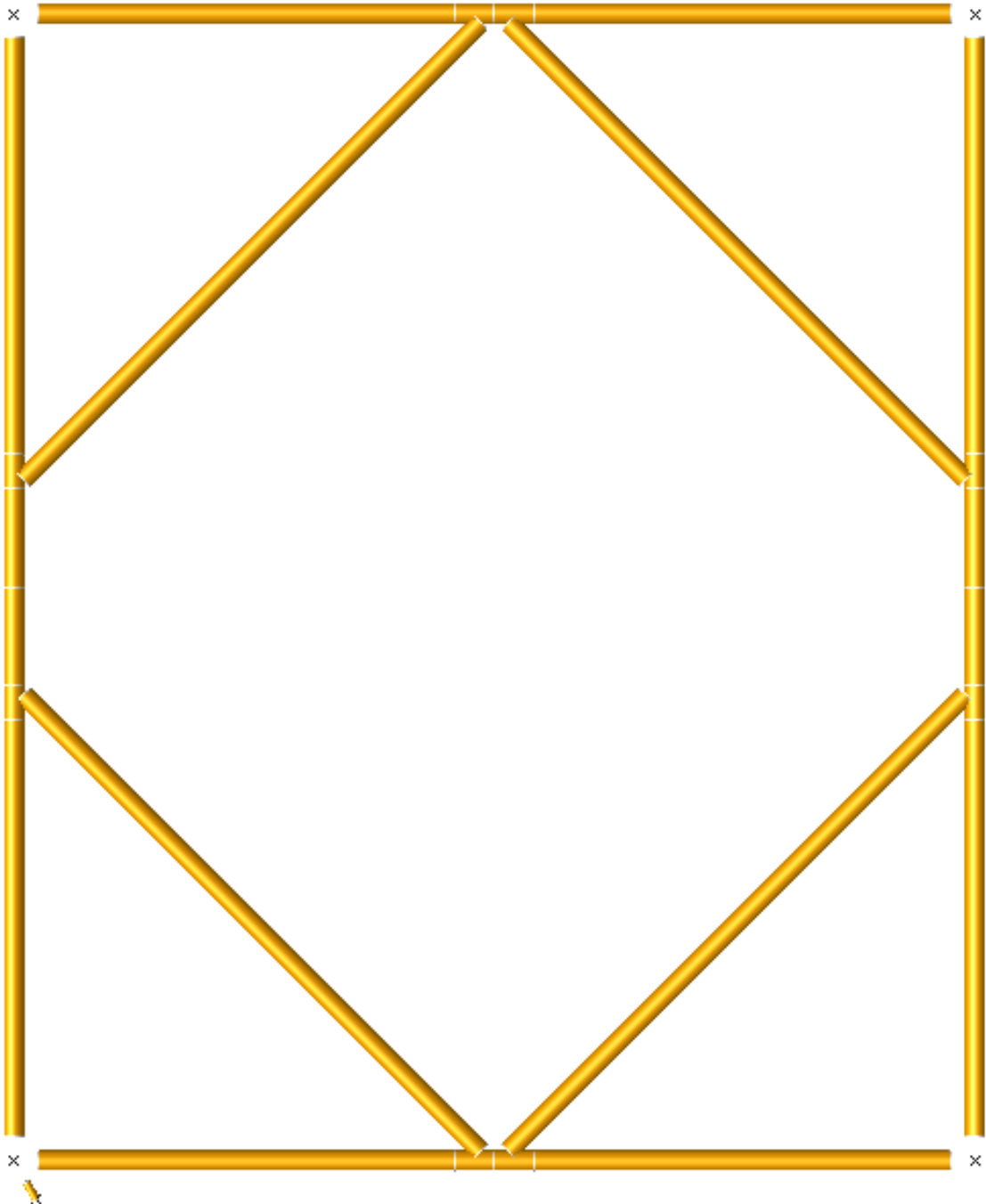
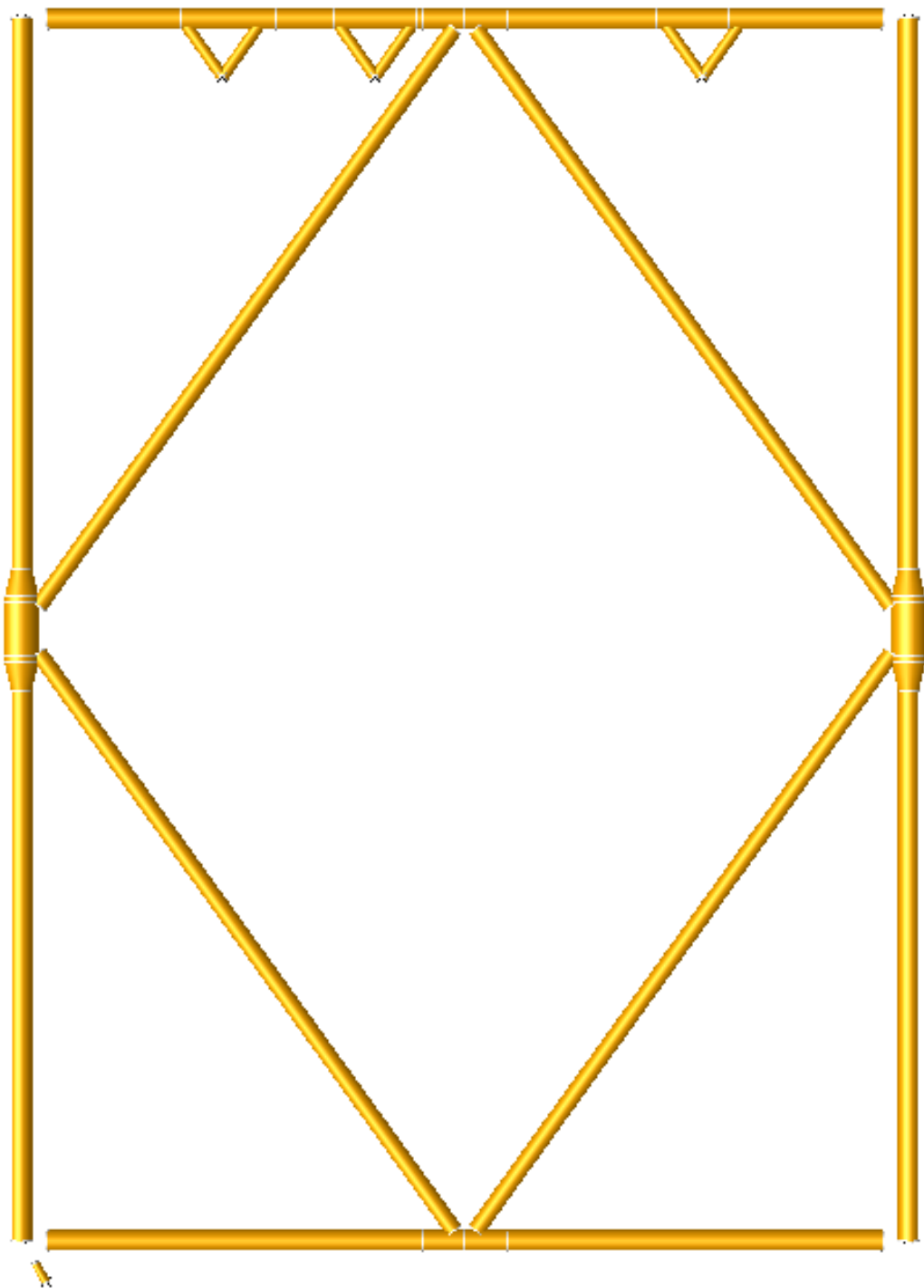


Figure 3-5 Face Row 2



**Figure 3-6 Plan at -41.285**





**Figure 3-7 Plan at -25.3**

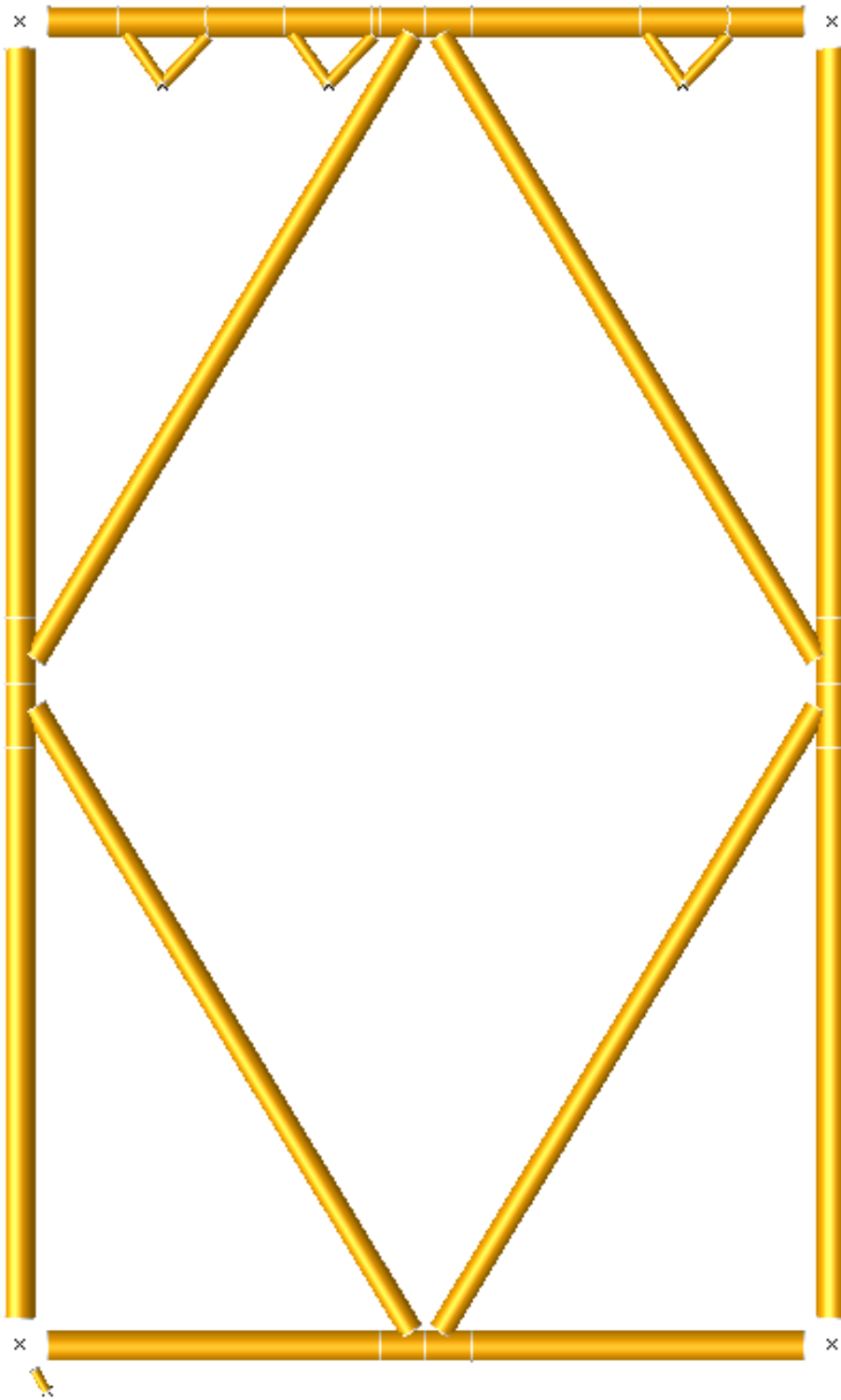


Figure 3-8 Plan at -9.0

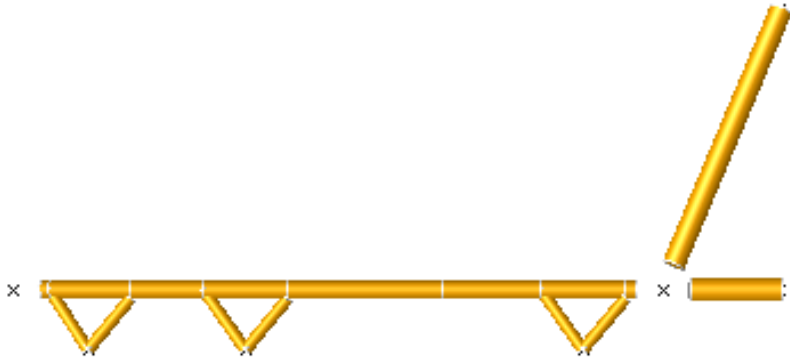


Figure 3-9 Plan at 5.0

The space frame structure consists of beam elements and the member intersections are modelled such that the resulting nominal member end stresses are consistent with their subsequent use in the fatigue analysis. In this regard, nominal brace stresses are normally computed at the intersections of the brace and chord centrelines except for large diameter chords or short braces. Later, more refined modelling is considered at the local joint geometry by offsetting the brace member to the face of the chord.

The model does not account for stress raising effects due to geometric discontinuity of the welded joints. However, these effects are incorporated using *Stress Concentration Factor (SCF)*. The design hot-spot SCF can be obtained by the finite element method, by parametric equations or from standard references.

The mass model includes all structural elements, miscellaneous attachments, marine growth, entrapped water and added mass using a consistent mass model to incorporate local dynamic response for fatigue assessment. For stiffness modelling, half of the corrosion allowance is considered when determining the wall thickness of members to represent the average condition during the life of the member. Main characteristics of this jacket and environmental data are listed in Table 3-1.

**Table 3-1 Platform General Data**

Jacket dimension at mud line (EL -41.3 m)	30.15 (m) × 36 (m)
Jacket dimension at work point (EL 7.3 m)	18 (m) × 36 (m)
Upper Deck dimension at EL 35.5 m	41.2 (m) × 23.2 (m)
Lower Deck dimension at EL 13.3 m	51.6 (m) × 23.2 (m)
Topside Operating Weight	1140 (MT)
Water Depth	42.72 m

The fixed jacket platform considered is supported by four legs. The analysis is performed for a water depth of 42.72 m corresponding to Mean Sea Level (MSL). The wave scatter diagram is used to represent the long-term statistics of the sea-state. The effect of wave frequency on wave loading and structural response is accounted through the use of hot spot stress transfer functions. The platform has four topside levels with a topside operating weight of 1,140 tones. The topside was installed using the *float over* method, so there are no braces at sea water level bay in the Y-direction and portal action is considered in this direction. The first two natural periods of the structure are 3.37 in the Y-direction and 1.90 in the X-direction, which are sway modes. The next mode is a torsional mode with a natural period of 1.37 seconds.

Frequency domain methods are generally applied to linear models; therefore, linearization of the foundation stiffness is performed at a suitable response level such that the foundation deflections and rotations are correctly reflected using the centre of fatigue damage sea-state. This will yield a lower response level compared to extreme sea-state and a correspondingly stiffer foundation, which is appropriate for fatigue analysis. For this purpose, a pile super element (pile stub) is developed within the pile solution module of SACS that yields the same deflections and rotations as the soil-pile system. Two files are used for the pile analysis, including structural input file and the PSI input file (refer to A.7).

Soil behaviour is simulated in the PSI input file by using the lateral and axial soil resistance deflection data (T-Z, P-Y, Q-Z) of the soil strata along the length (67.5 m) of the pile. The cyclic P-Y curve is used to properly simulate cyclic laterally loaded pile behaviour. Hence, the effect of cyclic loading on soil stiffness is considered in the assessment. The pile stub has the same properties as the pile (1.37 m diameter, 0.05 m thickness), but the relative equivalent length is much smaller and ranges from “ $4D$ ” to “ $10D$ ”, where “ $D$ ” is the pile diameter (1.37 m).

Non-linear behaviour of a piled foundation arises from non-linear characteristics of the soil, finite deflection of the pile (P- $\delta$  effect) and yielding in the pile. The nonlinear functions that define the cyclic soil behaviour vary from quasi-elastic at deep regions to strongly non-linear curves near the mud-line, which exhibits a complex plastic behaviour. Therefore, only the first soil layers are remarkably non-linear (Lima, 1985).

Due to non-linear behaviour of the pile-soil system, the structure-foundation stiffness is a function of displacement. In a linear analysis, the structural stiffness matrix is based on the undeformed structure and does not change as the structure deforms. However, due to the non-linearity involved, the stiffness matrix for the deformed shape cannot be determined until the deformed shape is obtained. The deformed shape, in turn, cannot be found until the stiffness matrix is found. Iterative methods have proven to be useful for solving this type of problems.

The soil-structure interaction considered in the research subject combines a linear analysis of the structure with a non-linear analysis of the piled foundation. The piles are represented by a linear or beam-column formulation and the non-linear soil (T-Z, P-Y and Q-Z curves) by piecewise linear springs at the *decoupling point* at the leg base; where there is no coupling between rotations and translations. This soil model implies a hysterical behaviour of the soil-structure interaction (Karunakaran, 1995). The solution involves "condensation" of the structural stiffness matrix to connection nodes at the pile heads, a non-linear iterative solution

of the foundation and structure to determine the pile head displacements and back-substitution of these displacements into the reduced equations of the structure to determine the displacements throughout the structure.

The process of condensation involves reducing the linear structure above the pile-head joints and loads to an equivalent linear stiffness matrix involving only the pile-head degrees of freedom and a set of forces applied to those degrees of freedom. Both the finite difference and finite element methods are used in offshore structural analysis programs to incorporate piled foundations characteristics.

A structure's dynamic behaviour is significantly affected by the soil characteristics and the pile-soil interaction. Since the natural period(s) of the structure is highly affected by the foundation stiffness, upper and lower bound foundation stiffness values are examined to avoid coincident of theoretical natural period with the cancellation point on the transfer function, which suppress the dynamic effects. Fatigue Demand is stated in terms of stress ranges that are produced by the variable loads imposed on the structure. This will require an appropriate structural analysis with due consideration of the boundary conditions (i.e. soil-structure interaction). It is now generally accepted that soil-foundation interaction is important and should be taken into account when calculating the response of the system. How important it is will depend on the particular soil and structure under consideration (Brebbia and Walker, 1979).

Analytical representations of the fluid-structure interaction are complicated due to the drag term and free surface effects. However, it is possible to approximate the influence of non-linear wave actions on the calculated stresses by an appropriate selection of the wave height input and suitable linearization of the results (ISO19902, 2007).

The modelling of the structure presents modest difficulties in comparison with an adequate description of the sea and the soil. Since prediction of structural safety and serviceability is the objective of the analysis, the structural response is of primary concern with due consideration of surrounding media, sea and soil. The thesis is a state of art report, describing a modelling that reflects present knowledge of physical properties, computational capabilities and economical restraints.

## 3.2 The basics of random process

For a zero-mean Gaussian process the spectral method is performed in the frequency domain analysis using structural transfer functions with appropriate spectral density functions (wave spectrum) to obtain the response spectrum and its statistical properties such as the standard deviation, zero-crossing period, etc. The frequency response function  $H(\omega)$  gives the steady state response of a system to a sine wave input. By measuring  $H(\omega)$  for all frequencies, we completely define the dynamic characteristics of the system. The need for measuring the dynamic characteristics of a system by monitoring its response to a random input signal arises from the idea that if these characteristics are known, then the operating conditions of the system can be optimized, so it runs at peak performance (Newland, 2012).

Spectral analysis is a practical method that is best able to represent the random nature of the wave environment and explicitly accounts for the influence of the frequency of excitation (the wave frequency) on actions as well as on the structural response. The method is applicable only to a linear system subjected to random excitation with simple form of input—output relations for spectral density. However, by suitable linearization of non-linear elements in the problem formulation (principally the drag term and wave surface effects around the still water level), this formal constraint can be adequately overcome as it is based on superimposition of many individual frequency components only applied in the analyses of moderate environmental conditions (i.e. fatigue analysis) where linearization gives satisfactory results. In a moderate environment (stationary random process), the statistical characteristics of the random sea does not change with time due to the existence of short periods. Therefore, we can obtain the probability density function for a random process  $p(x)$  during the time interval  $T$  as presented in Equation 3-1.

$$P(x)dx = \frac{(dt_1 + dt_2 + dt_3 + \dots)}{T} = \frac{\sum dt}{T} \quad \text{Equation 3-1}$$

If  $x$  is a random variable with a mean value of  $E[x]$  and standard deviation of  $\sigma$ , the variance,  $\sigma^2$ , is as defined in Equation 3-2.

$$\sigma^2 = E[(x - E[x])^2] = E[x^2] - (E[x])^2 \quad \text{Equation 3-2}$$

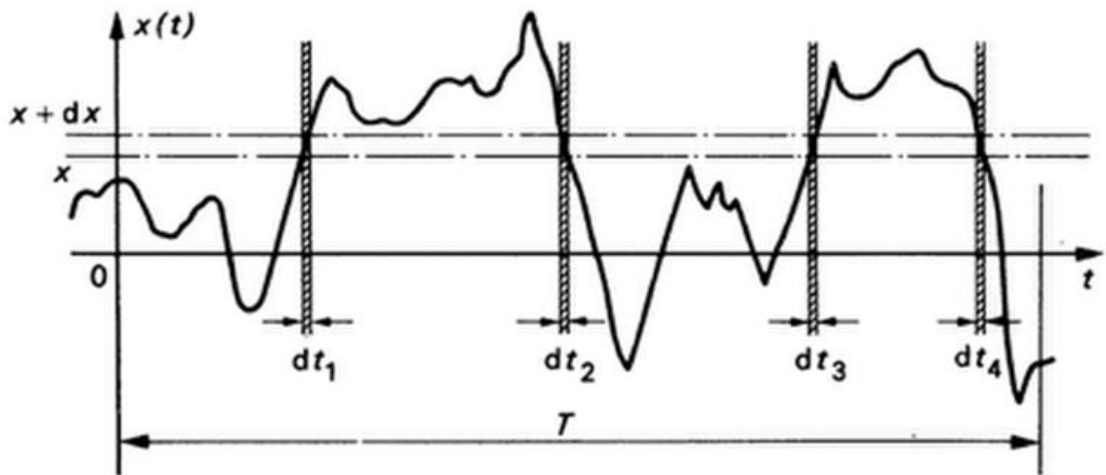


Figure 3-10 Probability density function  $p(x)$  for a random process

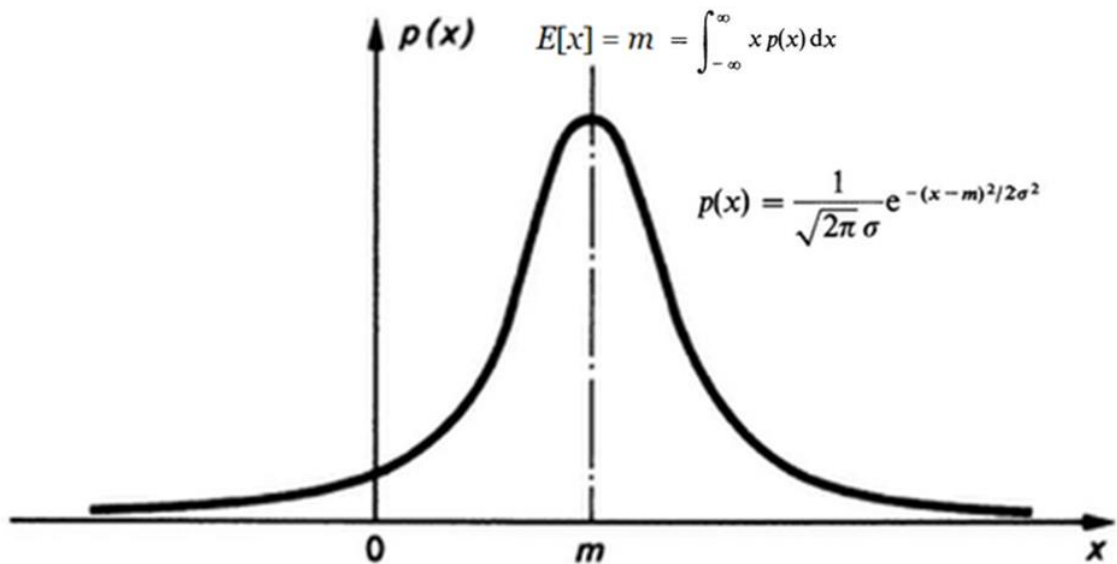


Figure 3-11 First-order probability density for a normal (or Gaussian) process

Random variables of  $x$  and  $y$  with mean values of  $m_x$  and  $m_y$  are statistically independent (non-correlated) if the normalized covariance  $\rho_{xy}$  (correlation coefficient) as defined in Equation 3-3 is zero.

$$\rho_{xy} = \frac{E[(x - m_x)(y - m_y)]}{\sigma_x \sigma_y} \quad \text{Equation 3-3}$$

The probability distribution function is used to describe the distribution of values of a random variable, and defined in Equation 3-4 as the shaded area under the probability density curve.



$$P(x) = \int_{-\infty}^x p(x)dx \quad \text{Equation 3-4}$$

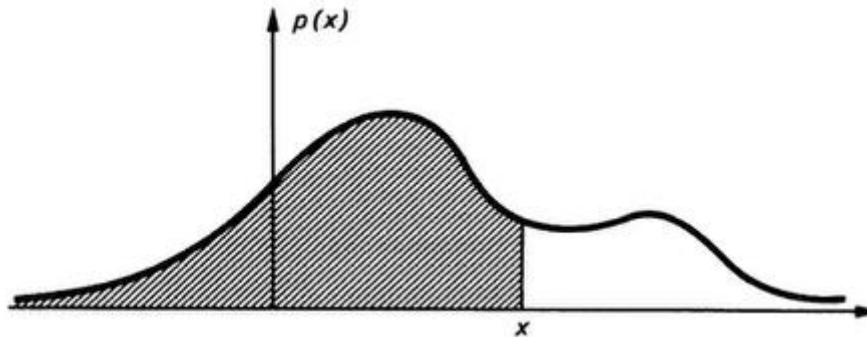


**Figure 3-12 Probability density function**

The first-order probability density function  $p(x)$  determines the probability  $p(x)dx$  that a random variable exists in the range of values  $x$  to  $x + dx$ . The second-order probability density function  $p(x, y)$  is obtained with an additional random variable  $y$ , refer to Figure 3-13.

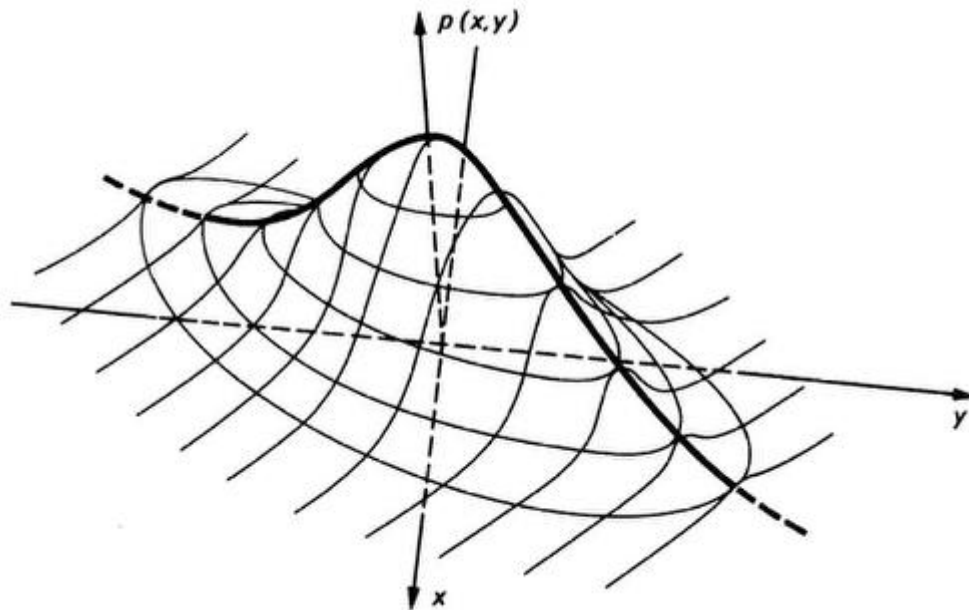


**Figure 3-13 Typical second-order or joint probability density function  $p(x, y)$**

In stationary random process, the first order probability distributions do not depend on absolute time, but the higher order probability distributions depend on the time separation between measuring points ( $\tau$ ).

The autocorrelation function  $R_x(\tau)$  for a random process  $x(t)$  is obtained as the mean value of the product  $x(t) \times x(t + \tau)$ . For a stationary process,  $R_x(\tau)$  depends only on the separation time  $\tau$  and not on the absolute time  $t$ , so  $R_x(\tau)$  is an even function of  $\tau$  as shown in Equation 3-5.

$$R_x(\tau) = E[x(t) \times x(t + \tau)] = E[x(t) \times x(t - \tau)] = R_x(-\tau) \quad \text{Equation 3-5}$$

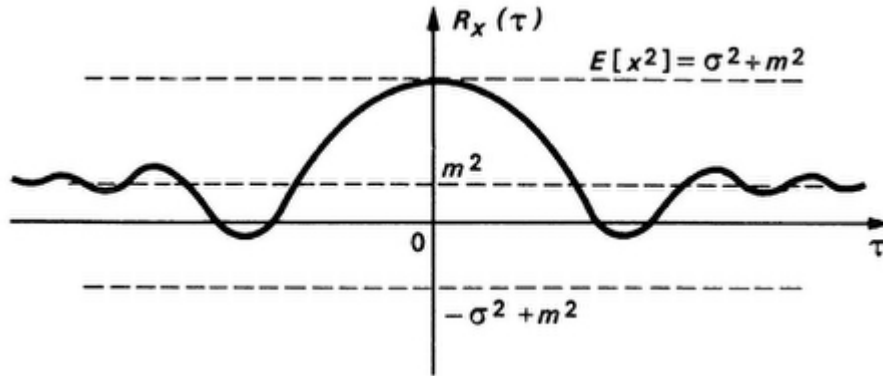


**Figure 3-14 Autocorrelation function  $R_x(\tau)$  of a stationary random process  $x(t)$**

The process would decay to zero in amplitude if the zero value of the random process  $x(t)$  is normalized, so the average value of the process  $m = E[x]$  is zero. Therefore, the Fourier transform of  $R_x(\tau)$  and its inverse are respectively given by Equation 3-6 and Equation 3-7.

$$S_x(\omega) = \frac{1}{2\pi} \int_{-\infty}^{\infty} R_x(\tau) e^{-i\omega\tau} d\tau \quad \text{Equation 3-6}$$

$$R_x(\tau) = \int_{-\infty}^{\infty} S_x(\omega) e^{i\omega\tau} d\omega \quad \text{Equation 3-7}$$

Where  $S_x(\omega)$  is the spectral density of the  $x$  process and is a function of angular frequency  $\omega$ .

When  $\tau = 0$ , the average square value of a stationary random process  $x$  is given by the area under a graph of spectral density  $S_x(\omega)$  against  $\omega$ , refer to Figure 3-15.

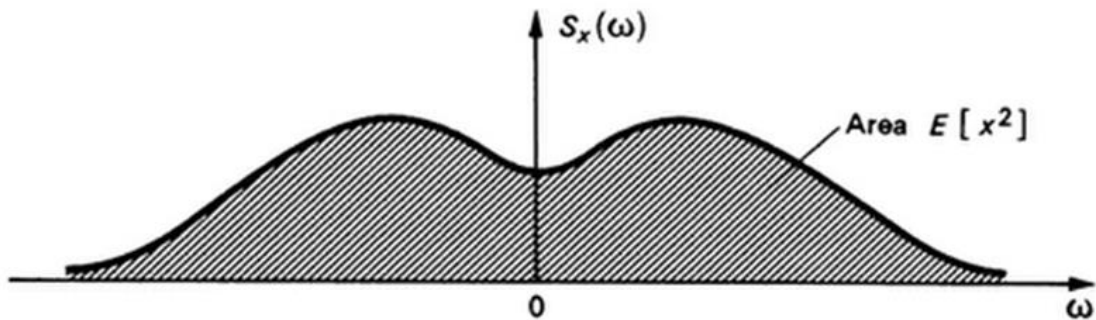


**Figure 3-15 spectral density curve for zero mean stationary process when  $\tau = 0$**

Here below are examples of narrow band and broad band processes.

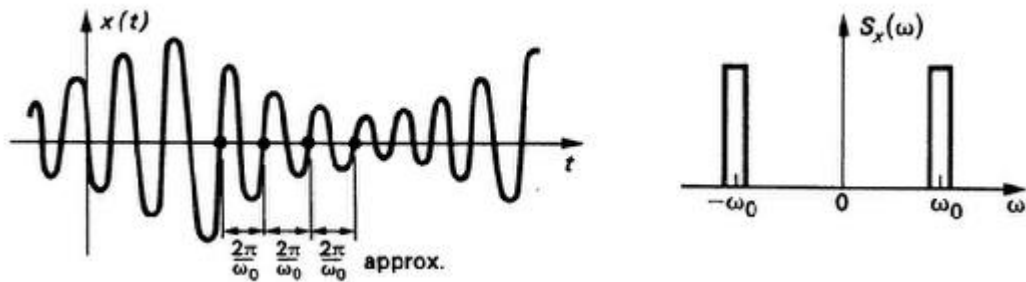


**Figure 3-16 Narrow band process**



**Figure 3-17 broad band process**

The cross correlation functions between two different stationary random functions of time  $x(t)$  and  $y(t)$  are obtained as the average value of the product  $x(t)y(t + \tau)$ , refer to Equation 3-8. Normally there is no correlation between  $x$  and  $y$  when the time separation  $\tau$  is very large and maximum correlation exists when  $\tau = \tau_0$ , as shown in Figure 3-18. Unlike the autocorrelation function, cross-correlation function is not even in  $\tau$ .

$$R_{xy}(\tau) = E[x(t)y(t + \tau)] = R_{yx}(-\tau) \quad \text{Equation 3-8}$$

The cross spectral density of a pair of random processes is defined as the Fourier transform of the subsequent cross correlation function for the two processes in Equation 3-9.

$$S_{xy}(\omega) = \frac{1}{2\pi} \int_{-\infty}^{\infty} R_{xy}(\tau) e^{-i\omega\tau} d\tau \quad \text{Equation 3-9}$$

And its inverse transform is given in Equation 3-10

$$R_{xy}(\tau) = \int_{-\infty}^{\infty} S_{xy}(\omega) e^{i\omega\tau} d\omega \quad \text{Equation 3-10}$$

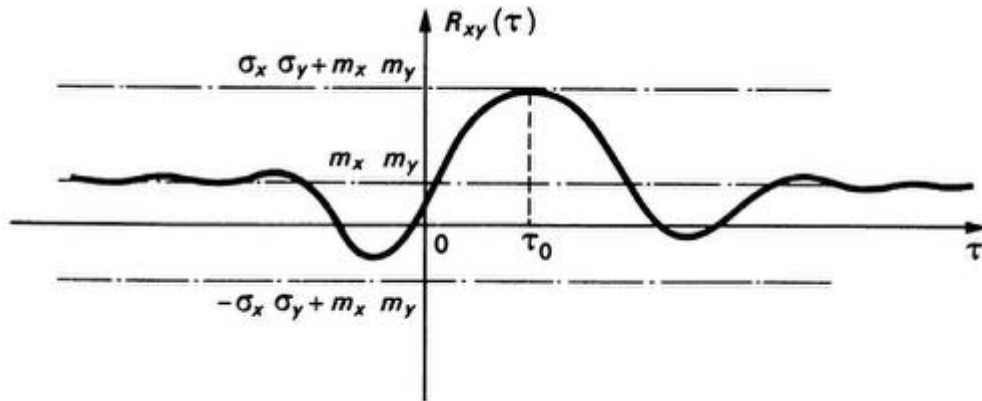


**Figure 3-18 Cross-correlation function  $R_{xy}(\tau)$  of stationary processes  $x(t)$  and  $y(t)$**

Cross spectral density  $S_{xy}(\omega)$  and  $S_{yx}(\omega)$  are similar but the sign of their imaginary parts is reversed. Therefore,  $S_{yx}(\omega)$  is the complex conjugate of  $S_{xy}(\omega)$ , refer to Equation 3-11.

$$S_{yx}(\omega) = S_{xy}^*(\omega) \quad \text{Equation 3-11}$$

Using the principle of superposition for linear vibrating systems (which does not change its characteristics with time), we can simplify the system so that the response to each input variable could be considered separately.

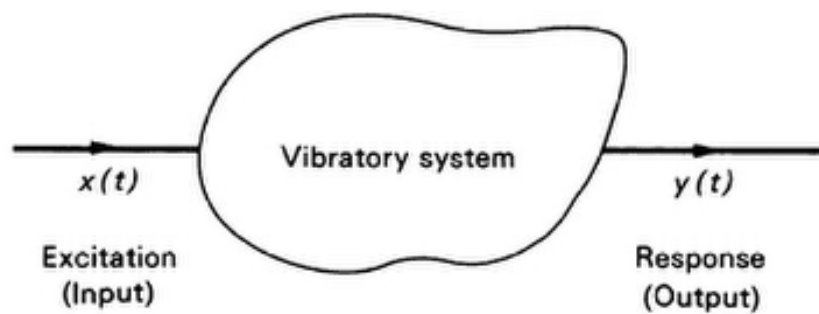


**Figure 3-19 Excitation and response parameters of a linear system**

If the input is a constant amplitude sine wave of fixed frequency (Equation 3-12), the steady state output will be as given in Equation 3-13.

$$x(t) = x_0 \sin \omega t \quad \text{Equation 3-12}$$

$$y(t) = y_0 \sin(\omega t - \phi) \quad \text{Equation 3-13}$$

The transfer function (transmission characteristics) of the system is then defined by evaluating the amplitude ratio  $y_0/x_0$  and the phase angle  $\phi$  at a series of closely spaced frequencies. If the frequency range extends from zero to infinity, then the frequency response characteristics of the system are theoretically defined as illustrated below for a linear spring-damper system.

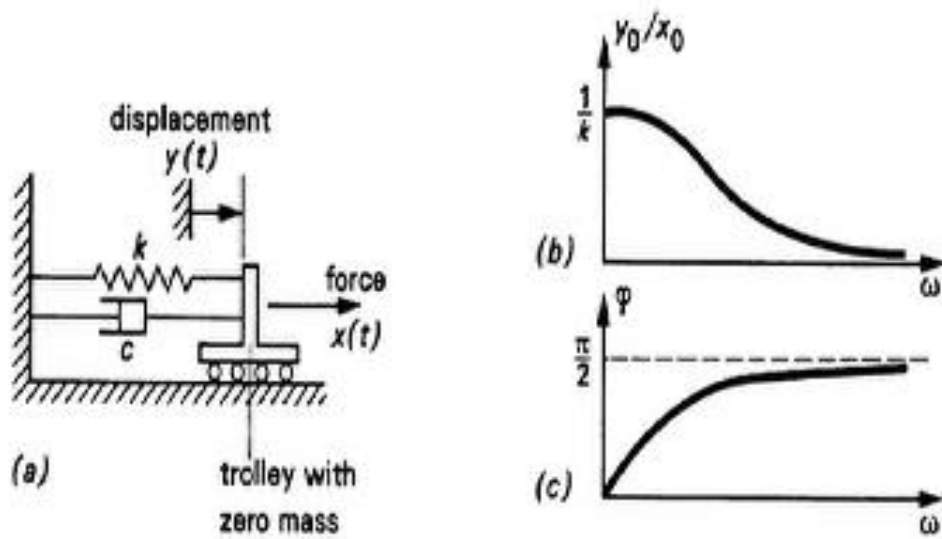


**Figure 3-20 Frequency response characteristics for a simple system**

The equation of motion for a linear spring of stiffness  $k$  and a linear viscous damper of coefficient  $c$ , is as follows:

$$ky + cy' = x(t) \quad \text{Equation 3-14}$$

Using the above equations, the amplitude ratio and phase angle are derived as respectively given in Equation 3-15 and Equation 3-16:

$$\frac{y_0}{x_0} = \frac{1}{\sqrt{(c^2 \omega^2 + k^2)}} \quad \text{Equation 3-15}$$

$$\phi = \tan^{-1} \frac{c\omega}{k} \quad \text{Equation 3-16}$$

It is conventional in vibration theory to represent the above quantities with a single complex number, which is called frequency response function  $H(\omega)$  as shown in Equation 3-17 and Equation 3-18.

$$H(\omega) = A(\omega) - iB(\omega) \quad \text{Equation 3-17}$$

$$|H(\omega)| = \sqrt{A^2 + B^2} = \frac{y_0}{x_0} ; \frac{B}{A} = \tan \phi \quad \text{Equation 3-18}$$

The frequency response function  $H(\omega)$  gives the steady state response of a system to a sine wave input. The dynamic characteristics of the system is completely define by measuring  $H(\omega)$  for all frequencies. Another method of defining a system's dynamic characteristics is to measure the transient response of an initially dormant system to an impulsive input. Refer to Figure 3-21 for a typical impulse response function. The unit impulse response function for the system shown in Figure 3-20(a) is illustrated in Figure 3-22.

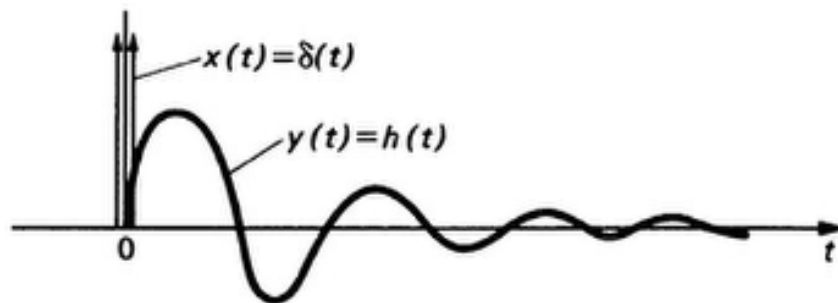


Figure 3-21 impulse response function

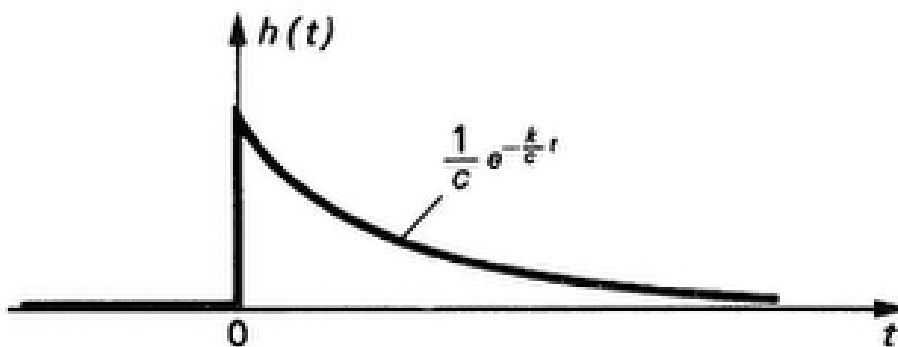


Figure 3-22 Unit impulse response function

If we take the Fourier transforms of both the impulsive input  $x(t) = \delta(t)$  and the transient output  $y(t) = h(t)$ , we obtain a very important relationship between the Fourier transforms of the input and output,  $X(\omega)$  and  $Y(\omega)$ , and the frequency response function  $H(\omega)$ , refer to Equation 3-19.

$$Y(\omega) = H(\omega)X(\omega) \quad \text{Equation 3-19}$$

A formal solution for the output  $y(t)$  is obtained in Equation 3-20, by taking the inverse transform of  $Y(\omega)$ , which is difficult to evaluate.

$$y(t) = \int_{-\infty}^{\infty} H(\omega) \left( \frac{1}{2\pi} \int_{-\infty}^{\infty} x(t) e^{-i\omega t} dt \right) e^{i\omega t} d\omega \quad \text{Equation 3-20}$$

However, by breaking down an arbitrary input  $x(t)$  into a series of impulses (refer to Figure 3-23), another formal solution for the response  $y(t)$  is obtained in Equation 3-20. This can be achieved using the principle of superposition for a passive linear system, which decays to static equilibrium.

$$y(t) = \int_{-\infty}^t h(t - \tau) x(\tau) d\tau \quad \text{Equation 3-21}$$

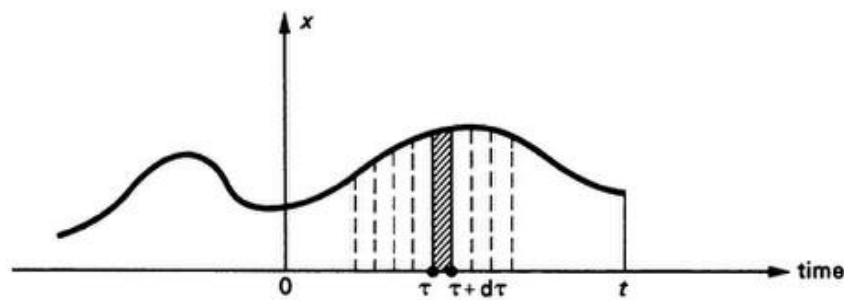


**Figure 3-23 Arbitrary input  $x(t)$**

The spectral density of the output process is derived by the Fourier transform of its autocorrelation function; refer to Equation 3-22.

$$S_y(\omega) = |H(\omega)|^2 S_x(\omega) \quad \text{Equation 3-22}$$

The mean response is obtained in Equation 3-23.

$$E[y^2] = \int_{-\infty}^{\infty} |H(\omega)|^2 S_x(\omega) d\omega \quad \text{Equation 3-23}$$

The cross spectral density between the input and output that obtained by the Fourier transform of its cross-correlation function is given in Equation 3-24.

$$S_{xy}(\omega) = H(\omega)S_x(\omega) = S_{xy}^* = H^*(\omega)S_x(\omega) \quad \text{Equation 3-24}$$

The output of a linear system subjected to Gaussian inputs is Gaussian and its probability distributions can be calculated if the respective mean values, variances and covariances (refer to Equation 3-3) are known. For non-Gaussian random processes, the theory becomes much more complicated. However, many naturally occurring random vibrations have the Gaussian probability distribution, refer to Figure 3-11. According to the central limit theorem, when a random process results from the summation of infinitely many random elementary events, then this process will tend to have Gaussian probability distributions. Furthermore, even when the excitation is non-Gaussian, a system's response may approximate to Gaussian if it is a narrow band response that is derived from a broad band excitation. The reason is because the convolution integral (Equation 3-20) may again be thought of as the limiting case of a linear sum of approximately independent random variables.

The characteristics of the excitation are modified by the response of the system. In most vibration problems, the system has at least one resonant frequency at which large amplitudes can be generated by small inputs. At other frequencies transmission is reduced and, at very high frequencies, the effective mass may be so high that the output is not measurable.

Since the output spectrum is confined to a narrow band of frequencies in the vicinity of the resonant frequency, the response  $y(t)$  is a narrow band random process and the typical time history of  $y(t)$  resembles a sine wave of varying amplitudes and phases, refer to Figure 3-24.

If the frequency response function has very sharp cut-offs above and below the resonant frequency (refer to Figure 3-25a), then its autocorrelation function is obtained from Equation 3-25.

$$R_y(\tau) = 4S_0 \frac{\sin(\frac{\Delta\omega\tau}{2})}{\tau} \cos \omega_0 \tau \quad \text{Equation 3-25}$$



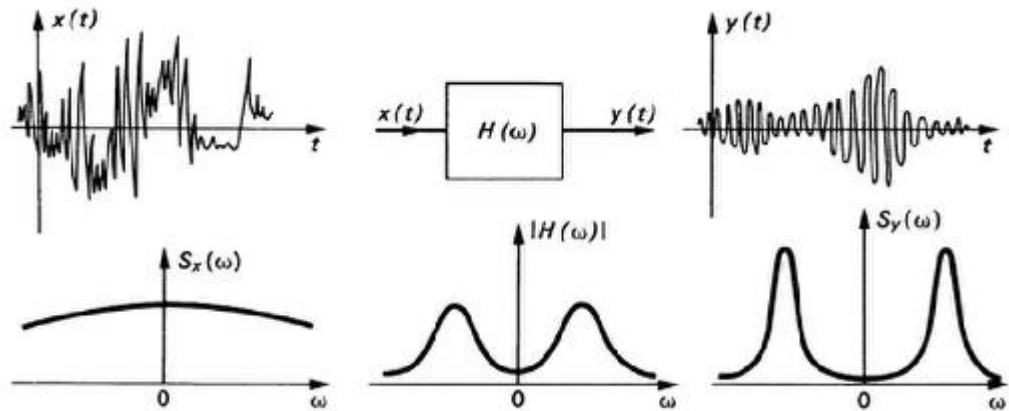


**Figure 3-24 Broad band noise transmission through resonant system**

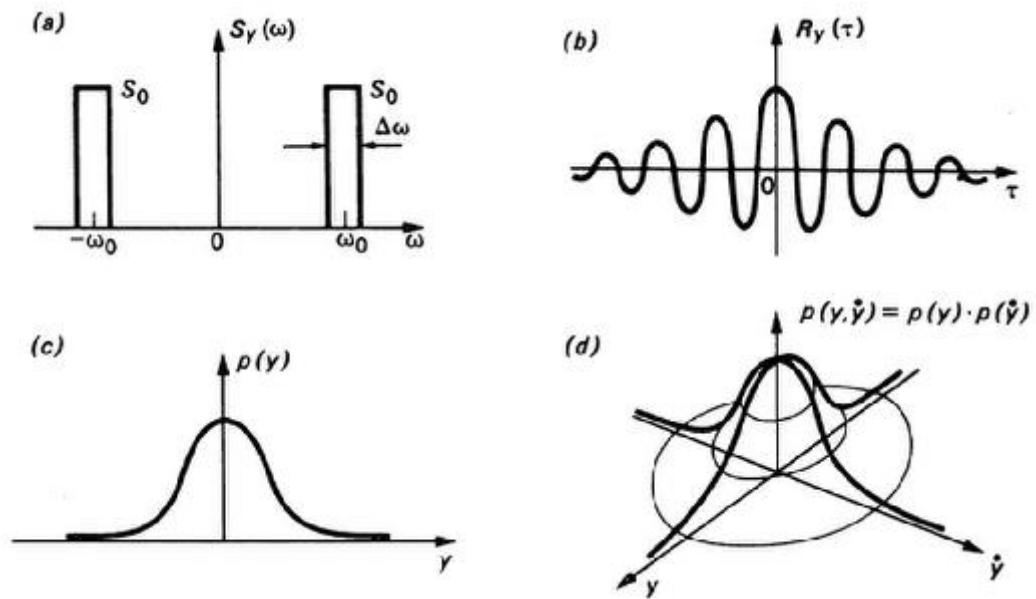


**Figure 3-25 stationary, Gaussian, narrow band process**

Provided that the excitation is Gaussian (refer to Figure 3-25c), then we can find the first order probability density function  $p(y)$  and the second order probability density function  $p(y, \dot{y})$  for the joint probability of  $y$  and its derivative  $\dot{y}$  from Equation 3-26 and Equation 3-27.

$$p(y) = \frac{1}{\sqrt{2\pi}\sigma_y} e^{\frac{-y^2}{2\sigma_y^2}} \quad \text{Equation 3-26}$$

$$p(y, \dot{y}) = \frac{1}{2\pi\sigma_y\sigma_{\dot{y}}} e^{-\frac{1}{2}\left(\frac{y^2}{\sigma_y^2} + \frac{\dot{y}^2}{\sigma_{\dot{y}}^2}\right)} = p(y)p(\dot{y}) \quad \text{Equation 3-27}$$

we need to know the frequency of crossings  $y = a$  to obtain the probability distribution of peaks, refer to Figure 3-26.

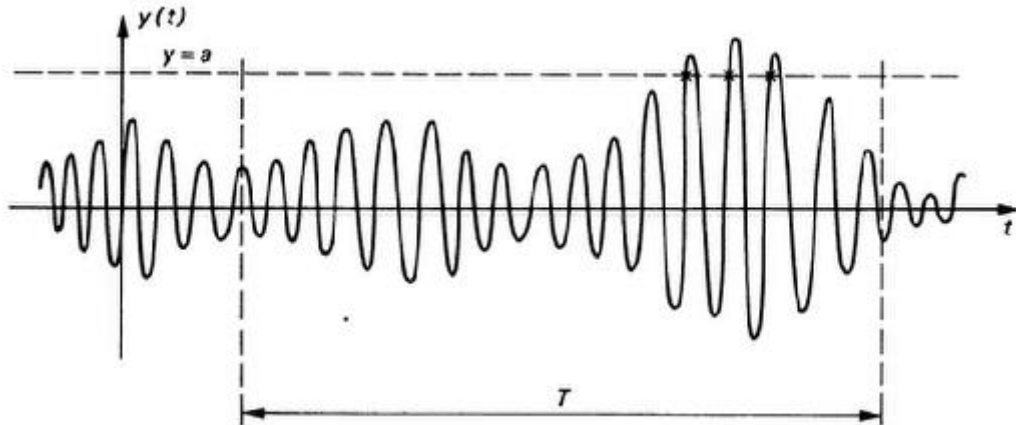


**Figure 3-26 Narrow band process**

For a stationary process, the average number of crossings is proportional to the time interval  $T$ , refer to Equation 3-28.

$$N_a^+(T) = v_a^+ T \quad \text{Equation 3-28}$$

Where  $v_a^+$  is the average frequency of crossing  $y = a$ .

$v_0$  is the average frequency for the process.

There will be a positive slope crossing of  $y = a$  in the next time interval  $dt$  if, at time  $t$ ,

$$y < a \text{ and } \frac{dy}{dt} > \frac{a - y}{dt}$$

In other words, if the values of  $y$  and  $\dot{y}$  lie within this shaded wedge (refer to Figure 3-27 b), then there will be a positive slope crossing of  $y = a$  in time  $dt$ . The probability that they do lie in the shaded wedge can be obtained from the joint probability density function  $p(y, \dot{y})$  and is just the shaded volume shown in Figure 3-27 a; i.e., the volume under the probability surface above the shaded wedge of acceptable values of  $y$  and  $\dot{y}$  as given below.

$$\text{Prob}\left(\begin{array}{l} \text{positive slope crossing} \\ \text{of } y=a \text{ in time } dt \end{array}\right) = \iint p(y, \dot{y}) dy d\dot{y} \quad \text{Equation 3-29}$$

Furthermore, the frequency parameter in terms of the joint probability density function is derived from Equation 3-30.

$$v_a^+ = \int_0^\infty p(a, \dot{y}) \dot{y} d\dot{y} \quad \text{Equation 3-30}$$

For a Gaussian process:

$$v_a^+ = \frac{\sigma_{\dot{y}}}{2\pi\sigma_y} e^{-a^2/2\sigma_y^2} \quad \text{Equation 3-31}$$

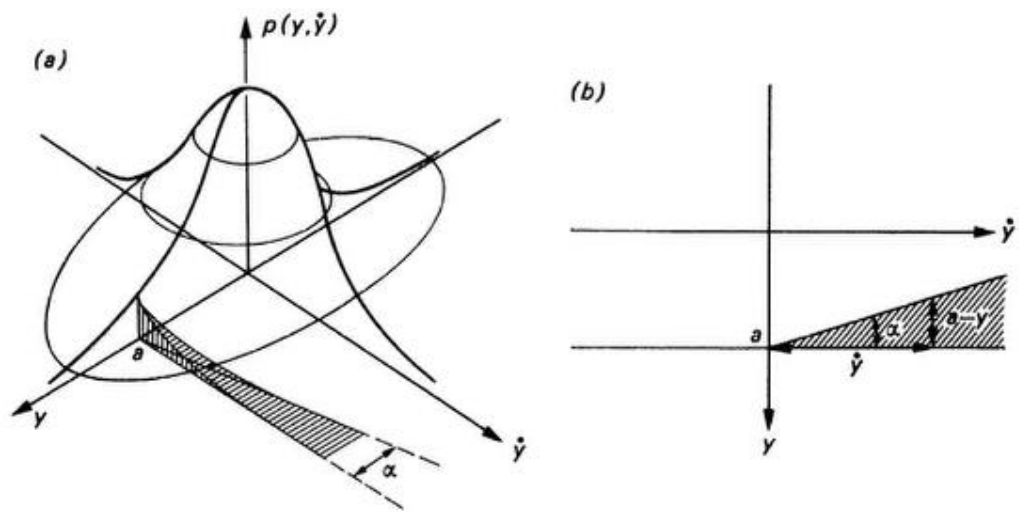


**Figure 3-27 Probability of crossing  $y= a$**

The probability that the magnitude of a peak, chosen at random, lies in the range  $a$  to  $a + da$ , is  $p_p(a)da$  (refer to Figure 3-28).

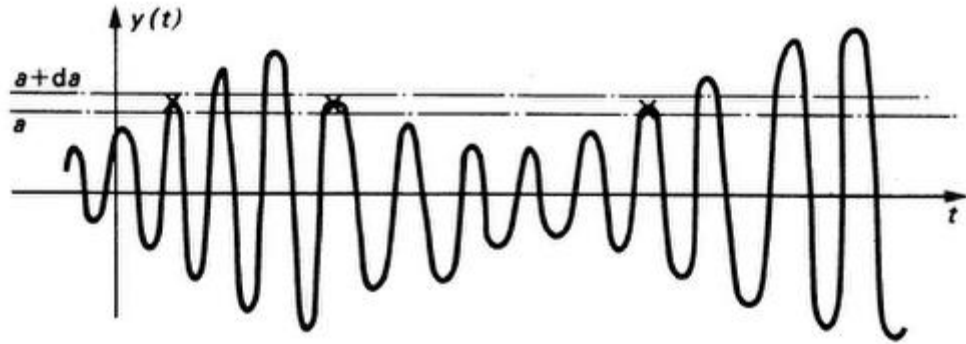


**Figure 3-28 Identification of peaks in the band  $y = a$  to  $y = a + da$**

The probability that any peak is greater than  $a$  is

$$\int_a^{\infty} p_p(a) da = \frac{v_a^+}{v_0^+} \quad \text{Equation 3-32}$$

Therefore, the probability density function for the occurrence of peaks is derived in Equation 3-33, provided that this is a smooth narrow band process with each cycle crossing the mean level  $y=0$ , so all the maxima occur above  $y=0$  and all the minima occur below  $y=0$ .

$$-p_p(a) = \frac{1}{v_0^+} \frac{d}{da} (v_a^+) \quad \text{Equation 3-33}$$

If  $y(t)$  is Gaussian, then the probability density of peaks will have a Rayleigh distribution as given in Equation 3-34 and shown in Figure 3-29.

$$p_p(a) = \frac{a}{\sigma_y^2} e^{-a^2/2\sigma_y^2} \quad 0 \leq a \leq \infty \quad \text{Equation 3-34}$$

The function  $p_p(a)$  has its maximum value at  $a = \sigma_y$ , which is the standard deviation of the  $y$  process. It is clear from Figure 3-29 that the majority of peaks are about this magnitude. The probability that any peak, chosen at random, exceeds  $a$  is,

$$\text{Prob}(\text{peak value exceeds } a) = e^{-a^2/2\sigma_y^2} \quad \text{Equation 3-35}$$

Our analysis of peaks that leads to the Rayleigh distribution for a Gaussian process is based on the assumption that the narrow band process  $y(t)$  resembles a sine wave of varying amplitude and phase.

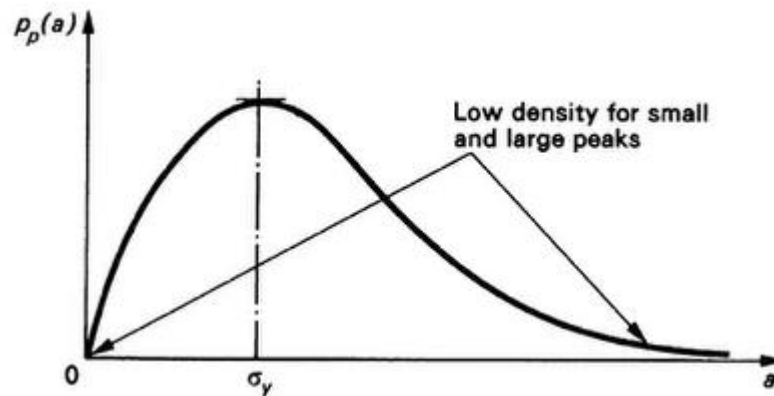


**Figure 3-29 Rayleigh distribution of peaks for a Gaussian narrow band process**

The existence of high frequency components in a more general narrow-band spectrum that is shown in Figure 3-30(a) introduces additional maxima in a narrow band process, which is illustrated in Figure 3-30(b). However, the Rayleigh distribution of peaks assumes only one maximum for each zero crossing, which means that irregularities in the smooth form of the sine wave approximation are not accepted.

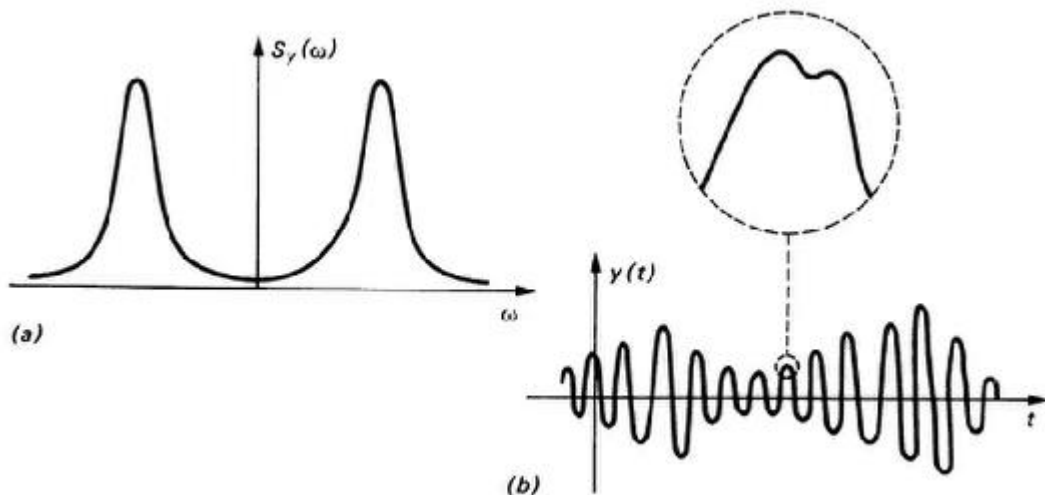


**Figure 3-30 irregularities in a narrow band process**

The above discussion was to clarify the basic mathematical theory of random process. The practical aspect of the subject involves experimental measurements with emphasis on measuring the spectral density of a random process or the cross-spectral density between two random processes. The spectral measurement is of prime importance since it simplifies the input-output relations for spectral density of a linear system subjected to random excitation.

The schematic of a spectrum analyser is shown in Figure 3-31. The input signal  $x(t)$ , which is a sample function of an ergodic (and therefore stationary) random process, is filtered to a narrow-band filter. The filter centre frequency is based on the predominant frequencies present in a vibration signal. The filter theoretical frequency response is shown in Figure 3-31(b). The average output of the spectrum analyser is proportional to the spectral density of the input process at the filter centre frequency. The mean output level is therefore a direct measure of the input spectral density.

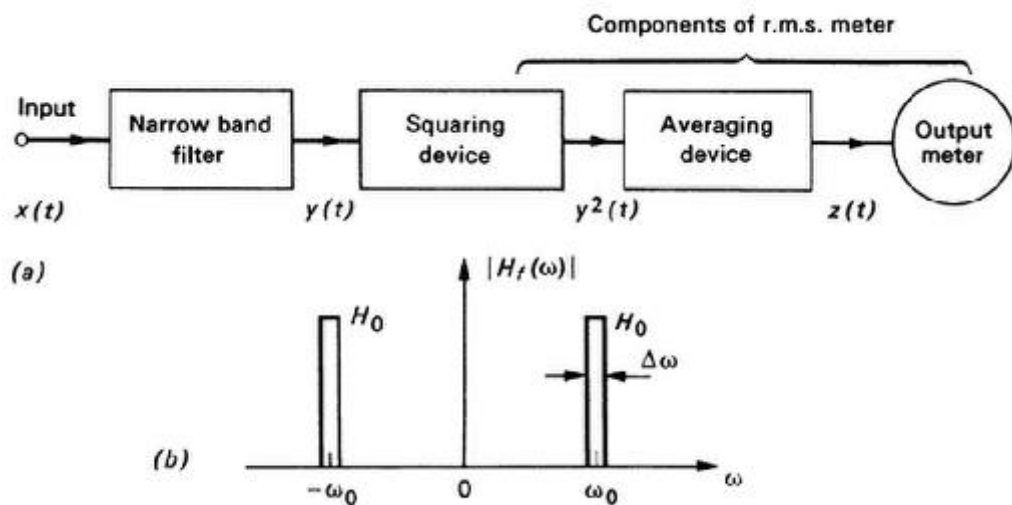


**Figure 3-31 Spectrum Analyser**

Selective filters are employed to transform time domain to frequency domain, which automatically reduce the effective bandwidth and therefore reduce the statistical reliability of the results that are obtained.

Until the late 1960s, Fourier transforms of correlation functions were employed to estimate spectra from measured data. By the advent of the fast Fourier transform (FFT), a computer algorithm for calculating discrete Fourier transforms (DFTs), spectral estimates are obtained directly from the original time series, which is quicker and more accurate. Furthermore, the most important development in signal analysis has been the wavelet transform. Unlike Fourier transforms that use sines and cosines as the basis functions for decomposing general signals, alternative families of orthogonal basis functions (wavelets) are employed in wavelet transforms.

Wavelet analysis provides an alternative way of breaking a signal down into its constituent parts overcoming the disadvantages of Fourier analysis where frequency information can only be extracted for the complete duration of a signal.

### 3.3 The applicability of the spectral method

The methodology used here is a frequency domain analysis using spectral density functions and the transfer function approach to model the response spectrum. The global structural analysis is carried out in the frequency domain with stochastic linearization for nonlinear forces and damping. Direct frequency response analysis for modal analysis is applied to determine the transfer functions. For simplicity, the model for short crested sea has been left out.

Ocean waves are the source of the fatigue inducing stress range acting on the structural system being analysed. The wave and current induced loads for a jacket type platform are likely to be drag dominated. This could be due to typical sizes of the submerged structural elements. Thus, methods based on linearized hydrodynamic loads should be used in a structural analysis. The spectral analysis method employed should reflect dynamic response characteristics of the structure in the fatigue assessment with due consideration of dynamic amplification.

Spectral based fatigue analysis technique is complex and numerically difficult to achieve. Since frequency domain formulation is based on probabilistic methods it will require the linearization of loads and structural response, so the superposition of stress range transfer functions from unit amplitude waves are considered valid.

The method is most applicable when there is a linear relationship between the wave height and the wave induced loads and the structural response to these loads is linear. This will require the existence of short periods during which wave statistics of the random sea may be assumed not to change (steady sea-states).

The main advantage of the spectral method in frequency domain analysis is that the computations are relatively efficient compared to time domain analysis methods (DNV, 2010). Other advantages are the successful use of wave power spectra to describe water surface elevation, the ease of handling nonlinear effects and the resulting solution being physically interpretable (Etube, 1999).

Determination of the frequency response function is the main task of spectral fatigue analysis. The frequency response function defines the relationship between the stresses at a specified structural location per unit wave height. For irregular waves, the sea-state is represented by a wave spectrum. The frequency domain method is well suited for systems exposed to random

wave environments, since the random response spectrum  $S_R(\omega)$  can be directly computed from the transfer function  $R(\omega)$  and the wave spectrum  $S_\eta(\omega)$  using the Equation 3-36.

$$S_R(\omega) = S_\eta(\omega)R^2(\omega) \quad \text{Equation 3-36}$$

Where  $\omega$  is angular frequency

Short term response statistics in each sea-state is determined with the assumption that the short term stress variation in a given sea-state is a random narrow banded stationary process. This will be the prerequisite to represent the short-term distribution of stress range by a Rayleigh distribution. Furthermore, the long-term response distribution can be obtained by accumulating the short term response statistics for all sea-states in the scatter diagram.

A spectral based fatigue assessment produce results in terms of fatigue induced damage or fatigue life using Miner's summation hypothesis, which is referred to as a direct method. This hypothesis applies for a narrow band process in which separate stress cycles can be identified, and suggests that if  $n_i$  cycles of stress occur at a level of stress at which  $N_i$  constant stress cycles would cause fracture, then the fractional damage done by the  $n_i$  cycles is  $n_i/N_i$ . Failure is to be expected when the sum of all the fractional damages is equal to one; i.e.,  $\Sigma(n_i/N_i)=1$ .

Fatigue damage is mostly associated with low or moderate seas; hence, confused short-crested sea conditions must be allowed. Confused short-crested seas result in a kinetic energy spread, which is modelled using the cosine-squared approach,  $(2/\pi) \cos^2\theta$ . Generally, cosine-squared spreading is assumed from +90 to -90 degrees on either side of the selected wave heading. Applying the wave spreading function modifies the spectral moment (ABS, 2010). However, for simplicity, the model for short crested sea has is ignored (Skjong, 1991). Although wave directionality and energy spreading generally reduce the structural response, their long term statistics are not yet commonly available (Kawamoto, 1982).

### 3.4 Uncertainty in the process

There is uncertainty involved in the evaluation of the response and its statistics. Wave forces and subsequent stresses involve certain nonlinear effects. The main source of uncertainty is the nonlinearity due to the drag term. Some potential errors when using a frequency domain analysis could be due to higher frequency harmonics in the wave force, underestimating wave forces in the wave crest when using linear kinematics up to the mean water level or nonlinear wave response on drag dominant structure.



The transfer function is no longer linear if it is dependent on the height of the regular wave that is selected. The evaluation of statistical extreme is more complex since the process is not Gaussian. In this regard, special care is required for wave height selection when generating the transfer function because the application of a spectral method requires a linear process to yield reasonable results with subsequent response calculations in view of the nonlinear nature of the drag forces (HSE, 2000).

In this context, linear means proportional to wave amplitude. It is assumed that the wave force on the structure is monotonic and that the responses are linear with wave height. Although this may not be the case, by suitable linearization it is still possible to use the powerful technique of spectral analysis with non-monotonic and nonlinear systems.

Fatigue in offshore structures is a typical high-cycle phenomenon, which is caused by many cycles with small stress ranges. A few extreme storms with return periods above one year are considered to be insignificant in fatigue damage. Consequently, the response of a structure in sea states with low wave heights and short wave periods (from the wave height of 0.3 m to the wave height corresponding to one year return period) is the response of interest in fatigue environment which linearization yields a good result.

### 3.5 Wave selection for transfer function

Wave selection should be considered based on the characteristics of the structure as well as the environment, so the transfer functions are adequately defined over the relevant frequency range. This range should include frequencies of sea-states with significant energy in the wave scatter diagram. High frequency cut-off should be considered for dynamic analysis.

An appropriate level of non-linear (drag) wave loading is introduced by proper selection of wave heights used for the transfer functions. Constant wave steepness is commonly used to provide a simple relationship between the wave height and frequency. The steepness is the ratio of wave height to wave length in the range of 1:15 to 1:25, which can be obtained by a suitable calibration process. The wave length is related to the frequency by the appropriate wave theory.

To accurately define the dynamic response peak, the natural frequency and three closely spaced frequencies on each side of the natural frequency should be included. Good definition of peaks and valleys of the transfer function can be verified on the base shear transfer function plot. The features of the frequency grid selection are shown in Figure 3-32 (repeat of Figure 1-2).

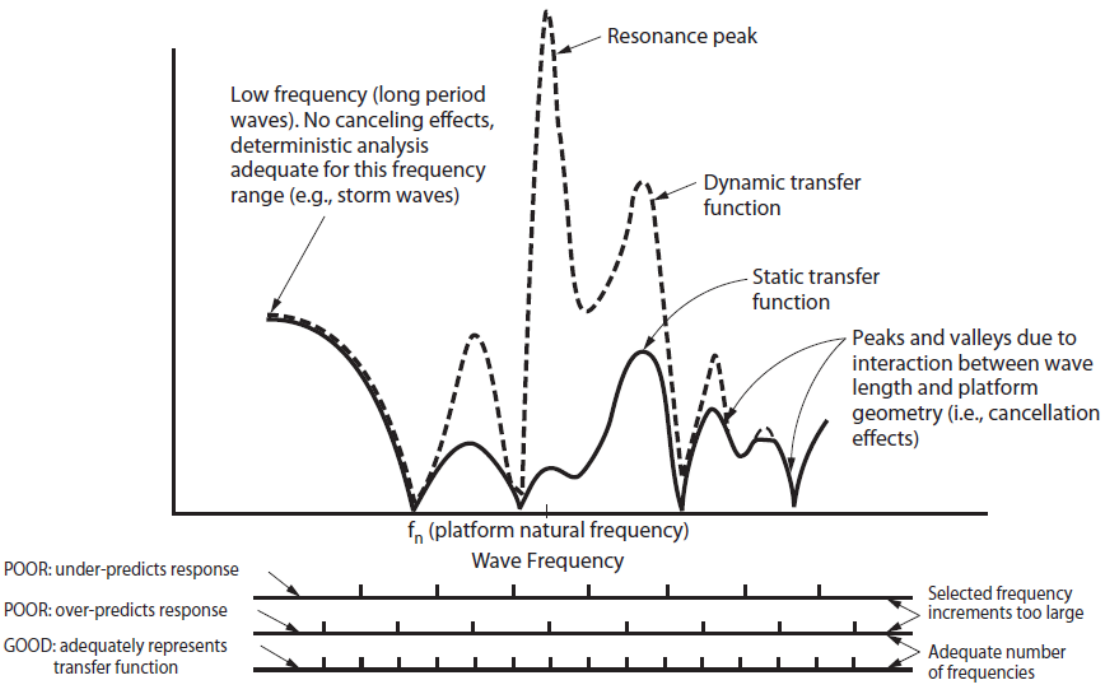


**Figure 3-32 Frequency grid selection**

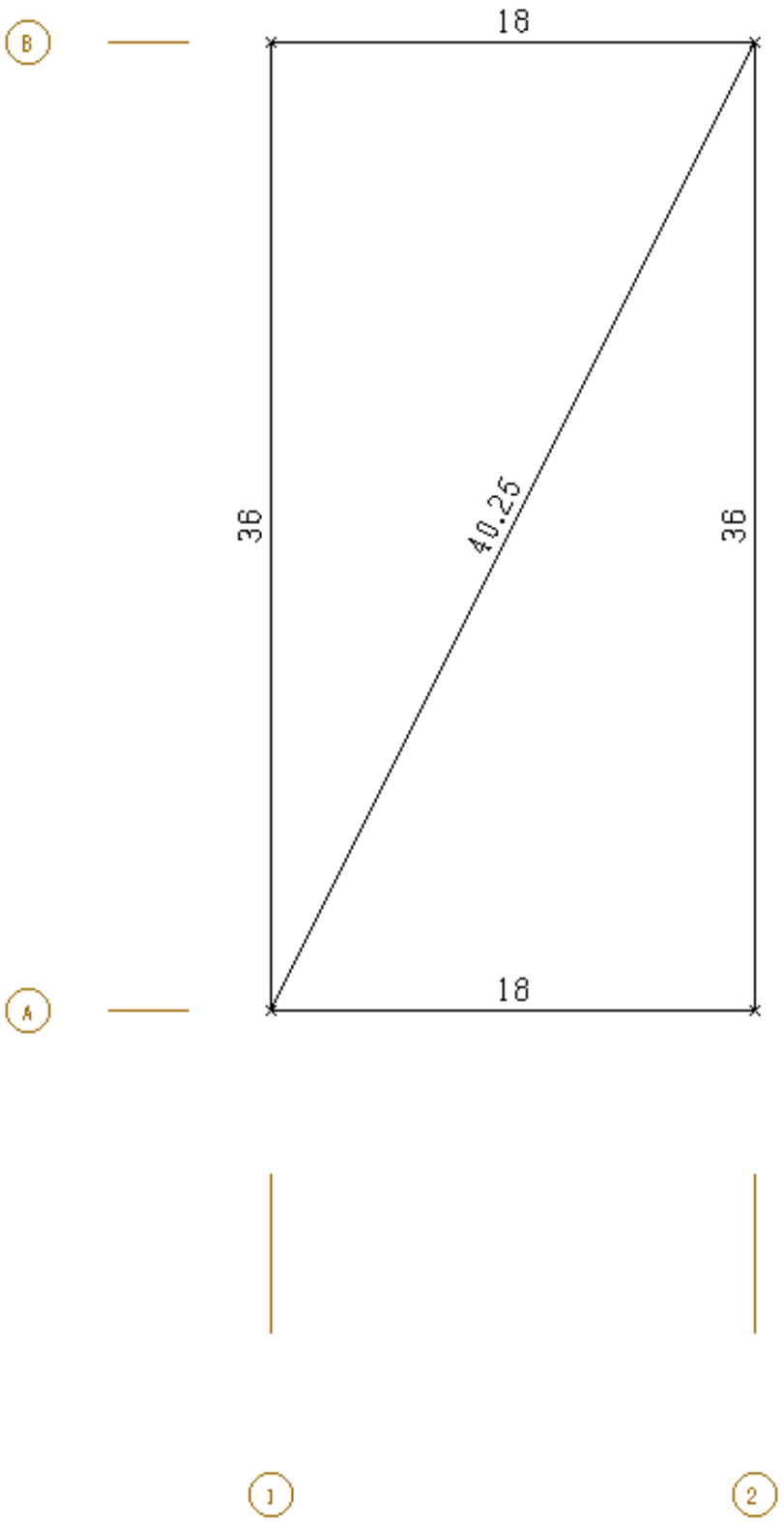


Figure 3-33 Leg spacing at Jacket work point (m)

**Table 3-2 First three modes of the structure**

Mode	Period (seconds)
1	3.372
2	1.901
3	1.374

**Table 3-3 Along Row A and B ( $d=18$  m)**

$n$	Enhancement wave		Cancellation wave	
	Period (sec)	Frequency (Hz)	Period (sec)	Frequency (Hz)
1	3.397	0.294	4.804	0.208
2	2.402	0.416	2.774	0.360
3	1.961	0.510	2.148	0.466

**Table 3-4 Along Row 1 and 2 ( $d = 36$ m)**

$n$	Enhancement wave		Cancellation wave	
	Period (sec)	Frequency (Hz)	Period (sec)	Frequency (Hz)
1	4.804	0.208	6.794	0.147
2	3.397	0.294	3.922	0.255
3	2.774	0.360	3.038	0.329

**Table 3-5 Along diagonal ( $d = 40.25$ )**

$n$	Enhancement wave		Cancellation wave	
	Period (sec)	Frequency (Hz)	Period (sec)	Frequency (Hz)
1	5.079	0.197	7.183	0.139
2	3.592	0.278	4.147	0.241
3	2.933	0.341	3.213	0.311

Wave cancelation and enhancement effects can be incorporated by selecting the wave frequencies in the vicinity of the troughs and peaks in the applied wave load transfer functions. These frequencies correspond to specific wave lengths as multiples or fractions of leg spacing.

Enhancement and cancelation wave periods ( $T_e$  and  $T_c$ ) correspond to wave lengths that are specific multiples or a fraction of key dimensions such as the main leg spacing, and are respectively given by Equation 3-37 and Equation 3-38.

$$T_e = \sqrt{d/1.56n} \quad \text{Equation 3-37}$$

$$T_c = \sqrt{d/1.56(n - 0.5)} \quad \text{Equation 3-38}$$

$d$ = leg spacing at jacket work point (m) as shown in Figure 3-33;  $n = 1, 2, 3$

Sufficient intermediate frequencies and selection of frequencies corresponding to peaks of the wave spectra included in the scatter diagram are required for accurate definition of wave input energy. The initial frequency grid is enhanced to include the first three modes of the structure (Table 3-2), enhancement/cancelation wave period (Table 3-3 to Table 3-5) and additional wave steps around the first period of the platform as given in Table 3-6. A comparison between initial and final frequency grid is presented in Figure 3-34 to Figure 3-37.

**Table 3-6 Enhanced Frequency Grid**

10 steps	From 10.00 seconds to 5.00 seconds at an interval of 0.50 seconds
4 steps	From 5.00 seconds to 4.00 seconds at an interval of 0.25 seconds
20 steps	From 4.00 seconds to 3.00 seconds at an interval of 0.05 seconds
21 steps	From 2.5 seconds to 1.00 seconds at an interval of 0.10 seconds

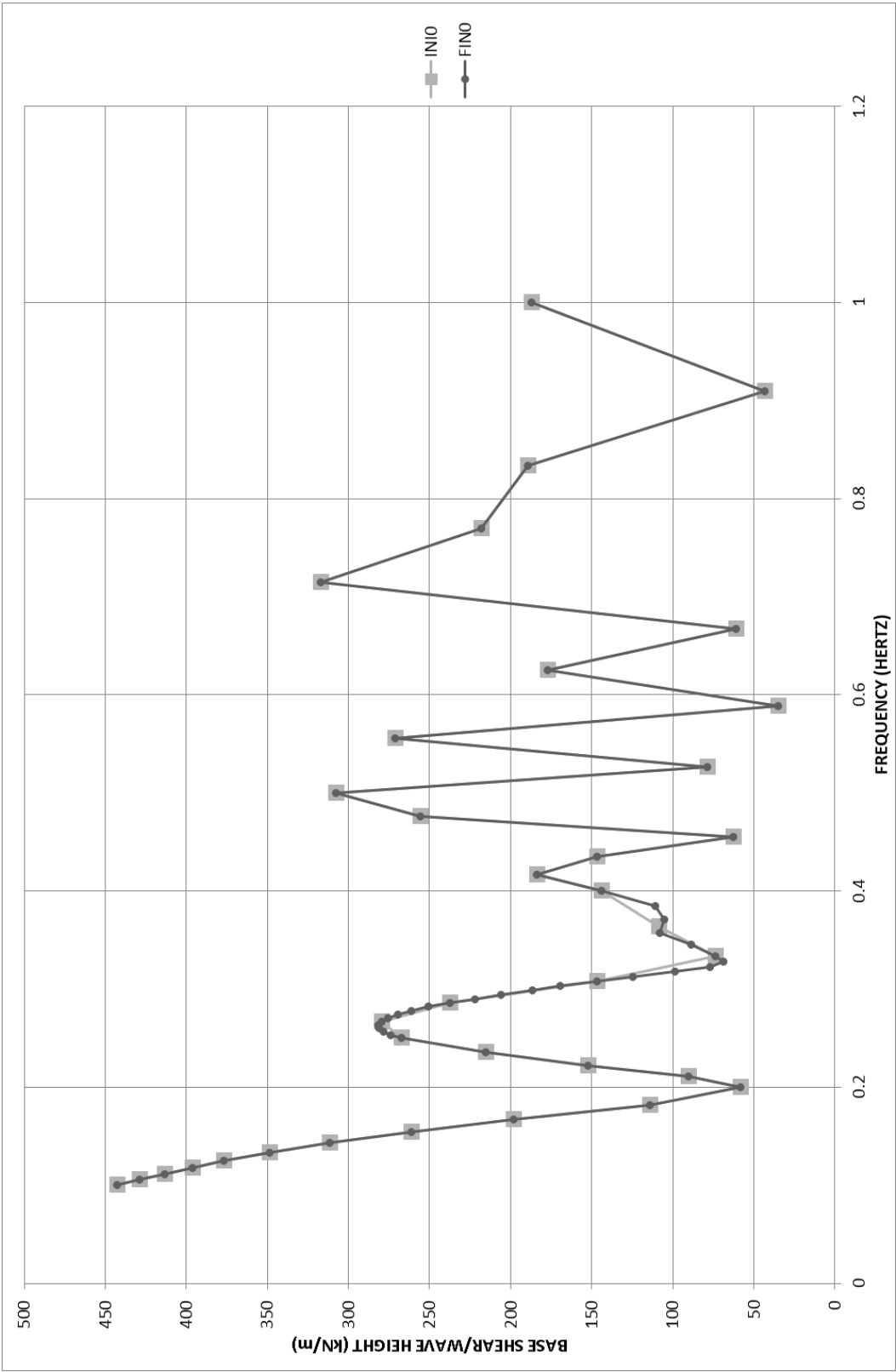


Figure 3-34 Initial and Final frequency grid comparison at 0°

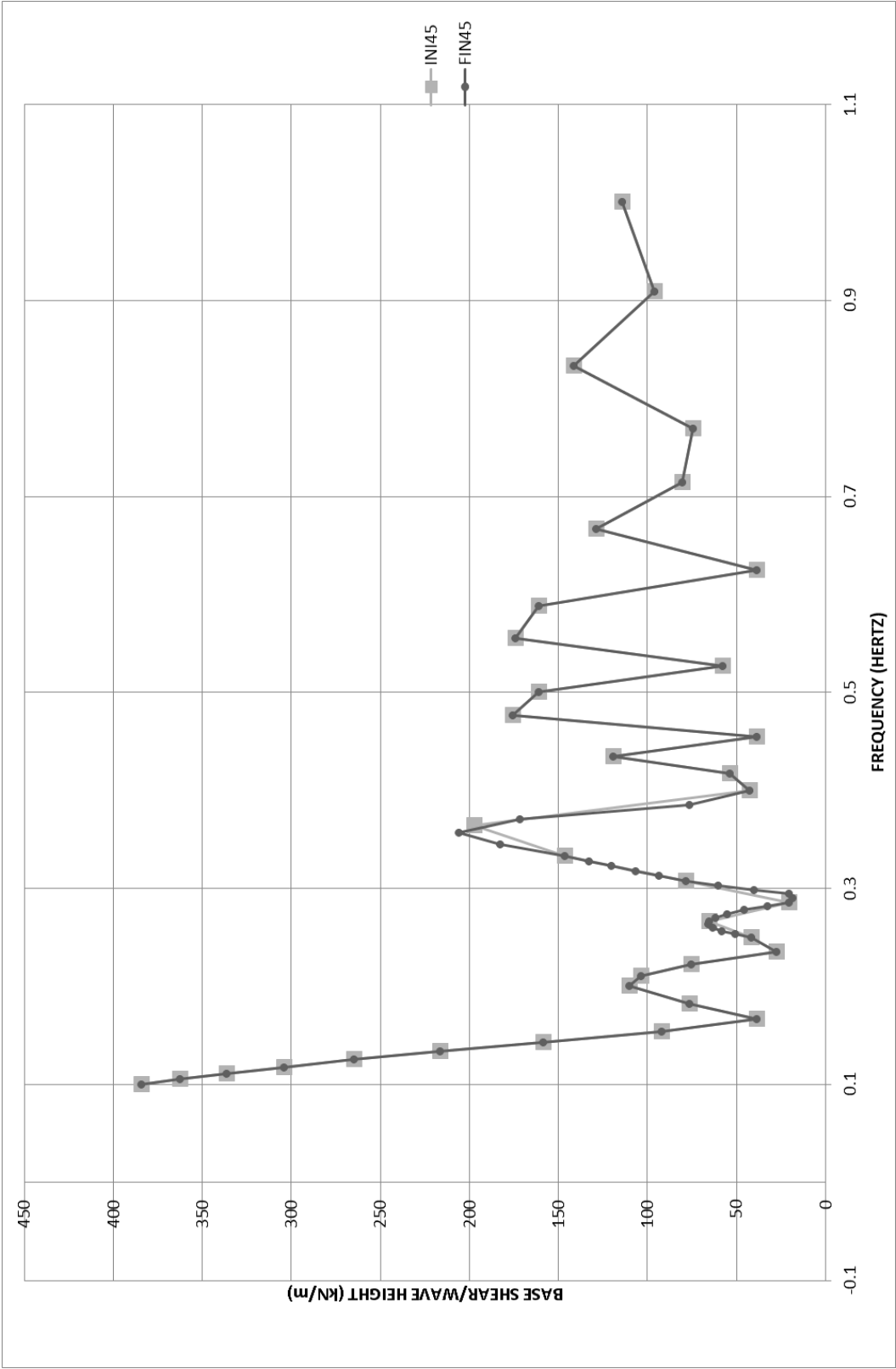


Figure 3-35 Initial and Final frequency grid comparison at 45°

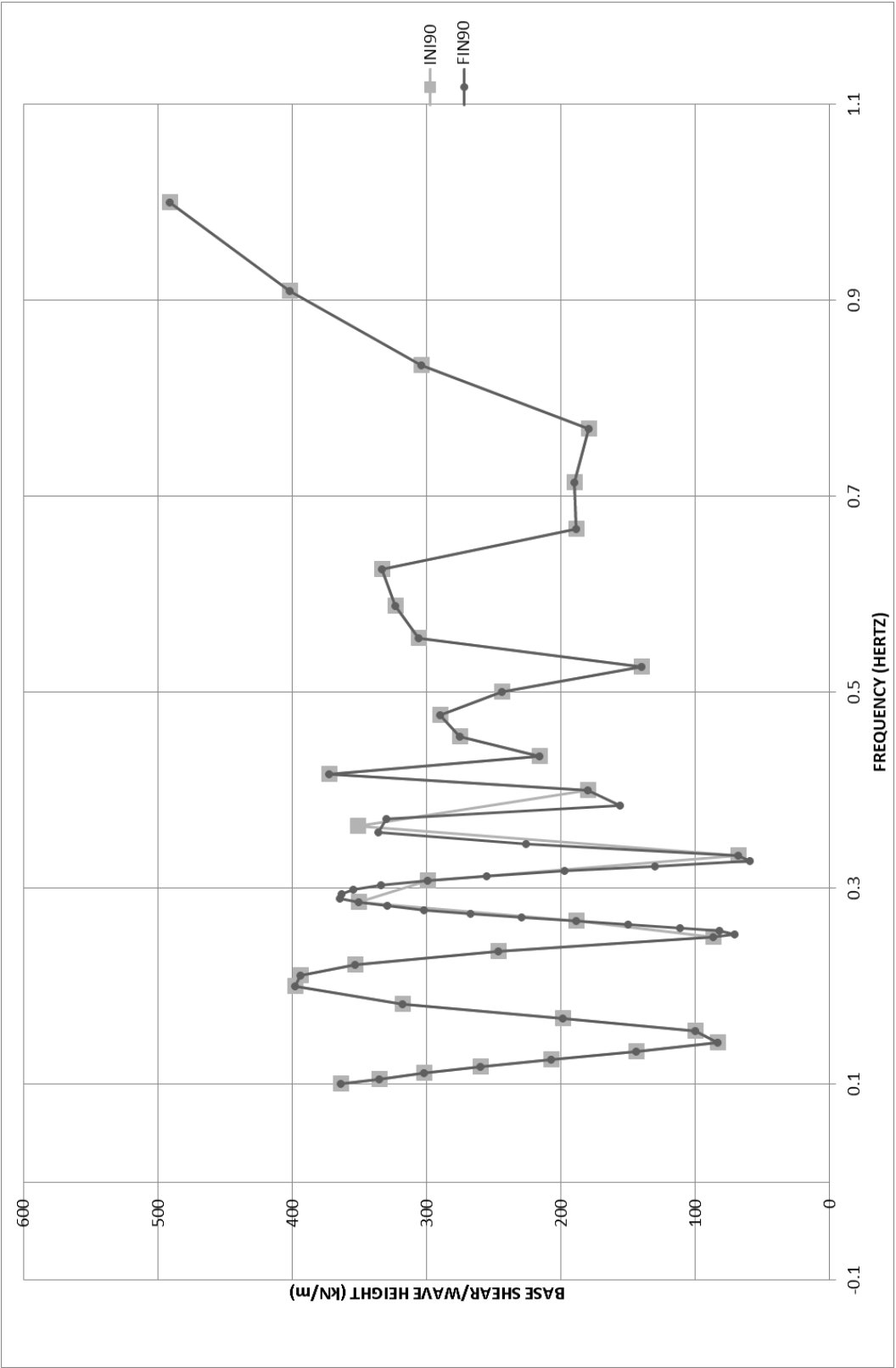


Figure 3-36 Initial and Final frequency grid comparison at 90°



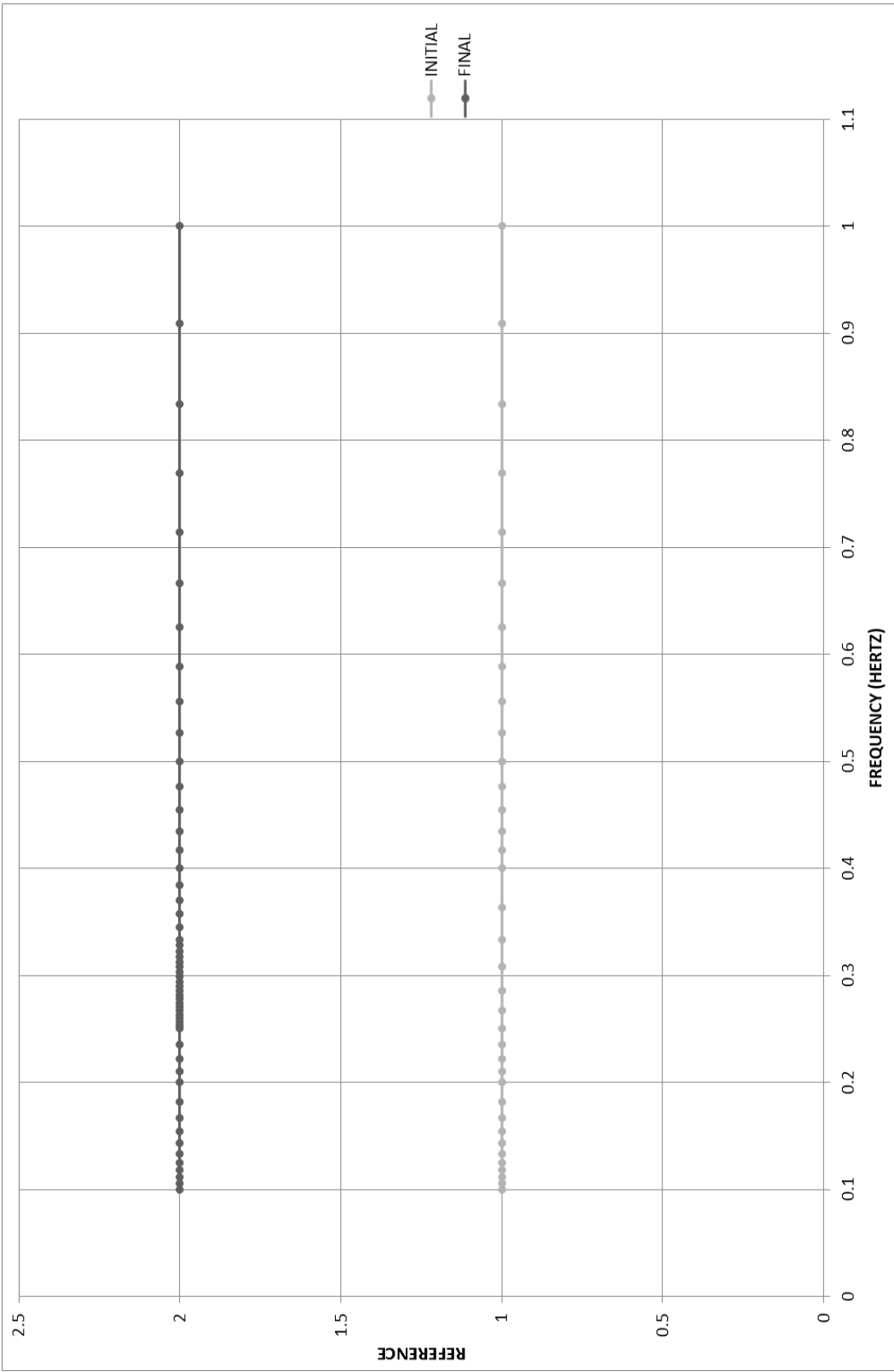


Figure 3-37 Frequency grid distribution

### 3.6 Calibration Method

The calibration is based on matching of global response parameters. For matching purposes, the base shear wave load is commonly used. The sea-state that contributes most to fatigue damage is considered. For this purpose, the centre of fatigue damage scatter diagrams along each direction are considered, as shown in Table 3-7 to Table 3-9.

**Table 3-7 Directional wave scatter diagram (0 degree)**

4.25								1		
3.75								1		
3.25							1	1		
2.75							5	1		
2.25						6	34			
1.75					1	165	39	1		
1.25				1	246	394	1			
0.75				705	1141	54				
0.25		1	100	1262	167					
Hs Tp	0.5	1.5	2.5	3.5	4.5	5.5	6.5	7.5	8.5	9.5

**Table 3-8 Directional wave scatter diagram (45 degree)**

4.25										
3.75										
3.25										
2.75										
2.25						2	4			
1.75						8	3			
1.25				3	25	35				
0.75			2	157	170	5				
0.25		1	83	574	47					
Hs Tp	0.5	1.5	2.5	3.5	4.5	5.5	6.5	7.5	8.5	9.5

**Table 3-9 Directional wave scatter diagram (90 degree)**

4.25										
3.75										
3.25										
2.75										
2.25										
1.75							1			
1.25					1	1				
0.75				22	20	2				
0.25			27	201	29					
Hs Tp	0.5	1.5	2.5	3.5	4.5	5.5	6.5	7.5	8.5	9.5

Dynamic Transfer functions are developed for the average wave steepness related to the weighted centre of damage in the scatter diagram and presented in Figure 3-48 to Figure 3-55. The weighing factor is the mean value of the normalized static base shear transfer function over the width of each cell in the scatter diagram as presented in Table 3-20 to Table 3-27. This weighing factor introduces a stress period dependency, which allows the cancellation effects to be reflected in the fatigue damage scatter diagram.

Fatigue damage is obtained from Equation 3-39 and presented in Table 3-28 to Table 3-30.

$$D_{ij} = N_{ij} \frac{(0.5(H_i + H_{i+1}))^m}{0.5(T_j + T_{j+1})} \quad \text{Equation 3-39}$$

Where;  $m = \text{slope of S-N curve} = 3$

The weighted fatigue damage is calculated using Equation 3-40 and presented in Table 3-31 to Table 3-33.

$$D_{ij} = N_{ij} * \frac{(W_j * 0.5 * (H_i + H_{i+1}))^m}{0.5 * (T_j + T_{j+1})} \quad \text{Equation 3-40}$$

Where  $D_{ij}$  is the weighted fatigue damage in each cell of the fatigue scatter diagram and  $W_j$  is the average period dependant weighing factor that is presented in Table 3-10.

**Table 3-10 Average Weighing factors ( $W_j$ )**

$T_p$ Dir.	0.5	1.5	2.5	3.5	4.5	5.5	6.5	7.5	8.5	9.5
0°	0.0	0.409	0.378	0.466	0.369	0.289	0.599	0.800	0.912	0.977
45°	0.0	0.306	0.314	0.191	0.195	0.209	0.261	0.568	0.797	0.945
90°	0.0	0.571	0.509	0.402	0.598	0.616	0.261	0.290	0.502	0.648

From fatigue damage calculations, the wave height ( $H_c$ ) and wave period ( $T_c$ ) at corresponding centre of fatigue damage scatter diagram is calculated by Equation 3-41.

$$\begin{cases} H_c = \frac{\sum D_{ij} H_{si}}{\sum D_{ij}} \\ T_c = \frac{\sum D_{ij} T_{pi}}{\sum D_{ij}} \end{cases} \quad \text{Equation 3-41}$$

From these values, the most probable maximum wave in the sea-state at the centre of the damage scatter diagram is determined from Equation 3-42 and presented in Table 3-11.

$$\begin{cases} H_{ref} = 1.86H_c \\ T_{ref} = T_c \end{cases} \quad \text{Equation 3-42}$$

**Table 3-11 Fatigue centroid**

	Fatigue Centroid					Weighted Fatigue Centroid				
	$H_c$	$T_c$	$H_{ref}$	$T_{ref}$	$H_{ref}/L_{ref}$	$H_c$	$T_c$	$H_{ref}$	$T_{ref}$	$H_{ref}/L_{ref}$
0°	1.46	5.19	2.72	5.19	1/15.5	2.02	5.82	3.75	5.82	1/14.1
45°	1.19	4.72	2.22	4.72	1/16	1.32	4.95	2.45	4.95	1/15.6
90°	0.84	4.27	1.55	4.27	1/18	0.81	4.36	1.50	4.36	1/19.7

This wave period is compared with the static base shear transfer function (Figure 3-39 to Figure 3-47) for the direction of interest to confirm that it does not fall in the valley of the transfer function. If it falls in the valley, then it is shifted to the adjacent peak depending on wave energy distribution as presented in Table 3-12.

**Table 3-12 Shifted fatigue centroid**

	$H_{ref}$	$T_{ref}$	$H_c$	$T_c$
0°	1.371	3.75	0.737	3.75
45°	2.438	5.00	1.311	5
90°	2.438	5.00	1.311	5

To account for the sensitivity of the structure, typically a broadside, an end-on and a diagonal direction are considered for calibration and a single representative steepness is chosen from these. In this case, an average design wave steepness of 1/16 is used. The wave height to be

used for each wave frequency in the fatigue analysis is calculated from Equation 3-43 using metric units.

$$\left\{ \begin{array}{l} L_{ref} = 1.56T_{ref}^2 \\ \text{wave steepness} = H_{ref}/L_{ref} \end{array} \right. \quad \text{Equation 3-43}$$

Use of the constant wave steepness will give unrealistically large wave heights at small wave frequencies. Therefore, a maximum height equal to the wave height with a one year return period and ending with a period corresponding to a wave height of 0.3 m should normally be used (API, 2007).

Root mean square (RMS) base shear wave loads are calculated for the sea-state at the centre of the fatigue damage scatter diagram, using standard spectral analysis techniques. For this, SACS (Offshore Structural Design and Analysis Software) modules are used by making the mass equal to zero (to eliminate inertial loads) and fully damping the structure (to make a low forcing frequency). Hence, the response calculated will be the static response of interest. This will provide an RMS base shear value for each wave steepness and direction as given in Table 3-13 and highlighted in SACS results as follows. Values of  $H_c$  and  $T_c$  are used to determine the static RMS (kN) values for the response function plots (refer to Figure 3-56 to Figure 3-64) along the three wave directions.

**Table 3-13 RMS base shear (kN)**

Wave Direction	Wave Steepness		
	1:25	1:20	1:15
0°	24.97	24.83	24.59
45°	22.01	21.68	21.06
90°	80.86	80.47	79.67

### Steepness 1:25

\*\*\*\*\* OVERTURNING MOMENT AND BASE SHEAR RMS VALUES \*\*\*\*\*

(SINGLE AMPLITUDE)

SPECTRUM NO.	TYPE	SIG. WAVE	DOMINANT	WAVE	** TRANSFER FUNCTION **			**** DYNAMIC RMS ****	
		HEIGHT	PERIOD	DIRECTION	FIRST	LAST	ALL	MOMENT	SHEAR
		M	SECS	DEGREES	WAVE	WAVE	CONVERGED	KN-M	KN
1	JS	0.74	3.75	0.000	1	36	YES	776.	<u>24.97</u>
2	JS	1.31	5.00	45.000	37	72	YES	614.	<u>22.01</u>
3	JS	1.31	5.00	90.000	73	108	YES	2504.	<u>80.86</u>

### Steepness 1:20

\*\*\*\*\* OVERTURNING MOMENT AND BASE SHEAR RMS VALUES \*\*\*\*\*

(SINGLE AMPLITUDE)

SPECTRUM NO.	TYPE	SIG. WAVE	DOMINANT	WAVE	** TRANSFER FUNCTION **			**** DYNAMIC RMS ****	
		HEIGHT	PERIOD	DIRECTION	FIRST	LAST	ALL	MOMENT	SHEAR
		M	SECS	DEGREES	WAVE	WAVE	CONVERGED	KN-M	KN
1	JS	0.74	3.75	0.000	1	36	YES	771.	<u>24.83</u>
2	JS	1.31	5.00	45.000	37	72	YES	603.	<u>21.68</u>
3	JS	1.31	5.00	90.000	73	108	YES	2490.	<u>80.47</u>

### Steepness 1:15

\*\*\*\*\* OVERTURNING MOMENT AND BASE SHEAR RMS VALUES \*\*\*\*\*

(SINGLE AMPLITUDE)

SPECTRUM NO.	TYPE	SIG. WAVE	DOMINANT	WAVE	** TRANSFER FUNCTION **			**** DYNAMIC RMS ****	
		HEIGHT	PERIOD	DIRECTION	FIRST	LAST	ALL	MOMENT	SHEAR
		M	SECS	DEGREES	WAVE	WAVE	CONVERGED	KN-M	KN
1	JS	0.74	3.75	0.000	1	36	YES	763.	<u>24.59</u>
2	JS	1.31	5.00	45.000	37	72	YES	588.	<u>21.06</u>
3	JS	1.31	5.00	90.000	73	108	YES	2473.	<u>79.67</u>

A stationary process is one whose statistics do not change with time. For every RMS stress there exists an average time,  $T_z$ , between zero crossings with a positive slope for a stationary Gaussian process with zero mean. This period is called the *Zero Crossing Period*. For a narrow band process, this is the average period or the reciprocal of the average frequency of the process. Assuming zero mean and a Rayleigh distribution of peaks, the most probable maximum [MPM] base shear wave load is found by using Equation 3-44 (HSE, 2000) and presented in Table 3-14.

$$\frac{MPM}{RMS} = \left[ 2 \ln \frac{T}{T_z} \right]^{0.5} \quad \text{Equation 3-44}$$

Where  $T$  is the 3 hours' duration of the storm in seconds ( $3 \times 60 \times 60 = 10,800$  seconds) and  $T_z$  is the mean zero crossing period of the wave in the sea-state at the centre of damage scatter diagram. This will provide the maximum base shear wave load from the spectral calculation for each wave steepness and direction. The corresponding base shear wave load range is double the MPM base shear wave load.

Wave power spectra can be generally classified into two characteristic forms. These are related to either the fetch-limited, developing sea conditions without swell, or the fully developed seas, and can be reasonably described by the JONSWAP and the Pierson-Moskowitz spectra, respectively. The shape of the stress (strain) power spectra is important because corrosion crack growth of the structural steels in tubular joints is sensitive to the frequency content. Therefore, it is necessary to simulate the correct frequency content, and hence power spectra, of typical wave loading (Kam, 1990). For sea-states described by a JONSWAP spectrum,  $T_z$  is assumed to be equal to  $T_p/1.28$ .

**Table 3-14 MPM VALUES**

Wave Direction	Wave Steepness		
	1:25	1:20	1:15
$0^0$	97.213	96.860	95.879
$45^0$	94.174	92.411	89.110
$90^0$	355.756	354.044	351.858

Spectral Base Shear Range is given as 2MPM for each wave direction and wave steepness in Table 3-15.

**Table 3-15 Spectral base shear**

Wave Direction	Wave Steepness		
	1:25	1:20	1:15
0°	194.426	193.720	191.758
45°	188.348	184.822	178.220
90°	711.512	708.088	703.716

Deterministic base shear is presented in Table 3-16 from values highlighted in SACS' results.

**Table 3-16 Deterministic base shear range**

0°	$136.366 + 136.260 = 272.626\text{kN}$
45°	$96.234 + 96.224 = 192.458\text{kN}$
90°	$348.209 + 348.113 = 696.322\text{kN}$



Deterministic base shear from SACS' results (refer to Table 3-16)

\*\*\*\* WAVE DESCRIPTION FOR LOAD CASE SW1 \*\*\*\*

WAVE THEORY \*\*\*\*\* CLASSICAL AIRY  
 WAVE HEIGHT \*\*\*\*\* 1.371 M  
 WATER DEPTH \*\*\*\*\* 42.720 M  
 WAVE PERIOD \*\*\*\*\* 3.750 SECS  
 WAVE LENGTH \*\*\*\*\* 21.948 M  
 ANGLE FROM X TOWARD Y \*\* 0.000 DEGREES  
 MUDLINE ELEVATION \*\*\*\*\* -41.600 M  
 WAVE CELERITY \*\*\*\*\* 5.853 M /SEC  
 MAX. NO. SEG/MEMBER \*\*\*\* 10  
 MIN. NO. SEG/MEMBER \*\*\*\* 1  
 CREST POSITION DETERMINED BY MAXIMUM SHEAR  
 STARTING CREST POSITION 0.000 M  
 NO. STEPS \*\*\*\*\* 36  
 STEP SIZE \*\*\*\*\* 0.610 M  
 CREST WATER DEPTH \*\*\*\*\* 42.72 M  
 TROUGH WATER DEPTH \*\*\*\*\* 42.72 M

\*\*\*\*\* SEASTATE LOADS FOR WAVE PASSING THROUGH STRUCTURE  
 \*\*\*\*\*

1.4 M. WAVE AT 0.0 DEG

	LOAD CONDITION	CREST POSITION M DEG	LOAD	MUDLINE ELEVATION
M	MAXIMUM MOMENT ABOUT MUDLINE	18.29 300.00	5085.233 KN-M	-41.60
M	MAXIMUM SHEAR AT MUDLINE	17.68 290.00	<u>136.366</u> KN	-41.60
M	MINIMUM MOMENT ABOUT MUDLINE	7.32 120.00	-4981.785 KN-M	-41.60
M	MINIMUM SHEAR AT MUDLINE	6.71 110.00	<u>-136.260</u> KN	-41.60
M	MAXIMUM FORCE UPWARD	1.83 30.00	33.716 KN	-41.60
M	MAXIMUM FORCE DOWNWARD	12.80 210.00	-21.916 KN	-41.60

\*\*\*\* WAVE DESCRIPTION FOR LOAD CASE SW2 \*\*\*\*

WAVE THEORY \*\*\*\*\* CLASSICAL AIRY  
 WAVE HEIGHT \*\*\*\*\* 2.438 M  
 WATER DEPTH \*\*\*\*\* 42.720 M  
 WAVE PERIOD \*\*\*\*\* 5.000 SECS  
 WAVE LENGTH \*\*\*\*\* 39.018 M  
 ANGLE FROM X TOWARD Y \*\* 45.000 DEGREES  
 MUDLINE ELEVATION \*\*\*\*\* -41.600 M  
 WAVE CELERITY \*\*\*\*\* 7.804 M /SEC  
 MAX. NO. SEG/MEMBER \*\*\*\*\* 10  
 MIN. NO. SEG/MEMBER \*\*\*\*\* 1  
 CREST POSITION DETERMINED BY MAXIMUM SHEAR  
 STARTING CREST POSITION 0.000 M  
 NO. STEPS \*\*\*\*\* 36  
 STEP SIZE \*\*\*\*\* 1.084 M  
 CREST WATER DEPTH \*\*\*\*\* 42.72 M  
 TROUGH WATER DEPTH \*\*\*\*\* 42.72 M

\*\*\*\*\*

\*\*\*\*\* SEASTATE LOADS FOR WAVE PASSING THROUGH STRUCTURE

2.4 M. WAVE AT 45.0 DEG

	LOAD CONDITION	CREST POSITION M DEG		LOAD	MUDLINE ELEVATION
M	MAXIMUM MOMENT ABOUT MUDLINE	32.52	300.00	3648.682 KN-M	-41.60
M	MAXIMUM SHEAR AT MUDLINE	10.84	100.00	<u>96.234</u> KN	-41.60
M	MINIMUM MOMENT ABOUT MUDLINE	13.01	120.00	-3379.133 KN-M	-41.60
M	MINIMUM SHEAR AT MUDLINE	30.35	280.00	<u>-96.224</u> KN	-41.60
M	MAXIMUM FORCE UPWARD	6.50	60.00	53.177 KN	-41.60
M	MAXIMUM FORCE DOWNWARD	26.01	240.00	-29.795 KN	-41.60

\*\*\*\* WAVE DESCRIPTION FOR LOAD CASE SW3 \*\*\*\*

WAVE THEORY \*\*\*\*\* CLASSICAL AIRY  
 WAVE HEIGHT \*\*\*\*\* 2.438 M  
 WATER DEPTH \*\*\*\*\* 42.720 M  
 WAVE PERIOD \*\*\*\*\* 5.000 SECS  
 WAVE LENGTH \*\*\*\*\* 39.018 M  
 ANGLE FROM X TOWARD Y \*\* 90.000 DEGREES  
 MUDLINE ELEVATION \*\*\*\*\* -41.600 M  
 WAVE CELERITY \*\*\*\*\* 7.804 M /SEC  
 MAX. NO. SEG/MEMBER \*\*\*\* 10  
 MIN. NO. SEG/MEMBER \*\*\*\* 1  
 CREST POSITION DETERMINED BY MAXIMUM SHEAR  
 STARTING CREST POSITION 0.000 M  
 NO. STEPS \*\*\*\*\* 36  
 STEP SIZE \*\*\*\*\* 1.084 M  
 CREST WATER DEPTH \*\*\*\*\* 42.72 M  
 TROUGH WATER DEPTH \*\*\*\*\* 42.72 M

\*\*\*\*\* SEASTATE LOADS FOR WAVE PASSING THROUGH STRUCTURE  
 \*\*\*\*\*

2.4 M. WAVE AT 90.0 DEG

	LOAD CONDITION	CREST POSITION M DEG	LOAD	MUDLINE ELEVATION
M	MAXIMUM MOMENT ABOUT MUDLINE	30.35 280.00	13019.681 KN-M	-41.60
M	MAXIMUM SHEAR AT MUDLINE	10.84 100.00	<u>348.209</u> KN	-41.60
M	MINIMUM MOMENT ABOUT MUDLINE	10.84 100.00	-12801.345 KN-M	-41.60
M	MINIMUM SHEAR AT MUDLINE	30.35 280.00	<u>-348.113</u> KN	-41.60
M	MAXIMUM FORCE UPWARD	3.25 30.00	95.008 KN	-41.60
M	MAXIMUM FORCE DOWNWARD	22.76 210.00	-72.506 KN	-41.60

The spectral base shear is compared against the deterministic base shear. In order to linearize the wave effects, the drag and inertia coefficients are enhanced by the ratio of deterministic base shear to spectral base shear, refer to the Table 3-17 and Table 3-18.

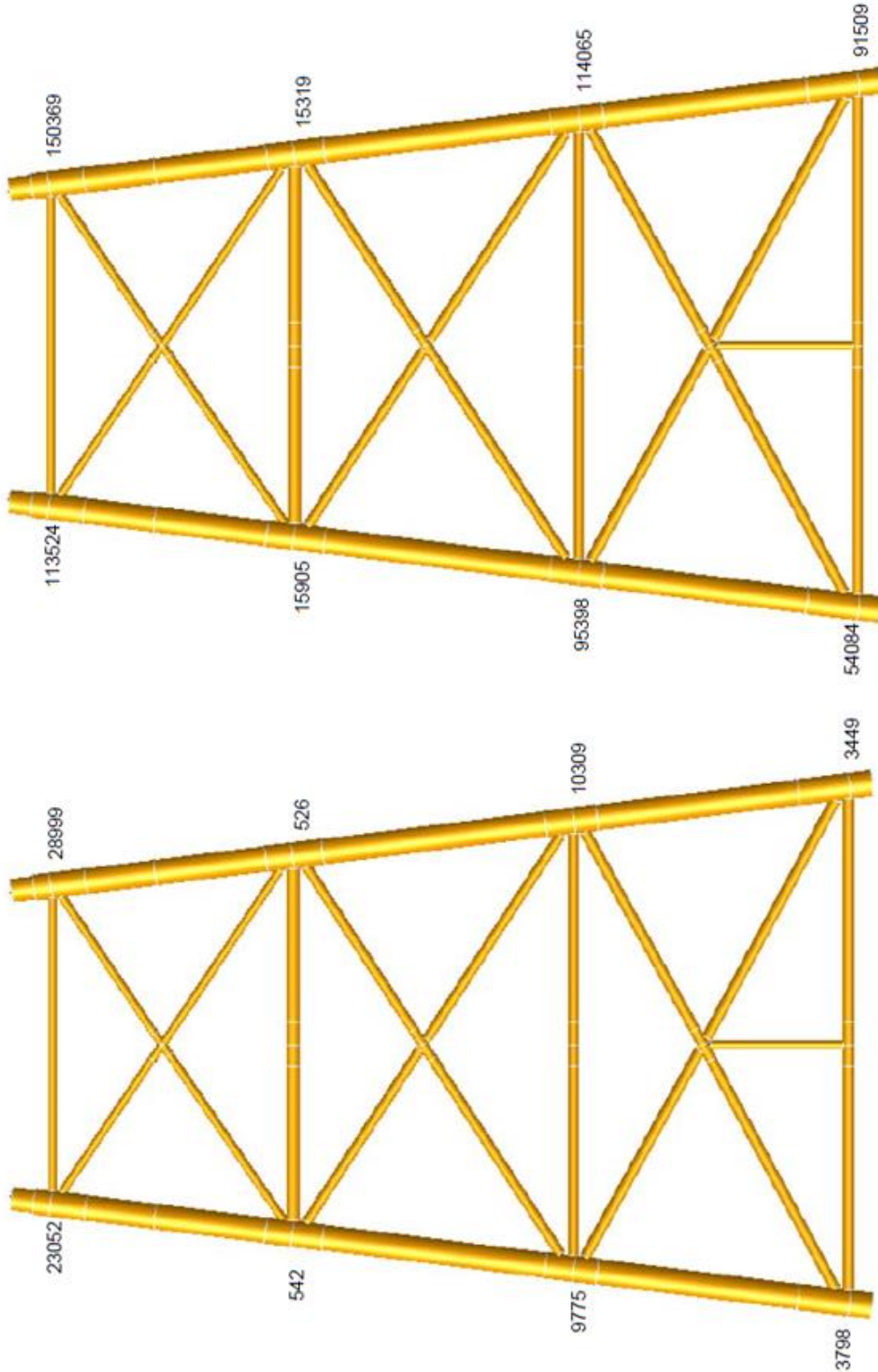
**Table 3-17 Enhanced drag coefficient**

$C_d$	Smooth members (initial = 0.6)			Rough members (initial = 0.7)		
	Wave Steepness			Wave Steepness		
Direction	1:25	1:20	1:15	1:25	1:20	1:15
00	0.808	0.813	0.821	0.943	0.948	0.957
450	0.659	0.669	0.689	0.769	0.780	0.803
900	0.649	0.652	0.659	0.757	0.761	0.768
$C_d$	0.821			0.957		

**Table 3-18 Enhanced mass coefficient**

$C_m$	Smooth members (initial = 2.0)			Rough members (initial = 2.0)		
	Wave Steepness			Wave Steepness		
Direction	1:25	1:20	1:15	1:25	1:20	1:15
0 <sup>0</sup>	2.694	2.709	2.736	2.694	2.709	2.736
45 <sup>0</sup>	2.196	2.230	2.295	2.196	2.230	2.295
90 <sup>0</sup>	2.163	2.174	2.195	2.163	2.174	2.195
$C_m$	2.736			2.736		

Fatigue demand and fatigue strength are established, then compared to one another to assess the adequacy of the structural component with respect to fatigue using a damage accumulation rule and a fatigue safety check. This approach is denoted as the *Miner Rule*. Calculated fatigue life is the computed life, in units of time (or number of cycles) for a particular structural detail considering its appropriate S-N curve (ABS, 2010). It can be clearly seen that fatigue life is overestimated (about four times) when the calibration process is not undertaken, refer to Figure 3-38.



(a) calibrated life (years)

(b) no calibration

Figure 3-38 Fatigue life comparison (years)

**Table 3-19 Weighing factor (steepness 1/25, 0°)**

0° T	Steepness 1/25		Transfer function	Weighing factor
	BS	Hs		
10.00	1747.209	5.920	295.14	
9.50	1581.797	5.424	291.63	0.986
9.00	1409.108	4.929	285.88	
8.50	1230.404	4.440	277.12	0.935
8.00	1048.718	3.960	264.83	
7.50	864.948	3.497	247.34	0.830
7.00	681.423	3.054	223.12	
6.50	499.823	2.636	189.61	0.628
6.00	321.940	2.247	143.28	
5.50	160.981	1.888	85.27	0.305
5.00	64.216	1.561	41.14	
4.75	93.086	1.409	66.07	
4.50	139.385	1.264	110.27	0.384
4.25	176.039	1.128	156.06	
4.00	192.362	0.999	192.55	
3.75	176.983	0.878	201.58	
3.50	130.647	0.765	170.78	0.489
3.25	66.350	0.659	100.68	
3.00	31.508	0.562	56.06	
2.75	37.796	0.472	80.08	
2.50	37.506	0.390	96.17	0.397
2.40	49.342	0.360	137.06	
2.30	36.594	0.330	110.89	
2.20	14.538	0.302	48.14	
2.10	50.760	0.275	184.58	
2.00	55.934	0.250	223.74	
1.90	14.438	0.225	64.17	
1.80	40.108	0.202	198.55	
1.70	4.942	0.180	27.46	
1.60	19.710	0.160	123.19	
1.50	6.544	0.140	46.74	0.429
1.40	28.754	0.122	235.69	
1.30	16.449	0.106	155.18	
1.20	12.434	0.090	138.16	
1.10	2.976	0.076	39.16	
1.00	8.780	0.062	141.61	

**Table 3-20 Weighing factor (steepness 1/20, 0°)**

0° T	Steepness 1/20		Transfer function	Weighing factor
	BS	Hs		
10.00	2241.665	7.400	302.93	
9.50	2012.340	6.780	296.81	0.979
9.00	1787.684	6.161	290.16	
8.50	1555.761	5.550	280.32	0.921
8.00	1320.969	4.950	266.86	
7.50	1085.162	4.371	248.26	0.812
7.00	850.753	3.817	222.89	
6.50	620.104	3.295	188.20	0.609
6.00	400.992	2.809	142.75	
5.50	196.796	2.361	83.35	0.295
5.00	81.378	1.951	41.71	
4.75	116.599	1.761	66.21	
4.50	174.848	1.580	110.66	0.374
4.25	220.120	1.410	156.11	
4.00	240.281	1.249	192.38	
3.75	219.504	1.097	200.09	
3.50	161.042	0.956	168.45	0.474
3.25	84.794	0.824	102.91	
3.00	37.912	0.702	54.01	
2.75	46.848	0.590	79.40	
2.50	46.716	0.488	95.73	0.383
2.40	59.544	0.449	132.61	
2.30	45.522	0.413	110.22	
2.20	18.124	0.378	47.95	
2.10	63.186	0.344	183.68	
2.00	69.882	0.312	223.98	
1.90	18.096	0.282	64.17	
1.80	50.076	0.253	197.93	
1.70	6.190	0.226	27.39	
1.60	24.162	0.200	120.81	
1.50	8.376	0.176	47.59	0.414
1.40	36.056	0.153	235.66	
1.30	20.612	0.132	156.15	
1.20	14.976	0.112	133.71	
1.10	3.268	0.094	34.77	
1.00	10.758	0.078	137.92	

**Table 3-21 Weighing factor (steepness 1/15, 0°)**

0° T	Steepness 1/15		Transfer function	Weighing factor
	BS	Hs		
10.00	3232.664	9.916	326.00	
9.50	2862.820	9.085	315.12	0.965
9.00	2500.432	8.256	302.86	
8.50	2142.750	7.437	288.12	0.881
8.00	1798.028	6.634	271.03	
7.50	1458.453	5.857	249.01	0.758
7.00	1132.472	5.115	221.40	
6.50	821.943	4.416	186.13	0.559
6.00	525.248	3.764	139.55	
5.50	245.842	3.163	77.72	0.268
5.00	116.404	2.614	44.53	
4.75	157.766	2.359	66.88	
4.50	235.090	2.117	111.05	0.350
4.25	294.299	1.889	155.80	
4.00	321.564	1.673	192.21	
3.75	290.794	1.471	197.68	
3.50	210.616	1.281	164.42	0.435
3.25	109.878	1.104	99.53	
3.00	52.190	0.941	55.46	
2.75	62.670	0.791	79.23	
2.50	62.520	0.654	95.60	0.354
2.40	78.922	0.602	131.10	
2.30	59.652	0.553	107.87	
2.20	24.742	0.506	48.90	
2.10	83.754	0.461	181.68	
2.00	93.174	0.418	222.90	
1.90	22.906	0.377	60.76	
1.80	66.144	0.339	195.12	
1.70	10.302	0.302	34.11	
1.60	32.344	0.268	120.69	
1.50	11.228	0.235	47.78	0.385
1.40	47.706	0.205	232.71	
1.30	28.632	0.177	161.76	
1.20	19.722	0.151	130.61	
1.10	4.216	0.127	33.20	
1.00	14.732	0.105	140.30	



**Table 3-22 Weighing factor (steepness 1/25, 45°)**

45° T	Steepness 1/25		Transfer function	Weighing factor
	BS	Hs		
10.00	1498.190	5.920	253.07	
9.50	1313.401	5.424	242.15	0.953
9.00	1124.608	4.929	228.16	
8.50	929.708	4.440	209.39	0.820
8.00	732.146	3.960	184.89	
7.50	536.146	3.497	153.32	0.597
7.00	352.333	3.054	115.37	
6.50	183.740	2.636	69.70	0.286
6.00	72.023	2.247	32.05	
5.50	109.297	1.888	57.89	0.226
5.00	127.918	1.561	81.95	
4.75	108.584	1.409	77.06	
4.50	70.059	1.264	55.43	0.210
4.25	21.537	1.128	19.09	
4.00	31.711	0.999	31.74	
3.75	43.683	0.878	49.75	
3.50	10.439	0.765	13.65	0.204
3.25	38.896	0.659	59.02	
3.00	58.136	0.562	103.44	
2.75	66.330	0.472	140.53	
2.50	13.480	0.390	34.56	0.333
2.40	13.952	0.360	38.76	
2.30	29.836	0.330	90.41	
2.20	8.232	0.302	27.26	
2.10	34.630	0.275	125.93	
2.00	28.320	0.250	113.28	
1.90	10.220	0.225	45.42	
1.80	25.436	0.202	125.92	
1.70	22.812	0.180	126.73	
1.60	4.668	0.160	29.18	
1.50	13.063	0.140	93.31	0.329
1.40	7.548	0.122	61.87	
1.30	6.418	0.106	60.55	
1.20	9.208	0.090	102.31	
1.10	5.490	0.076	72.24	
1.00	5.302	0.062	85.52	

**Table 3-23 Weighing factor (steepness 1/20, 45°)**

45° T	Steepness 1/20		Transfer function	Weighing factor
	BS	Hs		
10.00	1948.595	7.400	263.32	
9.50	1694.509	6.780	249.93	0.945
9.00	1434.859	6.161	232.89	
8.50	1175.751	5.550	211.85	0.798
8.00	917.609	4.950	185.38	
7.50	667.967	4.371	152.82	0.572
7.00	432.499	3.817	113.31	
6.50	219.804	3.295	66.71	0.266
6.00	83.687	2.809	29.79	
5.50	135.167	2.361	57.25	0.212
5.00	157.506	1.951	80.73	
4.75	132.576	1.761	75.28	
4.50	84.840	1.580	53.70	0.197
4.25	25.488	1.410	18.08	
4.00	39.688	1.249	31.78	
3.75	53.497	1.097	48.77	
3.50	12.311	0.956	12.88	0.192
3.25	48.802	0.824	59.23	
3.00	70.742	0.702	100.77	
2.75	83.622	0.590	141.73	
2.50	16.120	0.488	33.03	0.316
2.40	17.618	0.449	39.24	
2.30	35.602	0.413	86.20	
2.20	10.340	0.378	27.35	
2.10	43.142	0.344	125.41	
2.00	35.072	0.312	112.41	
1.90	12.590	0.282	44.65	
1.80	31.168	0.253	123.19	
1.70	27.398	0.226	121.23	
1.60	6.156	0.200	30.78	
1.50	16.310	0.176	92.67	0.307
1.40	9.066	0.153	59.25	
1.30	6.740	0.132	51.06	
1.20	11.725	0.112	104.69	
1.10	6.486	0.094	69.00	
1.00	6.334	0.078	81.21	

**Table 3-24 Weighing factor (steepness 1/15, 45°)**

45° T	Steepness 1/15		Transfer function	Weighing factor
	BS	Hs		
10.00	2784.367	9.916	280.80	
9.50	2398.803	9.085	264.04	0.936
9.00	2010.136	8.256	243.48	
8.50	1626.813	7.437	218.75	0.773
8.00	1251.270	6.634	188.61	
7.50	889.977	5.857	151.95	0.534
7.00	557.837	5.115	109.06	
6.50	271.259	4.416	61.43	0.232
6.00	93.998	3.764	24.97	
5.50	176.549	3.163	55.82	0.189
5.00	204.999	2.614	78.42	
4.75	169.905	2.359	72.02	
4.50	107.496	2.117	50.78	0.179
4.25	33.259	1.889	17.61	
4.00	54.547	1.673	32.60	
3.75	69.455	1.471	47.22	
3.50	16.352	1.281	12.77	0.179
3.25	64.856	1.104	58.75	
3.00	94.274	0.941	100.18	
2.75	111.570	0.791	141.05	
2.50	21.126	0.654	32.30	0.294
2.40	22.926	0.602	38.08	
2.30	46.898	0.553	84.81	
2.20	13.560	0.506	26.80	
2.10	57.142	0.461	123.95	
2.00	47.007	0.418	112.46	
1.90	16.346	0.377	43.36	
1.80	40.754	0.339	120.22	
1.70	34.892	0.302	115.54	
1.60	7.202	0.268	26.87	
1.50	21.170	0.235	90.09	0.282
1.40	11.976	0.205	58.42	
1.30	9.378	0.177	52.98	
1.20	15.258	0.151	101.05	
1.10	8.870	0.127	69.84	
1.00	8.476	0.105	80.72	

**Table 3-25 Weighing factor (steepness 1/25, 90°)**

90° T	Steepness 1/25		Transfer function	Weighing factor
	BS	Hs		
10.00	1392.544	5.920	235.23	
9.50	1191.226	5.424	219.62	0.608
9.00	985.026	4.929	199.84	
8.50	774.217	4.440	174.37	0.480
8.00	562.292	3.960	141.99	
7.50	351.373	3.497	100.48	0.284
7.00	192.735	3.054	63.11	
6.50	192.878	2.636	73.17	0.258
6.00	316.713	2.247	140.95	
5.50	428.654	1.888	227.04	0.610
5.00	450.657	1.561	288.70	
4.75	405.754	1.409	287.97	
4.50	321.507	1.264	254.36	0.598
4.25	200.413	1.128	177.67	
4.00	64.182	0.999	64.25	
3.75	121.003	0.878	137.82	
3.50	193.191	0.765	252.54	0.402
3.25	143.256	0.659	217.38	
3.00	27.966	0.562	49.76	
2.75	118.692	0.472	251.47	
2.50	53.046	0.390	136.02	0.510
2.40	98.760	0.360	274.33	
2.30	53.646	0.330	162.56	
2.20	60.156	0.302	199.19	
2.10	58.180	0.275	211.56	
2.00	45.008	0.250	180.03	
1.90	23.038	0.225	102.39	
1.80	44.766	0.202	221.61	
1.70	42.349	0.180	235.27	
1.60	38.620	0.160	241.38	
1.50	18.814	0.140	134.39	0.572
1.40	16.276	0.122	133.41	
1.30	14.324	0.106	135.13	
1.20	20.350	0.090	226.11	
1.10	22.078	0.076	290.50	
1.00	22.242	0.062	358.74	

**Table 3-26 Weighing factor (steepness 1/20, 90°)**

90° T	Steepness 1/20		Transfer function	Weighing factor
	BS	Hs		
10.00	1831.367	7.400	247.48	
9.50	1557.955	6.780	229.79	0.640
9.00	1280.816	6.161	207.89	
8.50	999.913	5.550	180.16	0.498
8.00	716.283	4.950	144.70	
7.50	446.066	4.371	102.05	0.289
7.00	239.459	3.817	62.73	
6.50	241.181	3.295	73.20	0.260
6.00	399.662	2.809	142.28	
5.50	537.809	2.361	227.79	0.615
5.00	561.646	1.951	287.88	
4.75	502.875	1.761	285.56	
4.50	399.819	1.580	253.05	0.597
4.25	248.615	1.410	176.32	
4.00	78.855	1.249	63.13	
3.75	150.511	1.097	137.20	
3.50	240.328	0.956	251.39	0.401
3.25	177.470	0.824	215.38	
3.00	34.439	0.702	49.06	
2.75	147.334	0.590	249.72	
2.50	65.474	0.488	134.17	0.508
2.40	121.526	0.449	270.66	
2.30	65.575	0.413	158.78	
2.20	75.242	0.378	199.05	
2.10	72.582	0.344	210.99	
2.00	55.824	0.312	178.92	
1.90	28.148	0.282	99.82	
1.80	56.090	0.253	221.70	
1.70	52.772	0.226	233.50	
1.60	47.550	0.200	237.75	
1.50	23.382	0.176	132.85	0.570
1.40	20.500	0.153	133.99	
1.30	17.392	0.132	131.76	
1.20	24.612	0.112	219.75	
1.10	27.292	0.094	290.34	
1.00	27.834	0.078	356.85	

**Table 3-27 Weighing factor (steepness 1/15, 90°)**

90° T	Steepness 1/15		Transfer function	Weighing factor
	BS	Hs		
10.00	2647.941	9.916	267.04	
9.50	2232.774	9.085	245.76	0.695
9.00	1818.108	8.256	220.22	
8.50	1401.359	7.437	188.43	0.529
8.00	990.273	6.634	149.27	
7.50	605.061	5.857	103.31	0.297
7.00	310.916	5.115	60.79	
6.50	324.625	4.416	73.51	0.266
6.00	549.272	3.764	145.93	
5.50	727.529	3.163	230.01	0.624
5.00	737.603	2.614	282.17	
4.75	664.157	2.359	281.54	
4.50	532.720	2.117	251.64	0.598
4.25	329.603	1.889	174.49	
4.00	102.145	1.673	61.05	
3.75	199.711	1.471	135.77	
3.50	319.707	1.281	249.58	0.402
3.25	233.088	1.104	211.13	
3.00	45.236	0.941	48.07	
2.75	197.634	0.791	249.85	
2.50	84.034	0.654	128.49	0.508
2.40	160.268	0.602	266.23	
2.30	86.191	0.553	155.86	
2.20	99.740	0.506	197.11	
2.10	95.586	0.461	207.34	
2.00	72.928	0.418	174.47	
1.90	37.426	0.377	99.27	
1.80	72.758	0.339	214.63	
1.70	69.692	0.302	230.77	
1.60	64.072	0.268	239.07	
1.50	31.294	0.235	133.17	0.570
1.40	27.522	0.205	134.25	
1.30	22.840	0.177	129.04	
1.20	32.370	0.151	214.37	
1.10	35.844	0.127	282.24	
1.00	36.891	0.105	351.34	

**Table 3-28 Fatigue damage (0 degree)**

4.25	0.00	0.00	0.00	0.00	0.00	0.00	0.00	10.24	0.00	0.00
3.75	0.00	0.00	0.00	0.00	0.00	0.00	0.00	7.03	0.00	0.00
3.25	0.00	0.00	0.00	0.00	0.00	0.00	0.00	5.28	4.58	0.00
2.75	0.00	0.00	0.00	0.00	0.00	0.00	0.00	16.00	2.77	0.00
2.25	0.00	0.00	0.00	0.00	0.00	12.43	59.58	0.00	0.00	0.00
1.75	0.00	0.00	0.00	0.00	1.19	160.78	32.16	0.71	0.00	0.00
1.25	0.00	0.00	0.00	0.56	106.77	139.91	0.30	0.00	0.00	0.00
0.75	0.00	0.00	0.00	84.98	106.97	4.14	0.00	0.00	0.00	0.00
0.25	0.00	0.01	0.63	5.63	0.58	0.00	0.00	0.00	0.00	0.00
Hs Tp	0.5	1.5	2.5	3.5	4.5	5.5	6.5	7.5	8.5	9.5

**Table 3-29 Fatigue damage (45 degree)**

4.25	0.00	0.00	0.00	0.00	0.00	0.00	0.00	0.00	0.00	0.00
3.75	0.00	0.00	0.00	0.00	0.00	0.00	0.00	0.00	0.00	0.00
3.25	0.00	0.00	0.00	0.00	0.00	0.00	0.00	0.00	0.00	0.00
2.75	0.00	0.00	0.00	0.00	0.00	0.00	0.00	0.00	0.00	0.00
2.25	0.00	0.00	0.00	0.00	0.00	4.14	7.01	0.00	0.00	0.00
1.75	0.00	0.00	0.00	0.00	0.00	7.80	2.47	0.00	0.00	0.00
1.25	0.00	0.00	0.00	1.67	10.85	12.43	0.00	0.00	0.00	0.00
0.75	0.00	0.00	0.34	18.92	15.94	0.38	0.00	0.00	0.00	0.00
0.25	0.00	0.01	0.52	2.56	0.16	0.00	0.00	0.00	0.00	0.00
Hs Tp	0.5	1.5	2.5	3.5	4.5	5.5	6.5	7.5	8.5	9.5

**Table 3-30 Fatigue damage (90 degree)**

4.25	0.00	0.00	0.00	0.00	0.00	0.00	0.00	0.00	0.00	0.00
3.75	0.00	0.00	0.00	0.00	0.00	0.00	0.00	0.00	0.00	0.00
3.25	0.00	0.00	0.00	0.00	0.00	0.00	0.00	0.00	0.00	0.00
2.75	0.00	0.00	0.00	0.00	0.00	0.00	0.00	0.00	0.00	0.00
2.25	0.00	0.00	0.00	0.00	0.00	0.00	0.00	0.00	0.00	0.00
1.75	0.00	0.00	0.00	0.00	0.00	0.00	0.82	0.00	0.00	0.00
1.25	0.00	0.00	0.00	0.00	0.43	0.36	0.00	0.00	0.00	0.00
0.75	0.00	0.00	0.00	2.65	1.88	0.15	0.00	0.00	0.00	0.00
0.25	0.00	0.00	0.17	0.90	0.10	0.00	0.00	0.00	0.00	0.00
Hs Tp	0.5	1.5	2.5	3.5	4.5	5.5	6.5	7.5	8.5	9.5

**Table 3-31 Weighted fatigue damage (0 degree)**

4.25	0.00	0.00	0.00	0.00	0.00	0.00	0.00	5.24	0.00	0.00
3.75	0.00	0.00	0.00	0.00	0.00	0.00	0.00	3.60	0.00	0.00
3.25	0.00	0.00	0.00	0.00	0.00	0.00	1.13	2.34	0.00	0.00
2.75	0.00	0.00	0.00	0.00	0.00	0.00	3.43	1.42	0.00	0.00
2.25	0.00	0.00	0.00	0.00	0.00	0.30	12.78	0.00	0.00	0.00
1.75	0.00	0.00	0.00	0.00	0.06	3.89	6.90	0.37	0.00	0.00
1.25	0.00	0.00	0.00	0.06	5.38	3.39	0.06	0.00	0.00	0.00
0.75	0.00	0.00	0.00	8.60	5.39	0.10	0.00	0.00	0.00	0.00
0.25	0.00	0.00	0.03	0.57	0.03	0.00	0.00	0.00	0.00	0.00
Hs Tp	0.5	1.5	2.5	3.5	4.5	5.5	6.5	7.5	8.5	9.5

**Table 3-32 Weighted fatigue damage (45 degree)**

4.25	0.00	0.00	0.00	0.00	0.00	0.00	0.00	0.00	0.00	0.00
3.75	0.00	0.00	0.00	0.00	0.00	0.00	0.00	0.00	0.00	0.00
3.25	0.00	0.00	0.00	0.00	0.00	0.00	0.00	0.00	0.00	0.00
2.75	0.00	0.00	0.00	0.00	0.00	0.00	0.00	0.00	0.00	0.00
2.25	0.00	0.00	0.00	0.00	0.00	0.04	0.13	0.00	0.00	0.00
1.75	0.00	0.00	0.00	0.00	0.00	0.07	0.04	0.00	0.00	0.00
1.25	0.00	0.00	0.00	0.01	0.08	0.11	0.00	0.00	0.00	0.00
0.75	0.00	0.00	0.01	0.13	0.12	0.00	0.00	0.00	0.00	0.00
0.25	0.00	0.00	0.02	0.02	0.00	0.00	0.00	0.00	0.00	0.00
Hs Tp	0.5	1.5	2.5	3.5	4.5	5.5	6.5	7.5	8.5	9.5

**Table 3-33 Weighted fatigue damage (90 degree)**

4.25	0.00	0.00	0.00	0.00	0.00	0.00	0.00	0.00	0.00	0.00
3.75	0.00	0.00	0.00	0.00	0.00	0.00	0.00	0.00	0.00	0.00
3.25	0.00	0.00	0.00	0.00	0.00	0.00	0.00	0.00	0.00	0.00
2.75	0.00	0.00	0.00	0.00	0.00	0.00	0.00	0.00	0.00	0.00
2.25	0.00	0.00	0.00	0.00	0.00	0.00	0.00	0.00	0.00	0.00
1.75	0.00	0.00	0.00	0.00	0.00	0.00	0.01	0.00	0.00	0.00
1.25	0.00	0.00	0.00	0.00	0.09	0.08	0.00	0.00	0.00	0.00
0.75	0.00	0.00	0.00	0.17	0.40	0.04	0.00	0.00	0.00	0.00
0.25	0.00	0.00	0.02	0.06	0.02	0.00	0.00	0.00	0.00	0.00
Hs Tp	0.5	1.5	2.5	3.5	4.5	5.5	6.5	7.5	8.5	9.5



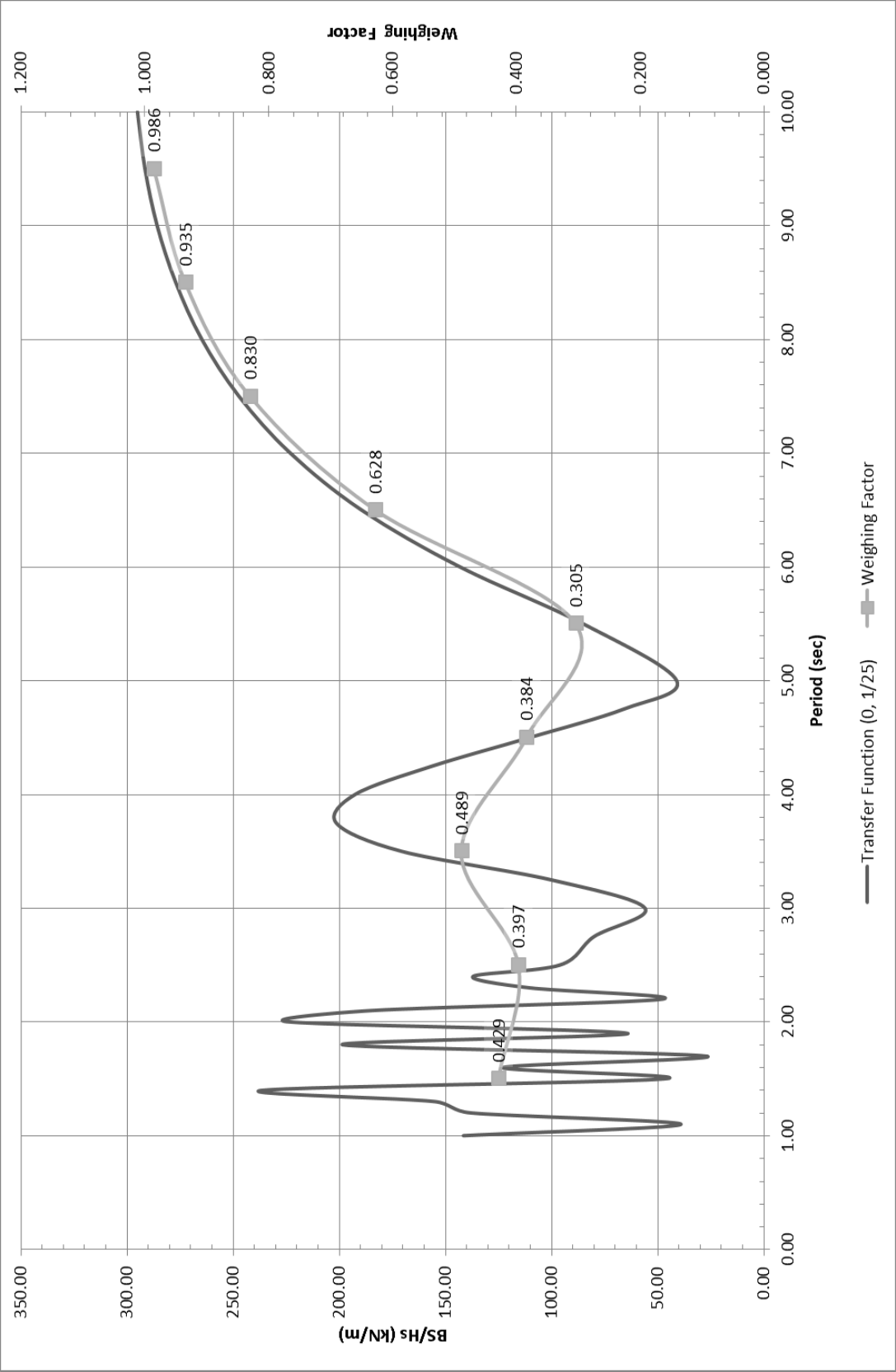


Figure 3-39 Static Transfer Function (0°, 1/25)

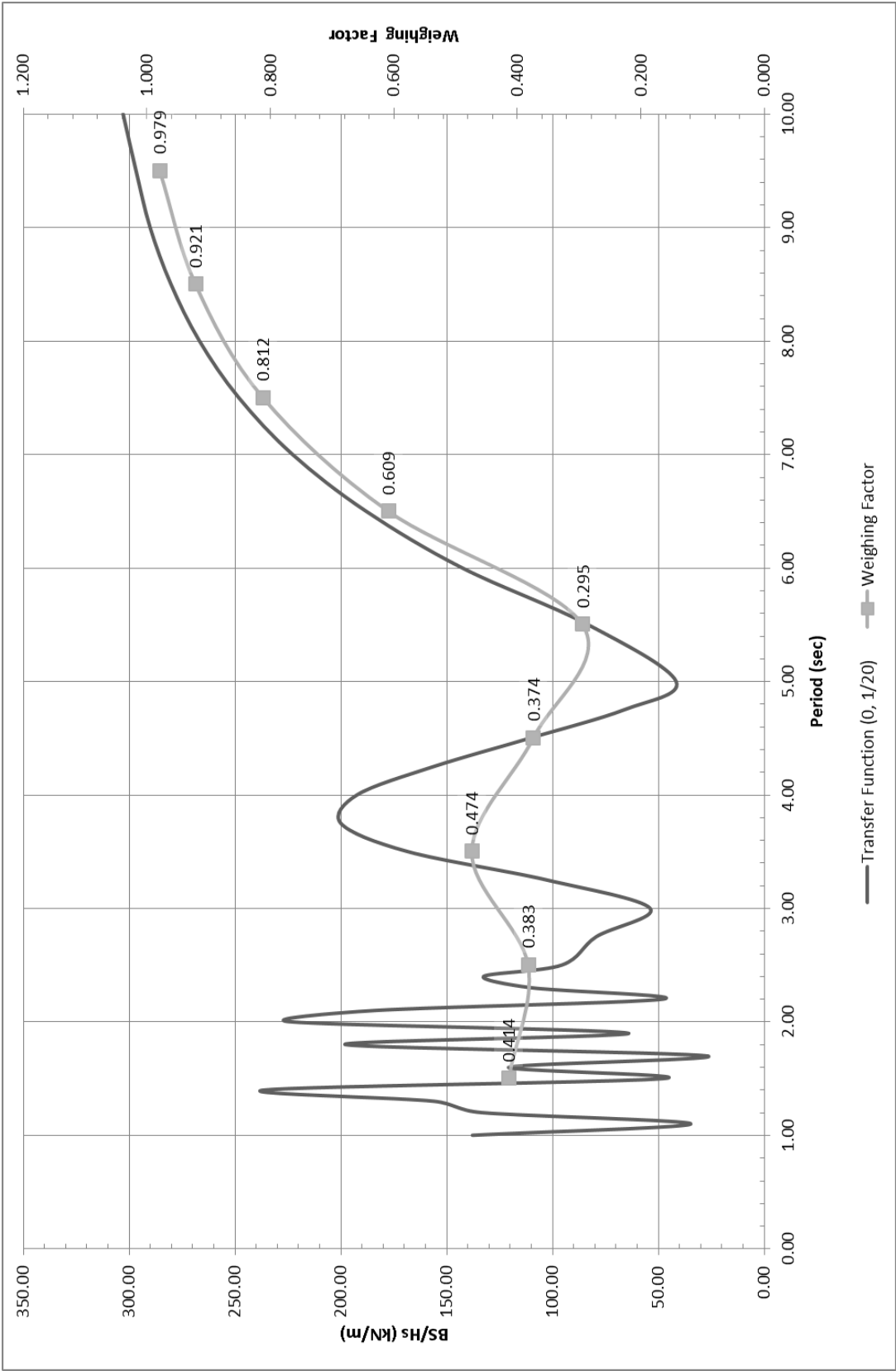


Figure 3-40 Static Transfer Function (0°, 1/20)

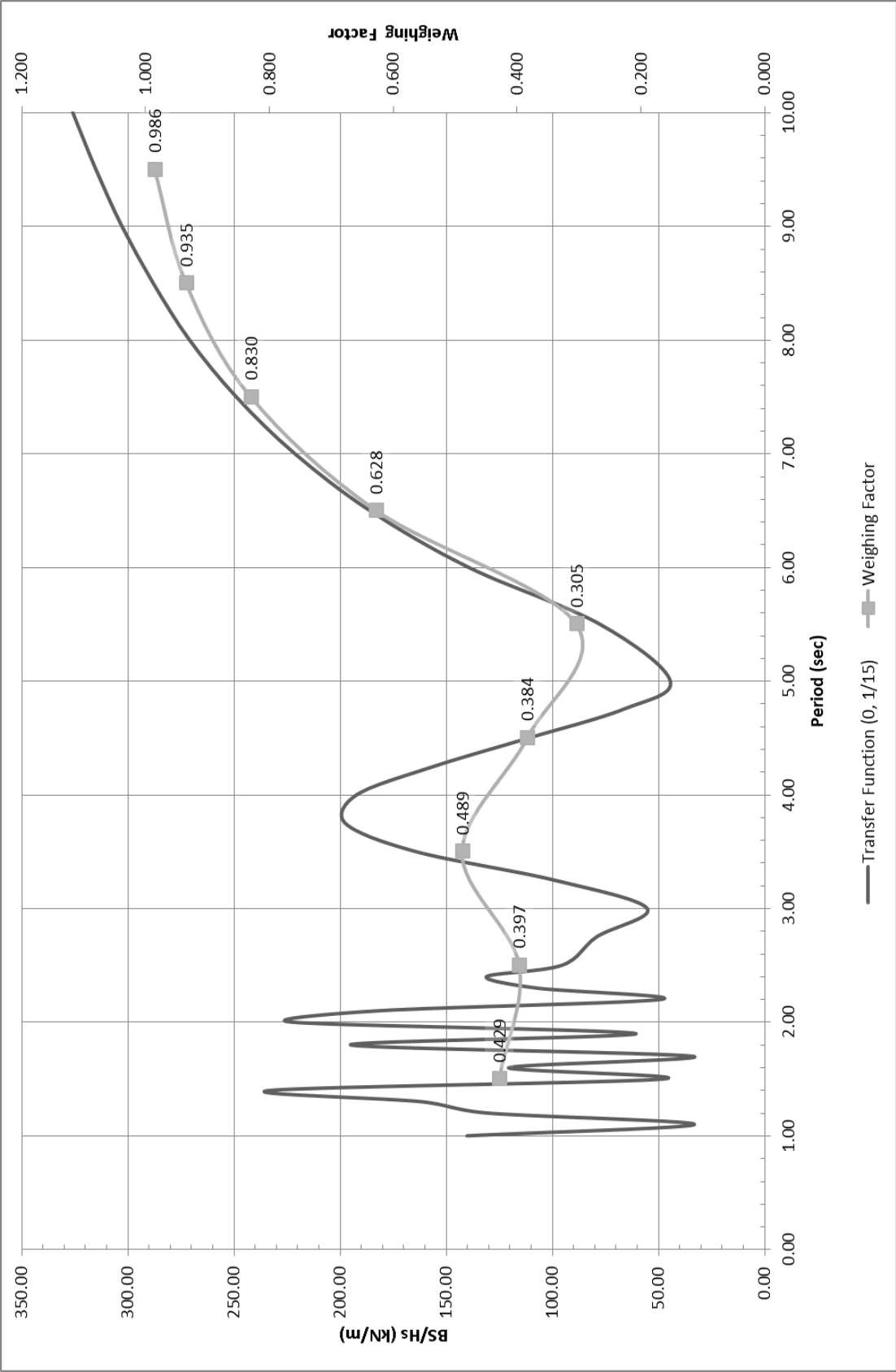


Figure 3-41 Static Transfer Function (0°, 1/15)

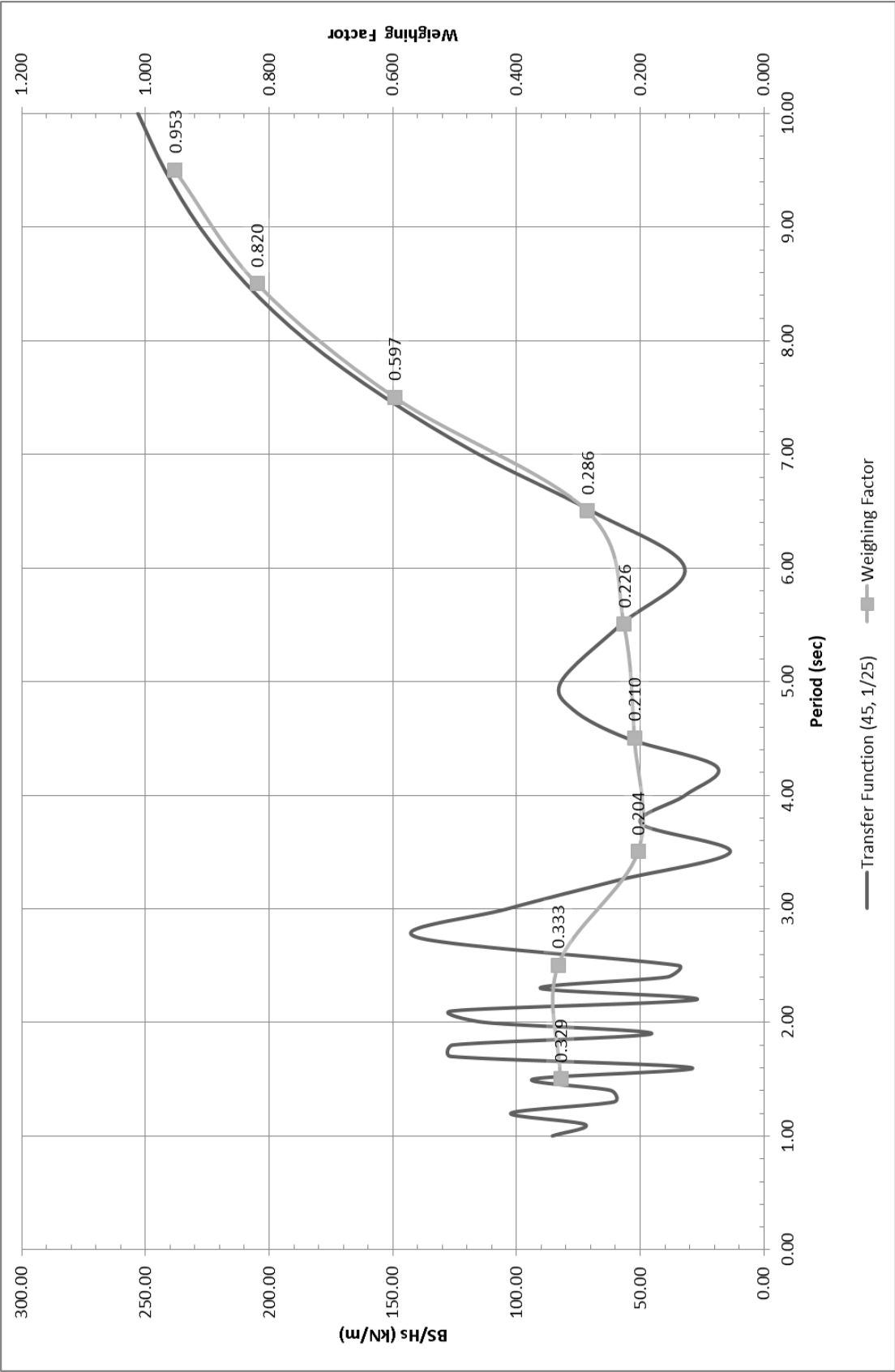


Figure 3-42 Static Transfer Function (45°, 1/25)

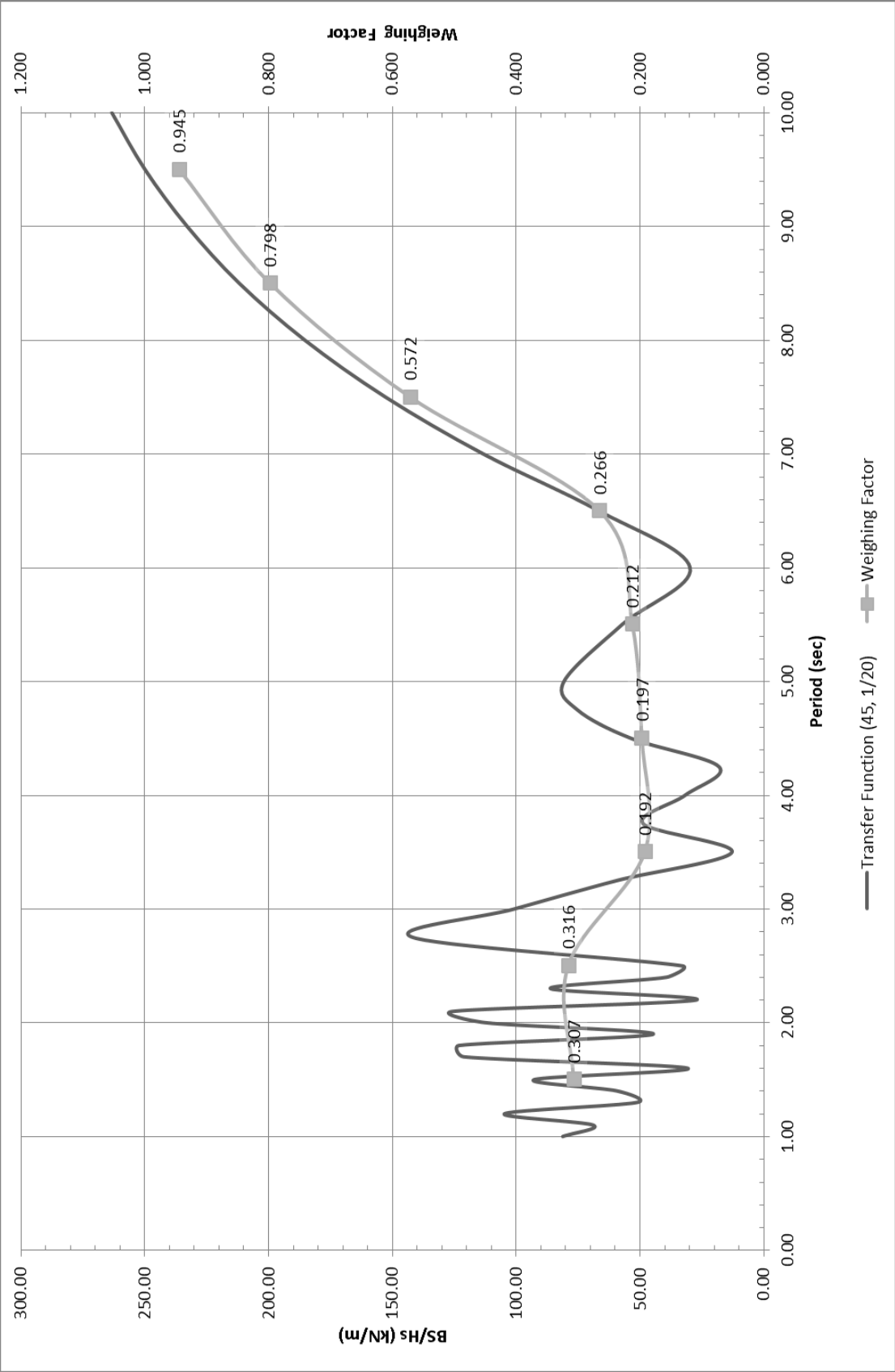


Figure 3-43 Static Transfer Function (45°, 1/20)

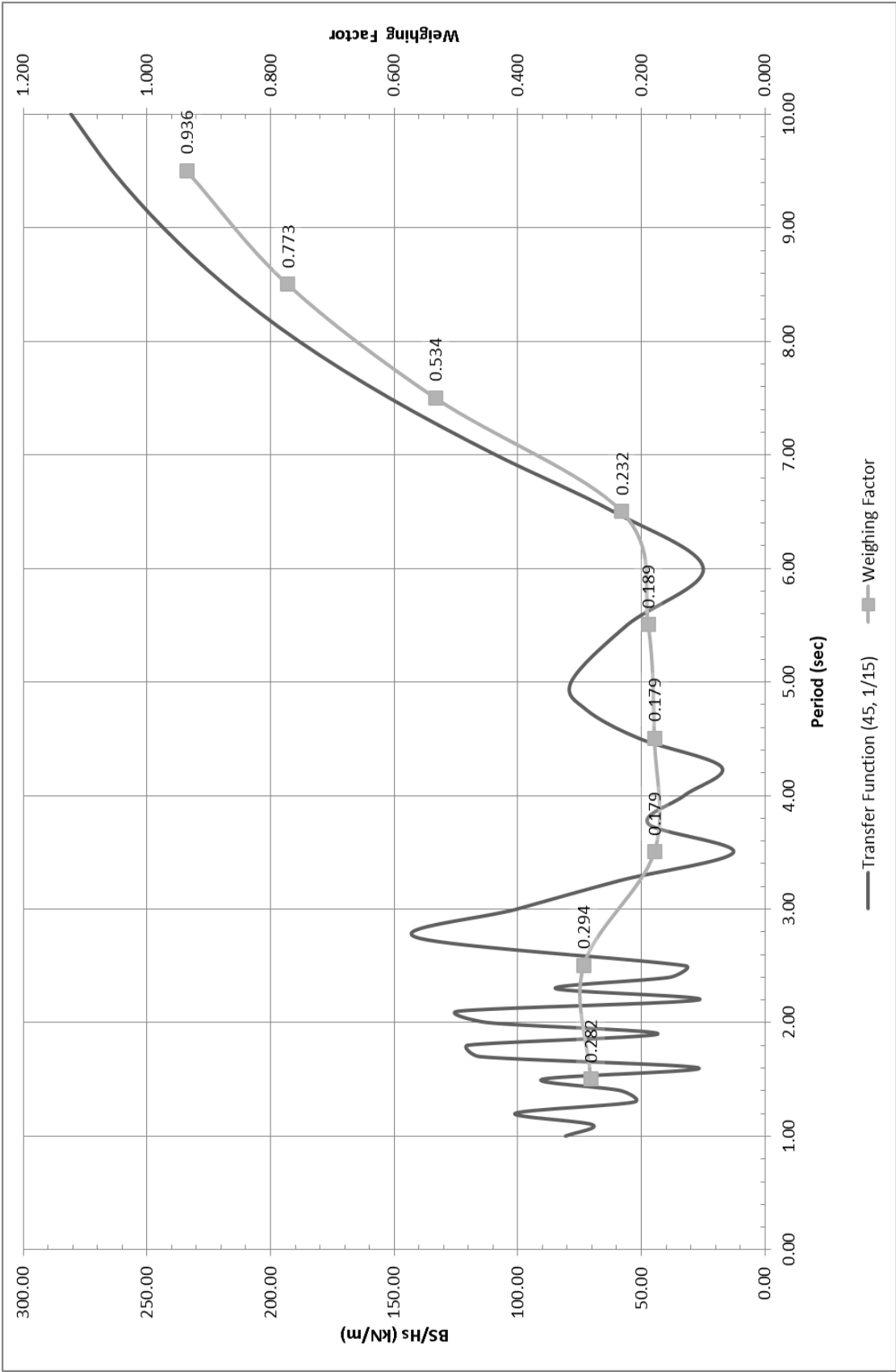


Figure 3-44 Static Transfer Function (45°, 1/15)

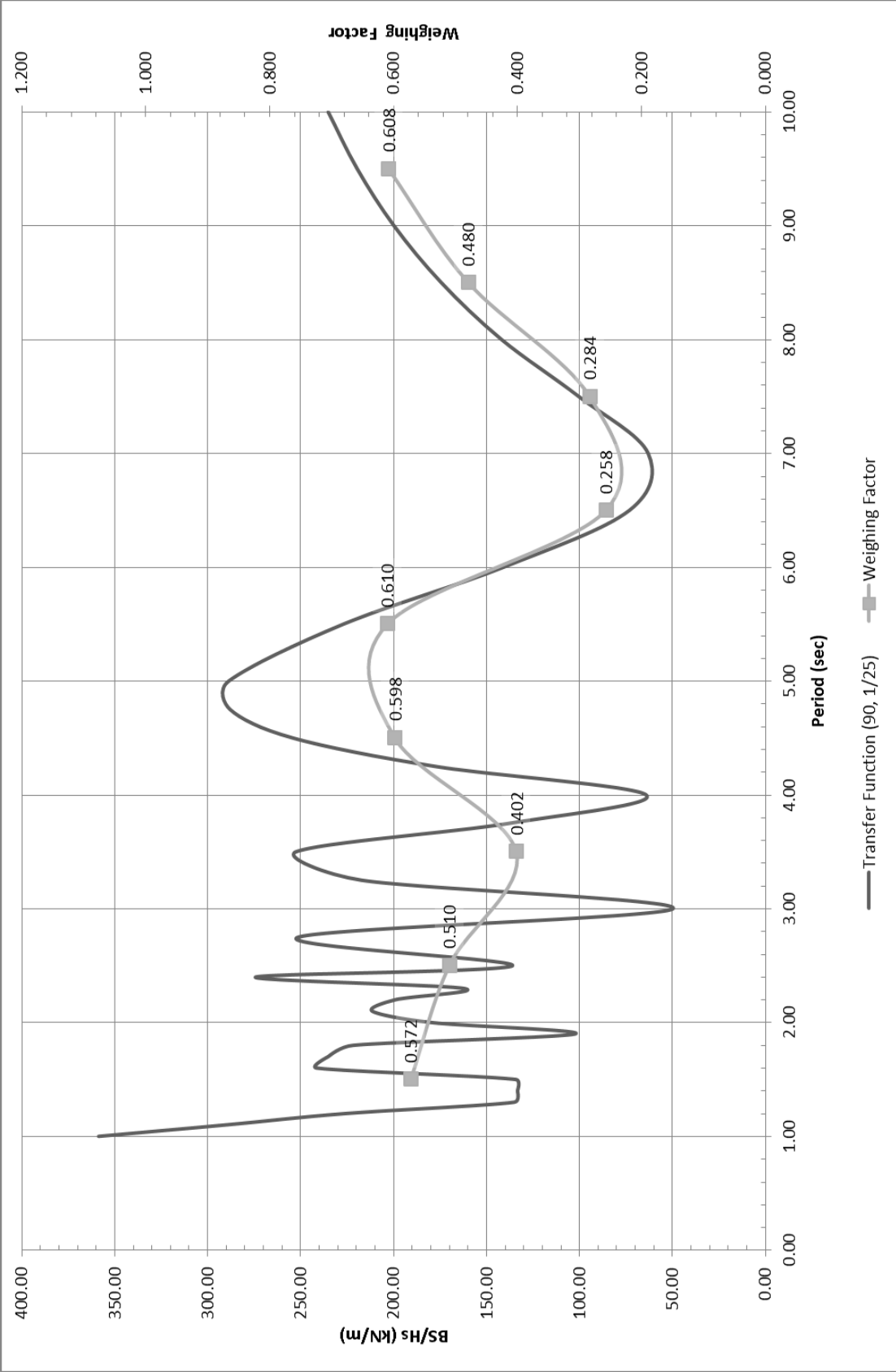


Figure 3-45 Static Transfer Function (90°, 1/25)

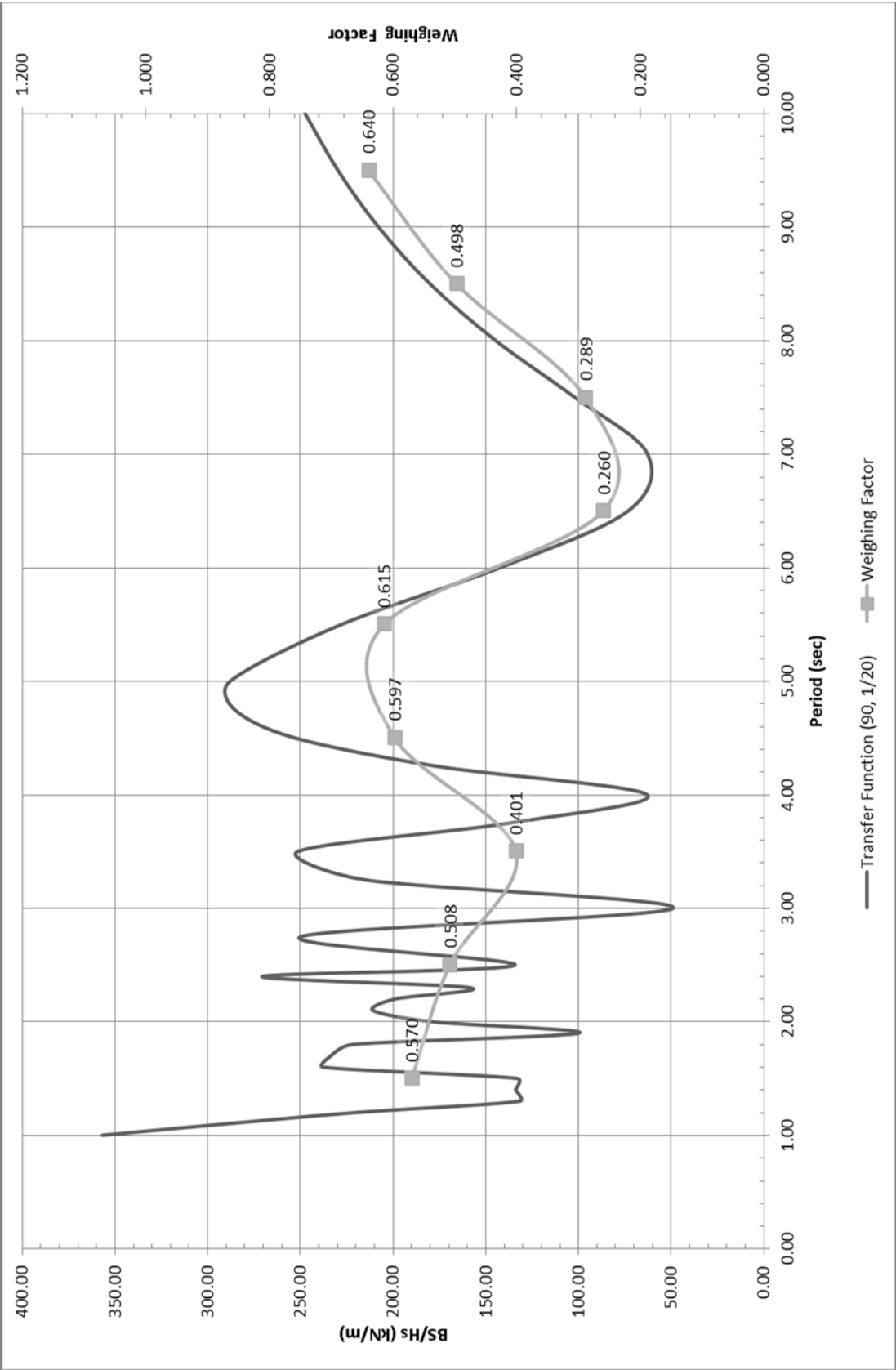


Figure 3-46 Static Transfer Function (90°, 1/20)



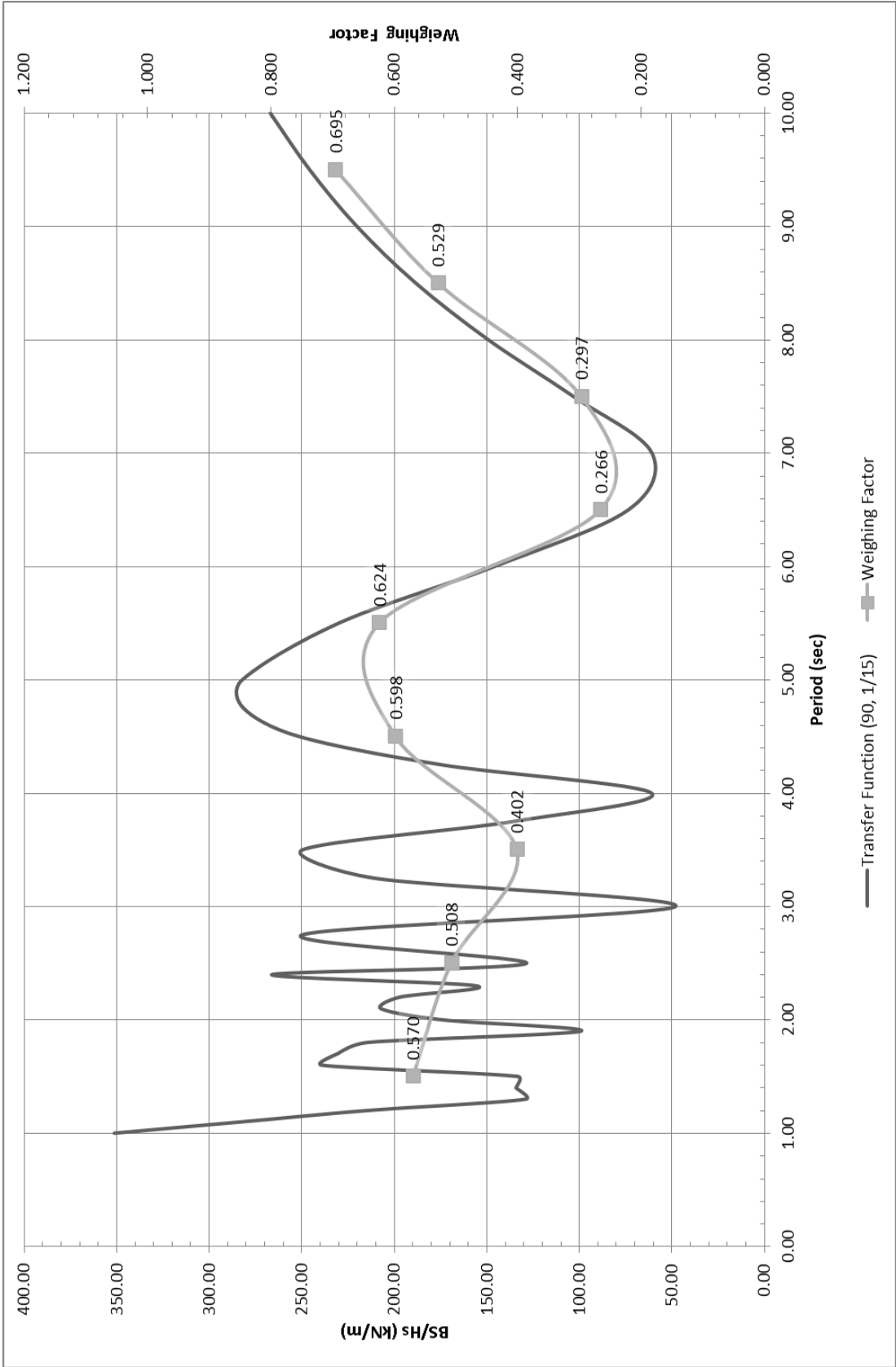


Figure 3-47 Static Transfer Function (90°, 1/15)

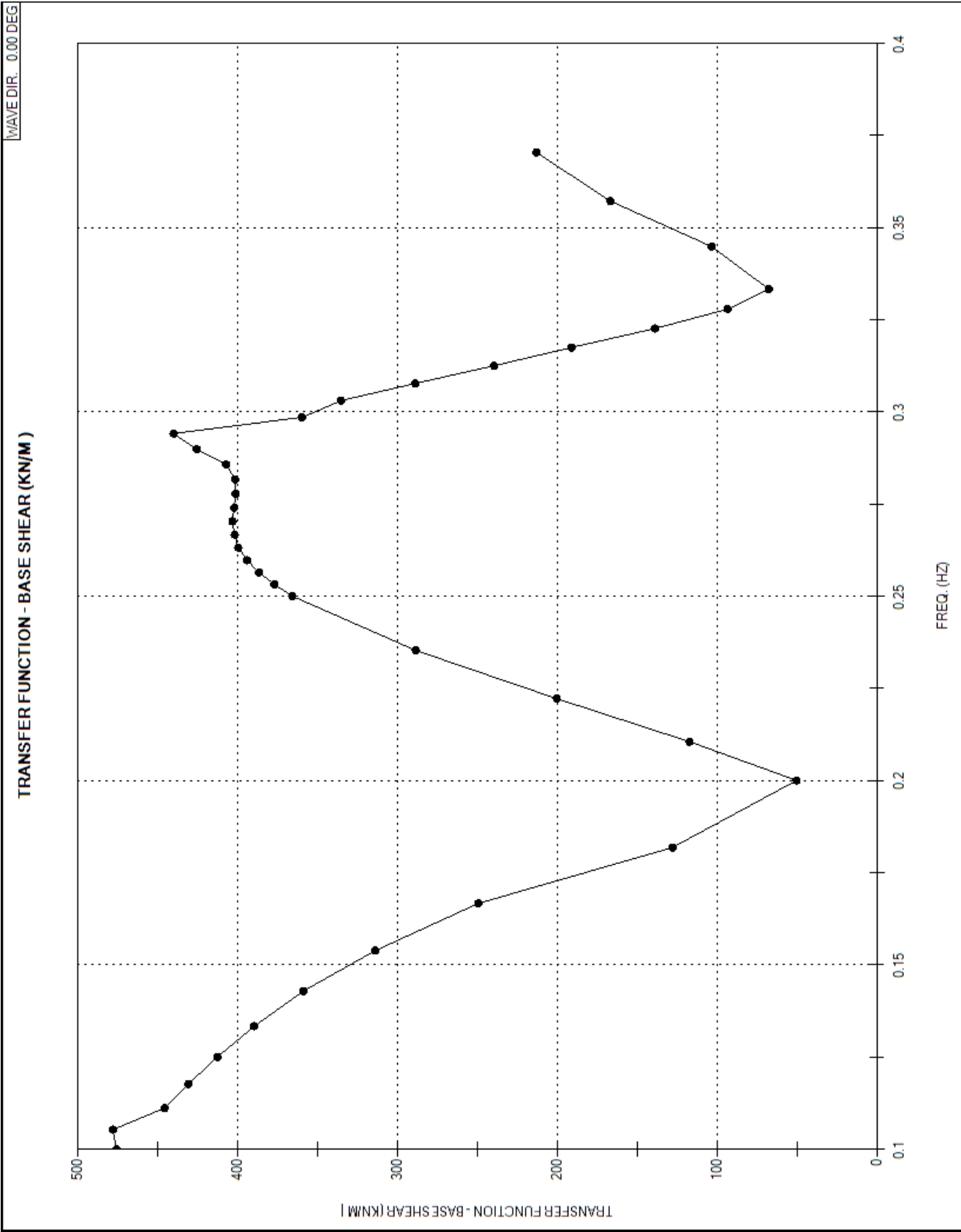


Figure 3-48 Dynamic Transfer Function (0°, 1/16)

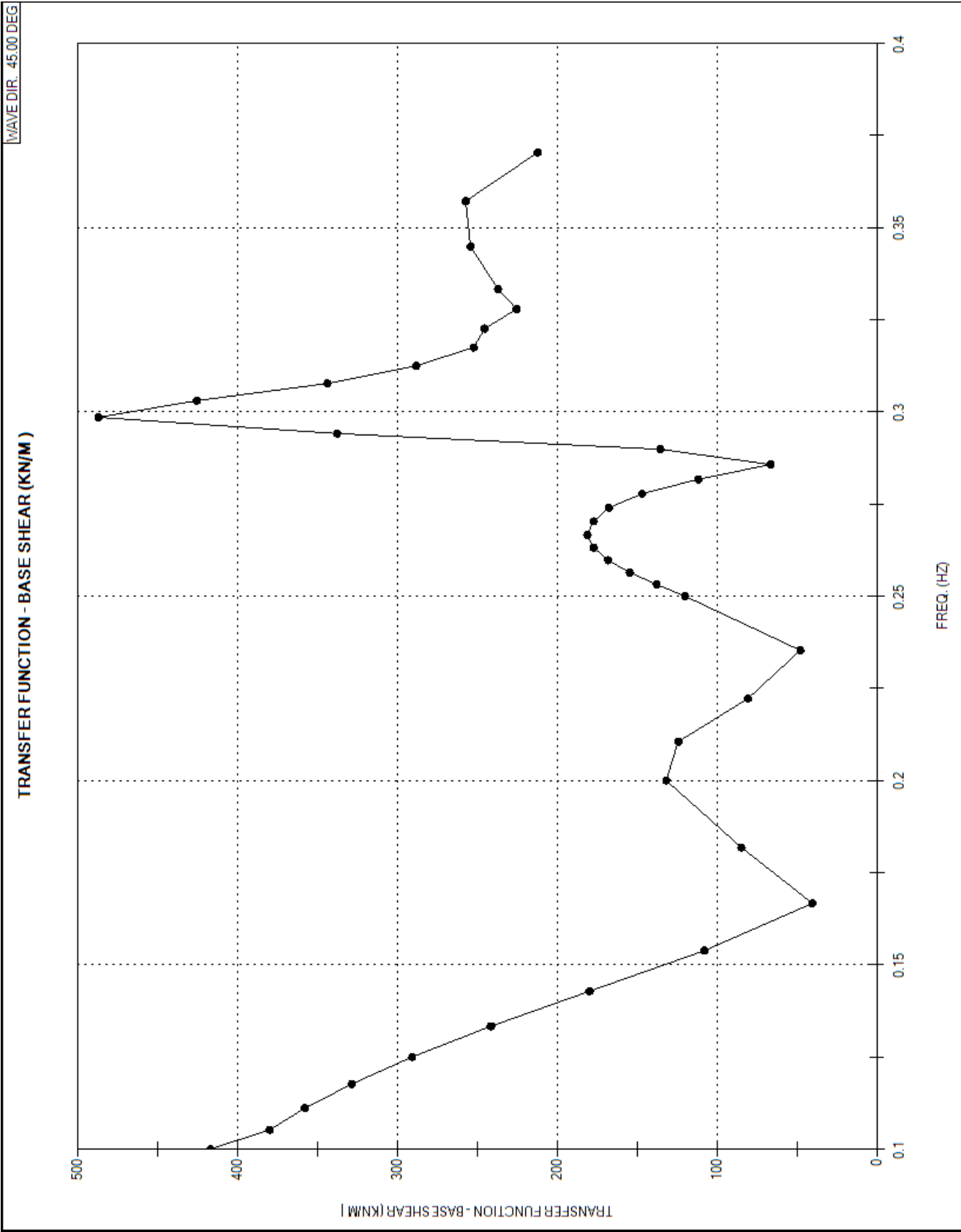


Figure 3-49 Dynamic Transfer Function (45°, 1/16)

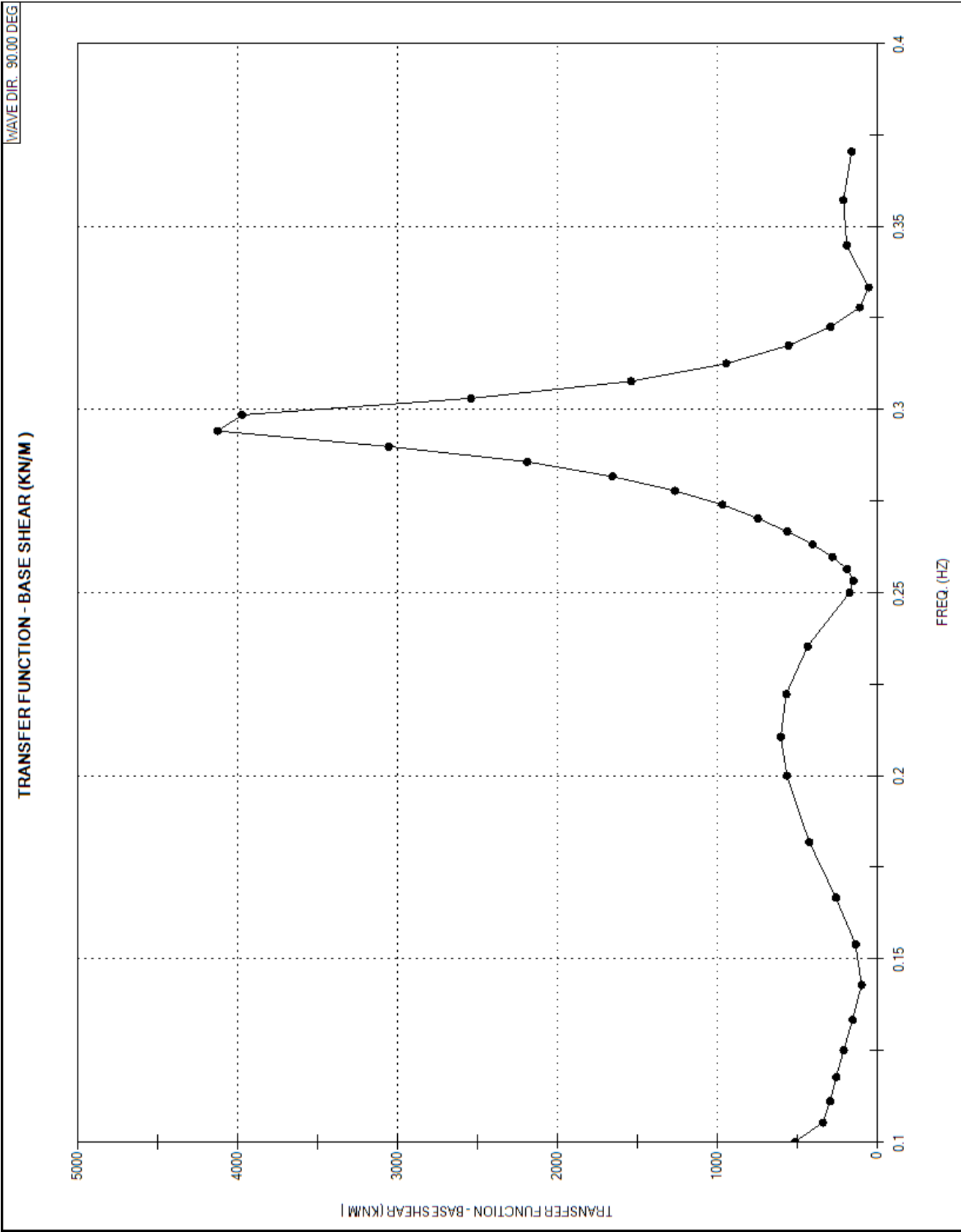


Figure 3-50 Dynamic Transfer Function (90°, 1/16)

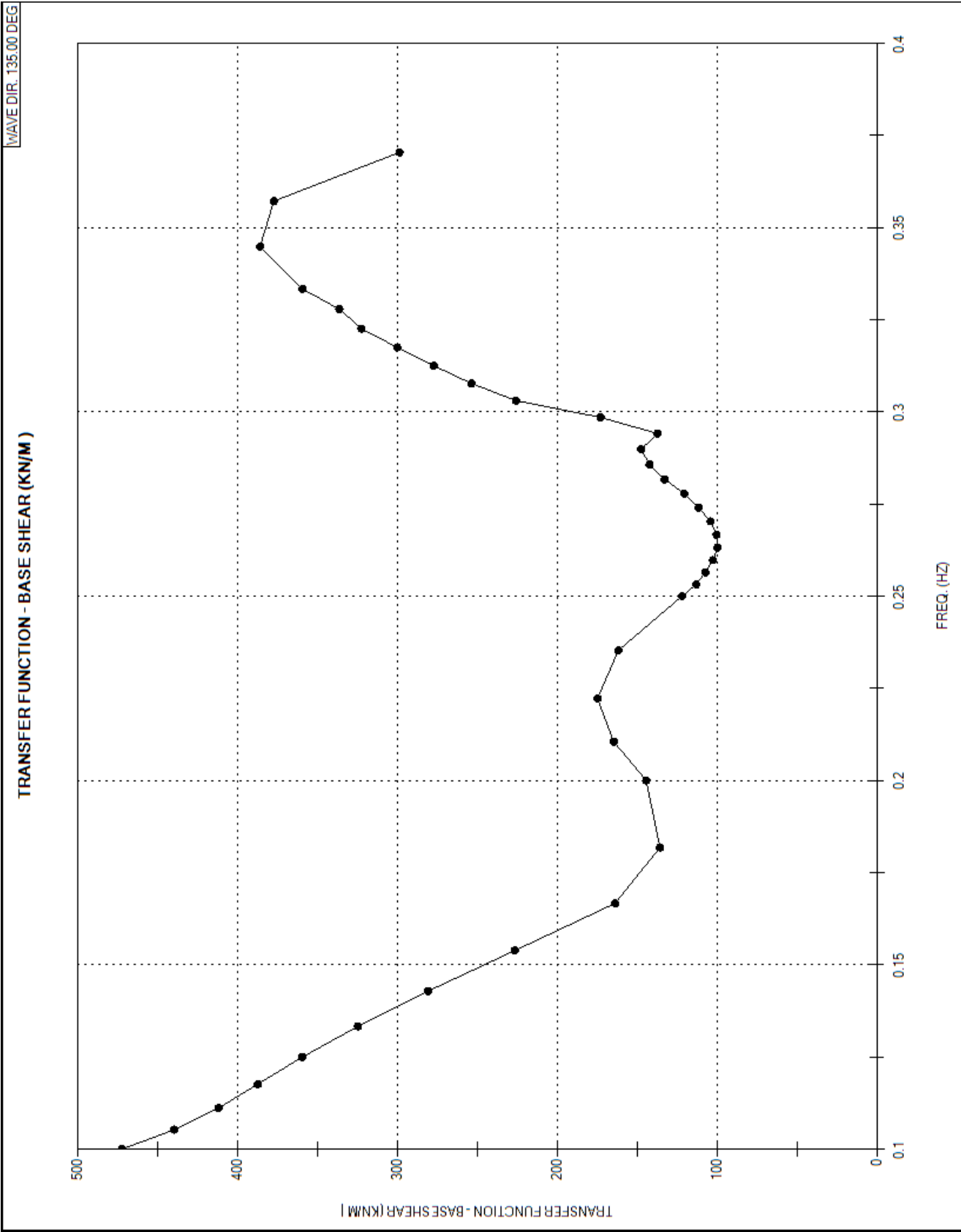


Figure 3-51 Dynamic Transfer Function (135°, 1/16)

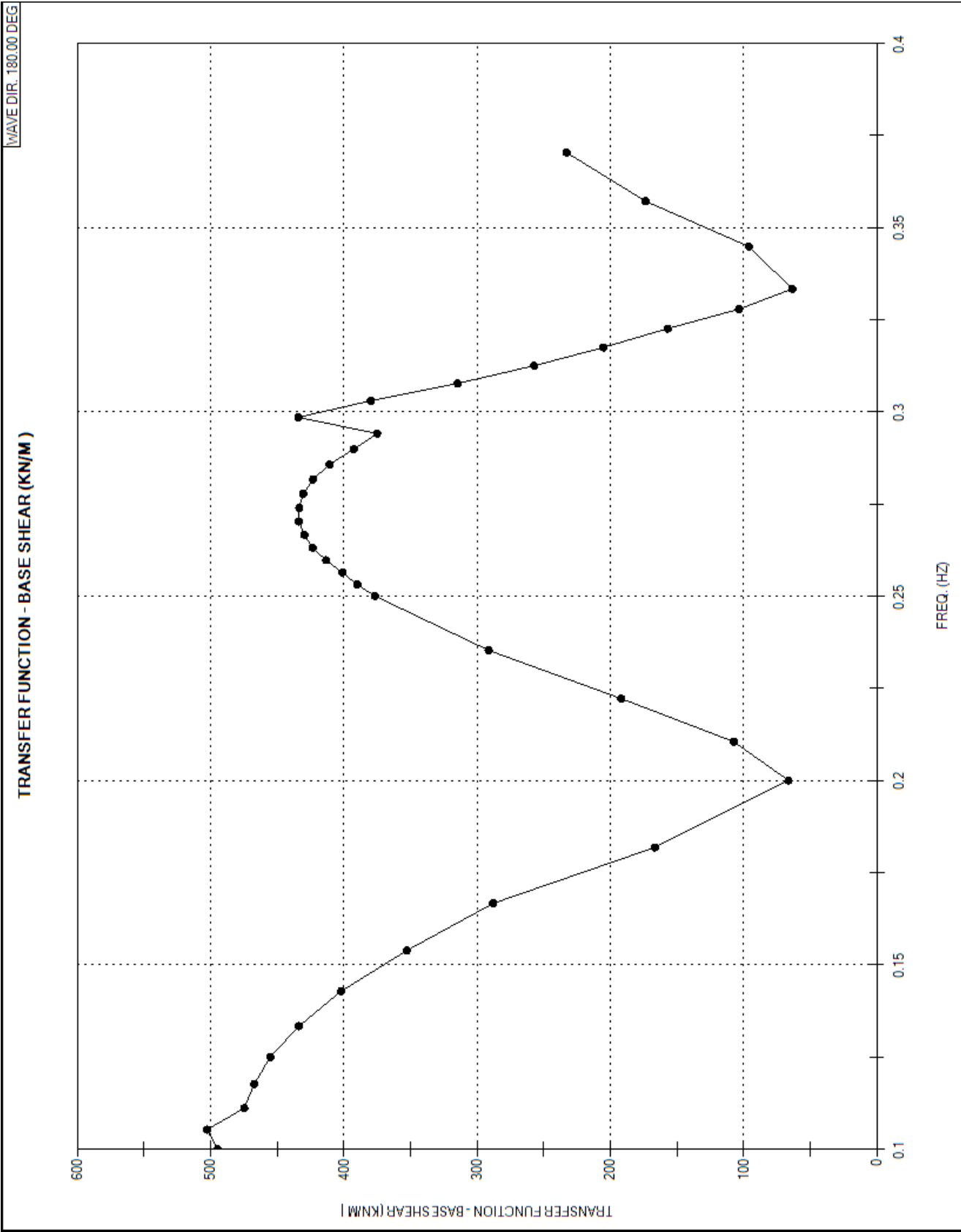


Figure 3-52 Dynamic Transfer Function (180°, 1/16)

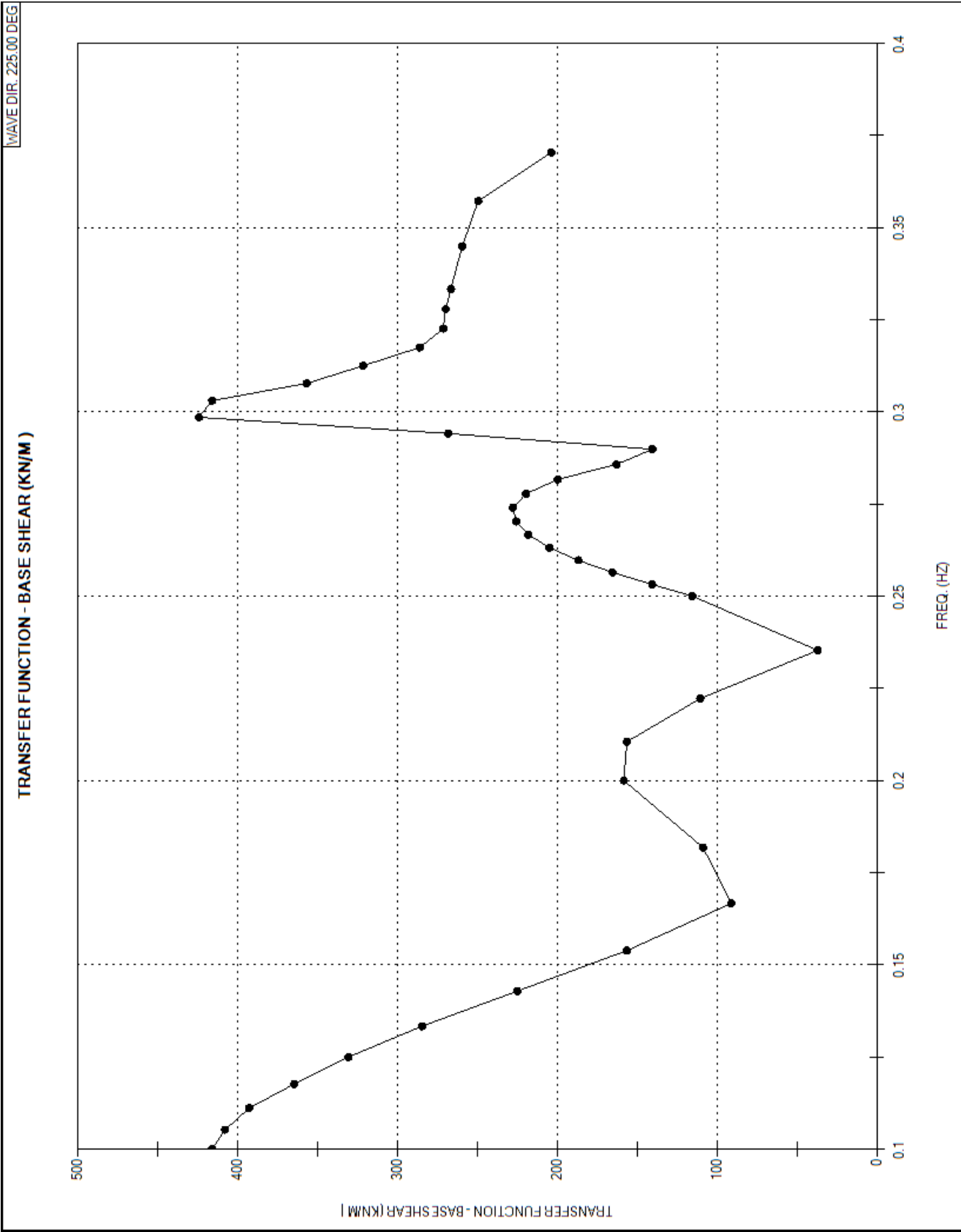


Figure 3-53 Dynamic Transfer Function (225°, 1/16)

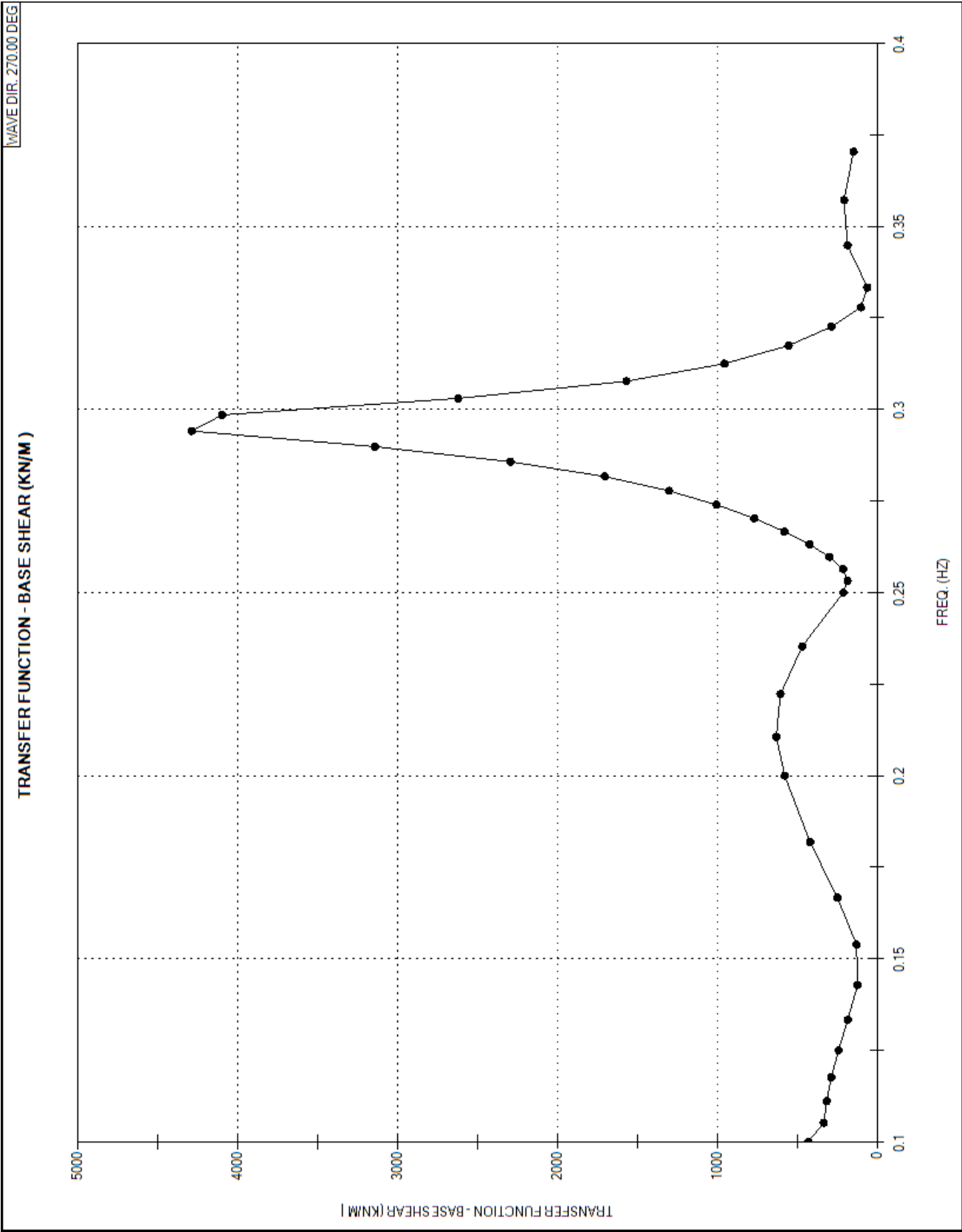


Figure 3-54 Dynamic Transfer Function (270°, 1/16)



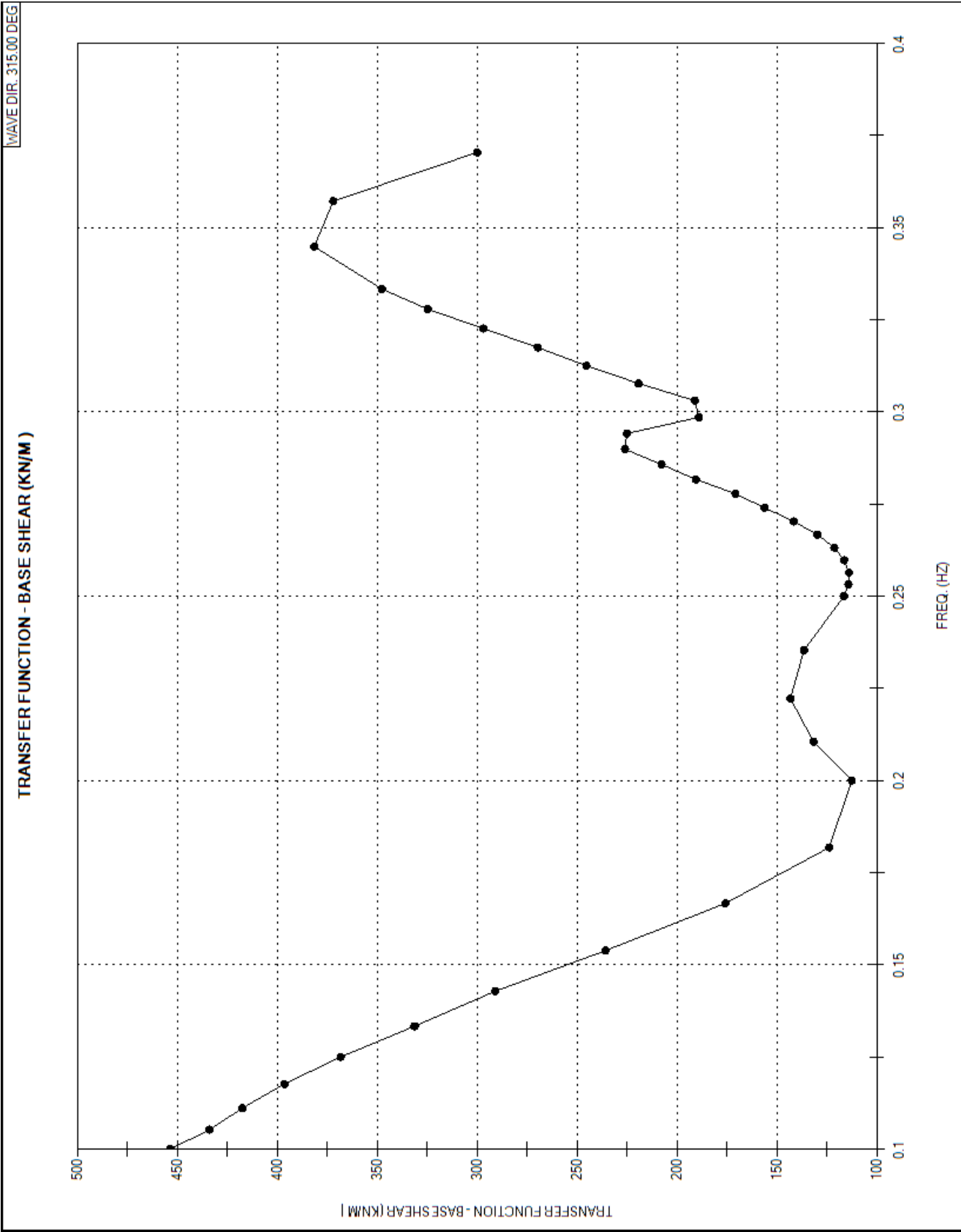


Figure 3-55 Dynamic Transfer Function (315°, 1/16)

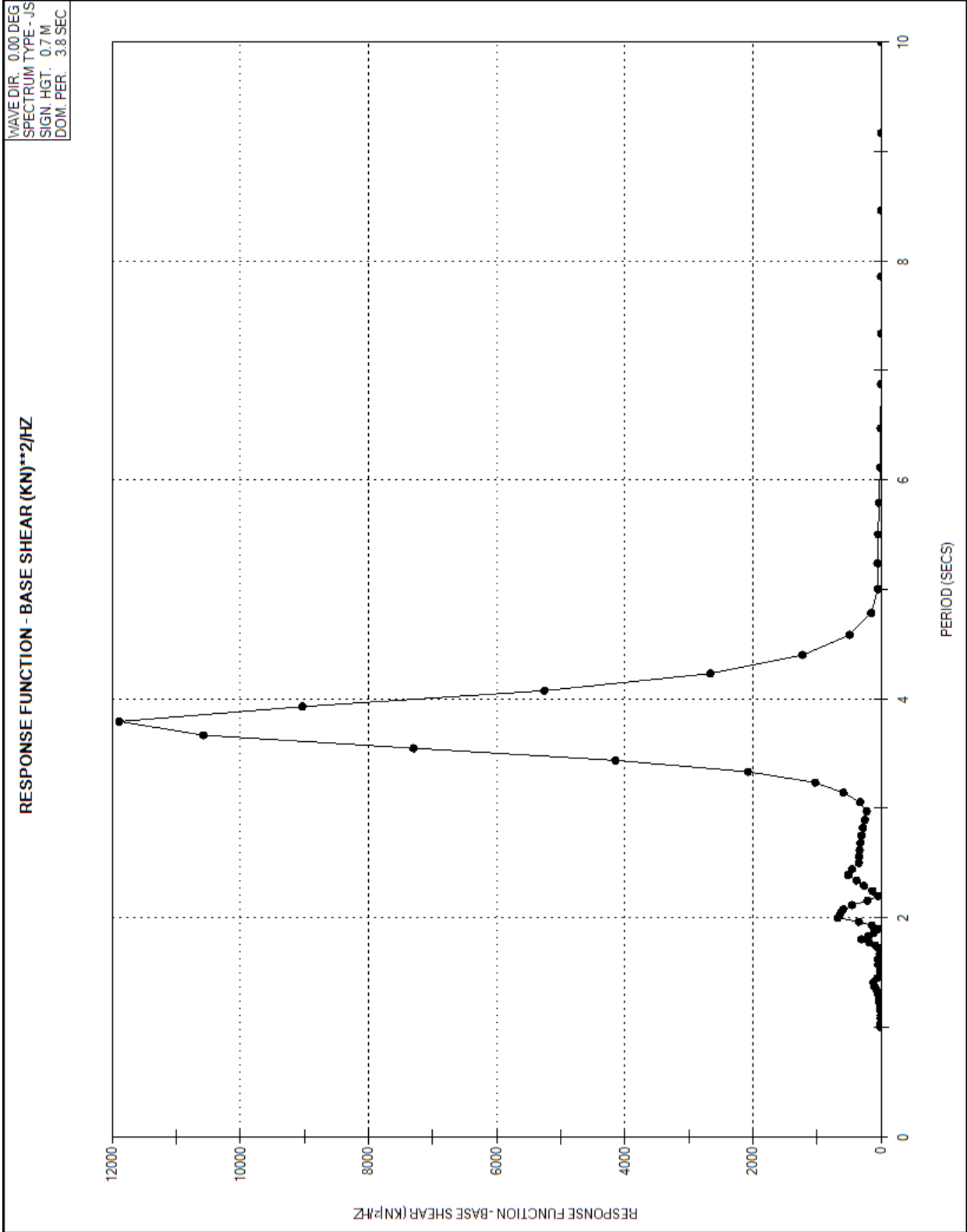


Figure 3-56 Response function (0°, 1/15)

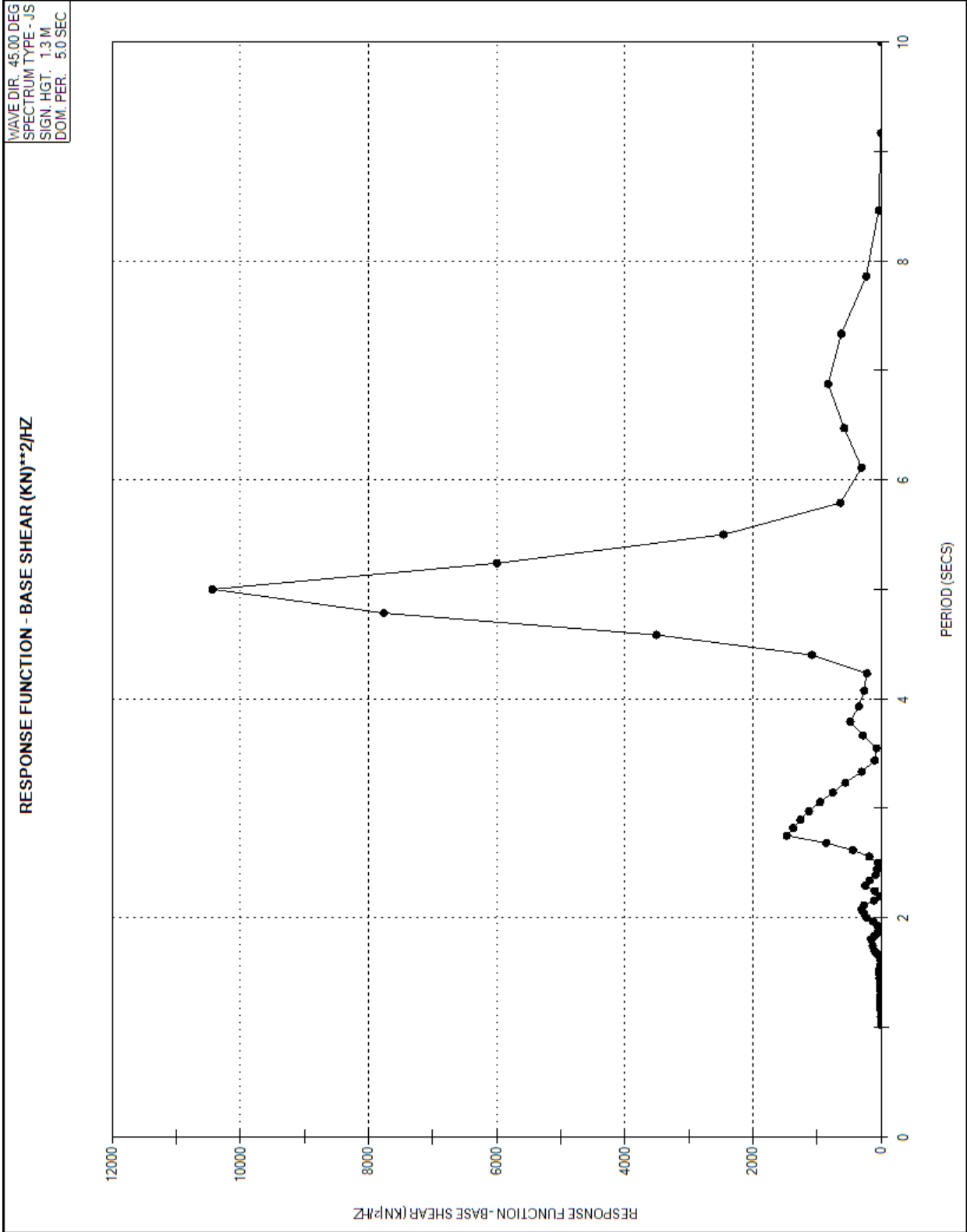


Figure 3-57 Response function (45°, 1/15)

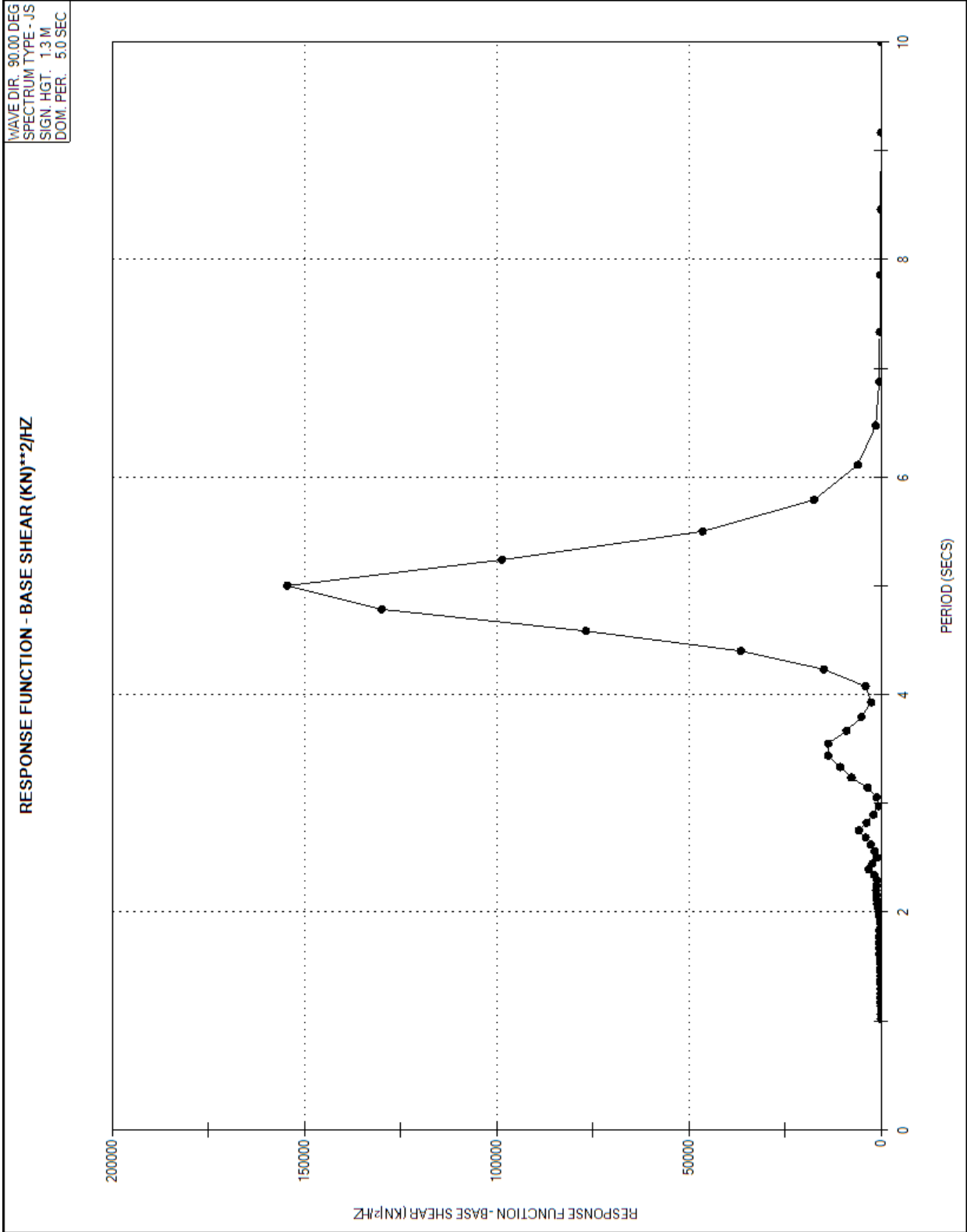


Figure 3-58 Response function (90°, 1/15)

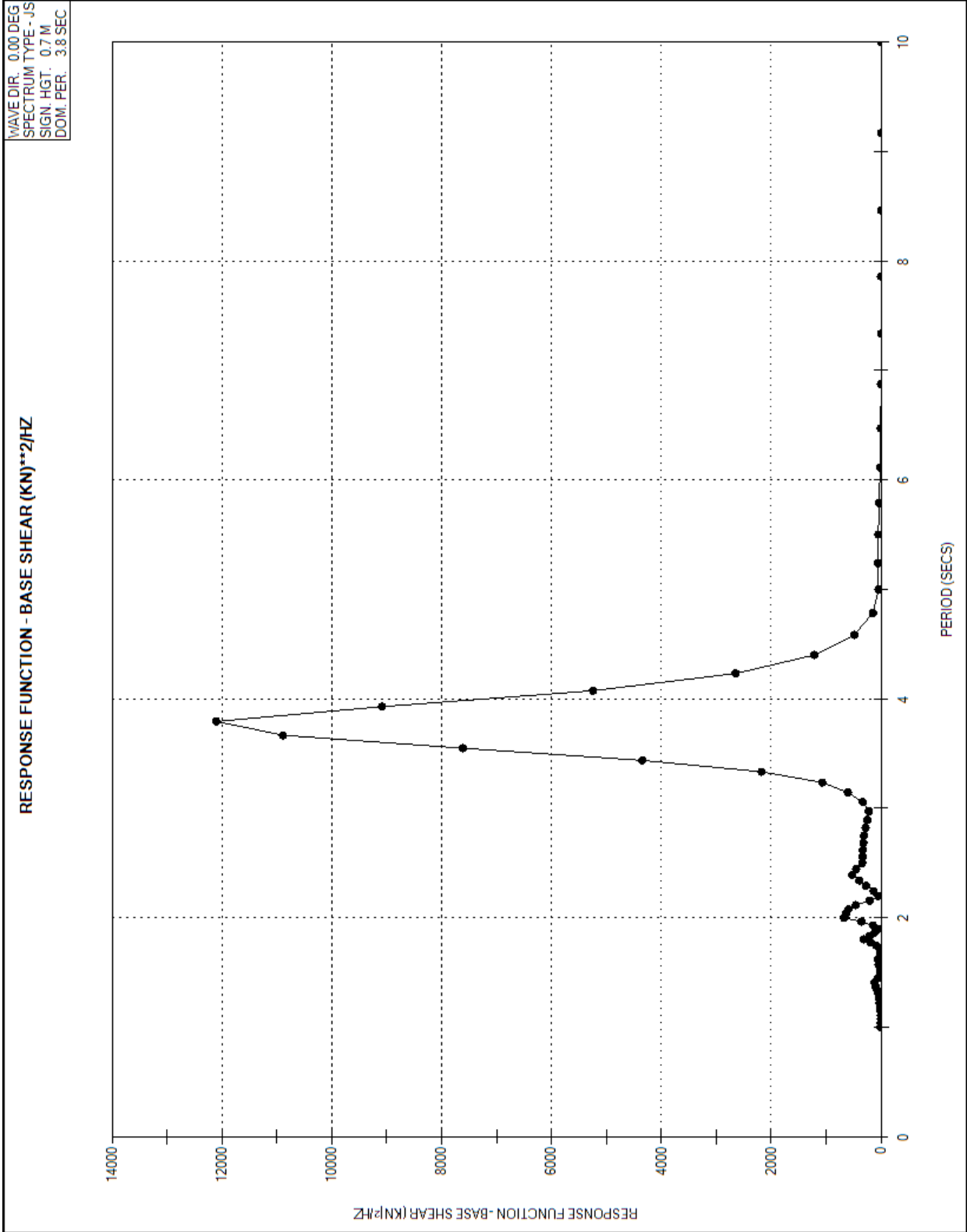


Figure 3-59 Response function (0°, 1/20)

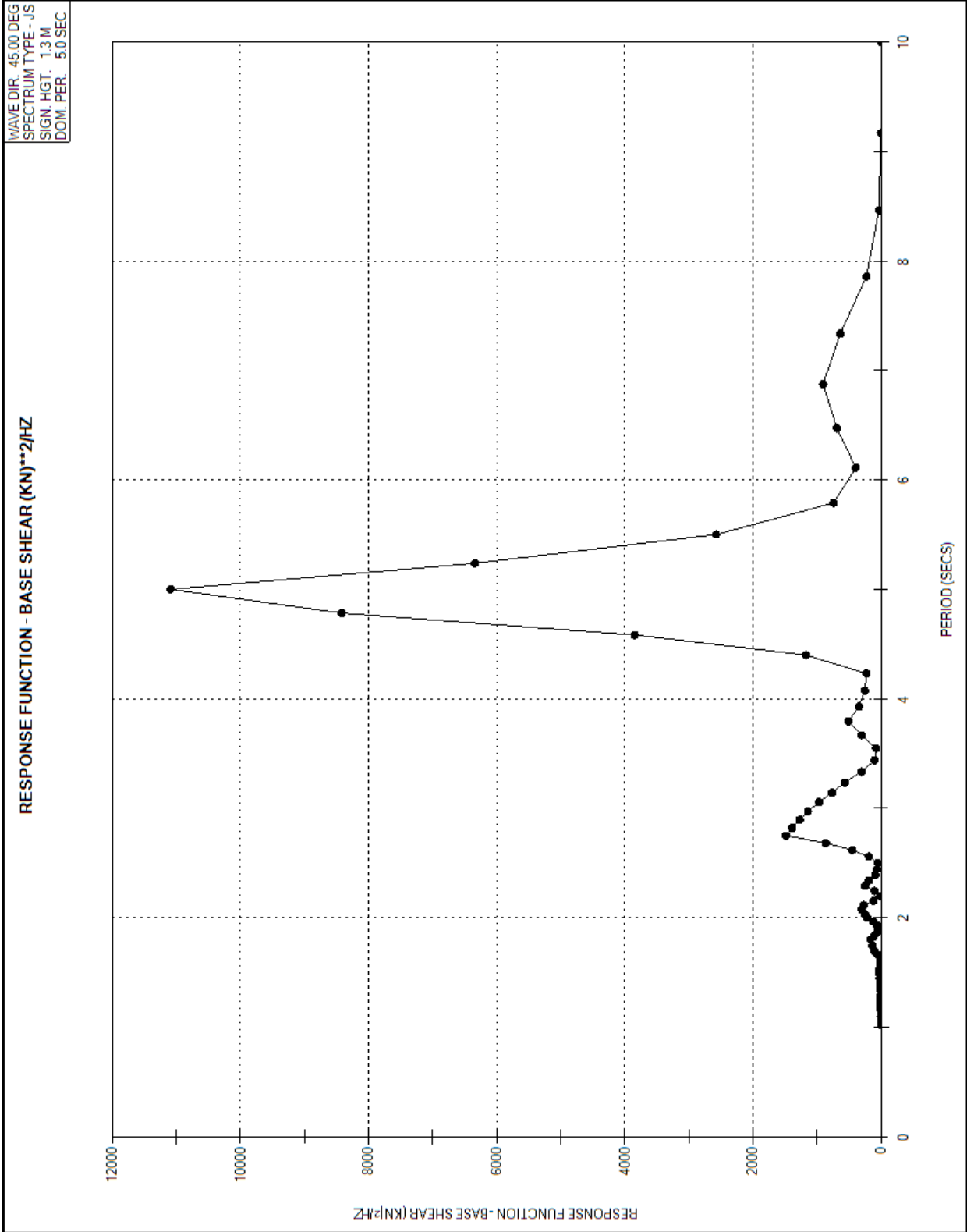


Figure 3-60 Response function (45°, 1/20)

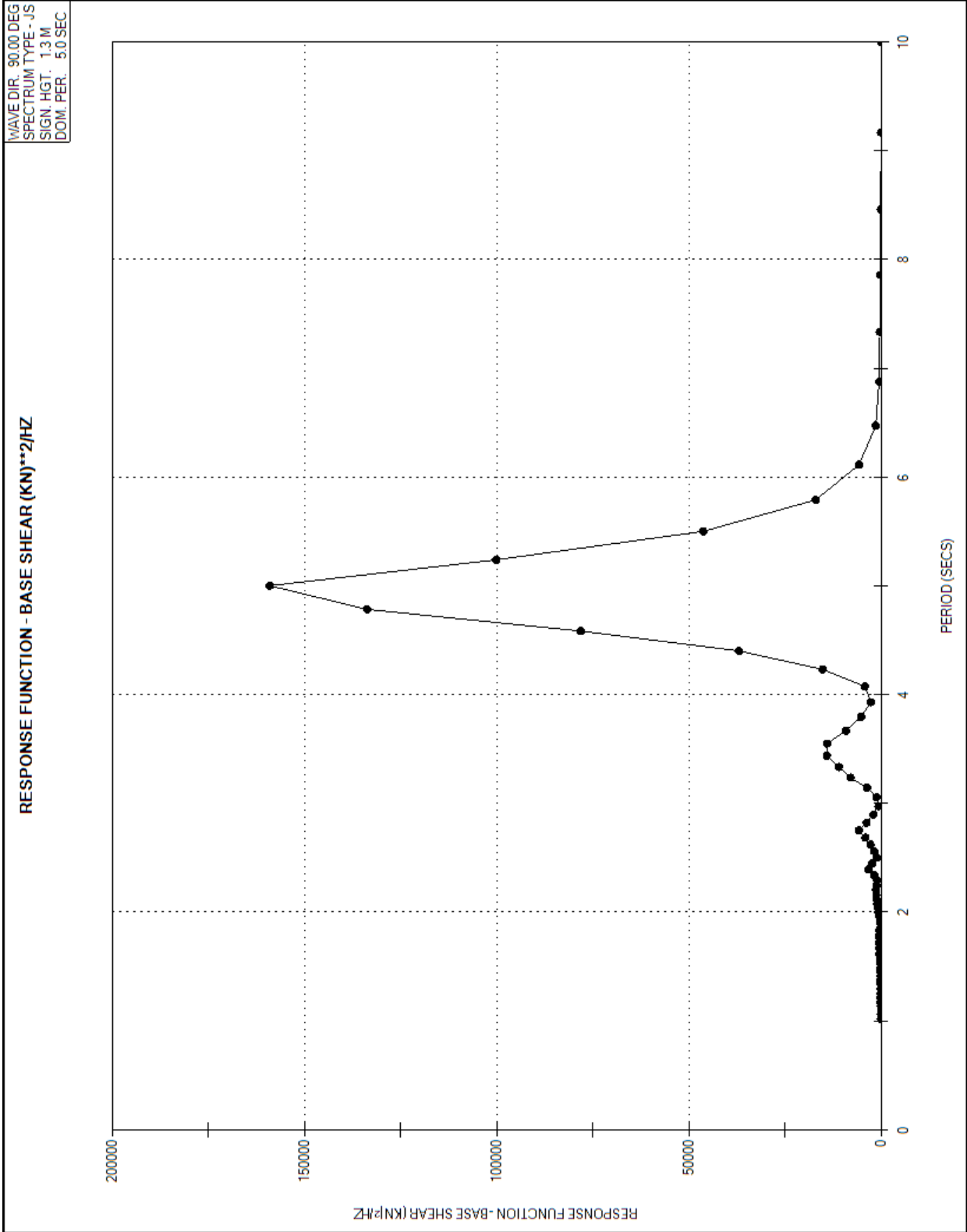


Figure 3-61 Response function (90°, 1/20)

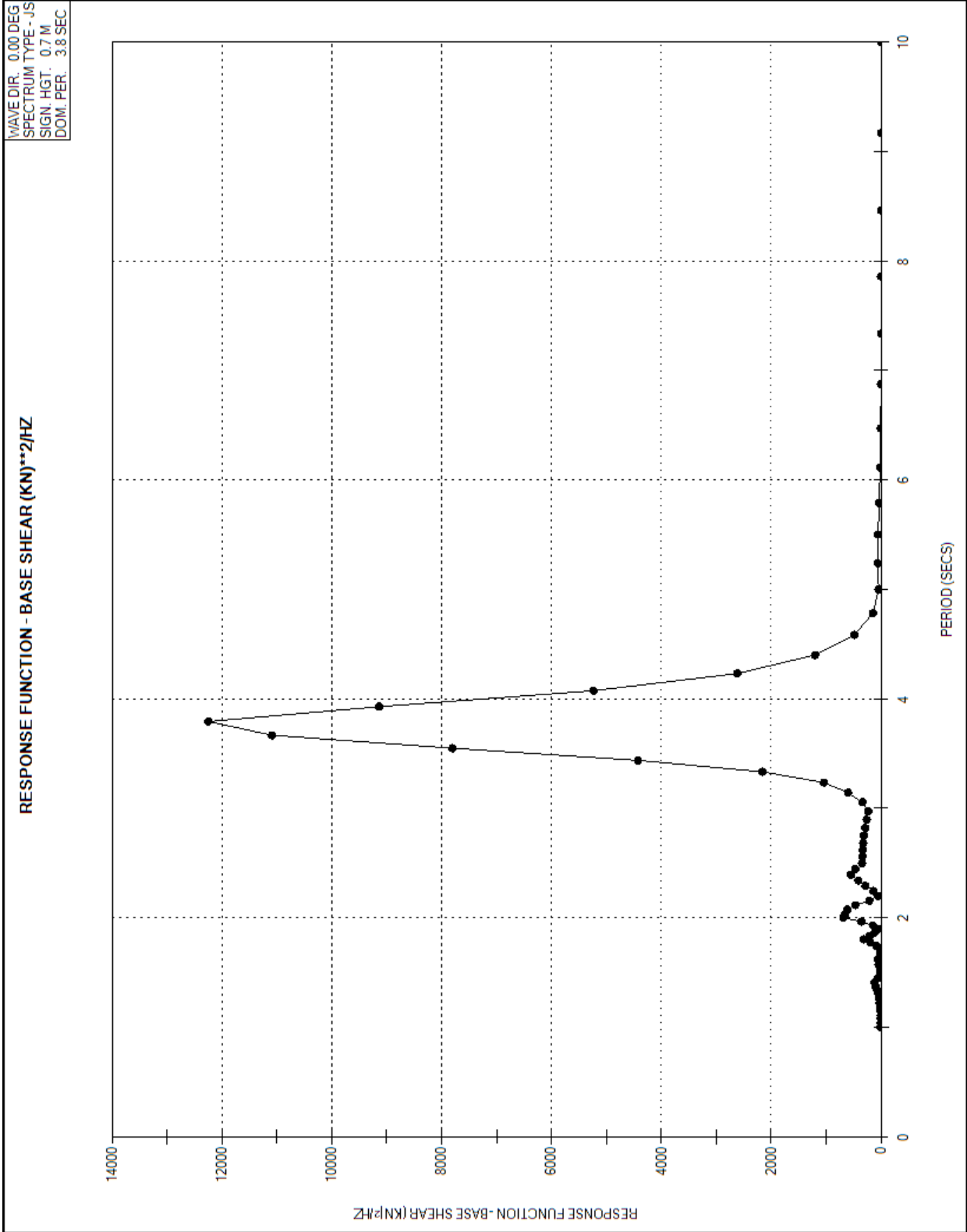


Figure 3-62 Response function (0°, 1/25)



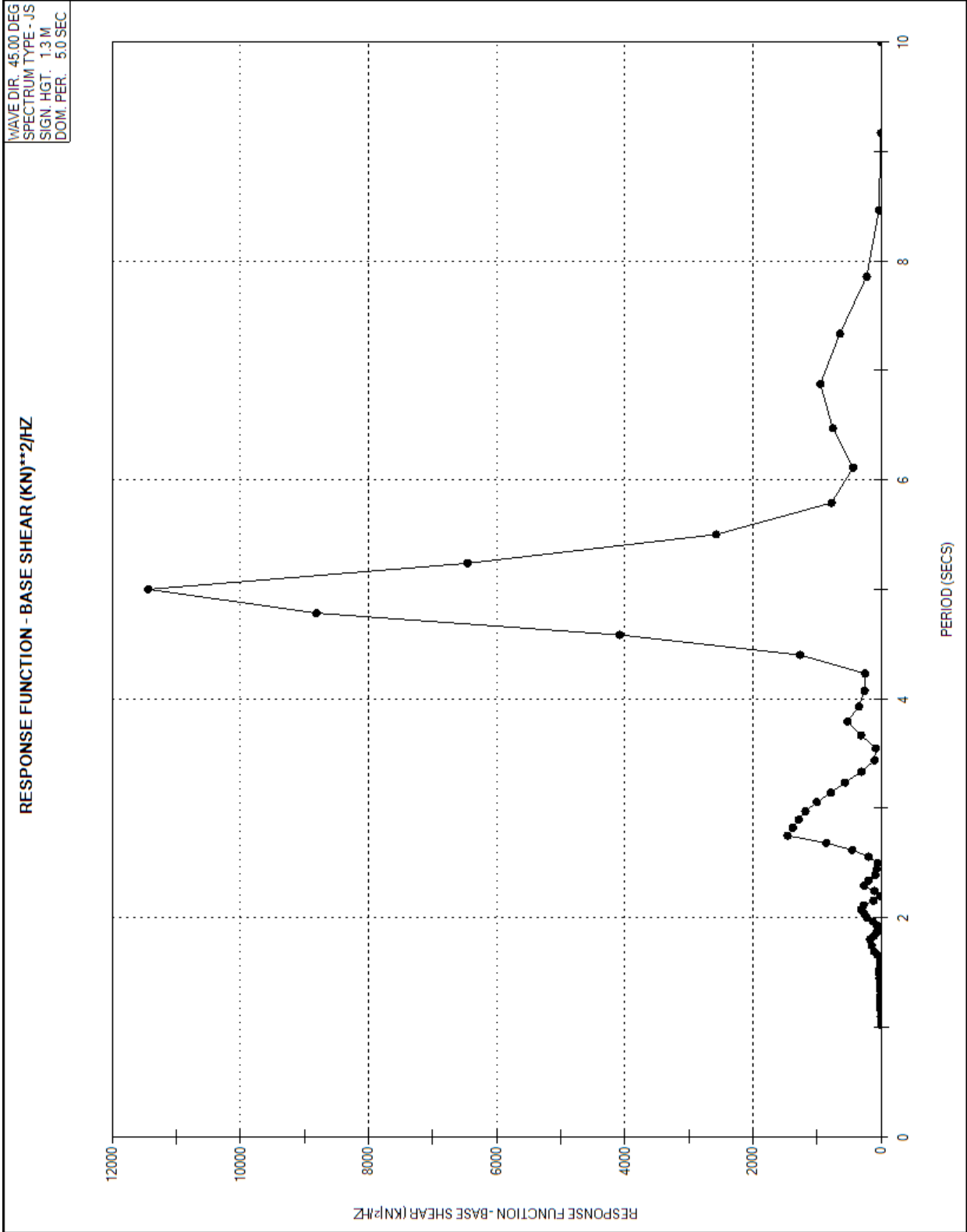


Figure 3-63 Response function (45°, 1/25)

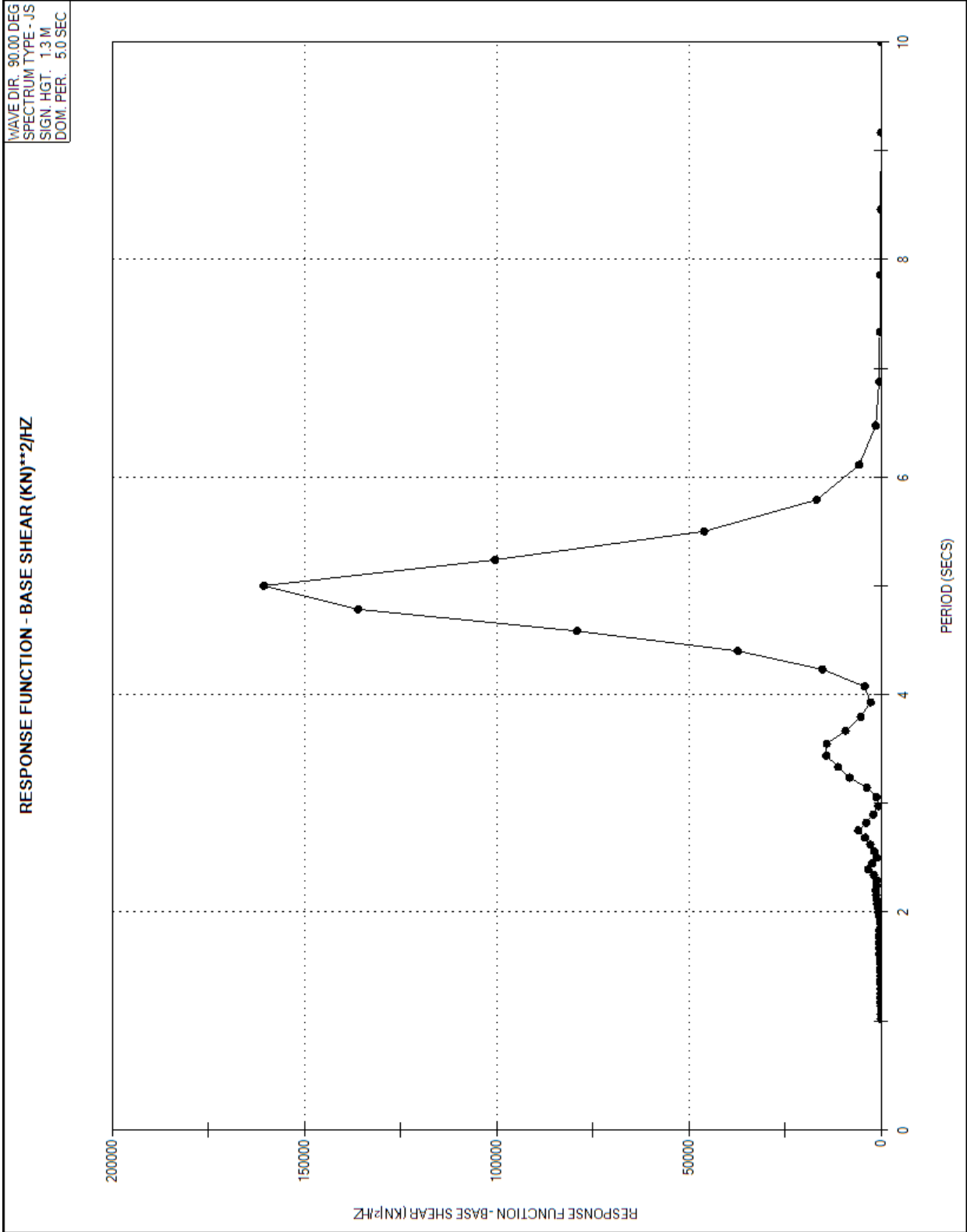


Figure 3-64 Response function (90°, 1/25)

## 3.7 Dynamic Analysis

For dynamically sensitive systems a dynamic analysis is required to assess the structural response. Such an analysis is required if the natural periods of the structure are in the range where there is sufficient wave energy to excite significant dynamic response. The natural periods of a structure are the most important indicators of the dynamic characteristics of the structure and depend on the stiffness distribution or mass distribution of the model.

The mass that will be dynamically excited and the distribution of that mass should be accurately represented in the dynamic analysis model. For fatigue analyses it is generally appropriate to consider a lower response level and a correspondingly stiffer foundation. Quasi static response analysis is performed using the dynamic analysis model with the mass and damping terms set to zero.

Since the dynamic module in SACS uses the linear theory (i.e. modal superposition), linearized foundation super elements are automatically created at each pile-head by the PSI program. To linearize the foundation for evaluation of fatigue damage, pile stubs of appropriate stiffness are modelled.

An equivalent solution to pile–soil interaction is considered using the pile stub to account for finite deflections of the pile (the  $P-\delta$  effect). For derivation of the pile stubs, the most probable maximum wave corresponding to the centre of fatigue damage scatter diagram is considered.

A normal in-place analysis with these waves is carried out to obtain the pile head forces. Using these forces, pile stub properties are determined by using “*SINGLE PILE*” module of SACS. Different load cases are used to calculate stiffness in each orthogonal direction as well as the diagonal direction.

With the spectral analysis method, dynamic response can be included by using a frequency domain dynamic solution instead of a quasi-static solution, for the structural analyses used to determine member nominal stresses. The steady state dynamic response to each of the regular waves stepped through the structure is thus included in the resulting hot spot stress range transfer functions.

The linearized (Airy) wave theory is adopted to model the wave elevation, water particle velocity and accelerations. However, this modelling is limited by the linearity of wave component superposition assumptions and does not include nonlinear wave characteristics. Since the fatigue damage accumulation experienced by jackets is mainly caused by wave

loadings due to small and medium sized waves, this linear assumption can normally yield sufficiently accurate wave loading calculation results (Jia, 2008).

Dynamic characteristics (mode shapes and frequencies) of the structure are generated with a reduced structural stiffness matrix and consistent mass approach. When dealing with very large structures (particularly lattice structures) the technique of *mass condensation* may be used (Guyan, 1965).

A set of master (retained) degrees of freedom are selected at each horizontal elevation on the main legs to extract the eigenvalues (periods) and eigenvectors (mode shapes), which includes all stiffness and mass properties related to the reduced degrees of freedom. After the modes are extracted using the master degrees of freedom, they are expanded to include the full 6 degrees of freedom for all joints in the structure.

A consistent mass approach is considered since it is more desirable for structures immersed in the fluid. The added mass is generated automatically by SACS and depends on the size, orientation and proximity of the member to the free surface. Entrapped mass is calculated for members designated as flooded in the model file. Refer to the weight and centre of gravity summary in Table 3-34. Hydrodynamic effects of marine growth are included in the program to account for the density and effective diameter due to marine growth.

For dynamic analyses, energy dissipation due to damping should be accounted for. The choice of damping value can have a profound effect. Offshore structures are very lightly damped. The physical sources of damping are difficult to determine and to quantify with any certainty. For the purpose of a fatigue analysis, damping shall be modelled by a viscous damping coefficient that accounts for all sources of damping including structural, foundation and hydrodynamic effects. For typical pile founded tubular space frame substructures, a total damping value of 2% of critical damping is appropriate.

A relative velocity formulation of the Morison equation inseparably links wave load excitation and hydrodynamic drag damping. It will reduce wave loading experienced and cause implicit additional hydrodynamic damping from drag forces. For small structural displacements, as are typical in fatigue loading conditions, this additional damping is not observed in measurements. Consequently, the relative velocity formulation should not be normally used in the fatigue analysis.

Where required, damping can normally be modelled by viscous damping using a damping ratio (a non-dimensional damping coefficient). Energy dissipation due to damping has a

profound effect on structural response calculations at and in the immediate vicinity of the resonant frequency or frequencies. Outside the resonance region, the influence of damping is negligible.

The eigenvalue parameters for the first 10 mode shapes are presented in Table 3-35. The maximum deflection for modes are presented in Table 3-36 and normalized degrees of freedom are highlighted in the same table. The mass participation factor for retained degrees of freedom (DoF) and expanded DoF are presented in Table 3-37 and Table 3-38 from the dynamic analysis results. The mass participation factor should be above 90% in at least two lateral directions.

Table 3-34 Weight and centre of gravity summary

***** ITEM DESCRIPTION *****	***** WEIGHT *****	***** CENTER OF GRAVITY *****
	X Y Z	X Y Z
	KN KN KN	M M M
PLATE ELEMENTS	2669.964 2669.964 2669.964	0.255 0.628 23.625
MEMBER ELEMENTS	23877.665 23877.665 23877.665	0.864 0.585 4.177
MEMBER ELEMENT NORMAL ADDED MASS	6802.370 6501.305 3587.666	0.344 1.844 -22.250
FLOODED MEMBER ELEMENT ENTRAPPED FLUID	2875.177 2875.177 2875.177	-0.559 2.369 -19.210
LOAD CASES CONVERTED TO WEIGHTS	44923.086 44923.086 44923.086	-0.033 0.784 23.879
***** TOTAL *****	81148.262 80847.196 77933.558	0.254 0.862 14.121

**Table 3-35 Frequencies and generalized mass**

MODE	FREQ. (CPS)	GEN. MASS	EIGENVALUE	PERIOD (SECS)
1	0.297	5.78E+03	2.88E-01	3.37
2	0.526	4.99E+03	9.17E-02	1.90
3	0.728	3.81E+03	4.78E-02	1.37
4	1.479	1.26E+02	1.16E-02	0.68
5	1.547	4.55E+02	1.06E-02	0.65
6	1.645	2.61E+03	9.36E-03	0.61
7	2.037	2.58E+03	6.10E-03	0.49
8	2.434	8.12E+03	4.28E-03	0.41
9	2.658	3.43E+03	3.59E-03	0.38
10	2.690	5.61E+03	3.50E-03	0.37

**Table 3-36 Maximum deflection for modes**

Mode	X-Defl. cm	Joint	Y-Defl. cm	Joint	Z-Defl. cm	Joint
1	-0.017	7520	<b>2.540</b>	<b>7120</b>	0.076	7110
2	<b>2.540</b>	<b>7520</b>	0.050	6101	-0.115	199
3	<b>2.540</b>	<b>7120</b>	-1.222	7501	0.072	101
4	0.013	181	<b>2.540</b>	<b>104</b>	-0.007	381
5	-0.027	399	<b>2.540</b>	<b>111</b>	-0.027	199
6	<b>2.540</b>	<b>281</b>	0.333	103	0.523	6120
7	<b>2.540</b>	<b>201</b>	-1.888	201	-0.407	301
8	-1.909	219	<b>2.540</b>	<b>7120</b>	1.818	6120
9	1.557	219	<b>2.540</b>	<b>115</b>	-1.877	7520
10	1.997	201	1.848	112	<b>2.540</b>	<b>7101</b>

**Table 3-37 Mass participation factor based on retained DoF**

Mode	X	Y	Z	Cumulative		
1	0.0000003	0.8306850	0.0000029	0.000000	0.830685	0.000003
2	0.8809174	0.0000001	0.0000022	0.880918	0.830685	0.000005
3	0.0001817	0.0000461	0.0000009	0.881099	0.830731	0.000006
4	0.0000383	0.0103685	0.0004366	0.881138	0.841100	0.000443
5	0.0000165	0.1512184	0.0000080	0.881154	0.992318	0.000451
6	0.0980083	0.0000015	0.0002527	0.979162	0.992320	0.000703
7	0.0001535	0.0000058	0.0000221	0.979316	0.992326	0.000726
8	0.0047990	0.0004347	0.0005199	0.984115	0.992760	0.001245
9	0.0052279	0.0001086	0.4845560	0.989343	0.992869	0.485801
10	0.0041544	0.0000377	0.4666680	0.993497	0.992907	0.952469

**Table 3-38 Mass participation factor based on expanded DoF**

Mode	X	Y	Z	Cumulative		
1	0.0000003	0.8400767	0.0000029	0.000000	0.840077	0.000003
2	0.8886507	0.0000001	0.0000022	0.888651	0.840077	0.000005
3	0.0001883	0.0000478	0.0000009	0.888839	0.840125	0.000006
4	0.0000365	0.0099481	0.0003967	0.888876	0.850073	0.000403
5	0.0000157	0.1427269	0.0000067	0.888891	0.992800	0.000409
6	0.0933678	0.0000012	0.0002533	0.982259	0.992801	0.000663
7	0.0001411	0.0000038	0.0000219	0.982400	0.992805	0.000685
8	0.0042038	0.0004773	0.0005203	0.986604	0.993282	0.001205
9	0.0044583	0.0001119	0.4847427	0.991063	0.993394	0.485948
10	0.0035019	0.0000491	0.4667915	0.994564	0.993443	0.952739

\*\*\* EFFECTIVE WEIGHT: X 81038.307 KN, Y 80728.788 KN, Z 77836.332 KN

Mode shapes for the first 10 mode of vibrations are presented in Figure 3-65 to Figure 3-74.



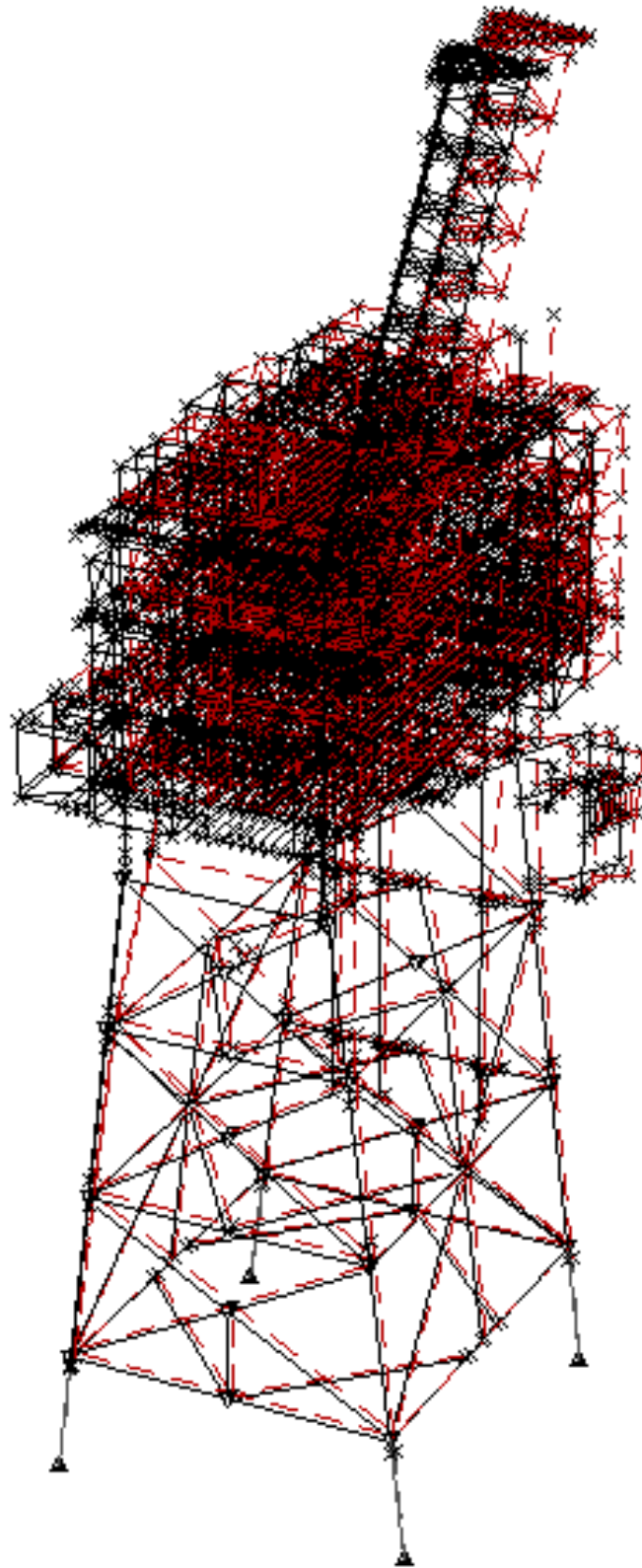
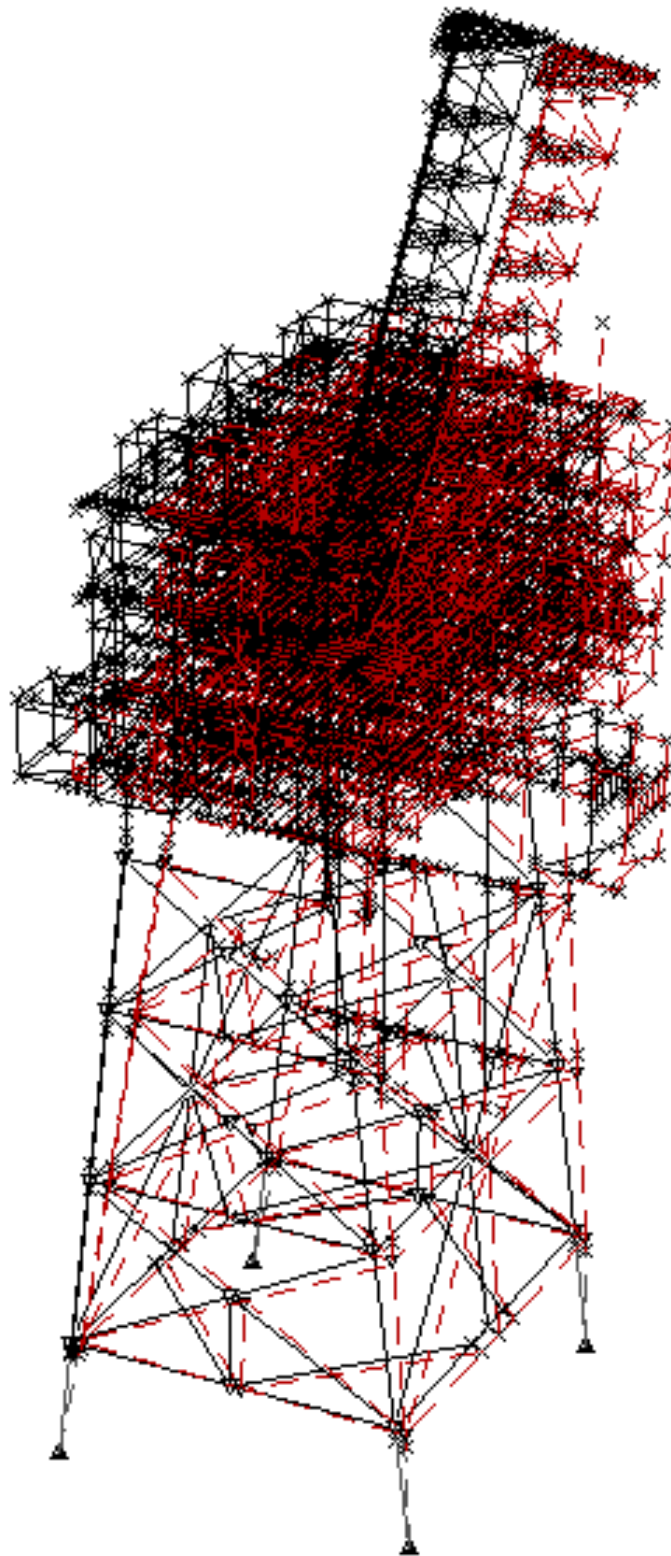
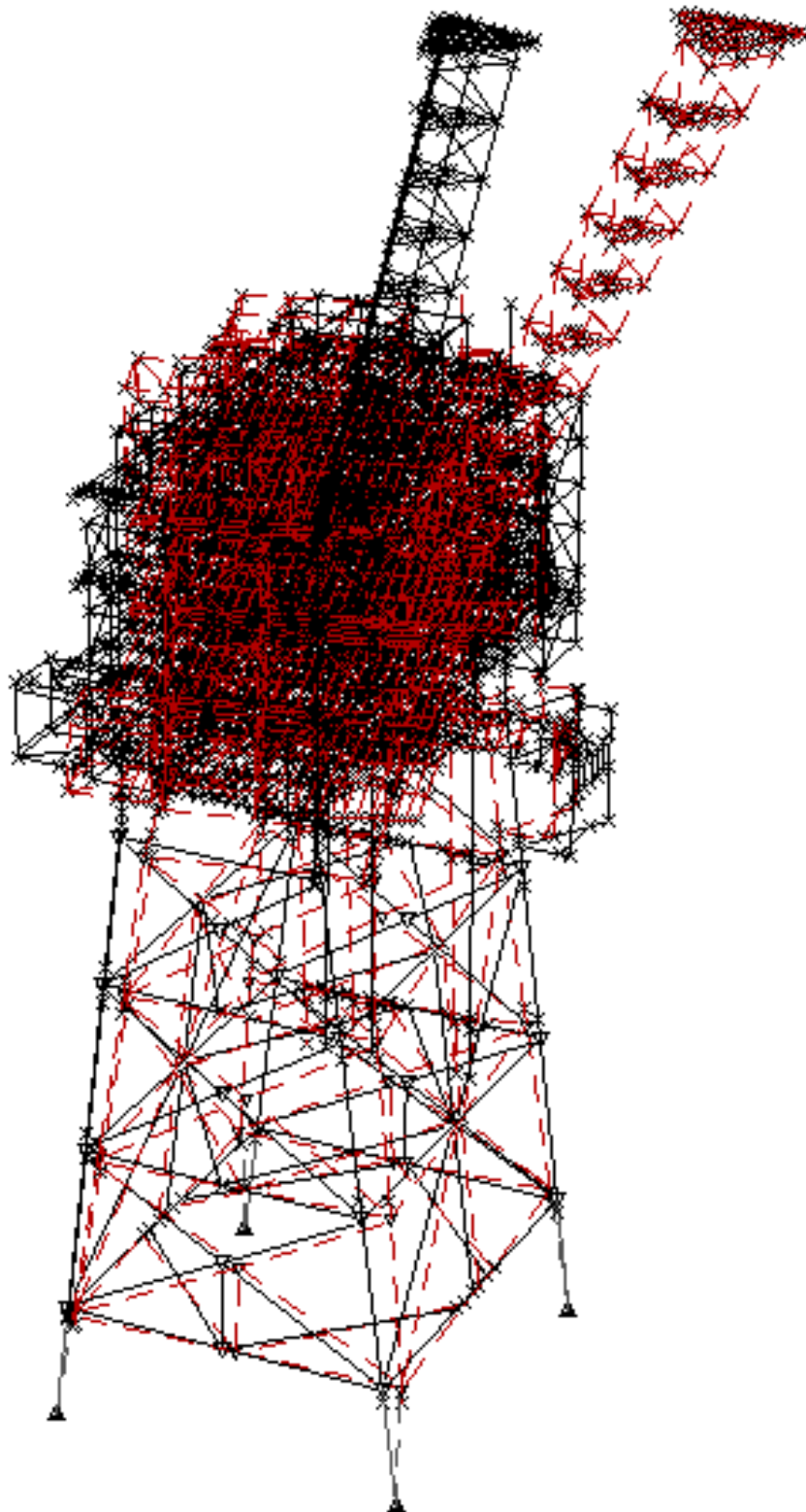


Figure 3-65 Deflected mode shape 1



**Figure 3-66 Deflected mode shape 2**



**Figure 3-67 Deflected mode shape 3**

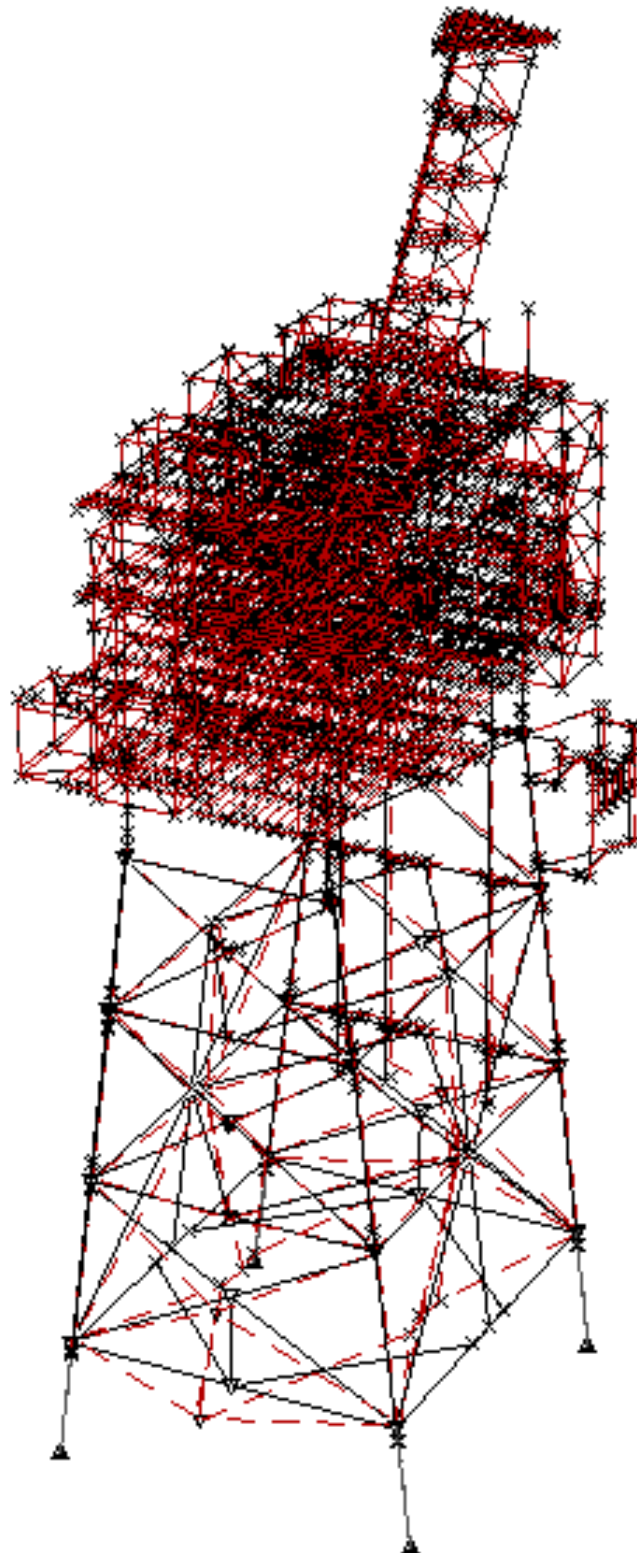
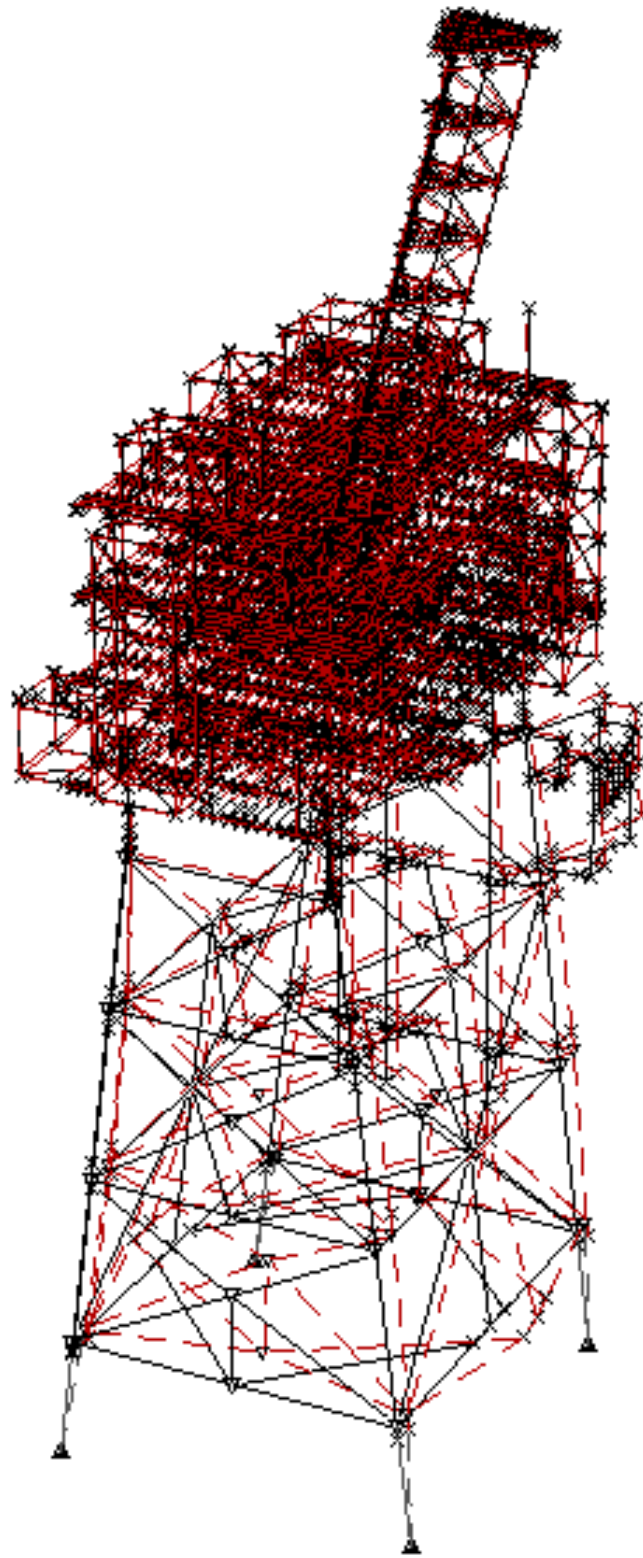
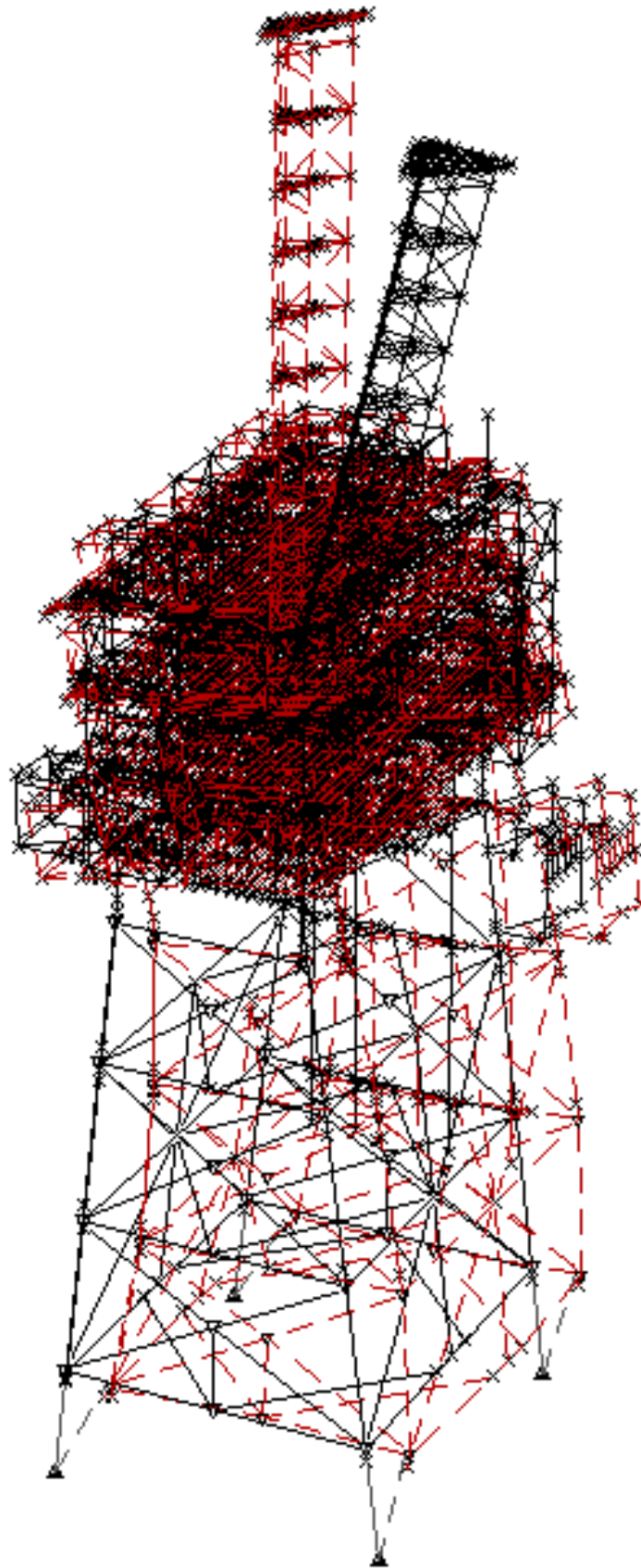


Figure 3-68 Deflected mode shape 4



**Figure 3-69 Deflected mode shape 5**





**Figure 3-70 Deflected mode shape 6**

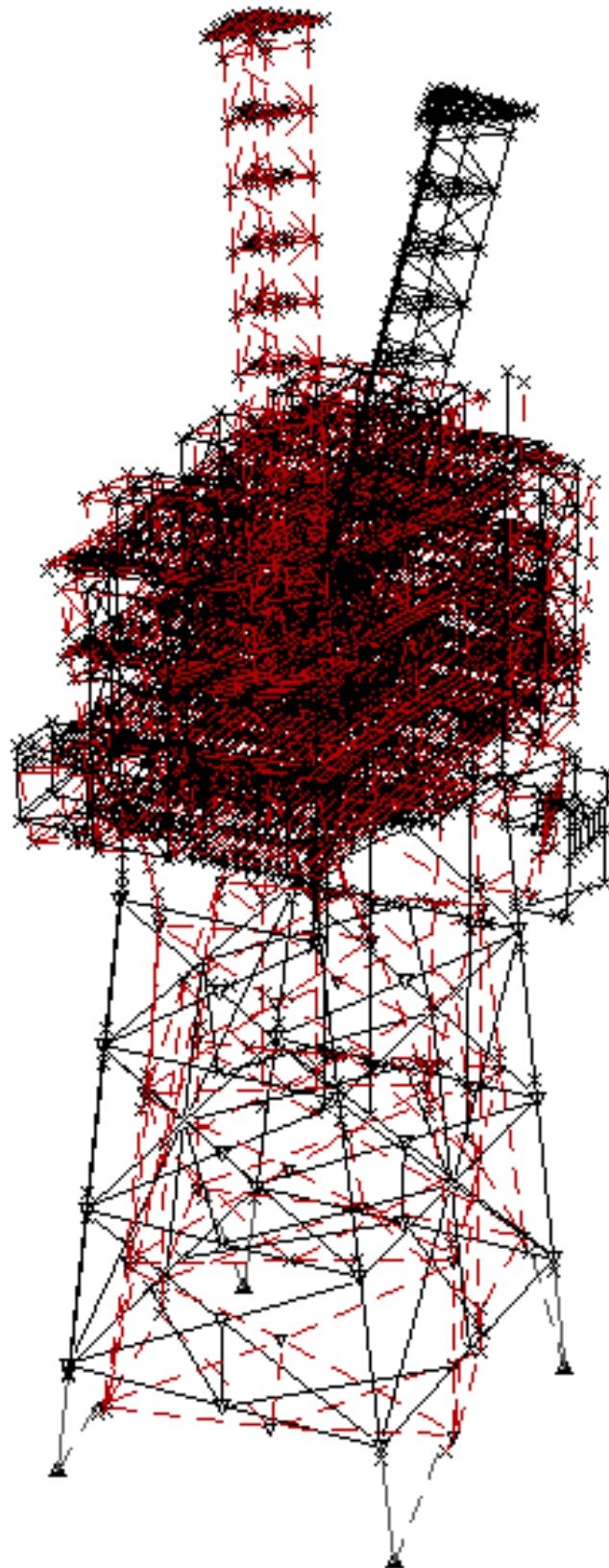


**Figure 3-71 Deflected mode shape 7**

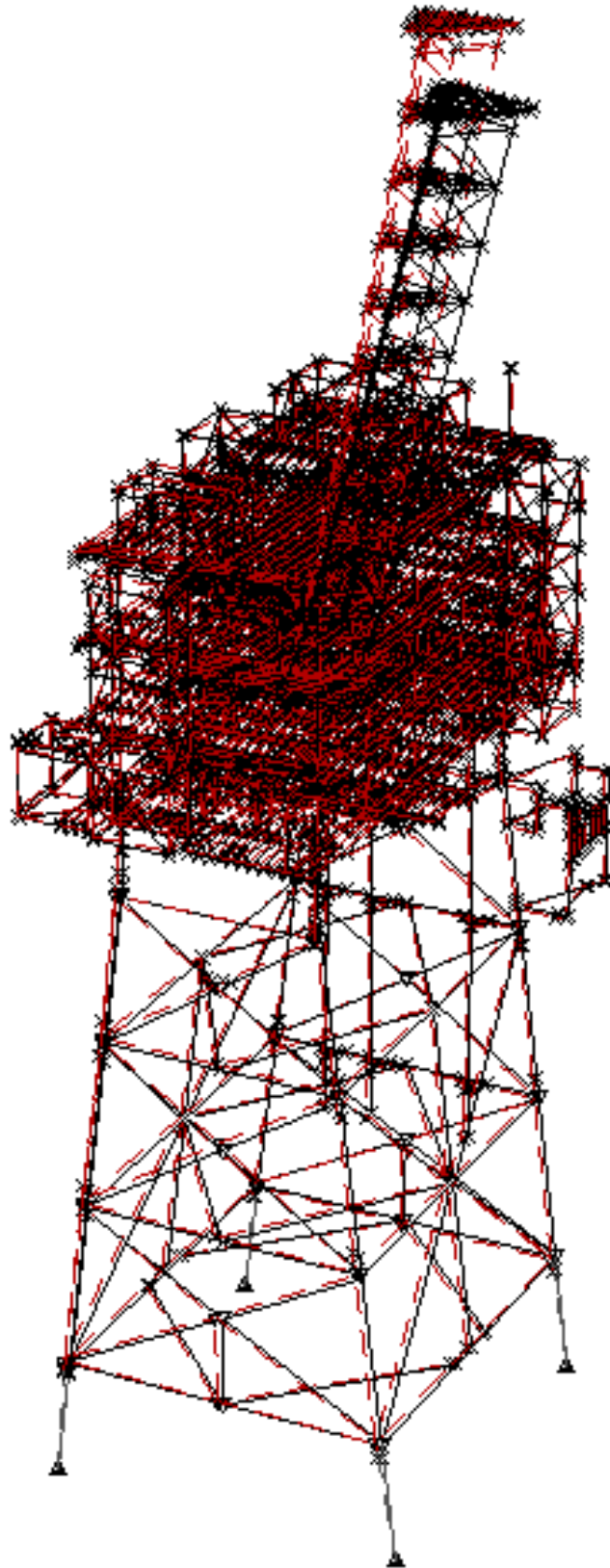


**Figure 3-72 Deflected mode shape 8**



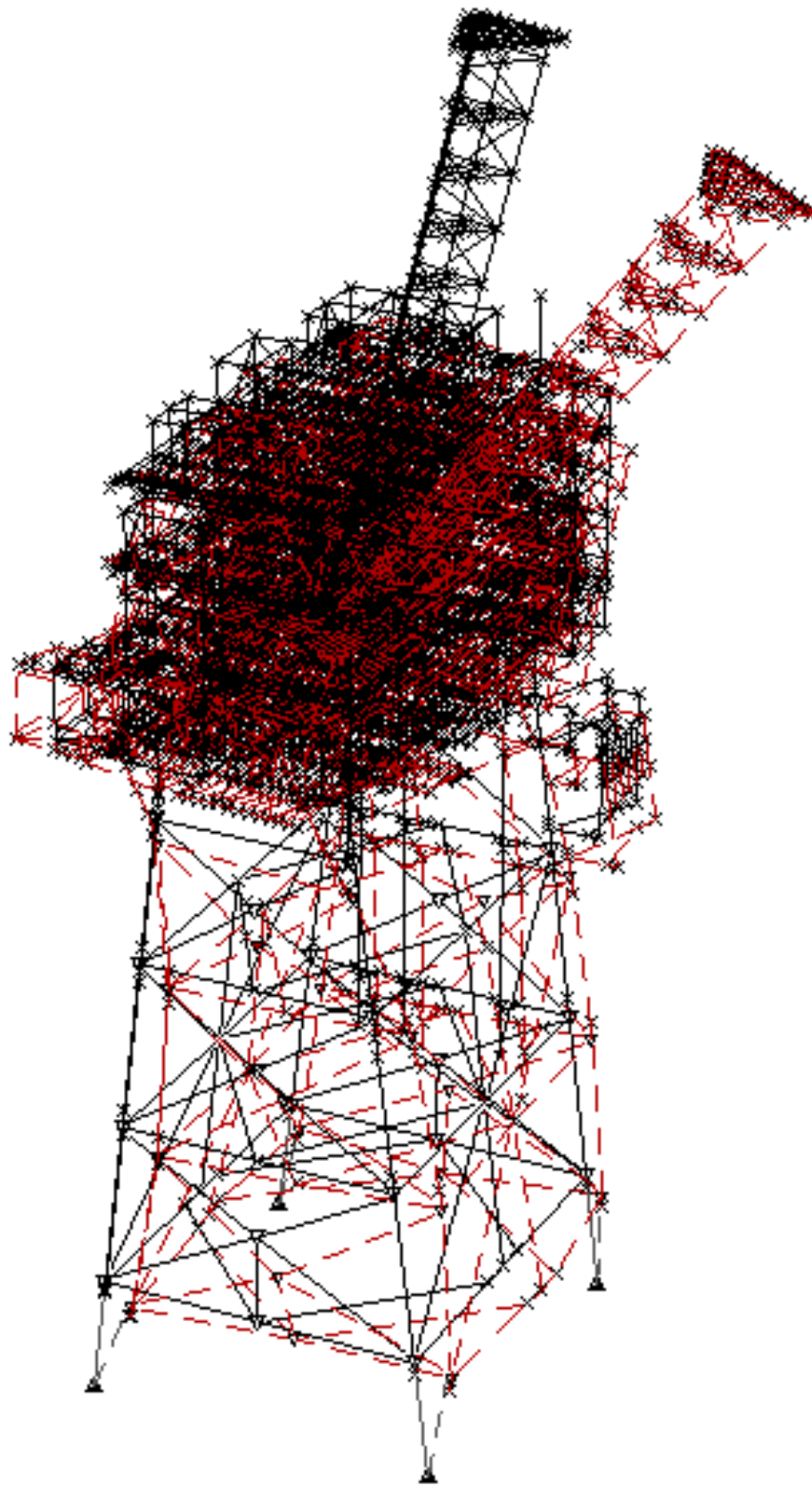


**Figure 3-73 Deflected mode shape 9**

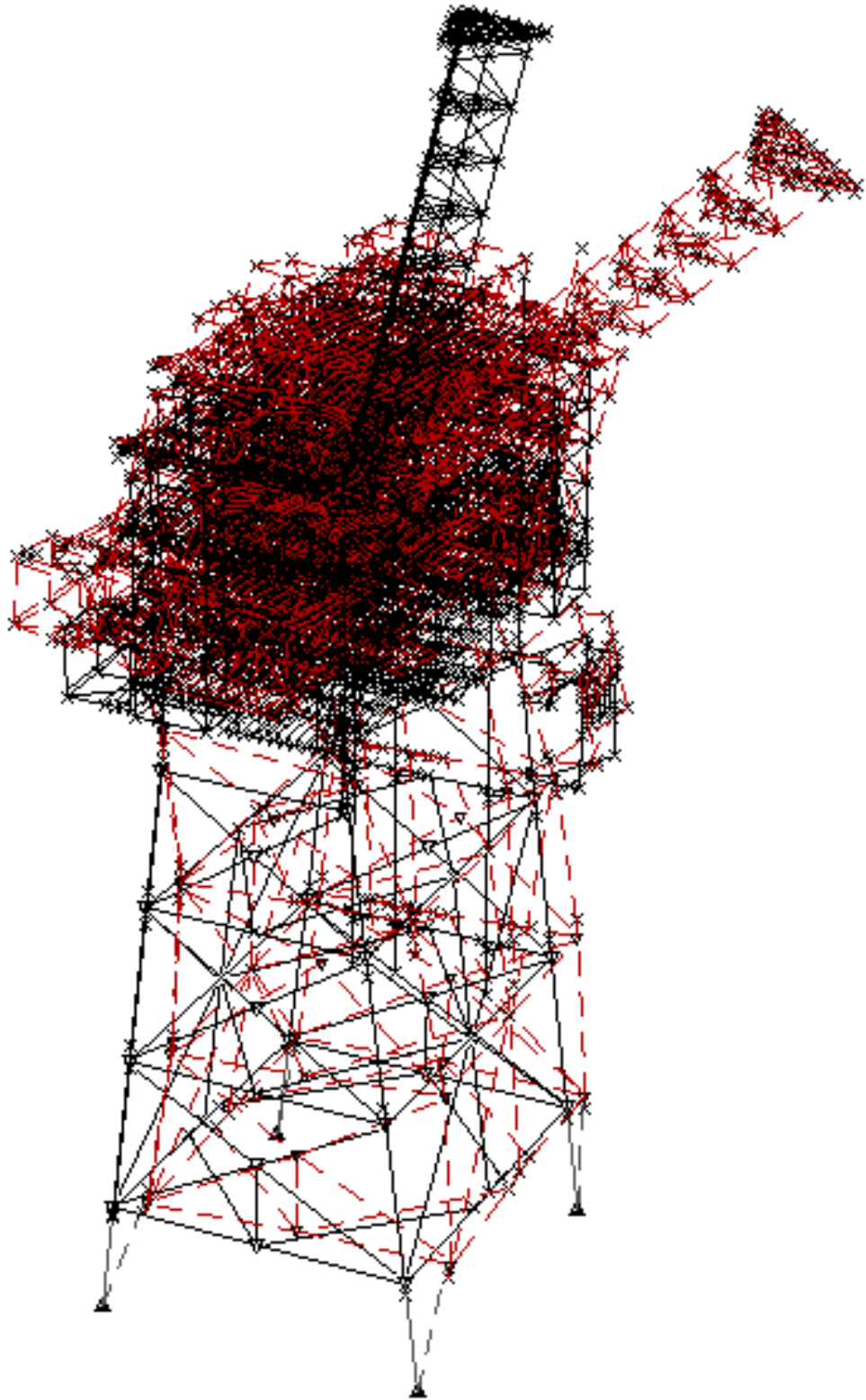


**Figure 3-74 Deflected mode shape 10**

# Chapter 4 Discussion

Modern offshore petroleum industry has been developed since 1947 at a fast pace through its significant milestones that have created a whole new phase of findings and producing crude oil and natural gas. The literature on fixed offshore structures is investigated to identify the significance of the procedure adopted for the study and its outcome.

The empirical techniques are calibrated against more advanced analysis techniques to take account of actual physical response process in a conservative manner. The outcome of adopted procedure is discussed in detail with a case study of parameters involved in design. A good balance is achieved between complexity and accuracy in the applied process.

## 4.1 Outline of the procedure

Studies on nonlinear environmental conditions and subsequent structural behaviour is discussed in detail. Nonlinear structural behaviour is studied using methods based on equivalent linearization and frequency domain expansions using transfer functions. Some of the data of the survey are attached in Appendix A.

A simplifying assumption was to neglect the effects of the relative movement of the structure with respect to the water velocities to linearize the structural behaviour. Otherwise this nonlinearity raises difficulties in solving the problem in the frequency domain and is restrictive to the procedure adopted. A further restraint is the application of Miner's rule which is assumed to be deterministic. However, the method has been developed to take account of randomness in the response process.

Dynamic effects of sea waves and their importance in fatigue degradation are discussed in the literature review. Further to that it is discussed how to incorporate these effects in the analysis in Sections 3.5 and 3.6. It is suggested to perform sensitivity analyses to obtain a clear representation of the structural dynamic behaviour. This can be performed by varying the key parameters, which are subject to change, e.g. the operating weight of the platform, the foundation stiffness and the structure's natural period.

The dynamic amplification effects could be severely suppressed if the natural period falls on the wave load cancelation point. Conversely with only a small shift in period a huge dynamic amplification is expected. Therefore, sensitivity analysis is important to verify the accuracy of the method as a practical and robust assessment tool. Dynamic response analysis methods are based on the matrix equilibrium equation (Equation 4-1).

$$M\ddot{r} + C\dot{r} + Kr = F(t) \quad \text{Equation 4-1}$$

Where;

$M$  = mass

$C$  = damping

$K$  = stiffness matrix

$r$  = nodal displacement vector

$F(t)$  = nodal load vector (includes relative velocities)

In the above equation dot superscript designates differentiation notation for time derivative. The right hand side of the Equation 4-1 (the force vector) contains all the possible nonlinear effects, like drag damping and free-surface variation, which means that the dynamic model can be simplified by linearization of the force vector with a proper linearization procedure taking account of linearization point.

Simplified methods are more applicable to fatigue environmental conditions compared to extreme environmental conditions. However, this practice will require a good awareness of dynamic response interaction with dynamic characteristics of the structure and excitation forces to properly reflect all dynamic effects in simplified methods.

For instance the dynamic transfer function in Figure 3-32 reveals considerable amplitudes particularly around the resonant frequency. This incident could be expected when excitation frequencies coincide with the natural frequency (Leira, 1990).

In the same figure cancellation/enhancement effects of hydrodynamic forces is observed as troughs/peaks of the transfer function curve at frequencies where the distance between the foremost and backmost leg is equal to a multiple of a half/full wavelength respectively.

A realistic dynamic response is expected with a reliable representation of the frequency content in the wave condition. The variation of design parameters like operating weight and water depth of the structure changes the amplitude and frequency content of the resulting time history. Therefore, a sensitivity analysis should be carried out to study the effect of water depth and operational weight on the model transfer function.

The concern of the present study is to investigate an analytical solution of the fatigue assessment through a statistical analysis that suits a random process. For this purpose the stress range PDF (Probability Density Function) is obtained directly from a power spectrum to predict fatigue damage. The other alternative is the application of Rain flow cycle counting to

obtain stress range histograms from time consuming measurements. Therefore, using the power spectrum of the associated stress time series is preferred to extensive simulation in the time domain method.

For stationary excitation, fatigue damage can be predicted with a minimum amount of data from the resulting stress range PDF with confidence, which makes the spectral method a desirable solution. Such stationary situations are limited in duration and the wave environment will not remain stationary for longer terms. As the result, the stress cycles for the random process may not be realized in the stationary situation (short term condition). Therefore, the description of the wave environment should be representative of the long term conditions.

The situation will not remain stationary nor Gaussian for long term wave climates. Consequently, relative phasing of periodic components becomes important in fatigue estimation. Considering that in the spectral method no phase information is retained in a power spectrum, this will make the response PDF more complex. Although there is no conventional method to obtain the response PDF for broad band processes, a system's response may approximate to Gaussian if its narrow band response derived from a broad band excitation. However, an assumed Gaussian PDF should be treated with uncertainty at the tails of the distribution.

For narrow band Gaussian processes, the PDF of the peaks and the resultant stress ranges are assumed with Rayleigh distributions, which means that the behaviour of the fatigue damage is only dependent on the current stress states as the case for the non-ageing effect process. Therefore, statistical modelling under random loading is simplified and fatigue damage can be obtained by the stress range and the number of cycles based on the Miner's rule. This implies that the load sequence interaction is negligible so that the total damage is the linear summation of the fractional damages caused by individual stress ranges.

The realistic distribution of wave energy over the relevant frequency range can be suitably accounted for using spectral analysis. Transfer functions are the corner stones of the spectral approach, which incorporates the dynamic characteristics of the structure. An appropriate frequency grid is selected with reliable interpolation routines to ensure a good definition of peaks and valleys in the global base shear transfer functions, refer to Figure 3-32. The frequency intervals obtained must be small enough for precise calculation of spectral moments.

The spectral moments are obtained from integrations of response spectra base on the frequency considered for integration points and wave direction in the case of multidirectional sea

spectrum. The locations of integration points are very important to avoid ambiguous integration results (Karadeniz, 2008). Furthermore, the termination of the calculation at the tail of the frequency range should be considered with care to prevent numerical errors due to ignoring a significant portion of the response.

Considering the above, the global base shear transfer functions are developed for the wave steepness related to the weighted centre of damage in the scatter diagram. The weighing factor is the mean value of the normalized static base shear transfer function over the width of each cell in the scatter diagram. This weighing factor introduces a stress period dependency, which allows the cancellation effects to be reflected in the fatigue damage scatter diagram.

Determination of wave height is obtained by a calibration process. Calibration of the wave steepness should be based on the matching of global response parameters, which are representative of the predominant wave action to which the structure is subjected to under fatigue conditions. The appropriate wave steepness is calibrated so that the spectral maximum base shear wave load range matches the deterministic value. Calibration is performed for a broadside, an end on and a diagonal wave direction.

Use of constant wave steepness gives unrealistically large wave heights at low wave frequencies (large wave lengths). Therefore, wave height at the low frequency side is capped to the wave height with a one year return period as a maximum. Moreover, if the dynamic amplification of the structural response is significant, special attention must be given to the high frequency cut off point.

It has been shown that for a more general narrow band spectrum, Figure 3-30 (a), the high frequency components introduce irregularities in the sine wave form approximation as additional maxima. Accordingly, a minimum wave height of 0.3 m is considered to avoid these irregularities.

The wave environment is characterized by the annual variability of the sea surface and directional spreading. The width of the spectral density and the directional spreading affect the nonlinear characteristics of the waves. Although wave directionality and energy spreading generally reduce the structural response, their effects in shallow water may be different than that of deep water situations (Prevosto, 1998).

The influence of wave directional spreading on the stress variations is investigated in a case study, which is of some significance (refer to Appendix B). In most cases the influence of wave directional spreading is of secondary importance and can be neglected. However, this

effect can be considered by choosing an appropriate wave spreading function if it is prominent (ISO19902, 2007). The results from case studies show that the fatigue life is increased in most of the joints using a cosine spreading function.

The space frame model for fatigue analysis includes all important characteristics of the stiffness and loading properties of the piled structure. The model stiffness includes the three dimensional distribution of platform stiffness (Figure 1-1). Offsets are specified for jacket tubular members so that braces are modelled to the face of the chord and a 5 cm gap (at the chord face) exists between braces. Member end stresses are then calculated at the face of the chord.

Member offsets are used to shorten or lengthen the member or to move the member when the neutral axis is not located on the line between its connecting joints. When offsets are specified, the program creates a rigid link between the neutral axis of the member end and the connecting joint. The offsets describe the length of the rigid link and should be used considering chord shell flexibility.

Structural components are considered in sufficient detail for fatigue analysis considering beam and finite elements (e.g. shear plates). The stiffness of appurtenances can be ignored unless it significantly changes the global stiffness of the structure. Deck plate is considered in sufficient detail using shear plates for coarse finite element mesh representation. Topside deck should be modelled in the detail in terms of topside stiffness, total topsides mass, centre of mass and the rotational inertia of the deck mass to present a realistic deck-jacket interface and precise torsional response. The equivalent linear foundation model (super element) is used due to requirement of linear theory (i.e. modal superposition) in dynamic analysis.

The super element is created for low deflection levels to represent the foundation stiffness for fatigue environment. Since the pile load-deflection curve is nonlinear, soil springs representing pile stiffness vary for different load levels. In mild environmental condition as is the case for fatigue waves spring stiffness is much greater than the spring stiffness appropriate for extreme wave loads (Kinra, 1979). Therefore, spring stiffness associated with extreme environmental conditions is not applicable for fatigue assessment.

The inertia effects of the structure substantially contribute to fatigue damage. The dynamic inertia force on a structure is due to its vibrations and calculated using a spectral technique and then scaled to match the global base shear response obtained from a Rayleigh distribution. There is uncertainty involved in the global response due to variation in the mass, damping and stiffness properties, which affects the calibration process. Therefore, the natural period of the



platform could be carefully mapped not to fall in a valley of the platform base shear transfer function. In other words, the period is to be shifted to the adjacent peak of the transfer function by attuning mass or stiffness within expected range, refer to Figure 3-39. Furthermore, sensitivity analysis may be carried out by varying the foundation stiffness. This will affect the member loads, especially near the mud line, which is prone to fatigue damage.

The mass model in dynamic analysis includes the topside and substructure weight, marine growth, entrapped water and added mass. A lumped mass model can be used for global structural response but it does not capture the local dynamic effects. Distribution of mass along the element can be considered by a consistent mass approach in which case the mass matrix created incorporates off-diagonal coupling terms between all degrees of freedom, including rotational DOFs. Since in the lumped mass approach off diagonal terms are assumed to be zero, it is not recommended when the element mass is not the same in all three directions. This could be the case when including effects of fluid added mass or virtual mass acting normal to the element. Considering the above, a consistent mass model is considered in the analysis.

Energy dissipation due to damping has a profound effect on the structural response at a resonant frequency. Instead of precise modelling, all sources of damping including structural, foundation and hydrodynamic effects are accounted for by considering an equivalent viscous damping that is 2% of critical damping. Damping modes in an offshore structure are hysteretic and friction damping; however, it is mathematically more convenient to obtain the correct energy loss per cycle by viscous damping. The relative velocity formulation is not used in the fatigue analysis since it will cause additional damping that is not observed in measurements (ISO19902, 2007).

In fatigue analysis the wave theory as well as drag and mass coefficients considered are different from those used in strength analyses for design wave loads (refer to 2.4). Furthermore, the current static effect can be neglected since we are dealing with the stress range. At the same time, current dynamic effect is complicated to account for in fatigue analysis. Although the analysis technology is lacking to incorporate these effects, it can only affect platform dynamics for large waves or currents, which is not the case for mild environments.

The effect of marine growth on the hydrodynamic actions is considered by increasing the cross-sectional dimensions of structural components at the marine growth zone as member drag diameter. Tubular structural members in this zone are classified as rough where the drag and inertia coefficient of rough members is considered in Morison's equation (API, 2007).

Marine growth weight is included in the mass model, which increases the platform added mass. The local and global wave loading will increase due to marine growth effects and cause further fatigue damage of members subjected to these additional loads.

Stress concentration factors consistent with corresponding S-N curve are utilized to evaluate local scale stresses. The fatigue life of the platform is evaluated using Miner cumulative damage summation on each sea state. The short term stress distribution is assessed using spectral methods assuming a narrow banded Rayleigh distribution in closed form for each sea state.

A calibration procedure is employed to compensate the uncertainties involved in wave action and resulting stress, which is discussed in more details in Section 3.6. Safety factors on the fatigue life are considered based on the component's criticality and in-service inspection requirements (API, 2007). Stress concentration factors are used for extrapolation of stresses to the weld toes. The S-N curve includes the local weld toe effects, such as notch stresses. Hot spot stress ranges are evaluated at eight locations termed saddle and crown (refer to Figure 4-1) around each tubular chord-brace intersection.

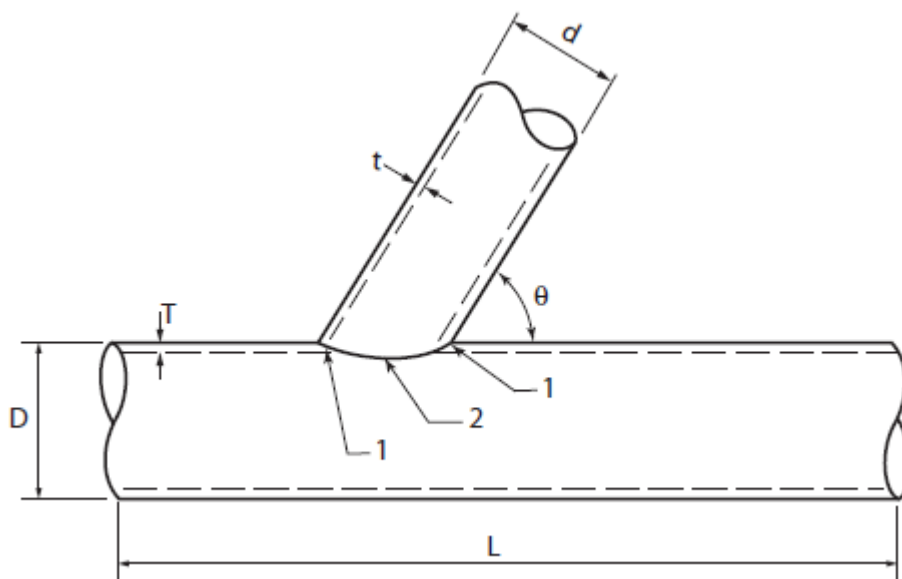


**Figure 4-1 Tubular intersection (1 crown, 2 saddle)**

Stress Concentration Factor (SCF) by Efthymiou is utilized, which is based on finite element analysis including all joint and load types. Miner summation law is adopted to predict fatigue life due to variable actions based on the following assumptions:

- A relation between stress range and the number of cycles to fail the material (S-N curve) can be found based on sinusoidal varying stresses.
- The same S-N curve can be used for varying stresses that are not sinusoidal where the difference between the maximum and minimum stresses in a cycle is taken as the stress range.
- An amount of damage for a material subjected to a stress range,  $s$ , for a number of cycles,  $n(s)$ , smaller than the number of cycles to failure is given by Equation 4-2

$$d = \frac{n(s)}{N(s)} \quad \text{Equation 4-2}$$

- A material subjected to different stress ranges will fail when the sum of damages for each stress range equals unity, that is:

$$\sum d_i = \sum \frac{n(s_i)}{N(s_i)} = 1.0 \quad \text{Equation 4-3}$$

Within the framework of the Miner theory the fatigue analysis is performed using the spectral (statistical) approach to yield more realistic and reliable results than the deterministic analysis.

## 4.2 Results

Wave induced dynamic force is the main contributor to fatigue damage of offshore platforms. It exposes lateral loads on the structure that cause member severance and consequent reduction in structural integrity. The fatigue inducing loads could excite dynamic response followed by intensified fatigue stresses in the structure since they are variable with time.

The dynamic effects and structural response to excitation forces are adequately modelled to study fatigue performance with realistic results. The results from different methods are compared to highlight the applicability of the analysis method to dynamically responding structures under random nonlinear wave loading.

As per the central limit theorem a random process may have a Gaussian probability distribution if it results from the summation of infinitely random elementary events. The effective bandwidth of the random process can be reduced using selective filters so that a time domain formulation can be transformed to frequency domain.

Only time varying loads are considered for the action model using the spectral method in the frequency domain. This method retains the random nature and frequency content of the random sea and is regarded as the most reliable method for fatigue assessment. The assessment delivers a usage factor representing the amount of fatigue damage using Miners rule of cumulative damage.

The purpose of the Dynpac program module is to generate dynamic characteristics (mode shapes and frequencies) of a structure. Modal analysis is performed to identify the structural characteristics that contribute to the dynamic response. For this purpose, a Guyan reduction is performed to reduce the structural stiffness matrix as well as the mass matrix. The eigenvalues are initially extracted for the master degrees of freedom and then expanded to reduced (slave) degrees of freedom, which will then be used in the calculation of the modal reactions.

The dynamic characteristics are considered in wave response analysis while generating the equivalent static loads. This includes hydrodynamic loading determined by Morison's equation as well as inertia loading determined from modal acceleration. An equivalent static load case is solved to obtain the nominal stresses. Nominal stresses from solution results are employed to create the transfer functions required for the spectral fatigue analysis.

The methods based on stochastic linearization are investigated using constant wave steepness. The empirical techniques are calibrated against more refined random analysis techniques using global response parameters to take account of actual physical response processes in a conservative manner. A calibration procedure is conducted by adjusting the wave steepness and parameters in Morison equation to obtain comparable results with conventionally calculated force levels. A good balance is achieved between complexity and accuracy in the applied process.

The spectral fatigue assessment is referred to as the direct method because it produces results in terms of fatigue damage. This method used is based on transfer functions, which require a linear relationship between wave height and wave induced loads. However, adjustments are made to the basic method to account for various nonlinearity. Transfer functions are obtained from a deterministic calculation and considered as the corner stone of probabilistic fatigue analysis.

Fatigue assessment is conducted with the aim for more economical design and reduced inspection without compromising the structural safety levels. Fatigue results are very sensitive to stress distribution due to an exponential relationship between the stress range and the allowable number of cycles; therefore, stress histories are precisely evaluated considering a

Rayleigh distribution of peak stresses, which yields accurate results (even for structures with significant nonlinearities) as compared to a Weibull fit of the peak distribution.

The nominal stresses are obtained from the global analysis based on the wave frequency and approach direction using linear (Airy) wave theory. The effect of nonlinear wave action is approximated by a suitable wave height selection. The computer model includes both the structural model and the action model for stress analysis. The structural model is adequately detailed in terms of geometry, stiffness, damping and mass distribution for precise evaluation of the torsional response. Static loads are included only for the determination of the equivalent pile stub. For stiffness modelling half of the corrosion allowance is considered for the average thickness during the life of the structure.

In low to moderate seas, which is applicable to the fatigue environment, a confused short crested sea condition is expected. Therefore, some case studies are carried out to examine short crested sea condition in fatigue assessment by applying the wave spreading functions, which modify the spectral moment. However, consistent relationship between the results may not exist due to the nonlinear nature of the wave environment.

Stress raisers from the global geometry of the connection are accounted for in stress concentration factors, which is referred to as the geometric hot spot stress. In fatigue analysis, stress concentration factors (SCF) are determined using load distribution through the connection. Analysis results are presented in tabulated forms in Table 4-1 for 8 different case studies. Extended detail results for the calibrated case is included in the Appendix B. A graphic display of the selected joint numbers is presented in Figure 4-2. Fatigue life comparison to the calibrated case is presented in Table 4-2. The interpretation of the results for case studies and their assumptions are discussed further in Section 5.1.

**Table 4-1 Fatigue life of selected joints for different case studies**

case Joint	C1	C2	C3	C4	C5	C6	C7	C8
101	3798	54084	38688	7883	26054	8091	3738	3798
201	9775	95398	60626	21579	64092	21577	9594	9775
301	542	15905	7520	1144	4327	1146	534	542
401	23052	113524	17553	10246	21264	13135	13758	23052
119	3449	91509	37892	6843	25454	7173	3406	3449
219	10309	114065	73969	23056	52002	22941	10142	10309
319	526	15319	7181	1107	4163	1111	519	526
419	28999	150369	24007	13213	28941	17026	17941	28998

**Table 4-2 Fatigue life comparison to calibrated case**

case Joint	C1/C1	C2/C1	C3/C1	C4/C1	C5/C1	C6/C1	C7/C1	C8/C1
101	1.00	14.2	10.2	2.1	6.9	2.1	0.98	1.00
201	1.00	9.8	6.2	2.2	6.6	2.2	0.98	1.00
301	1.00	29.3	13.9	2.1	8.0	2.1	0.99	1.00
401	1.00	4.9	0.8	0.4	0.9	0.6	0.60	1.00
119	1.00	26.5	11.0	2.0	7.4	2.1	0.99	1.00
219	1.00	11.1	7.2	2.2	5.0	2.2	0.98	1.00
319	1.00	29.1	13.7	2.1	7.9	2.1	0.99	1.00
419	1.00	5.2	0.8	0.5	1.0	0.6	0.62	1.00

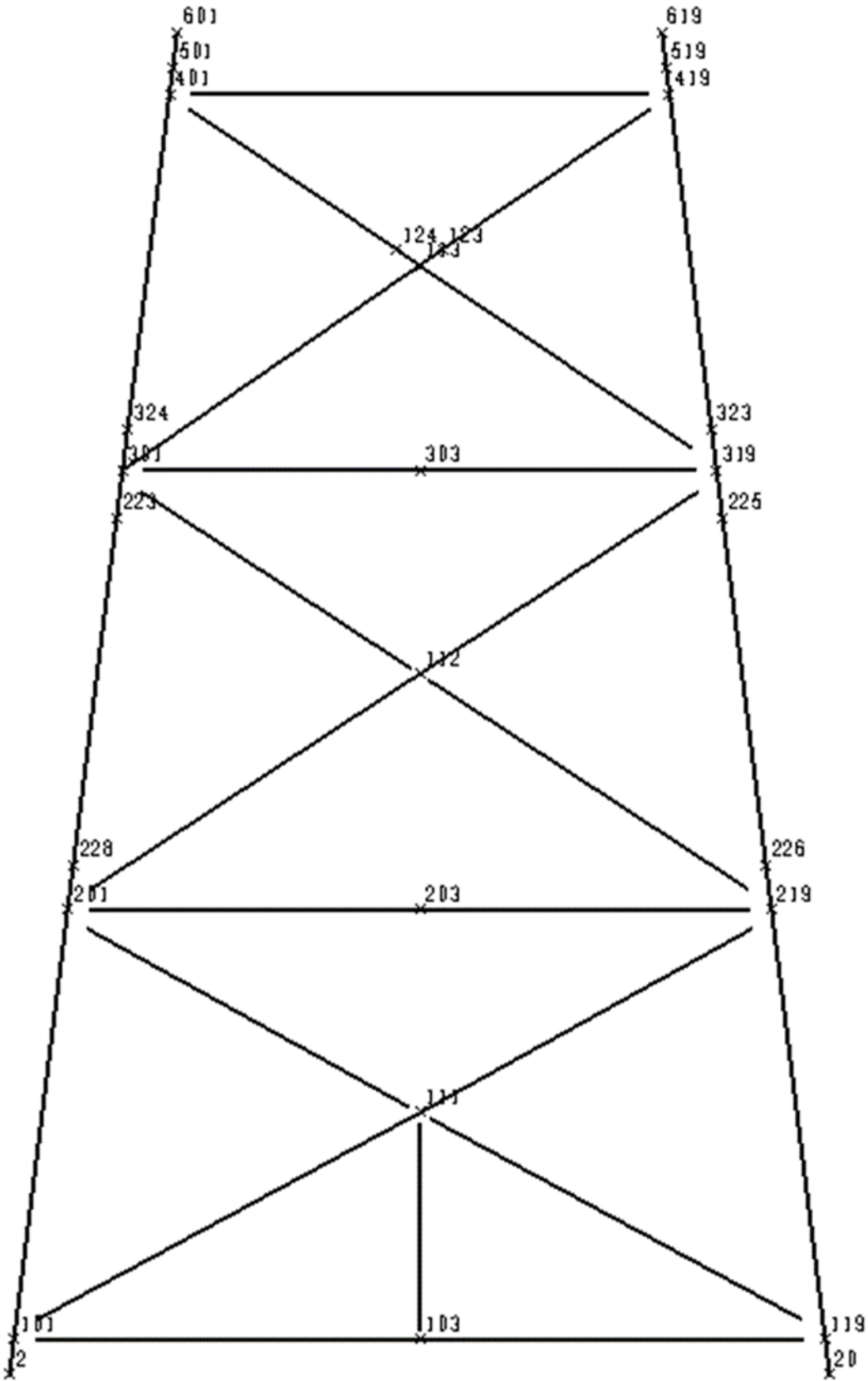


Figure 4-2 Face A joint numbers

# Chapter 5 Conclusion



The outcome of the research study has advanced the fatigue assessment procedure of offshore structures. The methodology used here is frequency domain analysis, which accounts for non-linear system responses with due consideration of the system vibration characteristics. In this regard a rigorous calibration process is employed to take account of the actual physical response process in a conservative manner. The applicability of the proposed approach is demonstrated in detail by applying the aforementioned methodology to a fixed jacket type offshore platform in the Persian Gulf.

## 5.1 Summary

In this thesis, a practical method for dynamic fatigue assessment of fixed offshore platforms is investigated. The literature review is conducted to identify the most appropriate design methods and their significance in meeting functionality, safety and economical aspects. The random nature of the wave environment is represented by frequency domain spectral methods using a suitable linearization in a moderate environment. The accuracy and efficiency of the method is verified by calibration techniques with due consideration of dynamic characteristics.

Fatigue damage is the main cause of structural failure in fixed offshore platforms and reduces overall structural integrity during its development. For platforms with periods greater than 3 seconds (refer to Table 3-35) the effects of dynamic and structural response which are incorporated through a calibration process become more important and must be adequately modelled to ensure that realistic results were obtained. The detailed description of analysis techniques are discussed in Chapter 3.

The response of the system to random excitation is monitored for optimization of its peak performance. In this regard some case studies are developed by varying the key parameters, which are subject to change. The results are tabulated in Table 4-1 and compared in Table 4-2. The assumptions and outcome of the case studies are discussed below.

1. Calibrated spectral dynamic fatigue results (C1)

The calibration method is discussed in detail in Section 3.6, which delivers the most accurate results for dynamic fatigue assessment of fixed offshore platforms using spectral techniques in frequency domain and a comparison of other case studies are conducted against this case.

2. Fatigue results ignoring calibration (C2)

A graphic display of fatigue life for selected joints is provided in Figure 3-38. For dynamically sensitive platforms, the dynamic effects and random nature of the wave environment are considered using calibrated spectral techniques against conventional techniques. The comparison of the results show that fatigue life ignoring calibration would be unrealistically higher than expected with the rigorous methods used in the research study. This shows the importance of using proper analysis techniques to obtain a realistic result with due consideration of dynamic effects.

### 3. Wave spreading options

- Wave spreading based on transfer function averaging (cosine distribution power 2, C3)
- Wave spreading based on API energy approach (cosine distribution power 2, C4)
- Wave spreading based on transfer function averaging (cosine distribution power 4, C5)
- Wave spreading based on API energy approach (cosine distribution power 4, C6)

Wave spreading is the basic component of the wave environment, which affects fatigue life estimates. An appropriate spreading function (e.g. cosine squared) may be used in conjunction with the wave spectrum to account for the effect of wave spreading on structural responses. Applying the wave spreading function modifies the spectral moment and reduces the structural response. However, their long term statistics are not yet commonly available and their effects in shallow waters may be different than that of deep water situations.

The influence of wave directional spreading on the stress variations is investigated in 4 case studies as mentioned above, which are of some significance. Cosine distribution power 4 is used when limited fetch restricts the degree of spread. The results from the case studies shows a significant increase in predicted fatigue life in most of the joints. However, there is uncertainty involved on the power in the cosine function. As a conservative recommendation, the most unfavourable condition should be adopted for the design of fixed offshore platforms.

### 4. Inclusion of crest or trough in Airy wave theory (C7)

The wave kinematics are computed using nonlinear Airy theory by inclusion of crest or trough. It is observed that the influence of nonlinear waves is most prevalent on the joints close to water surface with 40% reduction in fatigue life. However, this assumption is not consistent with linearity demand in spectral analysis; therefore, a direct conclusion cannot be drawn from this observation and a sensitivity study should be carried out to quantify this influence.

5. Unsorted equivalent static loads option saving execution time (C8)

The fatigue results will remain the same when using unsorted equivalent static loads in wave response analysis (US option). However, this method does not generate a modal response factor to save the execution time and recommended for fatigue analysis.

## 5.2 Recommendation

It is recommended to perform a rigorous calibration technique for fatigue design of fixed jacket type offshore platforms in hostile wave environments. The calibration process is discussed in detail in thesis subject, which has advanced fatigue assessment of offshore structures. This method is using frequency domain tools to account for non-linear system responses with due consideration of the system vibration characteristics. The applicability of the proposed approach is demonstrated in detail by applying the aforementioned methodology to a fixed jacket type offshore platform in the Persian Gulf as the most reliable fatigue assessment.

For future development work, it is recommended to include a sensitivity analysis by attuning the mass or stiffness within the expected range and comparing the response for the lower bound and upper bound estimate. It is anticipated that this will affect the member loads, especially near the mud line, which is prone to fatigue damage.

## References

- ABS 2004. Guidance notes on dynamic analysis procedure for self elevating drilling units. American Bureau of Shipping.
- ABS 2010. Guide for the fatigue assessment of offshore structures.
- API 2007. Recommended practice for planning, designing and constructing fixed offshore platforms. 2007.
- ASGARIAN, B. 2009. Pile-soil-structure interaction in pushover analysis of jacket offshore platforms using fiber elements. *Construction* 10.
- AZARHOUSHANG, A. 2010a. *Dynamic response of fixed offshore platforms to environmental loads*. MPhil, Curtin University.
- AZARHOUSHANG, A. 2010b. Nonlinear Water-Structure Interaction of Fixed Offshore Platform in Extreme Storm. *International Offshore and Polar Engineering Conference*. Beijing, China: The International Society of Offshore and Polar Engineers (ISOPE).
- BARLTROP, N. D. P. 1991. *Dynamics of Fixed Marine Structures*.
- BREBBIA, C. A. & WALKER, S. 1979. *Dynamic Analysis of Offshore Structures*, Butterworth & Co.
- CHOW, C. L. 1991. An analytical solution for fast fatigue assessment under wide-band random loading. *Int J Fatigue*, 10.
- CRUZ, A. M. 2008. Damage to offshore oil and gas facilities following hurricanes Katrina and Rita: An overview. *Journal of Loss Prevention in the Process Industries*, 21, 7.
- DNV 2010. ENVIRONMENTAL CONDITIONS AND ENVIRONMENTAL LOADS. In: VERITAS, D. N. (ed.).
- DNV 2011. SELF-ELEVATING UNITS.
- ETUBE, L. S. 1999. Modelling of jack-up response for fatigue under simulated service conditions. *Marine structures*, 22.
- FRIEZE, P. A. 1997. Fixed and Jack-up Platforms: Basis for Reliability Assessment. *Marine Structures*, 10.
- GOLAFSHANI, A. 2009. FEMA approaches in seismic assessment of jacket platforms. *Constructional Steel Research*, 65, 8.
- GREEVES, E. J. 1996. Evaluating Jack-up Dynamic Response Using Frequency Domain Methods and the Inertial Load Set Technique. *Marine Structures*, 9, 27.
- GUPTA, S. 2007. Fatigue damage in randomly vibrating jack-up platforms under non-Gaussian loads. *Applied ocean research*, 28, 13.
- GUYAN, R. J. 1965. Reduction of stiffness and mass matrices. *AIAA*, 3, 1.
- HILLIS, A. J. 2011. Structural health monitoring of fixed offshore structure using the bicoherence function of ambient vibration measurements. *Journal of Sound and Vibration*, 12.
- HSE 2000. Validation of wave response analysis for jack-up rigs. In: EXECUTIVE, H. A. S. (ed.).
- IRANINEJAD, B. 1988. *Dynamic Analysis of Fixed Offshore Platforms Subject to Non-linear Hydrodynamic Loading*. PhD, University of California.
- ISO19902 2007. Petroleum and natural gas industries-Fixed steel offshore structures.
- JIA, J. 2008. An efficient nonlinear dynamic approach for calculating wave induced fatigue damage of offshore structures and its industrial applications for lifetime extension. *Applied Ocean Research*, 30, 10.
- JOHANSEN, H. 2003. Fatigue Assessment.
- KAM, J. C. P. 1990. Recent development in the fast corrosion fatigue analysis of offshore structures subject to random wave loading. *Int J Fatigue* 11.
- KAM, J. C. P. 1992. Wave action standard history (wash) for fatigue testing offshore structures. *Applied Ocean Research*, 14, 10.

- KARADENIZ, H. An Integration Procedure to Calculate Response Spectral Moments of Offshore Structures. Proceedings of the Eighteenth (2008) International Offshore and Polar Engineering Conference, 2008 Vancouver, BC, Canada,. The International Society of Offshore and Polar Engineers (ISOPE).
- KARUNAKARAN, D. 1995. Nonlinear Dynamic Behavior of Jack-up Platforms. *Marine Structures*, 9, 30.
- KAWAMOTO, J. 1982. An assessment of uncertainties in fatigue analyses of steel jacket offshore platforms. *Applied ocean research*, 4, 8.
- KIM, C. H. 2008. *Nonlinear Waves and Offshore Structures*, World Scientific.
- KINRA, R. K. 1979. Fatigue Analysis of the Cognac Platform. *JOURNAL OF PETROLEUM TECHNOLOGY*, 13.
- KO, C. K. 1988. *Three Dimensional Dynamic Analysis of Fixed Offshore Platforms*. PhD, Austin University.
- LEIRA, B. J. 1990. Estimation of fatigue damage and extreme response for a jack-up platform. *Marine Structures*, 33.
- LIMA, E. C. P. E. A. 1985. Nonlinear Dynamic Analysis of a Jacket-Type Platform by Ritz Mode Superposition Method. *Offshore Technology Conference*, 11.
- NEWLAND, D. E. 2012. *An Introduction to Random Vibrations, Spectral & Wavelet Analysis*, Longman.
- PREVOSTO, M. 1998. Effect of Directional Spreading and Spectral Bandwidth on the Nonlinearity of the Irregular Waves. *The International Society of Offshore and Polar Engineers*, 3, 5.
- RAJASANKAR, J. 2003. Structural integrity assessment of offshore tubular joints based on reliability analysis. *International Journal of Fatigue*, 25, 11.
- SHABAKHTY, N. 2011. System failure probability of offshore jack-up platforms in the combination of fatigue and fracture. *Engineering failure analysis*, 21.
- SKJONG, R. 1991. Rational Methods for Fatigue Design and Inspection Planning of Offshore Structures. *Marine Structures*, 4, 26.
- VUGTS, J. H. 1978. Probabilistic Fatigue Analysis of Fixed Offshore Structures. *Journal of petroleum technology*, 11.
- WILSON, J. F. 2003. *Dynamics of Offshore Structures*, John Wiley & Sons, Inc.
- WIRSCHING, P. 1987. Considerations of Probability-Based Fatigue Design for Marine Structures. *Marine Structural Reliability Symposium*. Marine Structures.
- WIRSCHING, P. H. 1980. Fatigue reliability in welded joints of offshore structures. *INT. J. FATIGUE*, 7.
- ZIENKIEWICZ, O. C., LEWIS, R. W. & STAGG, K. G. 1978. *Numerical Methods in Offshore Engineering*, John Wiley & Sons, Inc.

*Every reasonable effort has been made to acknowledge the owners of copyright material. I would be pleased to hear from any copyright owner who has been omitted or incorrectly acknowledged.*

## Appendix A Input Files

## A.1 SACS Model

```

LDOPT      NF+Z  1.030   7.85  -41.60  42.72GLOBMN DYN      NP      K
SPECTRAL FATIGUE ANALYSIS
SACS MODEL FILE
OPTIONS      MN  DY  SDUC   3 3      PT
SECT
SECT CON1      TUB                      154.785.000137.105.000
SECT CON2      TUB                      154.785.000137.105.000
SECT CON3      TUB                      148.802.000137.105.000
SECT CON4      TUB                      155.805.500137.105.000
SECT CON5      TUB                      149.202.200137.105.000
SECT CON6      TUB                      154.204.700137.105.000
SECT CON7      TUB                      148.802.000137.105.000
SECT CONB0B    CON                      101.602.000 61.00
SECT DEQ      PRI1963.0613592.0306796.0306796.0 50.000      50.0001473.1473.
SECT DJPG0     PLG                      75.003.000120.002.500
SECT DJPG1     PLG                      120.005.000120.004.000
SECT DJPG10    WF                       50.005.000120.004.000
SECT DJPG11    PLG                      75.004.000120.001.500
SECT DJPG2     PLG                      120.003.000120.002.000
SECT DJPG3     PLG                      100.005.000120.003.000
SECT DJPG4     PLG                      50.005.000120.005.000
SECT DJPG5     PLG                      50.005.000120.002.500
SECT DJPG6     PLG                      120.003.000120.002.500
SECT DJPG7     PLG                      50.003.000120.002.500
SECT DJPG8     PLG                      75.004.000120.004.000
SECT DJPG9     PLG                      50.002.500120.002.000
SECT DLCON     CON                      152.404.500137.102.500 6.50
SECT DPB       PLG                      35.003.000 75.002.000
SECT DPG1      WF                       62.505.000120.003.000
SECT DPG10     PLG                      50.003.500120.001.500
SECT DPG12     PLG                      50.003.000120.001.500
SECT DPG13     PLG                      60.004.500120.001.500
SECT DPG2      PLG                      55.004.000120.003.000
SECT DPG3      PLG                      50.003.000120.002.500
SECT DPG4      PLG                      40.002.500120.001.500
SECT DPG5      PLG                      30.002.500120.001.500
SECT DPG7      PLG                      50.004.000120.001.500
SECT DPG9      PLG                      40.003.000120.001.500
SECT PILSTUB  PRI620.196503500.6503500.6503500. 10.000      10.000
GRUP
GRUP B0A       61.000 1.905 20.50 8.0034.50 1 .800.800      0.50N 7.849
GRUP B0A       61.000 2.540 20.50 8.0034.50 1 .800.800      0.50N 7.8491.25
GRUP B0B       61.000 1.905 20.50 8.0034.50 1 .800.800      0.50N 7.849
GRUP B0B       61.000 2.540 20.50 8.0034.50 1 .800.800      0.50N 7.8491.06
GRUP B0C       61.000 1.270 20.50 8.0035.50 1 .800.800      0.50N 7.849
GRUP B0D       61.000 2.540 20.50 8.0034.50 1 .800.800      0.50N 7.849
GRUP B1A       61.000 1.270 20.50 8.0035.50 1 .800.800      0.50N 7.849
GRUP B1A       61.000 2.060 20.50 8.0034.50 1 .800.800      0.50N 7.8491.25
GRUP B1B       101.60 4.500 20.50 8.0035.50 1 .800.800      0.50N 7.8491.75
    
```



GRUP B1B CONB0B		20.50	8.0035.50	1	.800.800	0.50N	7.8490.81
GRUP B1B	61.000	1.270	20.50	8.0035.50	1	.800.800	0.50N 7.849
GRUP B1C	50.800	1.270	20.50	8.0035.50	1	.800.800	0.50N 7.849
GRUP B1D	61.000	1.270	20.50	8.0035.50	1	.800.800	0.50N 7.849
GRUP B2A	81.300	2.000	20.50	8.0034.50	1	.800.800	0.50N 7.849
GRUP B2A	81.300	2.540	20.50	8.0034.50	1	.800.800	0.50N 7.8491.25
GRUP B2B	81.300	2.200	20.50	8.0034.50	1	.800.800	0.50N 7.849
GRUP B2B	81.300	2.540	20.50	8.0034.50	1	.800.800	0.50N 7.8491.75
GRUP B2C	66.000	1.750	20.50	8.0034.50	1	.800.800	0.50N 7.849
GRUP B2D	81.300	2.000	20.50	8.0034.50	1	.800.800	0.50N 7.849
GRUP B3A	50.800	1.588	20.50	8.0035.50	1	.800.800	0.50N 7.849
GRUP BLA	66.000	2.540	20.50	8.0034.50	1	1.001.00	0.50N 7.849
GRUP BLB	86.400	3.000	20.50	8.0034.50	1	1.001.00	0.50N 7.849
GRUP BLC	66.000	2.540	20.50	8.0034.50	1	1.001.00	0.50N 7.849
GRUP BLD	86.400	3.000	20.50	8.0034.50	1	1.001.00	0.50N 7.849
GRUP BLE	86.400	3.200	20.50	8.0034.50	1	1.001.00	0.50N 7.849
GRUP BLF	86.400	3.000	20.50	8.0034.50	1	1.001.00	0.50N 7.849
GRUP BLG	86.400	3.000	20.50	8.0034.50	1	1.001.00	0.50N 7.849
GRUP BLH	45.720	1.905	20.50	8.0034.50	1	1.001.00	0.50N 7.849
GRUP BLI	45.720	1.905	20.50	8.0034.50	1	1.001.00	0.50N 7.849
GRUP BLJ	45.720	1.905	20.50	8.0034.50	1	1.001.00	0.50N 7.849
GRUP CS1	35.560	1.270	20.50	8.0035.50	1	1.001.00	0.50N 7.849
GRUP CSA	90.000	2.540	20.50	8.0034.50	1	1.001.00	0.50F 7.849
GRUP CSB	90.000	2.540	20.50	8.0034.50	1	1.001.00	0.50F 7.849
GRUP CSC	90.000	2.540	20.50	8.0034.50	1	1.001.00	0.50F 7.849
GRUP CSZ	90.000	2.540	20.50	8.0024.80	1	1.001.00	0.50N 7.849
GRUP DB1	50.800	1.270	20.50	8.0035.50	1	1.001.00	0.50N 7.849
GRUP DB2	61.000	2.540	20.50	8.0034.50	1	1.001.00	0.50N 7.849
GRUP DB3	81.300	2.500	20.50	8.0034.50	1	1.001.00	0.50N 7.849
GRUP DB4	81.300	2.000	20.50	8.0034.50	1	1.001.00	0.50N 7.849
GRUP DB5	40.600	1.900	20.50	8.0034.50	1	1.001.00	0.50N 7.849
GRUP DB6	35.600	1.270	20.50	8.0027.50	1	1.001.00	0.50N 7.849
GRUP DB7	27.300	1.270	20.50	8.0027.50	1	1.001.00	0.50N 7.849
GRUP DB8	16.800	0.950	20.50	8.0027.50	1	1.001.00	0.50N 7.849
GRUP DC0 DJPG10		20.50	8.0034.00	1	1.001.00	0.50N	7.849
GRUP DC1 DPG7		20.50	8.0034.50	1	1.001.00	0.50N	7.849
GRUP DC2 DPG5		20.50	8.0034.50	1	1.001.00	0.50N	7.849
GRUP DC3 DPG4		20.50	8.0034.50	1	1.001.00	0.50N	7.849
GRUP DC4 IPE270		20.50	8.0027.50	1	1.001.00	1.00	0.50N 8.191
GRUP DC5 DJPG3		20.50	8.0034.50	1	1.001.00	0.50N	7.849
GRUP DC6 DJPG4		20.50	8.0034.00	1	1.001.00	0.50N	7.849
GRUP DC7 DJPG5		20.50	8.0034.00	1	1.001.00	0.50N	7.849
GRUP DC8 IPE600		20.50	8.0034.50	1	1.001.00	0.50N	7.849
GRUP DC9 DPG1		20.50	8.0034.00	1	1.001.00	0.50N	7.849
GRUP DCE HEB600		20.50	8.0034.50	1	1.001.00	0.50N	7.849
GRUP DCQ DEQ		20.50	8.0024.80	1	1.001.00	0.50N	0.001
GRUP DCW HEB600		20.50	8.0034.50	1	1.001.00	0.50N	7.849
GRUP DF1	45.720	1.270	20.50	8.0034.50	1	1.001.00	0.50N 7.849
GRUP DF2	40.640	1.270	20.50	8.0034.50	1	1.001.00	0.50N 7.849

GRUP DF3	27.300	0.927	20.50	8.0027.50	1	1.001.00	0.50N	7.849
GRUP DF4	21.910	0.953	20.50	8.0027.50	1	1.001.00	0.50N	7.849
GRUP DFB	27.300	1.270	20.50	8.0027.50	1	1.001.00	0.50N	7.849
GRUP DFC UPN220			20.50	8.0024.80	1	1.001.00	0.50N	7.849
GRUP DFG IPE220			20.50	8.0035.50	1	2.001.00	0.50N	7.849
GRUP DFH UPN220			20.50	8.0027.50	1	1.001.00	0.50N	7.849
GRUP DFK IPE220			20.50	8.0035.50	1	1.001.00	0.50N	7.849
GRUP DFL HEB300			20.50	8.0035.50	1	1.001.00	0.50N	7.849
GRUP DFP	40.600	1.270	20.50	8.0024.80	1	1.001.00	0.50N	7.849
GRUP DL1	137.10	6.500	20.50	8.0034.00	1	1.201.20	1.00	0.50N 7.849
GRUP DL2	152.40	2.500	20.50	8.0034.50	1	1.001.00	0.50N	7.849
GRUP DL3	152.40	2.500	20.50	8.0034.50	1	1.001.00	1.00	0.50N 7.849
GRUP DL4	152.40	2.500	20.50	8.0034.50	1	1.001.00	1.00	0.50N 7.849
GRUP DL5	152.40	2.500	20.50	8.0034.50	1	1.001.00	0.50N	7.849
GRUP DL5	152.40	4.000	20.50	8.0034.50	1	1.001.00	0.50N	7.8491.0
GRUP DL6	152.40	4.000	20.50	8.0034.50	1	1.001.00	0.50N	7.849
GRUP DLC DLCON			20.50	8.0034.50	1	1.001.00	0.50N	7.849
GRUP DLG	137.10	6.500	20.50	8.0034.00	1	1.201.20	1.00	0.50N 7.849
GRUP DM0 DJPG0			20.50	8.0034.50	1	1.001.00	0.50N	7.849
GRUP DM1 DPG12			20.50	8.0034.50	1	1.001.00	0.50N	7.849
GRUP DM2 DPG5			20.50	8.0034.50	1	1.001.00	0.50N	7.849
GRUP DM3 DPG10			20.50	8.0034.50	1	1.001.00	0.50N	7.849
GRUP DM4 DPG4			20.50	8.0034.50	1	1.001.00	0.50N	7.849
GRUP DM5 IPE270			20.50	8.0027.50	1	1.001.00	1.00	0.50N 8.191
GRUP DM6 DJPG2			20.50	8.0034.50	1	1.001.00	0.50N	7.849
GRUP DM7 IPE600			20.50	8.0034.50	1	1.001.00	0.50N	7.849
GRUP DM8 HEB600			20.50	8.0034.50	1	1.001.00	0.50N	7.849
GRUP DM9 DPG3			20.50	8.0034.50	1	1.001.00	0.50N	7.849
GRUP DME HEB600			20.50	8.0034.50	1	1.001.00	0.50N	7.849
GRUP DMQ DEQ			20.50	8.0024.80	1	1.001.00	0.50N	0.001
GRUP DS1	32.380	1.270	20.50	8.0027.50	1	1.001.00	0.50N	8.191
GRUP DS2 HEB300			20.50	8.0034.50	1	1.001.00	0.50N	8.191
GRUP DS3	27.300	1.270	20.50	8.0027.50	1	1.001.00	0.50N	8.191
GRUP DS4	16.800	1.097	20.50	8.0027.50	1	1.001.00	0.50N	8.191
GRUP DV1	121.90	3.000	20.50	8.0034.50	1	1.001.00	0.50N	7.849
GRUP DV2	61.000	3.000	20.50	8.0034.50	1	1.001.00	0.50N	7.849
GRUP DV3	50.800	1.430	20.50	8.0035.50	1	1.001.00	0.50N	7.849
GRUP DV4	50.800	1.270	20.50	8.0035.50	1	1.001.00	0.50N	7.849
GRUP DW0 DPG7			20.50	8.0034.50	1	1.001.00	0.50N	7.849
GRUP DW1 DPG12			20.50	8.0034.50	1	1.001.00	0.50N	7.849
GRUP DW2 DPG5			20.50	8.0034.50	1	1.001.00	0.50N	7.849
GRUP DW3 DPG9			20.50	8.0034.50	1	1.001.00	0.50N	7.849
GRUP DW4 IPE270			20.50	8.0027.50	1	1.001.00	1.00	0.50N 8.191
GRUP DW6 DJPG6			20.50	8.0034.50	1	1.001.00	0.50N	7.849
GRUP DW7 DJPG7			20.50	8.0034.50	1	1.001.00	0.50N	7.849
GRUP DW8 IPE600			20.50	8.0034.50	1	1.001.00	0.50N	7.849
GRUP DW9 DJPG8			20.50	8.0034.50	1	1.001.00	0.50N	7.849
GRUP DWB HEB300			20.50	8.0024.80	1	1.001.00	0.50N	0.001
GRUP DWC HEB300			20.50	8.0024.80	1	1.001.00	0.50N	0.001

GRUP DWD IPE270			20.50	8.0027.50	1	1.001.00	0.50N	0.010
GRUP DWN DPG2			20.50	8.0034.50	1	1.001.00	0.50N	7.849
GRUP DWS DJPG11			20.50	8.0034.50	1	1.001.00	0.50N	7.849
GRUP DWT	27.300	1.270	20.50	8.0024.80	1	1.001.00	0.50N	0.001
GRUP DWW HEB600			20.50	8.0034.50	1	1.001.00	0.50N	7.849
GRUP DZ0 DJPG9			20.50	8.0034.50	1	1.001.00	0.50N	7.849
GRUP DZ1 DPG7			20.50	8.0034.50	1	1.001.00	0.50N	7.849
GRUP DZ2 DPG5			20.50	8.0034.50	1	1.001.00	0.50N	7.849
GRUP DZ3 DPG4			20.50	8.0034.50	1	1.001.00	0.50N	7.849
GRUP DZ4 DPG13			20.50	8.0034.00	1	1.001.00	0.50N	7.849
GRUP DZ5 DPG9			20.50	8.0034.50	1	1.001.00	0.50N	7.849
GRUP DZ6 IPE270			20.50	8.0027.50	1	1.001.00	1.00	0.50N 8.191
GRUP DZ7 DJPG1			20.50	8.0034.50	1	1.001.00	0.50N	7.849
GRUP DZ8 IPE600			20.50	8.0034.50	1	1.001.00	0.50N	7.849
GRUP DZ9 HEB300			20.50	8.0027.50	1	1.001.00	0.50N	7.849
GRUP DZB HEB300			20.50	8.0035.50	1	1.001.00	0.50N	7.849
GRUP DZC DPB			20.50	8.0034.50	1	1.001.00	0.50N	7.849
GRUP DZE HEB600			20.50	8.0034.50	1	1.001.00	0.50N	7.849
GRUP DZQ DEQ			20.50	8.0024.80	1	1.001.00	0.50N	0.001
GRUP DZW HEB600			20.50	8.0034.50	1	1.001.00	0.50N	7.849
GRUP L31 CON7			20.50	8.0034.50	1	1.001.00	0.50F	7.849
GRUP L32 CON2			20.50	8.0034.00	1	1.001.00	0.50F	7.849
GRUP L33 CON4			20.50	8.0034.00	1	1.001.00	0.50F	7.849
GRUP L34 CON2			20.50	8.0034.00	1	1.001.00	0.50F	7.849
GRUP L35 CON2			20.50	8.0034.00	1	1.001.00	0.50F	7.849
GRUP L41 CON4			20.50	8.0034.00	1	1.001.00	0.50F	7.849
GRUP L42 CON3			20.50	8.0034.50	1	1.001.00	F	7.849
GRUP L42 CON5			20.50	8.0034.50	1	1.001.00	F10.4101.76	
GRUP L42 CON6			20.50	8.0034.50	1	1.001.00	F10.4100.75	
GRUP L43 CON6			20.50	7.8934.50	1	1.001.00	N	7.849
GRUP L44 CON4			20.50	8.0034.00	1	1.001.00	0.50F	7.849
GRUP L45 CON2			20.50	8.0034.00	1	1.001.00	0.50F	7.849
GRUP LG2 CON2			20.50	8.0034.00	1	1.001.00	0.50F	7.8493.0
GRUP LG2 CON3			20.50	8.0034.50	1	1.001.00	0.50F	7.849
GRUP LG2 CON2			20.50	8.0034.00	1	1.001.00	0.50F	7.8491.35
GRUP LG3 CON7			20.50	8.0034.50	1	1.001.00	0.50F	7.849
GRUP LG4 CON3			20.50	8.0034.50	1	1.001.00	0.50F	7.849
GRUP LG4 CON5			20.50	8.0034.50	1	1.001.00	0.50F10.4004.06	
GRUP LG4 CON6			20.50	8.0034.00	1	1.001.00	0.50F	8.9612.00
GRUP LG5 CON2			20.50	8.0034.00	1	1.001.00	0.50F	7.849
GRUP LG6	137.20	5.000	20.50	8.0034.50	1	1.001.00	0.50F	7.849
GRUP PL1 CON1			20.50	8.0034.00	1	1.001.00	0.50F	7.849
GRUP R1A	45.700	1.270	20.50	8.0035.50	1	.800.800	0.50N	7.849
GRUP R1B	45.700	1.270	20.50	8.0035.50	1	.800.800	0.50N	7.849
GRUP R1C	71.100	1.900	20.50	8.0034.50	1	.800.800	0.50N	7.849
GRUP R1D	71.100	1.900	20.50	8.0034.50	1	.800.800	0.50N	7.849
GRUP R1E	71.100	1.905	20.50	8.0035.50	1	.800.800	0.50N	7.849
GRUP R1F	71.100	1.905	20.50	8.0035.50	1	.800.800	0.50N	7.849
GRUP R2A	45.700	1.270	20.50	8.0035.50	1	.800.800	0.50N	7.849

Azin Azarhoushang  
Department of Civil Engineering

GRUP R2B	45.700	1.270	20.50	8.0035.50	1	.800.800	0.50N	7.849
GRUP R2C	71.100	1.900	20.50	8.0034.50	1	.800.800	0.50N	7.849
GRUP R2D	71.100	1.900	20.50	8.0034.50	1	.800.800	0.50N	7.849
GRUP R2E	71.100	1.905	20.50	8.0035.50	1	.800.800	0.50N	7.849
GRUP R2F	71.100	1.905	20.50	8.0035.50	1	.800.800	0.50N	7.849
GRUP RAA	45.720	1.588	20.50	8.0035.50	1	.800.800	0.50N	7.849
GRUP RAB	66.000	1.430	20.50	8.0035.50	1	.900.900	0.50N	7.849
GRUP RAB	66.000	2.540	20.50	8.0034.50	1	.900.900	0.50N	7.8491.0
GRUP RAC	66.000	1.430	20.50	8.0035.50	1	.900.900	0.50N	7.849
GRUP RAD	61.000	1.270	20.50	8.0035.50	1	.900.900	0.50N	7.849
GRUP RAD	61.000	2.060	20.50	8.0034.50	1	.900.900	0.50N	7.8491.0
GRUP RAE	61.000	1.270	20.50	8.0035.50	1	.900.900	0.50N	7.849
GRUP RAF	50.800	2.540	20.50	8.0034.50	1	.900.900	0.50N	7.849
GRUP RAG	50.200	2.240	20.50	8.0035.50	1	.900.900	0.50N	11.600
GRUP RAH	50.800	1.905	20.50	8.0034.50	1	.900.900	0.50N	7.849
GRUP RAJ	50.800	1.905	20.50	8.0034.50	1	.900.900	0.50N	7.849
GRUP RAJ	50.800	2.540	20.50	8.0034.50	1	.900.900	0.50N	7.8490.75
GRUP RAK	50.800	2.540	20.50	8.0034.50	1	.900.900	0.50N	7.849
GRUP RAK	50.800	2.540	20.50	8.0034.50	1	.900.900	0.50N	7.8490.75
GRUP RAL	66.000	1.270	20.50	8.0035.50	1	.900.900	0.50N	7.849
GRUP RAL	66.000	2.540	20.50	8.0035.50	1	.900.900	0.50N	7.8491.0
GRUP RAM	66.000	1.270	20.50	8.0035.50	1	.900.900	0.50N	7.849
GRUP RBA	45.720	1.588	20.50	8.0035.50	1	.800.800	0.50N	7.849
GRUP RBB	66.000	1.430	20.50	8.0035.50	1	.900.900	0.50N	7.849
GRUP RBB	66.000	2.540	20.50	8.0034.50	1	.900.900	0.50N	7.8491.0
GRUP RBC	66.000	1.430	20.50	8.0035.50	1	.900.900	0.50N	7.849
GRUP RBD	61.000	1.270	20.50	8.0035.50	1	.900.900	0.50N	7.849
GRUP RBD	61.000	2.060	20.50	8.0034.50	1	.900.900	0.50N	7.8491.0
GRUP RBE	61.000	1.270	20.50	8.0035.50	1	.900.900	0.50N	7.849
GRUP RBF	50.200	2.240	20.50	8.0034.50	1	.900.900	0.50N	11.600
GRUP RBG	50.800	2.540	20.50	8.0034.50	1	.900.900	0.50N	7.849
GRUP RBH	50.800	1.905	20.50	8.0034.50	1	.900.900	0.50N	7.849
GRUP RBH	50.800	2.540	20.50	8.0034.50	1	.900.900	0.50N	7.8490.75
GRUP RBJ	50.800	1.905	20.50	8.0034.50	1	.900.900	0.50N	7.849
GRUP RBK	50.800	2.540	20.50	8.0034.50	1	.900.900	0.50N	7.849
GRUP RBK	50.800	2.540	20.50	8.0034.50	1	.900.900	0.50N	7.8490.75
GRUP RBL	66.000	1.270	20.50	8.0035.50	1	.900.900	0.50N	7.849
GRUP RBM	66.000	1.270	20.50	8.0035.50	1	.900.900	0.50N	7.849
GRUP RBM	66.000	2.540	20.50	8.0034.50	1	.900.900	0.50N	7.8491.0
GRUP RIA	58.500	2.540	20.50	8.0035.50	1	1.001.00	0.50F	0.001
GRUP RS1	25.400	1.270	20.50	8.0035.50	1	1.001.00	0.50N	7.849
GRUP SEA	27.300	1.270	20.50	8.0034.00	1	1.001.00	0.50N	7.849
GRUP SEB	50.000	1.270	20.50	8.0024.80	1	1.001.00	0.50N	7.849
GRUP SEC	50.000	1.270	20.50	8.0024.80	1	1.001.00	0.50N	7.849
GRUP STB P1LSTUB			20.50	8.0034.50	9	1.001.00	0.50F	7.849
MEMBER								
.								
PGRUP								
PGRUP DPO	1.0000	20.000	0.250	24.800				0.001

PGRUP DP1	0.8000	20.000	0.25027.500	8.191
PGRUP DP2	0.8000	20.000	0.25027.500	8.191
PGRUP DP3	0.8000	20.000	0.25027.500	8.191
PGRUP DP4	0.8000	20.000	0.25027.500	8.191
PLATE				
.				
JOINT				
JOINT	2	-15.238	-18.000-42.600	1825422
JOINT	20	15.238	-18.000-42.600	2825424
JOINT	82	-15.238	18.000-42.600	3825427
JOINT	100	15.238	18.000-42.600	4825431
JOINT	101	-15.073	-18.000-41.285	5825436
JOINT	103	0.000	-18.000-41.285	6825442
JOINT	104	0.000	18.000-41.285	7825449
JOINT	105	-15.073	0.000-41.285	8825457
JOINT	106	15.073	0.000-41.285	9825466
JOINT	111	0.000	-18.000-32.861	10825476
JOINT	112	0.000	-18.000-16.566	11825487
JOINT	113	0.000	-18.000 -1.397	12825499
JOINT	114	0.000	18.000-32.861	13825512
JOINT	115	-0.001	18.000-16.565	14825526
JOINT	116	0.000	18.000 -1.397	15825541
JOINT	117	-15.073	-3.090-41.285	16825557
JOINT	118	-15.073	3.090-41.285	17825574
JOINT	119	15.073	-18.000-41.285	18825592
JOINT	121	15.073	3.090-41.285	19825611
JOINT	122	15.073	-3.090-41.285	20825631
JOINT	123	0.852	-18.000 -0.788	21825652
JOINT	124	-0.852	-18.000 -0.788	22825674
JOINT	125	0.852	18.000 -0.788	23825697
JOINT	126	-0.852	18.000 -0.790	24825721
JOINT	181	-15.073	18.000-41.285	25825746
JOINT	199	15.073	18.000-41.285	26825772
JOINT	201	-13.075	-18.000-25.300	27825799
JOINT	203	0.000	-18.000-25.300	28825827
JOINT	204	0.000	18.000-25.300	29825856
JOINT	205	-13.075	0.000-25.300	30825886
JOINT	206	13.075	0.000-25.300	31825917
JOINT	219	13.075	-18.000-25.300	32825949
JOINT	221	12.870	18.000-23.663	33825982
JOINT	222	11.255	18.000-10.736	34826016
JOINT	223	-11.255	-18.000-10.736	35826051
JOINT	224	-11.255	18.000-10.736	36826087
JOINT	225	11.255	-18.000-10.736	37826124
JOINT	226	12.870	-18.000-23.663	38826162
JOINT	227	-12.870	18.000-23.663	39826201
JOINT	228	-12.870	-18.000-23.663	40826241
JOINT	281	-13.075	18.000-25.300	41826282
JOINT	299	13.075	18.000-25.300	42826324

JOINT	301	-11.038-18.000	-9.000	43826367
JOINT	303	0.000-18.000	-9.000	44826411
JOINT	304	0.000 18.000	-9.000	45826456
JOINT	305	-11.038 0.000	-9.000	46826502
JOINT	306	11.038 0.000	-9.000	47826549
JOINT	319	11.038-18.000	-9.000	48826597
JOINT	321	10.707 18.000	-6.355	49826646
JOINT	322	-10.845 18.000	-7.452	50826696
JOINT	323	10.845-18.000	-7.452	51826747
JOINT	324	-10.845-18.000	-7.452	52826799
JOINT	381	-11.038 18.000	-9.000	53826852
JOINT	399	11.038 18.000	-9.000	54826906
JOINT	401	-9.288-18.000	5.000	55826961
JOINT	419	9.288-18.000	5.000	56827017
JOINT	481	-9.288 18.000	5.000	57827074
JOINT	499	9.288 18.000	5.000	58827132
JOINT	501	-9.163-18.000	6.000	59827191
JOINT	519	9.163-18.000	6.000	60827251
JOINT	581	-9.163 18.000	6.000	61827312
JOINT	599	9.163 18.000	6.000	62827374
JOINT	601	-9.000-18.000	7.300	63827437
JOINT	619	9.000-18.000	7.300	64827501
JOINT	631	-9.000-18.000	9.300	65827566
JOINT	649	9.000-18.000	9.300	66827632
JOINT	681	-9.000 18.000	7.300	67827699
JOINT	689	9.000 18.000	9.300	68827767
JOINT	691	-9.000 18.000	9.300	69827836
JOINT	699	9.000 18.000	7.300	70827906
JOINT	1001	12.663 18.000	5.000	71827977
JOINT	1002	12.663 18.000	1.000	72828049
JOINT	1004	9.788 18.000	1.000	73828122
JOINT	1005	12.663 18.000	3.800	74828196
JOINT	1006	15.663 18.000	3.800	75828271
JOINT	1007	15.663 18.000	-7.000	76828347
JOINT	1009	10.788 18.000	-7.000	77828424
JOINT	1010	12.663 26.000	5.000	78828502
JOINT	1011	12.663 26.000	1.000	79828581
JOINT	1012	14.663 18.000	-7.000	80828661
JOINT	1013	15.663 26.000	-7.000	81828742
JOINT	1015	14.663 24.359	-7.000	82828824
JOINT	1016	15.663 26.000	3.800	83828907
JOINT	1017	12.663 26.000	3.800	84828991
JOINT	1018	15.663 18.000	3.130	85829076
JOINT	1021	15.663 18.000	1.400	86829162
JOINT	1022	15.663 18.000	-1.500	87829249
JOINT	1023	15.663 26.000	-1.500	88829337
JOINT	1024	15.663 26.000	1.400	89829426
JOINT	1025	15.663 19.333	-1.500	90829516
JOINT	1026	15.663 20.667	-1.500	91829607

JOINT 1027	15.663	22.000	-1.500	92829699
JOINT 1028	15.663	23.333	-1.500	93829792
JOINT 1029	15.663	24.667	-1.500	94829886
JOINT 1030	15.663	19.333	1.400	95829981
JOINT 1031	15.663	20.667	1.400	96830077
JOINT 1032	15.663	22.000	1.400	97830174
JOINT 1033	15.663	23.333	1.400	98830272
JOINT 1034	15.663	24.667	1.400	99830371
JOINT 1035	15.663	19.333	3.130	100830471
JOINT 1036	15.663	20.667	3.130	101830572
JOINT 1101	-14.393	-19.247	-41.285	102830674
JOINT 1102	-12.355	-19.247	-25.300	103830777
JOINT 1103	-10.318	-19.247	-9.000	104830881
JOINT 1104	-8.443	-19.247	6.000	105830986
JOINT 1201	-5.950	18.000	5.000	106831092
JOINT 1202	3.000	18.000	5.000	107831199
JOINT 1203	8.200	18.000	5.000	108831307
JOINT 1204	-7.150	16.300	5.000	109831416
JOINT 1205	-2.650	16.300	5.000	110831526
JOINT 1206	7.000	16.300	5.000	111831637
JOINT 1207	-7.150	16.300	-9.000	112831749
JOINT 1208	-2.650	16.300	-9.000	113831862
JOINT 1209	7.000	16.300	-9.000	114831976
JOINT 1210	-5.950	18.000	-9.000	115832091
JOINT 1211	8.200	18.000	-9.000	116832207
JOINT 1212	5.800	18.000	-9.000	117832324
JOINT 1213	-7.150	16.300	-30.100	118832442
JOINT 1214	-2.650	16.300	-30.100	119832561
JOINT 1215	7.000	16.300	-30.100	120832681
JOINT 1216	7.000	16.300	-25.300	121832802
JOINT 1217	-7.150	16.300	-25.300	122832924
JOINT 1218	-2.650	16.300	-25.300	123833047
JOINT 1221	-5.950	18.000	-25.300	124833171
JOINT 1222	5.800	18.000	-25.300	125833296
JOINT 1223	8.200	18.000	-25.300	126833422
JOINT 1224	8.288	-17.000	5.000	127833549
JOINT 1225	-6.000	16.500	13.000	128833677
JOINT 1226	3.000	16.500	13.000	129833806
JOINT 1227	7.000	16.500	13.000	130833936
JOINT 1228	8.288	-17.000	13.000	131834067
JOINT 1229	8.288	-17.000	3.900	132834199
JOINT 3101	-9.000	-18.000	11.300	133834332
JOINT 3149	9.000	-18.000	11.300	134834466
JOINT 3201	-3.000	-5.000	10.300	135834601
JOINT 3203	0.000	-5.000	10.300	136834737
JOINT 3204	3.000	-5.000	10.300	137834874
JOINT 3205	6.000	-5.000	10.300	138835012
JOINT 3206	9.000	-5.000	10.300	139835151
JOINT 3207	-3.000	-2.000	10.300	140835291

JOINT 3208	9.000	-2.000	10.300	141835432
JOINT 3209	-3.000	1.000	10.300	142835574
JOINT 3210	0.000	1.000	10.300	143835717
JOINT 3211	3.000	1.000	10.300	144835861
JOINT 3212	6.000	1.000	10.300	145836006
JOINT 3213	9.000	1.000	10.300	146836152
JOINT 3214	-3.000	-4.000	10.300	147836299
JOINT 3215	-3.000	-3.000	10.300	148836447
JOINT 3216	-3.000	-1.000	10.300	149836596
JOINT 3217	-3.000	0.000	10.300	150836746
JOINT 3218	9.000	-4.000	10.300	151836897
JOINT 3219	9.000	-3.000	10.300	152837049
JOINT 3221	9.000	-1.000	10.300	153837202
JOINT 3222	9.000	0.000	10.300	154837356
JOINT 3223	0.000	-4.000	10.300	155837511
JOINT 3224	0.000	-3.000	10.300	156837667
JOINT 3225	0.000	-2.000	10.300	157837824
JOINT 3226	0.000	-1.000	10.300	158837982
JOINT 3227	0.000	0.000	10.300	159838141
JOINT 3228	3.000	-4.000	10.300	160838301
JOINT 3229	3.000	-3.000	10.300	161838462
JOINT 3230	3.000	-2.000	10.300	162838624
JOINT 3231	3.000	-1.000	10.300	163838787
JOINT 3232	3.000	0.000	10.300	164838951
JOINT 3233	6.000	-4.000	10.300	165839116
JOINT 3234	6.000	-3.000	10.300	166839282
JOINT 3235	6.000	-2.000	10.300	167839449
JOINT 3236	6.000	-1.000	10.300	168839617
JOINT 3237	6.000	0.000	10.300	169839786
JOINT 3251	-3.000	-4.500	10.300	170839956
JOINT 3252	0.000	-4.500	10.300	171840127
JOINT 3253	3.000	-4.500	10.300	172840299
JOINT 3254	6.000	-4.500	10.300	173840472
JOINT 3255	9.000	-4.500	10.300	174840646
JOINT 3501	-9.000	18.000	11.300	175840821
JOINT 3549	9.000	18.000	11.300	176840997
JOINT 4049	-10.734	-23.600	13.300	177841174
JOINT 4050	-9.867	-23.600	13.300	178841352
JOINT 4051	-9.000	-23.600	13.300	179841531
JOINT 4060	0.000	-23.600	13.300	180841711
JOINT 4062	1.000	-23.600	13.300	181841892
JOINT 4063	2.000	-23.600	13.300	182842074
JOINT 4064	3.000	-23.600	13.300	183842257
JOINT 4065	4.000	-23.600	13.300	184842441
JOINT 4066	5.000	-23.600	13.300	185842626
JOINT 4067	6.000	-23.600	13.300	186842812
JOINT 4068	7.000	-23.600	13.300	187842999
JOINT 4069	8.000	-23.600	13.300	188843187
JOINT 4070	9.000	-23.600	13.300	189843376



JOINT 4071	9.867-23.600	13.300	190843566
JOINT 4072	10.734-23.600	13.300	191843757
JOINT 4075	3.000-21.600	13.300	192843949
JOINT 4081	-9.000-20.600	13.300	193844142
JOINT 4083	0.000-20.600	13.300	194844336
JOINT 4084	-8.000-20.600	13.300	195844531
JOINT 4085	-1.000-20.600	13.300	196844727
JOINT 4086	-7.000-20.600	13.300	197844924
JOINT 4087	-6.000-20.600	13.300	198845122
JOINT 4089	-4.000-20.600	13.300	199845321
JOINT 4090	-3.000-20.600	13.300	200845521
JOINT 4091	-2.000-20.600	13.300	201845722
JOINT 4099	-10.734-18.000	13.300	202845924
JOINT 4100	-9.867-18.000	13.300	203846127
JOINT 4101	-9.000-18.000	13.300	204846331
JOINT 4102	-8.000-18.000	13.300	205846536
JOINT 4103	-7.000-18.000	13.300	206846742
JOINT 4104	-6.000-18.000	13.300	207846949
JOINT 4105	-5.000-18.000	13.300	208847157
JOINT 4106	-4.000-18.000	13.300	209847366
JOINT 4107	-3.000-18.000	13.300	210847576
JOINT 4108	-2.000-18.000	13.300	211847787
JOINT 4109	-1.000-18.000	13.300	212847999
JOINT 4110	0.000-18.000	13.300	213848212
JOINT 4112	1.000-18.000	13.300	214848426
JOINT 4113	2.000-18.000	13.300	215848641
JOINT 4114	3.000-18.000	13.300	216848857
JOINT 4115	4.000-18.000	13.300	217849074
JOINT 4116	5.000-18.000	13.300	218849292
JOINT 4117	6.000-18.000	13.300	219849511
JOINT 4118	7.000-18.000	13.300	220849731
JOINT 4119	8.000-18.000	13.300	221849952
JOINT 4120	9.000-18.000	13.300	222850174
JOINT 4121	9.867-18.000	13.300	223850397
JOINT 4122	10.734-18.000	13.300	224850621
JOINT 4123	-8.710-18.000	13.300	225850846
JOINT 4124	8.710-18.000	13.300	226851072
JOINT 4125	11.600 28.000	13.300	227851299
JOINT 4126	11.600 23.000	13.300	228851527
JOINT 4127	11.600 18.000	13.300	229851756
JOINT 4128	11.600 13.500	13.300	230851986
JOINT 4129	11.600 9.000	13.300	231852217
JOINT 4130	-9.000-17.240	13.300	232852449
JOINT 4131	-9.000 17.240	13.300	233852682
JOINT 4132	-9.000-18.730	13.300	234852916
JOINT 4133	-9.000 18.775	13.300	235853151
JOINT 4134	11.600 4.500	13.300	236853387
JOINT 4135	9.000-17.240	13.300	237853624
JOINT 4136	9.000 17.240	13.300	238853862

JOINT 4137	9.000	18.775	13.300	239854101
JOINT 4138	11.600	0.000	13.300	240854341
JOINT 4139	11.600-13.500		13.300	241854582
JOINT 4140	11.600	-4.500	13.300	242854824
JOINT 4141	11.600	-9.000	13.300	243855067
JOINT 4142	11.600-18.000		13.300	244855311
JOINT 4143	11.600-23.600		13.300	245855556
JOINT 4145	-11.600-13.500		13.300	246855802
JOINT 4146	-11.600	-4.500	13.300	247856049
JOINT 4147	-11.600	0.000	13.300	248856297
JOINT 4148	-11.600	4.500	13.300	249856546
JOINT 4149	-10.734-13.500		13.300	250856796
JOINT 4150	-9.867-13.500		13.300	251857047
JOINT 4151	-9.000-13.500		13.300	252857299
JOINT 4152	-8.000-13.500		13.300	253857552
JOINT 4153	-7.000-13.500		13.300	254857806
JOINT 4154	-6.000-13.500		13.300	255858061
JOINT 4155	-5.000-13.500		13.300	256858317
JOINT 4156	-4.000-13.500		13.300	257858574
JOINT 4157	-3.000-13.500		13.300	258858832
JOINT 4158	-2.000-13.500		13.300	259859091
JOINT 4159	-1.000-13.500		13.300	260859351
JOINT 4160	0.000-13.500		13.300	261859612
JOINT 4161	-11.600	9.000	13.300	262859874
JOINT 4162	1.000-13.500		13.300	263860137
JOINT 4163	2.000-13.500		13.300	264860401
JOINT 4164	3.000-13.500		13.300	265860666
JOINT 4165	4.000-13.500		13.300	266860932
JOINT 4166	5.000-13.500		13.300	267861199
JOINT 4167	6.000-13.500		13.300	268861467
JOINT 4168	7.000-13.500		13.300	269861736
JOINT 4169	8.000-13.500		13.300	270862006
JOINT 4170	9.000-13.500		13.300	271862277
JOINT 4171	9.867-13.500		13.300	272862549
JOINT 4172	10.734-13.500		13.300	273862822
JOINT 4173	-11.600	13.500	13.300	274863096
JOINT 4174	-11.600	28.000	13.300	275863371
JOINT 4175	-11.600-23.600		13.300	276863647
JOINT 4176	-11.600	-9.000	13.300	277863924
JOINT 4177	-11.600	18.000	13.300	278864202
JOINT 4178	-11.600	23.000	13.300	279864481
JOINT 4179	-11.600-18.000		13.300	280864761
JOINT 4180	-1.000-11.250		13.300	281865042
JOINT 4183	-1.000-24.700		16.600	282865324
JOINT 4184	-1.000-21.200		16.600	283865607
JOINT 4185	-8.000-24.700		16.600	284865891
JOINT 4186	-8.000-21.200		16.600	285866176
JOINT 4187	-17.300	9.000	16.600	286866462
JOINT 4188	-13.800	9.000	16.600	287866749

JOINT 4189	12.200	11.000	16.600	288867037
JOINT 4190	15.700	11.000	16.600	289867326
JOINT 4191	2.000-15.750	13.300	290867616	
JOINT 4199	-10.734	-9.000	13.300	291867907
JOINT 4200	-9.867	-9.000	13.300	292868199
JOINT 4201	-9.000	-9.000	13.300	293868492
JOINT 4202	-8.000	-9.000	13.300	294868786
JOINT 4203	-7.000	-9.000	13.300	295869081
JOINT 4204	-6.000	-9.000	13.300	296869377
JOINT 4205	-5.000	-9.000	13.300	297869674
JOINT 4206	-4.000	-9.000	13.300	298869972
JOINT 4207	-3.000	-9.000	13.300	299870271
JOINT 4208	-2.000	-9.000	13.300	300870571
JOINT 4209	-1.000	-9.000	13.300	301870872
JOINT 4210	0.000	-9.000	13.300	302871174
JOINT 4212	1.000	-9.000	13.300	303871477
JOINT 4213	2.000	-9.000	13.300	304871781
JOINT 4214	3.000	-9.000	13.300	305872086
JOINT 4215	4.000	-9.000	13.300	306872392
JOINT 4216	5.000	-9.000	13.300	307872699
JOINT 4217	6.000	-9.000	13.300	308873007
JOINT 4218	7.000	-9.000	13.300	309873316
JOINT 4219	8.000	-9.000	13.300	310873626
JOINT 4220	9.000	-9.000	13.300	311873937
JOINT 4221	9.867	-9.000	13.300	312874249
JOINT 4222	10.734	-9.000	13.300	313874562
JOINT 4225	12.600	-2.900	13.300	314874876
JOINT 4226	13.600	-2.900	13.300	315875191
JOINT 4227	14.600	-2.900	13.300	316875507
JOINT 4228	15.600	-2.900	13.300	317875824
JOINT 4229	9.000	-2.900	13.300	318876142
JOINT 4230	9.867	-2.900	13.300	319876461
JOINT 4232	9.000-18.730	13.300	320876781	
JOINT 4233	10.734	-2.900	13.300	321877102
JOINT 4234	11.600	-2.900	13.300	322877424
JOINT 4235	0.000-21.600	13.300	323877747	
JOINT 4237	-6.000-11.250	13.300	324878071	
JOINT 4238	-2.000-11.250	13.300	325878396	
JOINT 4239	3.000-15.750	13.300	326878722	
JOINT 4240	7.000-15.750	13.300	327879049	
JOINT 4241	15.600	-9.000	13.300	328879377
JOINT 4242	15.600	-4.500	13.300	329879706
JOINT 4243	12.600	-9.000	13.300	330880036
JOINT 4244	13.600	-9.000	13.300	331880367
JOINT 4245	14.600	-9.000	13.300	332880699
JOINT 4246	12.600	-4.500	13.300	333881032
JOINT 4247	13.600	-4.500	13.300	334881366
JOINT 4248	14.600	-4.500	13.300	335881701
JOINT 4249	-10.734	-4.500	13.300	336882037

JOINT 4250	-9.867	-4.500	13.300	337882374
JOINT 4251	-9.000	-4.500	13.300	338882712
JOINT 4252	-8.000	-4.500	13.300	339883051
JOINT 4253	-7.000	-4.500	13.300	340883391
JOINT 4254	-6.000	-4.500	13.300	341883732
JOINT 4255	-5.000	-4.500	13.300	342884074
JOINT 4256	-4.000	-4.500	13.300	343884417
JOINT 4257	-3.000	-4.500	13.300	344884761
JOINT 4258	-2.000	-4.500	13.300	345885106
JOINT 4259	-1.000	-4.500	13.300	346885452
JOINT 4260	0.000	-4.500	13.300	347885799
JOINT 4262	1.000	-4.500	13.300	348886147
JOINT 4263	2.000	-4.500	13.300	349886496
JOINT 4264	3.000	-4.500	13.300	350886846
JOINT 4265	4.000	-4.500	13.300	351887197
JOINT 4266	5.000	-4.500	13.300	352887549
JOINT 4267	6.000	-4.500	13.300	353887902
JOINT 4268	7.000	-4.500	13.300	354888256
JOINT 4269	8.000	-4.500	13.300	355888611
JOINT 4270	9.000	-4.500	13.300	356888967
JOINT 4271	9.867	-4.500	13.300	357889324
JOINT 4272	10.734	-4.500	13.300	358889682
JOINT 4275	-9.000	11.500	13.300	359890041
JOINT 4276	9.000	10.200	13.300	360890401
JOINT 4277	-9.000	6.500	13.300	361890762
JOINT 4278	9.000	6.500	13.300	362891124
JOINT 4279	-9.000	-11.500	13.300	363891487
JOINT 4280	9.000	-11.500	13.300	364891851
JOINT 4283	-9.000	-6.500	13.300	365892216
JOINT 4284	9.000	-6.500	13.300	366892582
JOINT 4299	-10.734	0.000	13.300	367892949
JOINT 4300	-9.867	0.000	13.300	368893317
JOINT 4301	-9.000	0.000	13.300	369893686
JOINT 4302	-8.000	0.000	13.300	370894056
JOINT 4303	-7.000	0.000	13.300	371894427
JOINT 4304	-6.000	0.000	13.300	372894799
JOINT 4305	-5.000	0.000	13.300	373895172
JOINT 4306	-4.000	0.000	13.300	374895546
JOINT 4307	-3.000	0.000	13.300	375895921
JOINT 4308	-2.000	0.000	13.300	376896297
JOINT 4309	-1.000	0.000	13.300	377896674
JOINT 4310	0.000	0.000	13.300	378897052
JOINT 4312	1.000	0.000	13.300	379897431
JOINT 4313	2.000	0.000	13.300	380897811
JOINT 4314	3.000	0.000	13.300	381898192
JOINT 4315	4.000	0.000	13.300	382898574
JOINT 4316	5.000	0.000	13.300	383898957
JOINT 4317	6.000	0.000	13.300	384899341
JOINT 4318	7.000	0.000	13.300	385899726

JOINT 4319	8.000	0.000	13.300	386900112
JOINT 4320	9.000	0.000	13.300	387900499
JOINT 4321	9.867	0.000	13.300	388900887
JOINT 4322	10.734	0.000	13.300	389901276
JOINT 4325	-8.000	-21.200	13.300	390901666
JOINT 4326	-1.000	-21.200	13.300	391902057
JOINT 4327	-8.000	-24.700	13.300	392902449
JOINT 4328	-1.000	-24.700	13.300	393902842
JOINT 4330	-9.000	-1.755	13.300	394903236
JOINT 4331	-9.000	-0.285	13.300	395903631
JOINT 4332	-9.000	0.285	13.300	396904027
JOINT 4333	9.000	-0.285	13.300	397904424
JOINT 4334	9.000	0.285	13.300	398904822
JOINT 4335	-9.000	1.755	13.300	399905221
JOINT 4336	9.000	-1.755	13.300	400905621
JOINT 4337	9.000	1.755	13.300	401906022
JOINT 4338	-9.000	-19.370	13.300	402906424
JOINT 4339	-9.000	-15.836	13.300	403906827
JOINT 4340	-9.000	16.000	13.300	404907231
JOINT 4341	-9.000	19.415	13.300	405907636
JOINT 4342	9.000	-19.370	13.300	406908042
JOINT 4343	9.000	-15.836	13.300	407908449
JOINT 4344	9.000	15.836	13.300	408908857
JOINT 4345	9.000	19.370	13.300	409909266
JOINT 4349	-10.734	4.500	13.300	410909676
JOINT 4350	-9.867	4.500	13.300	411910087
JOINT 4351	-9.000	4.500	13.300	412910499
JOINT 4352	-8.000	4.500	13.300	413910912
JOINT 4353	-7.000	4.500	13.300	414911326
JOINT 4354	-6.000	4.500	13.300	415911741
JOINT 4355	-5.000	4.500	13.300	416912157
JOINT 4356	-4.000	4.500	13.300	417912574
JOINT 4357	-3.000	4.500	13.300	418912992
JOINT 4358	-2.000	4.500	13.300	419913411
JOINT 4359	-1.000	4.500	13.300	420913831
JOINT 4360	0.000	4.500	13.300	421914252
JOINT 4362	1.000	4.500	13.300	422914674
JOINT 4363	2.000	4.500	13.300	423915097
JOINT 4364	3.000	4.500	13.300	424915521
JOINT 4365	4.000	4.500	13.300	425915946
JOINT 4366	5.000	4.500	13.300	426916372
JOINT 4367	6.000	4.500	13.300	427916799
JOINT 4368	7.000	4.500	13.300	428917227
JOINT 4369	8.000	4.500	13.300	429917656
JOINT 4370	9.000	4.500	13.300	430918086
JOINT 4371	9.867	4.500	13.300	431918517
JOINT 4372	10.734	4.500	13.300	432918949
JOINT 4375	12.200	18.000	13.300	433919382
JOINT 4376	15.700	18.000	13.300	434919816

JOINT 4377	15.700	11.000	13.300	435920251
JOINT 4378	12.200	11.000	13.300	436920687
JOINT 4379	-13.800	9.000	13.300	437921124
JOINT 4380	-17.300	9.000	13.300	438921562
JOINT 4383	-17.300	16.000	13.300	439922001
JOINT 4384	-13.800	16.000	13.300	440922441
JOINT 4385	9.000	1.000	13.300	441922882
JOINT 4386	9.000	-5.000	13.300	442923324
JOINT 4387	6.000	-5.000	13.300	443923767
JOINT 4388	3.000	-5.000	13.300	444924211
JOINT 4389	0.000	-5.000	13.300	445924656
JOINT 4390	-3.000	-5.000	13.300	446925102
JOINT 4391	-3.000	1.000	13.300	447925549
JOINT 4392	0.000	1.000	13.300	448925997
JOINT 4393	3.000	1.000	13.300	449926446
JOINT 4394	6.000	1.000	13.300	450926896
JOINT 4395	-3.000	-2.000	13.300	451927347
JOINT 4396	9.000	-2.000	13.300	452927799
JOINT 4399	-10.734	9.000	13.300	453928252
JOINT 4400	-9.867	9.000	13.300	454928706
JOINT 4401	-9.000	9.000	13.300	455929161
JOINT 4402	-8.000	9.000	13.300	456929617
JOINT 4403	-7.000	9.000	13.300	457930074
JOINT 4404	-6.000	9.000	13.300	458930532
JOINT 4405	-5.000	9.000	13.300	459930991
JOINT 4406	-4.000	9.000	13.300	460931451
JOINT 4407	-3.000	9.000	13.300	461931912
JOINT 4408	-2.000	9.000	13.300	462932374
JOINT 4409	-1.000	9.000	13.300	463932837
JOINT 4410	0.000	9.000	13.300	464933301
JOINT 4412	1.000	9.000	13.300	465933766
JOINT 4413	2.000	9.000	13.300	466934232
JOINT 4414	3.000	9.000	13.300	467934699
JOINT 4415	4.000	9.000	13.300	468935167
JOINT 4416	5.000	9.000	13.300	469935636
JOINT 4417	6.000	9.000	13.300	470936106
JOINT 4418	7.000	9.000	13.300	471936577
JOINT 4419	8.000	9.000	13.300	472937049
JOINT 4420	9.000	9.000	13.300	473937522
JOINT 4421	9.867	9.000	13.300	474937996
JOINT 4422	10.734	9.000	13.300	475938471
JOINT 4425	-6.000	16.500	13.300	476938947
JOINT 4426	3.000	16.500	13.300	477939424
JOINT 4427	7.000	16.500	13.300	478939902
JOINT 4449	-10.734	13.500	13.300	479940381
JOINT 4450	-9.867	13.500	13.300	480940861
JOINT 4451	-9.000	13.500	13.300	481941342
JOINT 4452	-8.000	13.500	13.300	482941824
JOINT 4453	-7.000	13.500	13.300	483942307

JOINT 4454	-6.000	13.500	13.300	484942791
JOINT 4455	-5.000	13.500	13.300	485943276
JOINT 4456	-4.000	13.500	13.300	486943762
JOINT 4457	-3.000	13.500	13.300	487944249
JOINT 4458	-2.000	13.500	13.300	488944737
JOINT 4459	-1.000	13.500	13.300	489945226
JOINT 4460	0.000	13.500	13.300	490945716
JOINT 4462	1.000	13.500	13.300	491946207
JOINT 4463	2.000	13.500	13.300	492946699
JOINT 4464	3.000	13.500	13.300	493947192
JOINT 4465	4.000	13.500	13.300	494947686
JOINT 4466	5.000	13.500	13.300	495948181
JOINT 4467	6.000	13.500	13.300	496948677
JOINT 4468	7.000	13.500	13.300	497949174
JOINT 4469	8.000	13.500	13.300	498949672
JOINT 4470	9.000	13.500	13.300	499950171
JOINT 4471	9.867	13.500	13.300	500950671
JOINT 4472	10.734	13.500	13.300	501951172
JOINT 4475	12.200	18.000	16.600	502951674
JOINT 4476	15.700	18.000	16.600	503952177
JOINT 4477	-17.300	16.000	16.600	504952681
JOINT 4478	-13.800	16.000	16.600	505953186
JOINT 4479	11.600	11.000	13.300	506953692
JOINT 4480	10.734	11.000	13.300	507954199
JOINT 4483	9.867	11.000	13.300	508954707
JOINT 4484	9.000	11.000	13.300	509955216
JOINT 4485	-11.600	16.000	13.300	510955726
JOINT 4486	-10.734	16.000	13.300	511956237
JOINT 4487	-9.867	16.000	13.300	512956749
JOINT 4499	-10.734	18.000	13.300	513957262
JOINT 4500	-9.867	18.000	13.300	514957776
JOINT 4501	-9.000	18.000	13.300	515958291
JOINT 4502	-8.000	18.000	13.300	516958807
JOINT 4503	-7.000	18.000	13.300	517959324
JOINT 4504	-6.000	18.000	13.300	518959842
JOINT 4505	-5.000	18.000	13.300	519960361
JOINT 4506	-4.000	18.000	13.300	520960881
JOINT 4507	-3.000	18.000	13.300	521961402
JOINT 4508	-2.000	18.000	13.300	522961924
JOINT 4509	-1.000	18.000	13.300	523962447
JOINT 4510	0.000	18.000	13.300	524962971
JOINT 4512	1.000	18.000	13.300	525963496
JOINT 4513	2.000	18.000	13.300	526964022
JOINT 4514	3.000	18.000	13.300	527964549
JOINT 4515	4.000	18.000	13.300	528965077
JOINT 4516	5.000	18.000	13.300	529965606
JOINT 4517	6.000	18.000	13.300	530966136
JOINT 4518	7.000	18.000	13.300	531966667
JOINT 4519	8.000	18.000	13.300	532967199

JOINT 4520	9.000	18.000	13.300	533967732
JOINT 4521	9.867	18.000	13.300	534968266
JOINT 4522	10.734	18.000	13.300	535968801
JOINT 4541	-15.500	23.000	13.300	536969337
JOINT 4542	-15.500	18.000	13.300	537969874
JOINT 4543	-15.500	-18.000	13.300	538970412
JOINT 4544	-15.500	-23.600	13.300	539970951
JOINT 4549	-10.734	23.000	13.300	540971491
JOINT 4550	-9.867	23.000	13.300	541972032
JOINT 4551	-9.000	23.000	13.300	542972574
JOINT 4552	-8.000	23.000	13.300	543973117
JOINT 4553	-7.000	23.000	13.300	544973661
JOINT 4554	-6.000	23.000	13.300	545974206
JOINT 4555	-5.000	23.000	13.300	546974752
JOINT 4556	-4.000	23.000	13.300	547975299
JOINT 4557	-3.000	23.000	13.300	548975847
JOINT 4558	-2.000	23.000	13.300	549976396
JOINT 4559	-1.000	23.000	13.300	550976946
JOINT 4560	0.000	23.000	13.300	551977497
JOINT 4562	1.000	23.000	13.300	552978049
JOINT 4563	2.000	23.000	13.300	553978602
JOINT 4564	3.000	23.000	13.300	554979156
JOINT 4565	4.000	23.000	13.300	555979711
JOINT 4566	5.000	23.000	13.300	556980267
JOINT 4567	6.000	23.000	13.300	557980824
JOINT 4568	7.000	23.000	13.300	558981382
JOINT 4569	8.000	23.000	13.300	559981941
JOINT 4570	9.000	23.000	13.300	560982501
JOINT 4571	9.867	23.000	13.300	561983062
JOINT 4572	10.734	23.000	13.300	562983624
JOINT 4575	-5.000	-20.600	13.300	563984187
JOINT 4576	4.000	-21.600	13.300	564984751
JOINT 4599	-10.734	28.000	13.300	565985316
JOINT 4600	-9.867	28.000	13.300	566985882
JOINT 4601	-9.000	28.000	13.300	567986449
JOINT 4602	-8.000	28.000	13.300	568987017
JOINT 4603	-7.000	28.000	13.300	569987586
JOINT 4604	-6.000	28.000	13.300	570988156
JOINT 4605	-5.000	28.000	13.300	571988727
JOINT 4606	-4.000	28.000	13.300	572989299
JOINT 4607	-3.000	28.000	13.300	573989872
JOINT 4608	-2.000	28.000	13.300	574990446
JOINT 4609	-1.000	28.000	13.300	575991021
JOINT 4610	0.000	28.000	13.300	576991597
JOINT 4612	1.000	28.000	13.300	577992174
JOINT 4613	2.000	28.000	13.300	578992752
JOINT 4614	3.000	28.000	13.300	579993331
JOINT 4615	4.000	28.000	13.300	580993911
JOINT 4616	5.000	28.000	13.300	581994492



Azin Azarhoushang  
Department of Civil Engineering

---

JOINT 4617	6.000	28.000	13.300	582995074
JOINT 4618	7.000	28.000	13.300	583995657
JOINT 4619	8.000	28.000	13.300	584996241
JOINT 4620	9.000	28.000	13.300	585996826
JOINT 4621	9.867	28.000	13.300	586997412
JOINT 4622	10.734	28.000	13.300	587997999
JOINT 4651	-2.000	-17.000	13.300	588998587
JOINT 4652	3.000	-17.000	13.300	589999176
JOINT 4653	-2.000	-14.500	13.300	590999766
JOINT 4654	3.000	-14.500	13.300	591 357
JOINT 4655	-7.000	-12.850	13.300	592 949
JOINT 4656	-2.000	-12.850	13.300	593 1542
JOINT 4657	-7.000	-10.450	13.300	594 2136
JOINT 4658	-2.000	-10.450	13.300	595 2731
JOINT 4659	-7.000	-12.850	14.800	596 3327
JOINT 4660	-7.000	-10.450	14.800	597 3924
JOINT 4661	-2.000	-12.850	14.800	598 4522
JOINT 4662	-2.000	-10.450	14.800	599 5121
JOINT 4663	-2.000	-17.000	16.100	600 5721
JOINT 4664	-2.000	-14.500	16.100	601 6322
JOINT 4665	3.000	-17.000	16.100	602 6924
JOINT 4666	3.000	-14.500	16.100	603 7527
JOINT 4667	-7.000	-12.850	15.100	604 8131
JOINT 4668	-7.000	-10.450	15.100	605 8736
JOINT 4669	-2.000	-12.850	15.100	606 9342
JOINT 4670	-2.000	-10.450	15.100	607 9949
JOINT 4671	-2.000	-17.000	16.400	608 10557
JOINT 4672	-2.000	-14.500	16.400	609 11166
JOINT 4673	3.000	-17.000	16.400	610 11776
JOINT 4674	3.000	-14.500	16.400	611 12387
JOINT 4675	-7.000	-11.650	14.800	612 12999
JOINT 4676	-2.000	-11.650	14.800	613 13612
JOINT 4677	-2.000	-15.750	16.100	614 14226
JOINT 4678	3.000	-15.750	16.100	615 14841
JOINT 4679	-2.000	-15.750	17.900	616 15457
JOINT 4680	3.000	-15.750	17.900	617 16074
JOINT 4683	-7.000	-11.650	16.500	618 16692
JOINT 4684	-2.000	-11.650	16.500	619 17311
JOINT 4685	-4.500	-12.850	14.800	620 17931
JOINT 4686	-4.500	-10.450	14.800	621 18552
JOINT 4687	0.500	-17.000	16.100	622 19174
JOINT 4688	0.500	-14.500	16.100	623 19797
JOINT 4689	-8.000	-11.650	16.500	624 20421
JOINT 4690	-1.000	-11.650	16.500	625 21046
JOINT 4691	-3.300	-15.750	17.900	626 21672
JOINT 4692	4.300	-15.750	17.900	627 22299
JOINT 4693	9.000	24.000	13.300	628 22927
JOINT 4694	9.000	27.000	13.300	629 23556
JOINT 4695	9.867	24.000	13.300	630 24186

JOINT 4696	8.000	24.000	13.300	631	24817
JOINT 4697	8.000	27.000	13.300	632	25449
JOINT 4698	9.867	27.000	13.300	633	26082
JOINT 4700	8.000	24.000	14.300	634	26716
JOINT 4703	9.000	24.000	14.300	635	27351
JOINT 4704	9.867	24.000	14.300	636	27987
JOINT 4705	8.000	27.000	14.300	637	28624
JOINT 4706	9.000	27.000	14.300	638	29262
JOINT 4707	9.867	27.000	14.300	639	29901
JOINT 4708	8.000	24.000	14.800	640	30541
JOINT 4709	9.000	24.000	14.800	641	31182
JOINT 4710	9.867	24.000	14.800	642	31824
JOINT 4711	8.000	27.000	14.800	643	32467
JOINT 4712	9.000	27.000	14.800	644	33111
JOINT 4713	9.867	27.000	14.800	645	33756
JOINT 4714	8.000	25.500	14.300	646	34402
JOINT 4715	9.867	25.500	14.300	647	35049
JOINT 4716	9.000	25.500	22.125	648	35697
JOINT 4717	-8.000	13.500	16.800	649	36346
JOINT 4718	-3.000	13.500	16.800	650	36996
JOINT 4721	2.000	13.500	16.800	651	37647
JOINT 4722	2.000	9.000	16.800	652	38299
JOINT 4723	2.000	4.500	16.800	653	38952
JOINT 4724	2.000	0.000	16.800	654	39606
JOINT 4725	-3.000	0.000	16.800	655	40261
JOINT 4726	-8.000	0.000	16.800	656	40917
JOINT 4727	-8.000	4.500	16.800	657	41574
JOINT 4728	-8.000	9.000	16.800	658	42232
JOINT 4729	7.000	0.000	16.800	659	42891
JOINT 4730	7.000	4.500	16.800	660	43551
JOINT 4731	-3.000	9.000	16.800	661	44212
JOINT 4732	-3.000	4.500	16.800	662	44874
JOINT 4733	-8.000	-4.500	16.800	663	45537
JOINT 4734	-3.000	-4.500	16.800	664	46201
JOINT 4735	2.000	-4.500	16.800	665	46866
JOINT 4736	7.000	-4.500	16.800	666	47532
JOINT 4737	5.000	24.000	13.300	667	48199
JOINT 4738	6.000	24.000	13.300	668	48867
JOINT 4739	5.000	25.500	13.300	669	49536
JOINT 4740	6.000	25.500	13.300	670	50206
JOINT 4741	5.000	24.000	14.300	671	50877
JOINT 4742	5.000	25.500	14.300	672	51549
JOINT 4743	6.000	25.500	14.300	673	52222
JOINT 4744	6.000	24.000	14.300	674	52896
JOINT 4745	5.000	24.000	14.800	675	53571
JOINT 4746	6.000	24.000	14.800	676	54247
JOINT 4747	5.000	25.500	14.800	677	54924
JOINT 4748	6.000	25.500	14.800	678	55602
JOINT 4749	5.500	24.750	22.125	679	56281

JOINT 5022	9.867-20.600	19.900	680	56961
JOINT 5031	11.600	13.500	681	57642
JOINT 5032	11.600	9.000	682	58324
JOINT 5033	11.600	4.500	683	59007
JOINT 5034	11.600	-9.000	684	59691
JOINT 5035	11.600-13.500	19.900	685	60376
JOINT 5036	11.600	0.000	686	61062
JOINT 5037	11.600	-4.500	687	61749
JOINT 5039	11.600-18.000	19.900	688	62437
JOINT 5040	11.600-20.600	19.900	689	63126
JOINT 5041	10.734	18.000	690	63816
JOINT 5049	-9.000-23.600	19.900	691	64507
JOINT 5051	-9.000-19.734	19.900	692	65199
JOINT 5055	-5.000-19.734	19.900	693	65892
JOINT 5060	0.000-19.734	19.900	694	66586
JOINT 5066	5.000-19.734	19.900	695	67281
JOINT 5070	9.000-20.600	19.900	696	67977
JOINT 5071	9.000-23.600	19.900	697	68674
JOINT 5072	10.734-20.600	19.900	698	69372
JOINT 5075	9.000-18.000	14.300	699	70071
JOINT 5076	9.000	18.000	700	70771
JOINT 5077	-9.000-18.000	14.300	701	71472
JOINT 5078	-9.000	18.000	702	72174
JOINT 5079	9.000-18.000	15.800	703	72877
JOINT 5080	9.000	18.000	704	73581
JOINT 5083	-9.000-18.000	15.800	705	74286
JOINT 5084	-9.000	18.000	706	74992
JOINT 5085	-1.000-24.700	23.900	707	75699
JOINT 5086	-1.000-21.200	23.900	708	76407
JOINT 5087	-17.300	16.000	709	77116
JOINT 5088	-13.800	16.000	710	77826
JOINT 5089	12.200	18.000	711	78537
JOINT 5090	15.700	18.000	712	79249
JOINT 5099	-11.100-18.000	19.900	713	79962
JOINT 5100	-10.050-18.000	19.900	714	80676
JOINT 5101	-9.000-18.000	19.900	715	81391
JOINT 5102	-8.000-18.000	19.900	716	82107
JOINT 5103	-7.000-18.000	19.900	717	82824
JOINT 5104	-6.000-18.000	19.900	718	83542
JOINT 5105	-5.000-18.000	19.900	719	84261
JOINT 5106	-4.000-18.000	19.900	720	84981
JOINT 5107	-3.000-18.000	19.900	721	85702
JOINT 5108	-2.000-18.000	19.900	722	86424
JOINT 5109	-1.000-18.000	19.900	723	87147
JOINT 5110	0.000-18.000	19.900	724	87871
JOINT 5112	1.000-18.000	19.900	725	88596
JOINT 5113	2.000-18.000	19.900	726	89322
JOINT 5114	3.000-18.000	19.900	727	90049
JOINT 5115	4.000-18.000	19.900	728	90777

JOINT 5116	5.000-18.000	19.900	729 91506
JOINT 5117	6.000-18.000	19.900	730 92236
JOINT 5118	7.000-18.000	19.900	731 92967
JOINT 5119	8.000-18.000	19.900	732 93699
JOINT 5120	9.000-18.000	19.900	733 94432
JOINT 5121	9.867-18.000	19.900	734 95166
JOINT 5122	10.734-18.000	19.900	735 95901
JOINT 5125	-8.435-18.000	19.900	736 96637
JOINT 5126	8.435-18.000	19.900	737 97374
JOINT 5131	-9.000 -9.610	19.900	738 98112
JOINT 5132	-9.000 -8.410	19.900	739 98851
JOINT 5133	-9.000 8.410	19.900	740 99591
JOINT 5134	-9.000 9.610	19.900	741100332
JOINT 5135	9.000 -9.610	19.900	742101074
JOINT 5136	9.000 -8.410	19.900	743101817
JOINT 5137	9.000 8.410	19.900	744102561
JOINT 5138	9.000 9.610	19.900	745103306
JOINT 5141	-13.200-19.734	19.900	746104052
JOINT 5143	-13.200 19.734	19.900	747104799
JOINT 5149	-11.100-13.500	19.900	748105547
JOINT 5150	-10.050-13.500	19.900	749106296
JOINT 5151	-9.000-13.500	19.900	750107046
JOINT 5152	-8.000-13.500	19.900	751107797
JOINT 5153	-7.000-13.500	19.900	752108549
JOINT 5154	-6.000-13.500	19.900	753109302
JOINT 5155	-5.000-13.500	19.900	754110056
JOINT 5156	-4.000-13.500	19.900	755110811
JOINT 5157	-3.000-13.500	19.900	756111567
JOINT 5158	-2.000-13.500	19.900	757112324
JOINT 5159	-1.000-13.500	19.900	758113082
JOINT 5160	0.000-13.500	19.900	759113841
JOINT 5162	1.000-13.500	19.900	760114601
JOINT 5163	2.000-13.500	19.900	761115362
JOINT 5164	3.000-13.500	19.900	762116124
JOINT 5165	4.000-13.500	19.900	763116887
JOINT 5166	5.000-13.500	19.900	764117651
JOINT 5167	6.000-13.500	19.900	765118416
JOINT 5168	7.000-13.500	19.900	766119182
JOINT 5169	8.000-13.500	19.900	767119949
JOINT 5170	9.000-13.500	19.900	768120717
JOINT 5171	9.867-13.500	19.900	769121486
JOINT 5172	10.734-13.500	19.900	770122256
JOINT 5175	-5.000 -6.750	19.900	771123027
JOINT 5176	-5.000 -2.250	19.900	772123799
JOINT 5177	-5.000 2.250	19.900	773124572
JOINT 5178	-5.000 6.750	19.900	774125346
JOINT 5179	5.000 6.750	19.900	775126121
JOINT 5180	5.000 2.250	19.900	776126897
JOINT 5183	5.000 -2.250	19.900	777127674

JOINT 5184	5.000	-6.750	19.900	778128452
JOINT 5199	-11.100	-9.000	19.900	779129231
JOINT 5200	-10.050	-9.000	19.900	780130011
JOINT 5201	-9.000	-9.000	19.900	781130792
JOINT 5202	-8.000	-9.000	19.900	782131574
JOINT 5203	-7.000	-9.000	19.900	783132357
JOINT 5204	-6.000	-9.000	19.900	784133141
JOINT 5205	-5.000	-9.000	19.900	785133926
JOINT 5206	-4.000	-9.000	19.900	786134712
JOINT 5207	-3.000	-9.000	19.900	787135499
JOINT 5208	-2.000	-9.000	19.900	788136287
JOINT 5209	-1.000	-9.000	19.900	789137076
JOINT 5210	0.000	-9.000	19.900	790137866
JOINT 5212	1.000	-9.000	19.900	791138657
JOINT 5213	2.000	-9.000	19.900	792139449
JOINT 5214	3.000	-9.000	19.900	793140242
JOINT 5215	4.000	-9.000	19.900	794141036
JOINT 5216	5.000	-9.000	19.900	795141831
JOINT 5217	6.000	-9.000	19.900	796142627
JOINT 5218	7.000	-9.000	19.900	797143424
JOINT 5219	8.000	-9.000	19.900	798144222
JOINT 5220	9.000	-9.000	19.900	799145021
JOINT 5221	9.867	-9.000	19.900	800145821
JOINT 5222	10.734	-9.000	19.900	801146622
JOINT 5223	-9.000	-10.910	19.900	802147424
JOINT 5224	-9.000	-7.042	19.900	803148227
JOINT 5225	-9.000	7.042	19.900	804149031
JOINT 5226	-9.000	10.910	19.900	805149836
JOINT 5227	9.000	-10.910	19.900	806150642
JOINT 5228	9.000	-7.042	19.900	807151449
JOINT 5229	9.000	7.042	19.900	808152257
JOINT 5230	9.000	11.000	19.900	809153066
JOINT 5231	-9.715	-18.000	19.900	810153876
JOINT 5232	-13.200	-20.600	19.900	811154687
JOINT 5233	-5.000	-20.600	19.900	812155499
JOINT 5234	0.000	-20.600	19.900	813156312
JOINT 5235	5.000	-20.600	19.900	814157126
JOINT 5236	-9.000	-20.600	19.900	815157941
JOINT 5237	9.000	-19.734	19.900	816158757
JOINT 5238	-13.200	20.600	19.900	817159574
JOINT 5239	-5.000	20.600	19.900	818160392
JOINT 5240	0.000	20.600	19.900	819161211
JOINT 5241	15.600	0.000	19.900	820162031
JOINT 5242	15.600	4.500	19.900	821162852
JOINT 5243	12.600	0.000	19.900	822163674
JOINT 5244	13.600	0.000	19.900	823164497
JOINT 5245	14.600	0.000	19.900	824165321
JOINT 5246	12.600	4.500	19.900	825166146
JOINT 5247	13.600	4.500	19.900	826166972

JOINT 5248	14.600	4.500	19.900	827167799
JOINT 5249	-11.100	-4.500	19.900	828168627
JOINT 5250	-10.050	-4.500	19.900	829169456
JOINT 5251	-9.000	-4.500	19.900	830170286
JOINT 5252	-8.000	-4.500	19.900	831171117
JOINT 5253	-7.000	-4.500	19.900	832171949
JOINT 5254	-6.000	-4.500	19.900	833172782
JOINT 5255	-5.000	-4.500	19.900	834173616
JOINT 5256	-4.000	-4.500	19.900	835174451
JOINT 5257	-3.000	-4.500	19.900	836175287
JOINT 5258	-2.000	-4.500	19.900	837176124
JOINT 5259	-1.000	-4.500	19.900	838176962
JOINT 5260	0.000	-4.500	19.900	839177801
JOINT 5261	5.000	20.600	19.900	840178641
JOINT 5262	1.000	-4.500	19.900	841179482
JOINT 5263	2.000	-4.500	19.900	842180324
JOINT 5264	3.000	-4.500	19.900	843181167
JOINT 5265	4.000	-4.500	19.900	844182011
JOINT 5266	5.000	-4.500	19.900	845182856
JOINT 5267	6.000	-4.500	19.900	846183702
JOINT 5268	7.000	-4.500	19.900	847184549
JOINT 5269	8.000	-4.500	19.900	848185397
JOINT 5270	9.000	-4.500	19.900	849186246
JOINT 5271	9.867	-4.500	19.900	850187096
JOINT 5272	10.734	-4.500	19.900	851187947
JOINT 5273	-9.000	20.600	19.900	852188799
JOINT 5274	9.000	20.600	19.900	853189652
JOINT 5275	-1.000	-20.600	19.900	854190506
JOINT 5276	-1.000	-19.734	19.900	855191361
JOINT 5277	-1.000	-18.867	19.900	856192217
JOINT 5280	-6.000	-6.750	19.900	857193074
JOINT 5283	-6.000	-2.250	19.900	858193932
JOINT 5284	-6.000	2.250	19.900	859194791
JOINT 5285	-6.000	6.750	19.900	860195651
JOINT 5286	6.000	6.750	19.900	861196512
JOINT 5287	6.000	2.250	19.900	862197374
JOINT 5288	6.000	-2.250	19.900	863198237
JOINT 5289	6.000	-6.750	19.900	864199101
JOINT 5299	-11.100	0.000	19.900	865199966
JOINT 5300	-10.050	0.000	19.900	866200832
JOINT 5301	-9.000	0.000	19.900	867201699
JOINT 5302	-8.000	0.000	19.900	868202567
JOINT 5303	-7.000	0.000	19.900	869203436
JOINT 5304	-6.000	0.000	19.900	870204306
JOINT 5305	-5.000	0.000	19.900	871205177
JOINT 5306	-4.000	0.000	19.900	872206049
JOINT 5307	-3.000	0.000	19.900	873206922
JOINT 5308	-2.000	0.000	19.900	874207796
JOINT 5309	-1.000	0.000	19.900	875208671

Azin Azarhoushang  
 Department of Civil Engineering

---

JOINT 5310	0.000	0.000	19.900	876209547
JOINT 5312	1.000	0.000	19.900	877210424
JOINT 5313	2.000	0.000	19.900	878211302
JOINT 5314	3.000	0.000	19.900	879212181
JOINT 5315	4.000	0.000	19.900	880213061
JOINT 5316	5.000	0.000	19.900	881213942
JOINT 5317	6.000	0.000	19.900	882214824
JOINT 5318	7.000	0.000	19.900	883215707
JOINT 5319	8.000	0.000	19.900	884216591
JOINT 5320	9.000	0.000	19.900	885217476
JOINT 5321	9.867	0.000	19.900	886218362
JOINT 5322	10.734	0.000	19.900	887219249
JOINT 5331	-13.200	9.000	19.900	888220137
JOINT 5332	-13.200	0.000	19.900	889221026
JOINT 5333	-13.200	-9.000	19.900	890221916
JOINT 5334	-15.500	18.000	19.900	891222807
JOINT 5335	-15.500	-18.000	19.900	892223699
JOINT 5336	-15.500	-23.600	19.900	893224592
JOINT 5337	-15.500	23.000	19.900	894225486
JOINT 5341	-13.200	13.500	19.900	895226381
JOINT 5342	-13.200	4.500	19.900	896227277
JOINT 5343	-13.200	-4.500	19.900	897228174
JOINT 5344	-13.200	-13.500	19.900	898229072
JOINT 5345	-13.200	18.000	19.900	899229971
JOINT 5346	-13.200	-18.000	19.900	900230871
JOINT 5347	-12.150	18.000	19.900	901231772
JOINT 5348	-12.150	13.500	19.900	902232674
JOINT 5349	-11.100	4.500	19.900	903233577
JOINT 5350	-10.050	4.500	19.900	904234481
JOINT 5351	-9.000	4.500	19.900	905235386
JOINT 5352	-8.000	4.500	19.900	906236292
JOINT 5353	-7.000	4.500	19.900	907237199
JOINT 5354	-6.000	4.500	19.900	908238107
JOINT 5355	-5.000	4.500	19.900	909239016
JOINT 5356	-4.000	4.500	19.900	910239926
JOINT 5357	-3.000	4.500	19.900	911240837
JOINT 5358	-2.000	4.500	19.900	912241749
JOINT 5359	-1.000	4.500	19.900	913242662
JOINT 5360	0.000	4.500	19.900	914243576
JOINT 5361	-12.150	9.000	19.900	915244491
JOINT 5362	1.000	4.500	19.900	916245407
JOINT 5363	2.000	4.500	19.900	917246324
JOINT 5364	3.000	4.500	19.900	918247242
JOINT 5365	4.000	4.500	19.900	919248161
JOINT 5366	5.000	4.500	19.900	920249081
JOINT 5367	6.000	4.500	19.900	921250002
JOINT 5368	7.000	4.500	19.900	922250924
JOINT 5369	8.000	4.500	19.900	923251847
JOINT 5370	9.000	4.500	19.900	924252771

JOINT 5371	9.867	4.500	19.900	925253696
JOINT 5372	10.734	4.500	19.900	926254622
JOINT 5373	-12.150	4.500	19.900	927255549
JOINT 5374	-12.150	0.000	19.900	928256477
JOINT 5375	-12.150	-4.500	19.900	929257406
JOINT 5376	-12.150	-9.000	19.900	930258336
JOINT 5377	-12.150	-13.500	19.900	931259267
JOINT 5378	-12.150	-18.000	19.900	932260199
JOINT 5381	12.200	18.000	19.900	933261132
JOINT 5383	15.700	18.000	19.900	934262066
JOINT 5384	12.200	11.000	19.900	935263001
JOINT 5385	15.700	11.000	19.900	936263937
JOINT 5386	-17.300	16.000	19.900	937264874
JOINT 5387	-13.800	16.000	19.900	938265812
JOINT 5388	-17.300	9.000	19.900	939266751
JOINT 5389	-13.800	9.000	19.900	940267691
JOINT 5390	11.600	19.734	19.900	941268632
JOINT 5391	11.600	18.867	19.900	942269574
JOINT 5392	0.000	23.500	19.900	943270517
JOINT 5393	5.000	23.500	19.900	944271461
JOINT 5394	0.000	21.567	19.900	945272406
JOINT 5395	0.000	22.533	19.900	946273352
JOINT 5396	5.000	21.567	19.900	947274299
JOINT 5397	5.000	22.533	19.900	948275247
JOINT 5398	9.000	21.567	19.900	949276196
JOINT 5399	-11.100	9.000	19.900	950277146
JOINT 5400	-10.050	9.000	19.900	951278097
JOINT 5401	-9.000	9.000	19.900	952279049
JOINT 5402	-8.000	9.000	19.900	953280002
JOINT 5403	-7.000	9.000	19.900	954280956
JOINT 5404	-6.000	9.000	19.900	955281911
JOINT 5405	-5.000	9.000	19.900	956282867
JOINT 5406	-4.000	9.000	19.900	957283824
JOINT 5407	-3.000	9.000	19.900	958284782
JOINT 5408	-2.000	9.000	19.900	959285741
JOINT 5409	-1.000	9.000	19.900	960286701
JOINT 5410	0.000	9.000	19.900	961287662
JOINT 5411	9.000	22.533	19.900	962288624
JOINT 5412	1.000	9.000	19.900	963289587
JOINT 5413	2.000	9.000	19.900	964290551
JOINT 5414	3.000	9.000	19.900	965291516
JOINT 5415	4.000	9.000	19.900	966292482
JOINT 5416	5.000	9.000	19.900	967293449
JOINT 5417	6.000	9.000	19.900	968294417
JOINT 5418	7.000	9.000	19.900	969295386
JOINT 5419	8.000	9.000	19.900	970296356
JOINT 5420	9.000	9.000	19.900	971297327
JOINT 5421	9.867	9.000	19.900	972298299
JOINT 5422	10.734	9.000	19.900	973299272



JOINT 5423	9.000	23.000	19.900	974300246
JOINT 5425	12.600	-1.600	19.900	975301221
JOINT 5426	13.600	-1.600	19.900	976302197
JOINT 5427	14.600	-1.600	19.900	977303174
JOINT 5428	15.600	-1.600	19.900	978304152
JOINT 5429	9.000	-1.600	19.900	979305131
JOINT 5430	9.867	-1.600	19.900	980306111
JOINT 5431	10.734	-1.600	19.900	981307092
JOINT 5432	11.600	-1.600	19.900	982308074
JOINT 5435	-8.000	-21.200	19.900	983309057
JOINT 5436	-8.000	-24.700	19.900	984310041
JOINT 5437	-1.000	-21.200	19.900	985311026
JOINT 5438	-1.000	-24.700	19.900	986312012
JOINT 5440	-8.000	-20.600	19.900	987312999
JOINT 5441	-8.000	-19.734	19.900	988313987
JOINT 5442	-8.000	-18.867	19.900	989314976
JOINT 5449	-11.100	13.500	19.900	990315966
JOINT 5450	-10.050	13.500	19.900	991316957
JOINT 5451	-9.000	13.500	19.900	992317949
JOINT 5452	-8.000	13.500	19.900	993318942
JOINT 5453	-7.000	13.500	19.900	994319936
JOINT 5454	-6.000	13.500	19.900	995320931
JOINT 5455	-5.000	13.500	19.900	996321927
JOINT 5456	-4.000	13.500	19.900	997322924
JOINT 5457	-3.000	13.500	19.900	998323922
JOINT 5458	-2.000	13.500	19.900	999324921
JOINT 5459	-1.000	13.500	19.900	1000325921
JOINT 5460	0.000	13.500	19.900	1001326922
JOINT 5462	1.000	13.500	19.900	1002327924
JOINT 5463	2.000	13.500	19.900	1003328927
JOINT 5464	3.000	13.500	19.900	1004329931
JOINT 5465	4.000	13.500	19.900	1005330936
JOINT 5466	5.000	13.500	19.900	1006331942
JOINT 5467	6.000	13.500	19.900	1007332949
JOINT 5468	7.000	13.500	19.900	1008333957
JOINT 5469	8.000	13.500	19.900	1009334966
JOINT 5470	9.000	13.500	19.900	1010335976
JOINT 5471	9.867	13.500	19.900	1011336987
JOINT 5472	10.734	13.500	19.900	1012337999
JOINT 5475	12.200	11.000	23.900	1013339012
JOINT 5476	15.700	11.000	23.900	1014340026
JOINT 5477	-17.300	9.000	23.900	1015341041
JOINT 5478	-13.800	9.000	23.900	1016342057
JOINT 5479	-8.000	-24.700	23.900	1017343074
JOINT 5480	-8.000	-21.200	23.900	1018344092
JOINT 5481	11.600	11.000	19.900	1019345111
JOINT 5483	10.734	11.000	19.900	1020346131
JOINT 5484	9.867	11.000	19.900	1021347152
JOINT 5485	-13.200	16.000	19.900	1022348174

JOINT 5486	-12.150	16.000	19.900	1023349197
JOINT 5487	-11.100	16.000	19.900	1024350221
JOINT 5488	-10.050	16.000	19.900	1025351246
JOINT 5489	-9.000	16.000	19.900	1026352272
JOINT 5499	-11.100	18.000	19.900	1027353299
JOINT 5500	-10.050	18.000	19.900	1028354327
JOINT 5501	-9.000	18.000	19.900	1029355356
JOINT 5502	-8.000	18.000	19.900	1030356386
JOINT 5503	-7.000	18.000	19.900	1031357417
JOINT 5504	-6.000	18.000	19.900	1032358449
JOINT 5505	-5.000	18.000	19.900	1033359482
JOINT 5506	-4.000	18.000	19.900	1034360516
JOINT 5507	-3.000	18.000	19.900	1035361551
JOINT 5508	-2.000	18.000	19.900	1036362587
JOINT 5509	-1.000	18.000	19.900	1037363624
JOINT 5510	0.000	18.000	19.900	1038364662
JOINT 5512	1.000	18.000	19.900	1039365701
JOINT 5513	2.000	18.000	19.900	1040366741
JOINT 5514	3.000	18.000	19.900	1041367782
JOINT 5515	4.000	18.000	19.900	1042368824
JOINT 5516	5.000	18.000	19.900	1043369867
JOINT 5517	6.000	18.000	19.900	1044370911
JOINT 5518	7.000	18.000	19.900	1045371956
JOINT 5519	8.000	18.000	19.900	1046373002
JOINT 5520	9.000	18.000	19.900	1047374049
JOINT 5521	9.867	18.000	19.900	1048375097
JOINT 5522	11.600	18.000	19.900	1049376146
JOINT 5523	-5.000	18.867	19.900	1050377196
JOINT 5524	0.000	18.867	19.900	1051378247
JOINT 5525	5.000	18.867	19.900	1052379299
JOINT 5526	-9.000	18.867	19.900	1053380352
JOINT 5527	-8.435	18.000	19.900	1054381406
JOINT 5528	8.435	18.000	19.900	1055382461
JOINT 5529	-9.715	18.000	19.900	1056383517
JOINT 5530	9.000	18.867	19.900	1057384574
JOINT 5531	-13.200	18.867	19.900	1058385632
JOINT 5532	-13.200	-18.867	19.900	1059386691
JOINT 5533	-9.000	-18.867	19.900	1060387751
JOINT 5534	-5.000	-18.867	19.900	1061388812
JOINT 5535	0.000	-18.867	19.900	1062389874
JOINT 5536	5.000	-18.867	19.900	1063390937
JOINT 5537	9.000	-18.867	19.900	1064392001
JOINT 5540	11.600	20.600	19.900	1065393066
JOINT 5551	-9.000	19.734	19.900	1066394132
JOINT 5555	-5.000	19.734	19.900	1067395199
JOINT 5560	0.000	19.734	19.900	1068396267
JOINT 5566	5.000	19.734	19.900	1069397336
JOINT 5570	9.000	19.734	19.900	1070398406
JOINT 5601	-9.000	23.000	19.900	1071399477

JOINT 5620	9.000	23.500	19.900	1072400549
JOINT 5625	-15.500	-22.100	19.900	1073401622
JOINT 5626	-9.000	-22.100	19.900	1074402696
JOINT 5627	-12.250	-22.100	19.900	1075403771
JOINT 5628	-15.500	21.500	19.900	1076404847
JOINT 5629	-9.000	21.500	19.900	1077405924
JOINT 5630	-12.250	21.500	19.900	1078407002
JOINT 5635	-10.500	23.000	19.900	1079408081
JOINT 5636	-14.500	23.000	19.900	1080409161
JOINT 5637	-14.500	21.500	19.900	1081410242
JOINT 5638	-10.500	21.500	19.900	1082411324
JOINT 5639	-10.500	-23.600	19.900	1083412407
JOINT 5640	-14.500	-23.600	19.900	1084413491
JOINT 5641	-14.500	-22.100	19.900	1085414576
JOINT 5642	-10.500	-22.100	19.900	1086415662
JOINT 5651	-6.000	-6.000	19.900	1087416749
JOINT 5652	6.000	-6.000	19.900	1088417837
JOINT 5653	-6.000	6.000	19.900	1089418926
JOINT 5654	6.000	6.000	19.900	1090420016
JOINT 5655	-6.000	-2.500	19.900	1091421107
JOINT 5656	6.000	-2.500	19.900	1092422199
JOINT 5657	-6.000	-5.500	19.900	1093423292
JOINT 5658	6.000	-5.500	19.900	1094424386
JOINT 5659	-6.000	5.500	19.900	1095425481
JOINT 5660	6.000	5.500	19.900	1096426577
JOINT 5661	-6.000	2.500	19.900	1097427674
JOINT 5662	6.000	2.500	19.900	1098428772
JOINT 5663	-6.000	-9.000	20.800	1099429871
JOINT 5664	-6.000	-6.000	20.800	1100430971
JOINT 5665	6.000	-9.000	20.800	1101432072
JOINT 5666	6.000	-6.000	20.800	1102433174
JOINT 5667	-6.000	-5.500	20.800	1103434277
JOINT 5668	-6.000	-2.500	20.800	1104435381
JOINT 5669	6.000	-5.500	20.800	1105436486
JOINT 5670	6.000	-2.500	20.800	1106437592
JOINT 5671	-6.000	2.500	20.800	1107438699
JOINT 5672	-6.000	5.500	20.800	1108439807
JOINT 5673	6.000	2.500	20.800	1109440916
JOINT 5674	6.000	5.500	20.800	1110442026
JOINT 5675	-6.000	6.000	20.800	1111443137
JOINT 5676	-6.000	9.000	20.800	1112444249
JOINT 5677	6.000	6.000	20.800	1113445362
JOINT 5678	6.000	9.000	20.800	1114446476
JOINT 5679	-6.000	-7.500	20.800	1115447591
JOINT 5680	-6.000	-4.000	20.800	1116448707
JOINT 5683	-6.000	4.000	20.800	1117449824
JOINT 5684	-6.000	7.500	20.800	1118450942
JOINT 5685	6.000	-7.500	20.800	1119452061
JOINT 5686	6.000	-4.000	20.800	1120453181

JOINT 5687	6.000	4.000	20.800	1121454302
JOINT 5688	6.000	7.500	20.800	1122455424
JOINT 5689	-2.000	-9.000	20.800	1123456547
JOINT 5690	2.000	-9.000	20.800	1124457671
JOINT 5691	-2.000	-6.000	20.800	1125458796
JOINT 5692	2.000	-6.000	20.800	1126459922
JOINT 5693	-2.000	-5.500	20.800	1127461049
JOINT 5694	2.000	-5.500	20.800	1128462177
JOINT 5695	-2.000	-2.500	20.800	1129463306
JOINT 5696	2.000	-2.500	20.800	1130464436
JOINT 5697	-2.000	2.500	20.800	1131465567
JOINT 5698	2.000	2.500	20.800	1132466699
JOINT 5700	-2.000	5.500	20.800	1133467832
JOINT 5701	2.000	5.500	20.800	1134468966
JOINT 5703	-2.000	6.000	20.800	1135470101
JOINT 5704	2.000	6.000	20.800	1136471237
JOINT 5705	-2.000	9.000	20.800	1137472374
JOINT 5706	2.000	9.000	20.800	1138473512
JOINT 5707	-6.000	-9.000	21.100	1139474651
JOINT 5708	-6.000	-6.000	21.100	1140475791
JOINT 5709	-6.000	-5.500	21.100	1141476932
JOINT 5710	-6.000	-2.500	21.100	1142478074
JOINT 5711	-6.000	2.500	21.100	1143479217
JOINT 5712	-6.000	5.500	21.100	1144480361
JOINT 5713	-6.000	6.000	21.100	1145481506
JOINT 5714	-6.000	9.000	21.100	1146482652
JOINT 5715	6.000	-9.000	21.100	1147483799
JOINT 5716	6.000	-6.000	21.100	1148484947
JOINT 5717	6.000	-5.500	21.100	1149486096
JOINT 5718	6.000	-2.500	21.100	1150487246
JOINT 5721	6.000	2.500	21.100	1151488397
JOINT 5722	6.000	5.500	21.100	1152489549
JOINT 5723	6.000	6.000	21.100	1153490702
JOINT 5724	6.000	9.000	21.100	1154491856
JOINT 5725	-6.000	-7.500	23.500	1155493011
JOINT 5726	-6.000	-4.000	23.500	1156494167
JOINT 5727	-6.000	4.000	23.500	1157495324
JOINT 5728	-6.000	7.500	23.500	1158496482
JOINT 5729	6.000	-7.500	23.500	1159497641
JOINT 5730	6.000	-4.000	23.500	1160498801
JOINT 5731	6.000	4.000	23.500	1161499962
JOINT 5732	6.000	7.500	23.500	1162501124
JOINT 5733	-7.500	-7.500	23.500	1163502287
JOINT 5734	-7.500	-4.000	23.500	1164503451
JOINT 5735	-7.500	4.000	23.500	1165504616
JOINT 5736	-7.500	7.500	23.500	1166505782
JOINT 5737	7.500	-7.500	23.500	1167506949
JOINT 5738	7.500	-4.000	23.500	1168508117
JOINT 5739	7.500	4.000	23.500	1169509286

JOINT 5740	7.500	7.500	23.500	1170510456
JOINT 6021	9.867-14.404	27.900		1171511627
JOINT 6022	9.867-17.133	27.900		1172512799
JOINT 6023	11.600	13.500	27.900	1173513972
JOINT 6024	11.600	0.000	27.900	1174515146
JOINT 6025	11.600	-4.500	27.900	1175516321
JOINT 6026	11.600	-9.000	27.900	1176517497
JOINT 6027	10.734	18.000	27.900	1177518674
JOINT 6028	11.600	9.000	27.900	1178519852
JOINT 6029	11.600	4.500	27.900	1179521031
JOINT 6030	11.600-13.500	27.900		1180522211
JOINT 6031	11.600-18.000	27.900		1181523392
JOINT 6033	-11.600-20.600	27.900		1182524574
JOINT 6034	-11.600-18.000	27.900		1183525757
JOINT 6035	-11.600-13.500	27.900		1184526941
JOINT 6036	-11.600	-9.000	27.900	1185528126
JOINT 6037	-11.600	-4.500	27.900	1186529312
JOINT 6038	-11.600	0.000	27.900	1187530499
JOINT 6039	-11.600	4.500	27.900	1188531687
JOINT 6040	-11.600	9.000	27.900	1189532876
JOINT 6041	-11.600	13.500	27.900	1190534066
JOINT 6042	-10.734	18.000	27.900	1191535257
JOINT 6051	-9.000-20.600	27.900		1192536449
JOINT 6055	-5.000-20.600	27.900		1193537642
JOINT 6060	0.000-23.600	27.900		1194538836
JOINT 6066	4.757-23.600	27.900		1195540031
JOINT 6070	9.000-23.600	27.900		1196541227
JOINT 6075	-5.000-11.250	27.900		1197542424
JOINT 6076	1.000-11.250	27.900		1198543622
JOINT 6077	-5.000	-6.750	27.900	1199544821
JOINT 6078	1.000	-6.750	27.900	1200546021
JOINT 6079	-5.000	-2.250	27.900	1201547222
JOINT 6080	1.000	-2.250	27.900	1202548424
JOINT 6083	-5.000	2.250	27.900	1203549627
JOINT 6084	1.000	2.250	27.900	1204550831
JOINT 6085	-5.000	6.750	27.900	1205552036
JOINT 6086	1.000	6.750	27.900	1206553242
JOINT 6087	-5.000	11.250	27.900	1207554449
JOINT 6088	1.000	11.250	27.900	1208555657
JOINT 6099	-10.734-18.000	27.900		1209556866
JOINT 6100	-9.867-18.000	27.900		1210558076
JOINT 6101	-9.000-18.000	27.900		1211559287
JOINT 6102	-8.000-18.000	27.900		1212560499
JOINT 6103	-7.000-18.000	27.900		1213561712
JOINT 6104	-6.000-18.000	27.900		1214562926
JOINT 6105	-5.000-18.000	27.900		1215564141
JOINT 6106	-4.000-18.000	27.900		1216565357
JOINT 6107	-3.000-18.000	27.900		1217566574
JOINT 6108	-2.000-18.000	27.900		1218567792

JOINT 6109	-1.000-18.000	27.900	1219569011
JOINT 6110	0.000-18.000	27.900	1220570231
JOINT 6112	1.000-18.000	27.900	1221571452
JOINT 6113	2.000-18.000	27.900	1222572674
JOINT 6114	3.000-18.000	27.900	1223573897
JOINT 6115	4.000-18.000	27.900	1224575121
JOINT 6116	4.757-18.000	27.900	1225576346
JOINT 6117	6.000-18.000	27.900	1226577572
JOINT 6118	7.000-18.000	27.900	1227578799
JOINT 6119	8.000-18.000	27.900	1228580027
JOINT 6120	9.000-18.000	27.900	1229581256
JOINT 6121	9.867-18.000	27.900	1230582486
JOINT 6122	10.734-18.000	27.900	1231583717
JOINT 6125	-8.465-18.000	27.900	1232584949
JOINT 6126	8.465-18.000	27.900	1233586182
JOINT 6127	-8.000-21.200	27.900	1234587416
JOINT 6128	-1.000-21.200	27.900	1235588651
JOINT 6129	-8.000-24.700	27.900	1236589887
JOINT 6130	-1.000-24.700	27.900	1237591124
JOINT 6131	5.000-13.500	27.900	1238592362
JOINT 6132	11.203-15.797	27.900	1239593601
JOINT 6133	6.878-20.121	27.900	1240594841
JOINT 6137	12.433-13.500	27.900	1241596082
JOINT 6138	14.100-13.500	27.900	1242597324
JOINT 6139	12.433-18.000	27.900	1243598567
JOINT 6140	14.100-18.000	27.900	1244599811
JOINT 6142	14.100-23.600	27.900	1245601056
JOINT 6145	10.734-15.308	27.900	1246602302
JOINT 6146	10.734-16.266	27.900	1247603549
JOINT 6149	-10.734-13.500	27.900	1248604797
JOINT 6150	-9.867-13.500	27.900	1249606046
JOINT 6151	-9.000-13.500	27.900	1250607296
JOINT 6152	-8.000-13.500	27.900	1251608547
JOINT 6153	-7.000-13.500	27.900	1252609799
JOINT 6154	-6.000-13.500	27.900	1253611052
JOINT 6155	-5.000-13.500	27.900	1254612306
JOINT 6156	-4.000-13.500	27.900	1255613561
JOINT 6157	-3.000-13.500	27.900	1256614817
JOINT 6158	-2.000-13.500	27.900	1257616074
JOINT 6159	-1.000-13.500	27.900	1258617332
JOINT 6160	0.000-13.500	27.900	1259618591
JOINT 6162	1.000-13.500	27.900	1260619851
JOINT 6163	2.000-13.500	27.900	1261621112
JOINT 6164	3.000-13.500	27.900	1262622374
JOINT 6165	4.000-13.500	27.900	1263623637
JOINT 6166	4.757-13.500	27.900	1264624901
JOINT 6167	6.000-13.500	27.900	1265626166
JOINT 6168	7.000-13.500	27.900	1266627432
JOINT 6169	8.000-13.500	27.900	1267628699

JOINT 6170	9.000-13.500	27.900	1268629967
JOINT 6171	9.867-13.500	27.900	1269631236
JOINT 6172	10.734-13.500	27.900	1270632506
JOINT 6175	-11.600-19.733	27.900	1271633777
JOINT 6176	-11.600-18.867	27.900	1272635049
JOINT 6177	-5.000-19.733	27.900	1273636322
JOINT 6178	-5.000-18.867	27.900	1274637596
JOINT 6179	-9.000-19.733	27.900	1275638871
JOINT 6180	-9.000-18.867	27.900	1276640147
JOINT 6183	0.000-18.867	27.900	1277641424
JOINT 6184	0.000-19.733	27.900	1278642702
JOINT 6185	0.000-20.600	27.900	1279643981
JOINT 6186	4.757-18.867	27.900	1280645261
JOINT 6187	4.757-19.733	27.900	1281646542
JOINT 6188	4.757-20.600	27.900	1282647824
JOINT 6189	14.100-18.867	27.900	1283649107
JOINT 6190	14.100-19.733	27.900	1284650391
JOINT 6191	14.100-20.600	27.900	1285651676
JOINT 6192	9.000-20.600	27.900	1286652962
JOINT 6193	9.000-19.733	27.900	1287654249
JOINT 6194	9.000-18.867	27.900	1288655537
JOINT 6195	0.000-22.600	27.900	1289656826
JOINT 6196	0.000-21.600	27.900	1290658116
JOINT 6197	4.757-22.600	27.900	1291659407
JOINT 6198	4.757-21.600	27.900	1292660699
JOINT 6199	-10.734 -9.000	27.900	1293661992
JOINT 6200	-9.867 -9.000	27.900	1294663286
JOINT 6201	-9.000 -9.000	27.900	1295664581
JOINT 6202	-8.000 -9.000	27.900	1296665877
JOINT 6203	-7.000 -9.000	27.900	1297667174
JOINT 6204	-6.000 -9.000	27.900	1298668472
JOINT 6205	-5.000 -9.000	27.900	1299669771
JOINT 6206	-4.000 -9.000	27.900	1300671071
JOINT 6207	-3.000 -9.000	27.900	1301672372
JOINT 6208	-2.000 -9.000	27.900	1302673674
JOINT 6209	-1.000 -9.000	27.900	1303674977
JOINT 6210	0.000 -9.000	27.900	1304676281
JOINT 6211	9.000-22.600	27.900	1305677586
JOINT 6212	1.000 -9.000	27.900	1306678892
JOINT 6213	2.000 -9.000	27.900	1307680199
JOINT 6214	3.000 -9.000	27.900	1308681507
JOINT 6215	4.000 -9.000	27.900	1309682816
JOINT 6216	5.000 -9.000	27.900	1310684126
JOINT 6217	6.000 -9.000	27.900	1311685437
JOINT 6218	7.000 -9.000	27.900	1312686749
JOINT 6219	8.000 -9.000	27.900	1313688062
JOINT 6220	9.000 -9.000	27.900	1314689376
JOINT 6221	9.867 -9.000	27.900	1315690691
JOINT 6222	10.734 -9.000	27.900	1316692007

JOINT 6223	-9.000	-9.974	27.900	1317693324
JOINT 6224	-9.000	-8.053	27.900	1318694642
JOINT 6225	-9.000	8.053	27.900	1319695961
JOINT 6226	-9.000	9.974	27.900	1320697281
JOINT 6227	9.000	-9.974	27.900	1321698602
JOINT 6228	9.000	-8.053	27.900	1322699924
JOINT 6229	9.000	8.053	27.900	1323701247
JOINT 6230	9.000	10.600	27.900	1324702571
JOINT 6231	8.944	-22.187	31.600	1325703896
JOINT 6232	13.235	-17.916	31.600	1326705222
JOINT 6233	9.000	-18.000	34.800	1327706549
JOINT 6234	9.000	-21.600	27.900	1328707877
JOINT 6235	14.100	-22.600	27.900	1329709206
JOINT 6236	14.100	-21.600	27.900	1330710536
JOINT 6237	5.624	-18.867	27.900	1331711867
JOINT 6238	8.133	-18.867	27.900	1332713199
JOINT 6239	6.490	-19.733	27.900	1333714532
JOINT 6240	7.266	-19.733	27.900	1334715866
JOINT 6241	15.600	4.500	27.900	1335717201
JOINT 6242	15.600	9.000	27.900	1336718537
JOINT 6243	12.600	4.500	27.900	1337719874
JOINT 6244	13.600	4.500	27.900	1338721212
JOINT 6245	14.600	4.500	27.900	1339722551
JOINT 6246	12.600	9.000	27.900	1340723891
JOINT 6247	13.600	9.000	27.900	1341725232
JOINT 6248	14.600	9.000	27.900	1342726574
JOINT 6249	-10.734	-4.500	27.900	1343727917
JOINT 6250	-9.867	-4.500	27.900	1344729261
JOINT 6251	-9.000	-4.500	27.900	1345730606
JOINT 6252	-8.000	-4.500	27.900	1346731952
JOINT 6253	-7.000	-4.500	27.900	1347733299
JOINT 6254	-6.000	-4.500	27.900	1348734647
JOINT 6255	-5.000	-4.500	27.900	1349735996
JOINT 6256	-4.000	-4.500	27.900	1350737346
JOINT 6257	-3.000	-4.500	27.900	1351738697
JOINT 6258	-2.000	-4.500	27.900	1352740049
JOINT 6259	-1.000	-4.500	27.900	1353741402
JOINT 6260	0.000	-4.500	27.900	1354742756
JOINT 6262	1.000	-4.500	27.900	1355744111
JOINT 6263	2.000	-4.500	27.900	1356745467
JOINT 6264	3.000	-4.500	27.900	1357746824
JOINT 6265	4.000	-4.500	27.900	1358748182
JOINT 6266	5.000	-4.500	27.900	1359749541
JOINT 6267	6.000	-4.500	27.900	1360750901
JOINT 6268	7.000	-4.500	27.900	1361752262
JOINT 6269	8.000	-4.500	27.900	1362753624
JOINT 6270	9.000	-4.500	27.900	1363754987
JOINT 6271	9.867	-4.500	27.900	1364756351
JOINT 6272	10.734	-4.500	27.900	1365757716



JOINT 6275	-8.000-20.600	27.900	1366759082
JOINT 6276	-1.000-20.600	27.900	1367760449
JOINT 6277	-8.000-19.733	27.900	1368761817
JOINT 6278	-8.000-18.867	27.900	1369763186
JOINT 6279	-1.000-19.733	27.900	1370764556
JOINT 6280	-1.000-18.867	27.900	1371765927
JOINT 6281	-8.000-24.700	31.700	1372767299
JOINT 6283	-8.000-21.200	31.700	1373768672
JOINT 6284	-17.300 9.000	31.700	1374770046
JOINT 6285	-13.800 9.000	31.700	1375771421
JOINT 6286	12.200 11.000	31.700	1376772797
JOINT 6287	15.700 11.000	31.700	1377774174
JOINT 6290	0.000 23.500	27.900	1378775552
JOINT 6299	-10.734 0.000	27.900	1379776931
JOINT 6300	-9.867 0.000	27.900	1380778311
JOINT 6301	-9.000 0.000	27.900	1381779692
JOINT 6302	-8.000 0.000	27.900	1382781074
JOINT 6303	-7.000 0.000	27.900	1383782457
JOINT 6304	-6.000 0.000	27.900	1384783841
JOINT 6305	-5.000 0.000	27.900	1385785226
JOINT 6306	-4.000 0.000	27.900	1386786612
JOINT 6307	-3.000 0.000	27.900	1387787999
JOINT 6308	-2.000 0.000	27.900	1388789387
JOINT 6309	-1.000 0.000	27.900	1389790776
JOINT 6310	0.000 0.000	27.900	1390792166
JOINT 6312	1.000 0.000	27.900	1391793557
JOINT 6313	2.000 0.000	27.900	1392794949
JOINT 6314	3.000 0.000	27.900	1393796342
JOINT 6315	4.000 0.000	27.900	1394797736
JOINT 6316	5.000 0.000	27.900	1395799131
JOINT 6317	6.000 0.000	27.900	1396800527
JOINT 6318	7.000 0.000	27.900	1397801924
JOINT 6319	8.000 0.000	27.900	1398803322
JOINT 6320	9.000 0.000	27.900	1399804721
JOINT 6321	9.867 0.000	27.900	1400806121
JOINT 6322	10.734 0.000	27.900	1401807522
JOINT 6325	13.266-13.500	27.900	1402808924
JOINT 6326	13.266-18.000	27.900	1403810327
JOINT 6328	-11.600 20.600	27.900	1404811731
JOINT 6329	-9.000 20.600	27.900	1405813136
JOINT 6330	-6.000 20.600	27.900	1406814542
JOINT 6331	-4.000 20.600	27.900	1407815949
JOINT 6332	0.000 20.600	27.900	1408817357
JOINT 6333	3.000 20.600	27.900	1409818766
JOINT 6334	9.000 20.600	27.900	1410820176
JOINT 6335	11.600 20.600	27.900	1411821587
JOINT 6349	-10.734 4.500	27.900	1412822999
JOINT 6350	-9.867 4.500	27.900	1413824412
JOINT 6351	-9.000 4.500	27.900	1414825826

JOINT 6352	-8.000	4.500	27.900	1415827241
JOINT 6353	-7.000	4.500	27.900	1416828657
JOINT 6354	-6.000	4.500	27.900	1417830074
JOINT 6355	-5.000	4.500	27.900	1418831492
JOINT 6356	-4.000	4.500	27.900	1419832911
JOINT 6357	-3.000	4.500	27.900	1420834331
JOINT 6358	-2.000	4.500	27.900	1421835752
JOINT 6359	-1.000	4.500	27.900	1422837174
JOINT 6360	0.000	4.500	27.900	1423838597
JOINT 6362	1.000	4.500	27.900	1424840021
JOINT 6363	2.000	4.500	27.900	1425841446
JOINT 6364	3.000	4.500	27.900	1426842872
JOINT 6365	4.000	4.500	27.900	1427844299
JOINT 6366	5.000	4.500	27.900	1428845727
JOINT 6367	6.000	4.500	27.900	1429847156
JOINT 6368	7.000	4.500	27.900	1430848586
JOINT 6369	8.000	4.500	27.900	1431850017
JOINT 6370	9.000	4.500	27.900	1432851449
JOINT 6371	9.867	4.500	27.900	1433852882
JOINT 6372	10.734	4.500	27.900	1434854316
JOINT 6375	-1.000-24.700	31.700		1435855751
JOINT 6376	-1.000-21.200	31.700		1436857187
JOINT 6381	12.200	18.000	27.900	1437858624
JOINT 6383	15.700	18.000	27.900	1438860062
JOINT 6384	12.200	11.000	27.900	1439861501
JOINT 6385	15.700	11.000	27.900	1440862941
JOINT 6386	-17.300	16.000	27.900	1441864382
JOINT 6387	-13.800	16.000	27.900	1442865824
JOINT 6388	-17.300	9.000	27.900	1443867267
JOINT 6389	-13.800	9.000	27.900	1444868711
JOINT 6399	-10.734	9.000	27.900	1445870156
JOINT 6400	-9.867	9.000	27.900	1446871602
JOINT 6401	-9.000	9.000	27.900	1447873049
JOINT 6402	-8.000	9.000	27.900	1448874497
JOINT 6403	-7.000	9.000	27.900	1449875946
JOINT 6404	-6.000	9.000	27.900	1450877396
JOINT 6405	-5.000	9.000	27.900	1451878847
JOINT 6406	-4.000	9.000	27.900	1452880299
JOINT 6407	-3.000	9.000	27.900	1453881752
JOINT 6408	-2.000	9.000	27.900	1454883206
JOINT 6409	-1.000	9.000	27.900	1455884661
JOINT 6410	0.000	9.000	27.900	1456886117
JOINT 6412	1.000	9.000	27.900	1457887574
JOINT 6413	2.000	9.000	27.900	1458889032
JOINT 6414	3.000	9.000	27.900	1459890491
JOINT 6415	4.000	9.000	27.900	1460891951
JOINT 6416	5.000	9.000	27.900	1461893412
JOINT 6417	6.000	9.000	27.900	1462894874
JOINT 6418	7.000	9.000	27.900	1463896337

JOINT 6419	8.000	9.000	27.900	1464897801
JOINT 6420	9.000	9.000	27.900	1465899266
JOINT 6421	9.867	9.000	27.900	1466900732
JOINT 6422	10.734	9.000	27.900	1467902199
JOINT 6425	12.200	18.000	31.700	1468903667
JOINT 6426	15.700	18.000	31.700	1469905136
JOINT 6427	-17.300	16.000	31.700	1470906606
JOINT 6428	-13.800	16.000	31.700	1471908077
JOINT 6431	11.600	10.600	27.900	1472909549
JOINT 6432	10.734	10.600	27.900	1473911022
JOINT 6433	9.867	10.600	27.900	1474912496
JOINT 6435	15.600	10.600	27.900	1475913971
JOINT 6436	12.600	10.600	27.900	1476915447
JOINT 6437	13.600	10.600	27.900	1477916924
JOINT 6438	14.600	10.600	27.900	1478918402
JOINT 6449	-10.734	13.500	27.900	1479919881
JOINT 6450	-9.867	13.500	27.900	1480921361
JOINT 6451	-9.000	13.500	27.900	1481922842
JOINT 6452	-8.000	13.500	27.900	1482924324
JOINT 6453	-7.000	13.500	27.900	1483925807
JOINT 6454	-6.000	13.500	27.900	1484927291
JOINT 6455	-5.000	13.500	27.900	1485928776
JOINT 6456	-4.000	13.500	27.900	1486930262
JOINT 6457	-3.000	13.500	27.900	1487931749
JOINT 6458	-2.000	13.500	27.900	1488933237
JOINT 6459	-1.000	13.500	27.900	1489934726
JOINT 6460	0.000	13.500	27.900	1490936216
JOINT 6462	1.000	13.500	27.900	1491937707
JOINT 6463	2.000	13.500	27.900	1492939199
JOINT 6464	3.000	13.500	27.900	1493940692
JOINT 6465	4.000	13.500	27.900	1494942186
JOINT 6466	5.000	13.500	27.900	1495943681
JOINT 6467	6.000	13.500	27.900	1496945177
JOINT 6468	7.000	13.500	27.900	1497946674
JOINT 6469	8.000	13.500	27.900	1498948172
JOINT 6470	9.000	13.500	27.900	1499949671
JOINT 6471	9.867	13.500	27.900	1500951171
JOINT 6472	10.734	13.500	27.900	1501952672
JOINT 6475	-11.600	16.000	27.900	1502954174
JOINT 6476	-10.734	16.000	27.900	1503955677
JOINT 6477	-9.867	16.000	27.900	1504957181
JOINT 6478	-9.000	16.000	27.900	1505958686
JOINT 6479	11.600	11.000	27.900	1506960192
JOINT 6480	10.734	11.000	27.900	1507961699
JOINT 6481	2.000	-11.250	27.900	1508963207
JOINT 6483	9.867	11.000	27.900	1509964716
JOINT 6484	9.000	11.000	27.900	1510966226
JOINT 6485	2.000	-6.750	27.900	1511967737
JOINT 6486	2.000	-2.250	27.900	1512969249

JOINT 6487	2.000	2.250	27.900	1513970762
JOINT 6488	2.000	6.750	27.900	1514972276
JOINT 6489	2.000	11.250	27.900	1515973791
JOINT 6499	-11.600	18.000	27.900	1516975307
JOINT 6500	-9.867	18.000	27.900	1517976824
JOINT 6501	-9.000	18.000	27.900	1518978342
JOINT 6502	-8.000	18.000	27.900	1519979861
JOINT 6503	-7.000	18.000	27.900	1520981381
JOINT 6504	-6.000	18.000	27.900	1521982902
JOINT 6505	-5.000	18.000	27.900	1522984424
JOINT 6506	-4.000	18.000	27.900	1523985947
JOINT 6507	-3.000	18.000	27.900	1524987471
JOINT 6508	-2.000	18.000	27.900	1525988996
JOINT 6509	-1.000	18.000	27.900	1526990522
JOINT 6510	0.000	18.000	27.900	1527992049
JOINT 6512	1.000	18.000	27.900	1528993577
JOINT 6513	2.000	18.000	27.900	1529995106
JOINT 6514	3.000	18.000	27.900	1530996636
JOINT 6515	4.000	18.000	27.900	1531998167
JOINT 6516	5.000	18.000	27.900	1532999699
JOINT 6517	6.000	18.000	27.900	1533 1232
JOINT 6518	7.000	18.000	27.900	1534 2766
JOINT 6519	8.000	18.000	27.900	1535 4301
JOINT 6520	9.000	18.000	27.900	1536 5837
JOINT 6521	9.867	18.000	27.900	1537 7374
JOINT 6522	11.600	18.000	27.900	1538 8912
JOINT 6523	-9.000	18.867	27.900	1539 10451
JOINT 6524	-6.000	18.867	27.900	1540 11991
JOINT 6525	0.000	18.867	27.900	1541 13532
JOINT 6526	3.000	18.867	27.900	1542 15074
JOINT 6527	-8.465	18.000	27.900	1543 16617
JOINT 6528	8.465	18.000	27.900	1544 18161
JOINT 6529	9.000	18.867	27.900	1545 19706
JOINT 6530	-11.600	18.867	27.900	1546 21252
JOINT 6531	11.600	18.867	27.900	1547 22799
JOINT 6535	-9.000	26.000	27.900	1548 24347
JOINT 6536	-11.600	26.000	27.900	1549 25896
JOINT 6537	6.000	18.867	27.900	1550 27446
JOINT 6538	6.000	19.734	27.900	1551 28997
JOINT 6539	6.000	20.600	27.900	1552 30549
JOINT 6540	3.000	26.000	27.900	1553 32102
JOINT 6541	-11.600	21.680	27.900	1554 33656
JOINT 6542	-11.600	22.760	27.900	1555 35211
JOINT 6543	-11.600	23.840	27.900	1556 36767
JOINT 6544	-11.600	24.920	27.900	1557 38324
JOINT 6545	-9.000	21.680	27.900	1558 39882
JOINT 6546	-9.000	22.760	27.900	1559 41441
JOINT 6547	-9.000	23.840	27.900	1560 43001
JOINT 6548	-9.000	24.920	27.900	1561 44562

JOINT 6549	-11.600	19.734	27.900	1562	46124
JOINT 6550	3.000	21.680	27.900	1563	47687
JOINT 6551	-9.000	19.734	27.900	1564	49251
JOINT 6552	3.000	22.760	27.900	1565	50816
JOINT 6553	3.000	23.840	27.900	1566	52382
JOINT 6554	3.000	24.920	27.900	1567	53949
JOINT 6555	-6.000	19.734	27.900	1568	55517
JOINT 6556	-8.000	24.920	27.900	1569	57086
JOINT 6557	-7.000	24.920	27.900	1570	58656
JOINT 6558	-6.000	24.920	27.900	1571	60227
JOINT 6559	-5.000	24.920	27.900	1572	61799
JOINT 6560	0.000	19.734	27.900	1573	63372
JOINT 6561	-4.000	24.920	27.900	1574	64946
JOINT 6562	-3.000	24.920	27.900	1575	66521
JOINT 6563	-2.000	24.920	27.900	1576	68097
JOINT 6564	-1.000	24.920	27.900	1577	69674
JOINT 6565	-8.000	21.680	27.900	1578	71252
JOINT 6566	3.000	19.734	27.900	1579	72831
JOINT 6567	-7.000	21.680	27.900	1580	74411
JOINT 6568	-6.000	21.680	27.900	1581	75992
JOINT 6569	-5.000	21.680	27.900	1582	77574
JOINT 6570	9.000	19.734	27.900	1583	79157
JOINT 6571	-4.000	21.680	27.900	1584	80741
JOINT 6572	11.600	19.734	27.900	1585	82326
JOINT 6573	-4.000	18.867	27.900	1586	83912
JOINT 6574	-4.000	19.734	27.900	1587	85499
JOINT 6575	-3.000	21.680	27.900	1588	87087
JOINT 6576	0.000	26.000	27.900	1589	88676
JOINT 6577	-2.000	21.680	27.900	1590	90266
JOINT 6578	-1.000	21.680	27.900	1591	91857
JOINT 6579	-6.000	26.000	27.900	1592	93449
JOINT 6580	-3.000	26.000	27.900	1593	95042
JOINT 6583	-9.000	23.000	27.900	1594	96636
JOINT 6584	0.000	21.680	27.900	1595	98231
JOINT 6585	0.000	22.760	27.900	1596	99827
JOINT 6586	0.000	23.840	27.900	1597	101424
JOINT 6587	0.000	24.920	27.900	1598	103022
JOINT 6651	-5.000	2.600	27.900	1599	104621
JOINT 6652	2.000	2.600	27.900	1600	106221
JOINT 6653	-5.000	5.400	27.900	1601	107822
JOINT 6654	2.000	5.400	27.900	1602	109424
JOINT 6655	-5.000	8.200	27.900	1603	111027
JOINT 6656	2.000	8.200	27.900	1604	112631
JOINT 6657	-5.000	11.000	27.900	1605	114236
JOINT 6658	2.000	11.000	27.900	1606	115842
JOINT 6659	-5.000	-11.000	27.900	1607	117449
JOINT 6660	2.000	-11.000	27.900	1608	119057
JOINT 6661	-5.000	-8.200	27.900	1609	120666
JOINT 6662	2.000	-8.200	27.900	1610	122276

JOINT 6663	-5.000	-5.400	27.900	1611123887
JOINT 6664	2.000	-5.400	27.900	1612125499
JOINT 6665	-5.000	-2.600	27.900	1613127112
JOINT 6666	2.000	-2.600	27.900	1614128726
JOINT 6667	-5.000	11.000	28.800	1615130341
JOINT 6668	2.000	11.000	28.800	1616131957
JOINT 6669	-5.000	8.200	28.800	1617133574
JOINT 6670	2.000	8.200	28.800	1618135192
JOINT 6671	-5.000	5.400	28.800	1619136811
JOINT 6672	2.000	5.400	28.800	1620138431
JOINT 6673	-5.000	2.600	28.800	1621140052
JOINT 6674	2.000	2.600	28.800	1622141674
JOINT 6675	-5.000	-2.600	28.800	1623143297
JOINT 6676	2.000	-2.600	28.800	1624144921
JOINT 6677	-5.000	-5.400	28.800	1625146546
JOINT 6678	2.000	-5.400	28.800	1626148172
JOINT 6679	-5.000	-8.200	28.800	1627149799
JOINT 6680	2.000	-8.200	28.800	1628151427
JOINT 6683	-5.000	-11.000	28.800	1629153056
JOINT 6684	2.000	-11.000	28.800	1630154686
JOINT 6685	-5.000	-11.000	29.100	1631156317
JOINT 6686	-5.000	-8.200	29.100	1632157949
JOINT 6687	2.000	-11.000	29.100	1633159582
JOINT 6688	2.000	-8.200	29.100	1634161216
JOINT 6689	-5.000	-5.400	29.100	1635162851
JOINT 6690	-5.000	-2.600	29.100	1636164487
JOINT 6691	2.000	-5.400	29.100	1637166124
JOINT 6692	-5.000	2.600	29.100	1638167762
JOINT 6693	2.000	-2.600	29.100	1639169401
JOINT 6694	-5.000	5.400	29.100	1640171041
JOINT 6695	2.000	2.600	29.100	1641172682
JOINT 6696	2.000	5.400	29.100	1642174324
JOINT 6697	-5.000	8.200	29.100	1643175967
JOINT 6698	-5.000	11.000	29.100	1644177611
JOINT 6700	2.000	8.200	29.100	1645179256
JOINT 6703	2.000	11.000	29.100	1646180902
JOINT 6704	-5.000	-9.600	30.900	1647182549
JOINT 6705	2.000	-9.600	30.900	1648184197
JOINT 6706	-5.000	-4.000	30.900	1649185846
JOINT 6707	2.000	-4.000	30.900	1650187496
JOINT 6708	-5.000	4.000	30.900	1651189147
JOINT 6709	-5.000	9.600	30.900	1652190799
JOINT 6710	2.000	4.000	30.900	1653192452
JOINT 6711	2.000	9.600	30.900	1654194106
JOINT 6712	-6.700	-9.600	30.900	1655195761
JOINT 6713	-6.700	-4.000	30.900	1656197417
JOINT 6714	-6.700	4.000	30.900	1657199074
JOINT 6715	-6.700	9.600	30.900	1658200732
JOINT 6716	3.700	-9.600	30.900	1659202391

JOINT 6717	3.700	-4.000	30.900	1660204051
JOINT 6718	3.700	4.000	30.900	1661205712
JOINT 6721	3.700	9.600	30.900	1662207374
JOINT 6722	-5.000	-9.600	28.800	1663209037
JOINT 6723	2.000	-9.600	28.800	1664210701
JOINT 6724	-5.000	-4.000	28.800	1665212366
JOINT 6725	2.000	-4.000	28.800	1666214032
JOINT 6726	-5.000	4.000	28.800	1667215699
JOINT 6727	2.000	4.000	28.800	1668217367
JOINT 6728	2.000	9.600	28.800	1669219036
JOINT 6729	-5.000	9.600	28.800	1670220706
JOINT 6730	-2.667	-11.000	28.800	1671222377
JOINT 6731	-0.333	-11.000	28.800	1672224049
JOINT 6732	-2.667	-8.200	28.800	1673225722
JOINT 6733	-0.333	-8.200	28.800	1674227396
JOINT 6734	-2.667	-5.400	28.800	1675229071
JOINT 6735	-0.333	-5.400	28.800	1676230747
JOINT 6736	-2.667	-2.600	28.800	1677232424
JOINT 6737	-0.333	-2.600	28.800	1678234102
JOINT 6738	-2.667	2.600	28.800	1679235781
JOINT 6739	-0.333	2.600	28.800	1680237461
JOINT 6740	-2.667	5.400	28.800	1681239142
JOINT 6741	-0.333	5.400	28.800	1682240824
JOINT 6742	-2.667	8.200	28.800	1683242507
JOINT 6743	-0.333	8.200	28.800	1684244191
JOINT 6744	-2.667	11.000	28.800	1685245876
JOINT 6745	-0.333	11.000	28.800	1686247562
JOINT 6751	-7.000	21.680	28.800	1687249249
JOINT 6752	-7.000	24.920	28.800	1688250937
JOINT 6753	-1.000	21.680	28.800	1689252626
JOINT 6754	-1.000	24.920	28.800	1690254316
JOINT 6755	-7.000	21.680	29.100	1691256007
JOINT 6756	-7.000	24.920	29.100	1692257699
JOINT 6757	-1.000	21.680	29.100	1693259392
JOINT 6758	-1.000	24.920	29.100	1694261086
JOINT 6759	-7.000	23.300	28.800	1695262781
JOINT 6760	-1.000	23.300	28.800	1696264477
JOINT 6761	-7.000	23.300	30.900	1697266174
JOINT 6762	-1.000	23.300	30.900	1698267872
JOINT 6763	-8.500	23.300	30.900	1699269571
JOINT 6764	0.500	23.300	30.900	1700271271
JOINT 6765	-5.000	21.680	28.800	1701272972
JOINT 6766	-3.000	21.680	28.800	1702274674
JOINT 6767	-5.000	24.920	28.800	1703276377
JOINT 6768	-3.000	24.920	28.800	1704278081
JOINT 7021	-11.600	20.600	35.500	1705279786
JOINT 7022	-9.000	20.600	35.500	1706281492
JOINT 7023	-5.000	20.600	35.500	1707283199
JOINT 7024	0.000	20.600	35.500	1708284907

JOINT 7025	5.000	20.600	35.500	1709286616
JOINT 7026	9.000	20.600	35.500	1710288326
JOINT 7027	11.600	20.600	35.500	1711290037
JOINT 7028	-11.600	-20.600	35.500	1712291749
JOINT 7029	-9.000	-20.600	35.500	1713293462
JOINT 7030	-5.000	-20.600	35.500	1714295176
JOINT 7031	-1.000	-20.600	35.500	1715296891
JOINT 7032	4.757	-20.600	35.500	1716298607
JOINT 7033	6.491	-19.734	35.500	1717300324
JOINT 7034	10.734	-15.308	35.500	1718302042
JOINT 7035	11.600	13.500	35.500	1719303761
JOINT 7036	11.600	9.600	35.500	1720305481
JOINT 7037	11.600	4.500	35.500	1721307202
JOINT 7038	11.600	0.000	35.500	1722308924
JOINT 7039	11.600	-4.500	35.500	1723310647
JOINT 7040	11.600	-9.000	35.500	1724312371
JOINT 7041	11.600	-13.500	35.500	1725314096
JOINT 7042	10.734	18.000	35.500	1726315822
JOINT 7043	-11.600	-13.500	35.500	1727317549
JOINT 7044	-11.600	-9.000	35.500	1728319277
JOINT 7045	-11.600	-4.500	35.500	1729321006
JOINT 7046	-11.600	0.000	35.500	1730322736
JOINT 7047	-11.600	4.500	35.500	1731324467
JOINT 7048	-11.600	9.600	35.500	1732326199
JOINT 7049	-11.600	-19.734	35.500	1733327932
JOINT 7050	-11.600	13.500	35.500	1734329666
JOINT 7051	-9.000	-19.734	35.500	1735331401
JOINT 7052	-10.733	-18.000	35.500	1736333137
JOINT 7053	-10.733	18.000	35.500	1737334874
JOINT 7055	-5.000	-19.734	35.500	1738336612
JOINT 7060	-1.000	-19.734	35.500	1739338351
JOINT 7066	4.757	-19.734	35.500	1740340091
JOINT 7075	-8.000	-20.600	35.500	1741341832
JOINT 7076	-8.000	-19.734	35.500	1742343574
JOINT 7077	-8.000	-18.867	35.500	1743345317
JOINT 7099	-11.600	-18.000	35.500	1744347061
JOINT 7100	-9.867	-18.000	35.500	1745348806
JOINT 7101	-9.000	-18.000	35.500	1746350552
JOINT 7102	-8.000	-18.000	35.500	1747352299
JOINT 7103	-7.000	-18.000	35.500	1748354047
JOINT 7104	-6.000	-18.000	35.500	1749355796
JOINT 7105	-5.000	-18.000	35.500	1750357546
JOINT 7106	-4.000	-18.000	35.500	1751359297
JOINT 7107	-3.000	-18.000	35.500	1752361049
JOINT 7108	-2.000	-18.000	35.500	1753362802
JOINT 7109	-1.000	-18.000	35.500	1754364556
JOINT 7110	0.000	-18.000	35.500	1755366311
JOINT 7112	1.000	-18.000	35.500	1756368067
JOINT 7113	2.000	-18.000	35.500	1757369824



Azin Azarhoushang  
Department of Civil Engineering

---

JOINT 7114	3.000-18.000	35.500	1758371582
JOINT 7115	4.000-18.000	35.500	1759373341
JOINT 7116	4.757-18.000	35.500	1760375101
JOINT 7117	6.000-18.000	35.500	1761376862
JOINT 7118	7.000-18.000	35.500	1762378624
JOINT 7119	8.000-18.000	35.500	1763380387
JOINT 7120	9.000-18.000	35.500	1764382151
JOINT 7123	4.757-13.500	35.500	1765383916
JOINT 7125	-8.000-21.200	35.500	1766385682
JOINT 7126	-8.000-24.700	35.500	1767387449
JOINT 7127	-1.000-21.200	35.500	1768389217
JOINT 7128	-1.000-24.700	35.500	1769390986
JOINT 7131	-9.000-17.380	35.500	1770392756
JOINT 7132	-9.000 17.380	35.500	1771394527
JOINT 7135	9.000-17.380	35.500	1772396299
JOINT 7136	9.000 17.380	35.500	1773398072
JOINT 7149	-10.734-13.500	35.500	1774399846
JOINT 7150	-9.867-13.500	35.500	1775401621
JOINT 7151	-9.000-13.500	35.500	1776403397
JOINT 7152	-8.000-13.500	35.500	1777405174
JOINT 7153	-7.000-13.500	35.500	1778406952
JOINT 7154	-6.000-13.500	35.500	1779408731
JOINT 7155	-5.000-13.500	35.500	1780410511
JOINT 7156	-4.000-13.500	35.500	1781412292
JOINT 7157	-3.000-13.500	35.500	1782414074
JOINT 7158	-2.000-13.500	35.500	1783415857
JOINT 7159	-1.000-13.500	35.500	1784417641
JOINT 7160	0.000-13.500	35.500	1785419426
JOINT 7162	1.000-13.500	35.500	1786421212
JOINT 7163	2.000-13.500	35.500	1787422999
JOINT 7164	3.000-13.500	35.500	1788424787
JOINT 7165	4.000-13.500	35.500	1789426576
JOINT 7166	5.000-13.500	35.500	1790428366
JOINT 7167	6.000-13.500	35.500	1791430157
JOINT 7168	7.000-13.500	35.500	1792431949
JOINT 7169	8.000-13.500	35.500	1793433742
JOINT 7170	9.000-13.500	35.500	1794435536
JOINT 7171	9.867-13.500	35.500	1795437331
JOINT 7172	10.734-13.500	35.500	1796439127
JOINT 7175	8.133-18.867	35.500	1797440924
JOINT 7176	7.265-19.734	35.500	1798442722
JOINT 7177	10.734-16.266	35.500	1799444521
JOINT 7178	9.867-17.133	35.500	1800446321
JOINT 7181	-9.000 9.000	35.500	1801448122
JOINT 7183	-11.600 9.000	35.500	1802449924
JOINT 7184	-10.734 9.000	35.500	1803451727
JOINT 7185	-9.867 9.000	35.500	1804453531
JOINT 7199	-10.734 -9.000	35.500	1805455336
JOINT 7200	-9.867 -9.000	35.500	1806457142

JOINT 7201	-9.000	-9.000	35.500	1807458949
JOINT 7202	-8.000	-9.000	35.500	1808460757
JOINT 7203	-7.000	-9.000	35.500	1809462566
JOINT 7204	-6.000	-9.000	35.500	1810464376
JOINT 7205	-5.000	-9.000	35.500	1811466187
JOINT 7206	-4.000	-9.000	35.500	1812467999
JOINT 7207	-3.000	-9.000	35.500	1813469812
JOINT 7208	-2.000	-9.000	35.500	1814471626
JOINT 7209	-1.000	-9.000	35.500	1815473441
JOINT 7210	0.000	-9.000	35.500	1816475257
JOINT 7212	1.000	-9.000	35.500	1817477074
JOINT 7213	2.000	-9.000	35.500	1818478892
JOINT 7214	3.000	-9.000	35.500	1819480711
JOINT 7215	4.000	-9.000	35.500	1820482531
JOINT 7216	5.000	-9.000	35.500	1821484352
JOINT 7217	6.000	-9.000	35.500	1822486174
JOINT 7218	7.000	-9.000	35.500	1823487997
JOINT 7219	8.000	-9.000	35.500	1824489821
JOINT 7220	9.000	-9.000	35.500	1825491646
JOINT 7221	9.867	-9.000	35.500	1826493472
JOINT 7222	10.734	-9.000	35.500	1827495299
JOINT 7223	-9.000	-1.356	35.500	1828497127
JOINT 7224	-9.000	1.356	35.500	1829498956
JOINT 7225	9.000	-1.356	35.500	1830500786
JOINT 7226	9.000	1.356	35.500	1831502617
JOINT 7227	-9.000	-16.170	35.500	1832504449
JOINT 7228	-9.000	16.000	35.500	1833506282
JOINT 7229	9.000	-16.170	35.500	1834508116
JOINT 7230	9.000	16.170	35.500	1835509951
JOINT 7231	0.000	-18.867	35.500	1836511787
JOINT 7232	0.000	-19.734	35.500	1837513624
JOINT 7233	0.000	-20.600	35.500	1838515462
JOINT 7249	-10.734	-4.500	35.500	1839517301
JOINT 7250	-9.867	-4.500	35.500	1840519141
JOINT 7251	-9.000	-4.500	35.500	1841520982
JOINT 7252	-8.000	-4.500	35.500	1842522824
JOINT 7253	-7.000	-4.500	35.500	1843524667
JOINT 7254	-6.000	-4.500	35.500	1844526511
JOINT 7255	-5.000	-4.500	35.500	1845528356
JOINT 7256	-4.000	-4.500	35.500	1846530202
JOINT 7257	-3.000	-4.500	35.500	1847532049
JOINT 7258	-2.000	-4.500	35.500	1848533897
JOINT 7259	-1.000	-4.500	35.500	1849535746
JOINT 7260	0.000	-4.500	35.500	1850537596
JOINT 7262	1.000	-4.500	35.500	1851539447
JOINT 7263	2.000	-4.500	35.500	1852541299
JOINT 7264	3.000	-4.500	35.500	1853543152
JOINT 7265	4.000	-4.500	35.500	1854545006
JOINT 7266	5.000	-4.500	35.500	1855546861

JOINT 7267	6.000	-4.500	35.500	1856548717
JOINT 7268	7.000	-4.500	35.500	1857550574
JOINT 7269	8.000	-4.500	35.500	1858552432
JOINT 7270	9.000	-4.500	35.500	1859554291
JOINT 7271	9.867	-4.500	35.500	1860556151
JOINT 7272	10.734	-4.500	35.500	1861558012
JOINT 7275	-17.300	16.000	35.500	1862559874
JOINT 7276	-13.800	16.000	35.500	1863561737
JOINT 7277	-17.300	9.000	35.500	1864563601
JOINT 7278	-13.800	9.000	35.500	1865565466
JOINT 7279	12.200	18.000	35.500	1866567332
JOINT 7280	15.700	18.000	35.500	1867569199
JOINT 7283	12.200	11.000	35.500	1868571067
JOINT 7284	15.700	11.000	35.500	1869572936
JOINT 7299	-10.734	0.000	35.500	1870574806
JOINT 7300	-9.867	0.000	35.500	1871576677
JOINT 7301	-9.000	0.000	35.500	1872578549
JOINT 7302	-8.000	0.000	35.500	1873580422
JOINT 7303	-7.000	0.000	35.500	1874582296
JOINT 7304	-6.000	0.000	35.500	1875584171
JOINT 7305	-5.000	0.000	35.500	1876586047
JOINT 7306	-4.000	0.000	35.500	1877587924
JOINT 7307	-3.000	0.000	35.500	1878589802
JOINT 7308	-2.000	0.000	35.500	1879591681
JOINT 7309	-1.000	0.000	35.500	1880593561
JOINT 7310	0.000	0.000	35.500	1881595442
JOINT 7312	1.000	0.000	35.500	1882597324
JOINT 7313	2.000	0.000	35.500	1883599207
JOINT 7314	3.000	0.000	35.500	1884601091
JOINT 7315	4.000	0.000	35.500	1885602976
JOINT 7316	5.000	0.000	35.500	1886604862
JOINT 7317	6.000	0.000	35.500	1887606749
JOINT 7318	7.000	0.000	35.500	1888608637
JOINT 7319	8.000	0.000	35.500	1889610526
JOINT 7320	9.000	0.000	35.500	1890612416
JOINT 7321	9.867	0.000	35.500	1891614307
JOINT 7322	10.734	0.000	35.500	1892616199
JOINT 7349	-10.734	4.500	35.500	1893618092
JOINT 7350	-9.867	4.500	35.500	1894619986
JOINT 7351	-9.000	4.500	35.500	1895621881
JOINT 7352	-8.000	4.500	35.500	1896623777
JOINT 7353	-7.000	4.500	35.500	1897625674
JOINT 7354	-6.000	4.500	35.500	1898627572
JOINT 7355	-5.000	4.500	35.500	1899629471
JOINT 7356	-4.000	4.500	35.500	1900631371
JOINT 7357	-3.000	4.500	35.500	1901633272
JOINT 7358	-2.000	4.500	35.500	1902635174
JOINT 7359	-1.000	4.500	35.500	1903637077
JOINT 7360	0.000	4.500	35.500	1904638981

JOINT 7362	1.000	4.500	35.500	1905640886
JOINT 7363	2.000	4.500	35.500	1906642792
JOINT 7364	3.000	4.500	35.500	1907644699
JOINT 7365	4.000	4.500	35.500	1908646607
JOINT 7366	5.000	4.500	35.500	1909648516
JOINT 7367	6.000	4.500	35.500	1910650426
JOINT 7368	7.000	4.500	35.500	1911652337
JOINT 7369	8.000	4.500	35.500	1912654249
JOINT 7370	9.000	4.500	35.500	1913656162
JOINT 7371	9.867	4.500	35.500	1914658076
JOINT 7372	10.734	4.500	35.500	1915659991
JOINT 7375	-9.000	3.000	35.500	1916661907
JOINT 7376	-8.000	3.000	35.500	1917663824
JOINT 7377	-7.000	3.000	35.500	1918665742
JOINT 7378	-6.000	3.000	35.500	1919667661
JOINT 7379	-5.000	3.000	35.500	1920669581
JOINT 7380	-4.000	3.000	35.500	1921671502
JOINT 7383	-3.000	3.000	35.500	1922673424
JOINT 7384	-9.867	3.000	35.500	1923675347
JOINT 7385	-2.000	3.000	35.500	1924677271
JOINT 7386	-11.600	16.000	35.500	1925679196
JOINT 7387	-10.733	16.000	35.500	1926681122
JOINT 7388	-9.867	16.000	35.500	1927683049
JOINT 7389	11.600	11.000	35.500	1928684977
JOINT 7390	10.734	11.000	35.500	1929686906
JOINT 7391	9.867	11.000	35.500	1930688836
JOINT 7392	9.000	11.000	35.500	1931690767
JOINT 7399	-10.734	9.600	35.500	1932692699
JOINT 7400	-9.867	9.600	35.500	1933694632
JOINT 7401	-9.000	9.600	35.500	1934696566
JOINT 7402	-8.000	9.600	35.500	1935698501
JOINT 7403	-7.000	9.600	35.500	1936700437
JOINT 7404	-6.000	9.600	35.500	1937702374
JOINT 7405	-5.000	9.600	35.500	1938704312
JOINT 7406	-4.000	9.600	35.500	1939706251
JOINT 7407	-3.000	9.600	35.500	1940708191
JOINT 7408	-2.000	9.600	35.500	1941710132
JOINT 7409	-1.000	9.600	35.500	1942712074
JOINT 7410	0.000	9.600	35.500	1943714017
JOINT 7412	1.000	9.600	35.500	1944715961
JOINT 7413	2.000	9.600	35.500	1945717906
JOINT 7414	3.000	9.600	35.500	1946719852
JOINT 7415	4.000	9.600	35.500	1947721799
JOINT 7416	5.000	9.600	35.500	1948723747
JOINT 7417	6.000	9.600	35.500	1949725696
JOINT 7418	7.000	9.600	35.500	1950727646
JOINT 7419	8.000	9.600	35.500	1951729597
JOINT 7420	9.000	9.600	35.500	1952731549
JOINT 7421	9.867	9.600	35.500	1953733502

JOINT 7422	10.734	9.600	35.500	1954735456
JOINT 7449	-10.734	13.500	35.500	1955737411
JOINT 7450	-9.867	13.500	35.500	1956739367
JOINT 7451	-9.000	13.500	35.500	1957741324
JOINT 7452	-8.000	13.500	35.500	1958743282
JOINT 7453	-7.000	13.500	35.500	1959745241
JOINT 7454	-6.000	13.500	35.500	1960747201
JOINT 7455	-5.000	13.500	35.500	1961749162
JOINT 7456	-4.000	13.500	35.500	1962751124
JOINT 7457	-3.000	13.500	35.500	1963753087
JOINT 7458	-2.000	13.500	35.500	1964755051
JOINT 7459	-1.000	13.500	35.500	1965757016
JOINT 7460	0.000	13.500	35.500	1966758982
JOINT 7462	1.000	13.500	35.500	1967760949
JOINT 7463	2.000	13.500	35.500	1968762917
JOINT 7464	3.000	13.500	35.500	1969764886
JOINT 7465	4.000	13.500	35.500	1970766856
JOINT 7466	5.000	13.500	35.500	1971768827
JOINT 7467	6.000	13.500	35.500	1972770799
JOINT 7468	7.000	13.500	35.500	1973772772
JOINT 7469	8.000	13.500	35.500	1974774746
JOINT 7470	9.000	13.500	35.500	1975776721
JOINT 7471	9.867	13.500	35.500	1976778697
JOINT 7472	10.734	13.500	35.500	1977780674
JOINT 7499	-11.600	18.000	35.500	1978782652
JOINT 7500	-9.867	18.000	35.500	1979784631
JOINT 7501	-9.000	18.000	35.500	1980786611
JOINT 7502	-8.000	18.000	35.500	1981788592
JOINT 7503	-7.000	18.000	35.500	1982790574
JOINT 7504	-6.000	18.000	35.500	1983792557
JOINT 7505	-5.000	18.000	35.500	1984794541
JOINT 7506	-4.000	18.000	35.500	1985796526
JOINT 7507	-3.000	18.000	35.500	1986798512
JOINT 7508	-2.000	18.000	35.500	1987800499
JOINT 7509	-1.000	18.000	35.500	1988802487
JOINT 7510	0.000	18.000	35.500	1989804476
JOINT 7512	1.000	18.000	35.500	1990806466
JOINT 7513	2.000	18.000	35.500	1991808457
JOINT 7514	3.000	18.000	35.500	1992810449
JOINT 7515	4.000	18.000	35.500	1993812442
JOINT 7516	5.000	18.000	35.500	1994814436
JOINT 7517	6.000	18.000	35.500	1995816431
JOINT 7518	7.000	18.000	35.500	1996818427
JOINT 7519	8.000	18.000	35.500	1997820424
JOINT 7520	9.000	18.000	35.500	1998822422
JOINT 7521	9.867	18.000	35.500	1999824421
JOINT 7522	11.600	18.000	35.500	2000826421
JOINT 7523	-9.000	18.867	35.500	2001828422
JOINT 7524	-5.000	18.867	35.500	2002830424

JOINT 7525	0.000	18.867	35.500	2003832427
JOINT 7526	5.000	18.867	35.500	2004834431
JOINT 7527	9.000	18.867	35.500	2005836436
JOINT 7528	-9.000	-18.867	35.500	2006838442
JOINT 7529	-5.000	-18.867	35.500	2007840449
JOINT 7530	9.000	18.000	43.000	2008842457
JOINT 7531	-1.000	-18.867	35.500	2009844466
JOINT 7532	4.757	-18.867	35.500	2010846476
JOINT 7533	7.357	-20.600	35.500	2011848487
JOINT 7534	5.624	-18.867	35.500	2012850499
JOINT 7535	9.867	-14.404	35.500	2013852512
JOINT 7536	11.600	-16.211	35.500	2014854526
JOINT 7537	-11.600	18.867	35.500	2015856541
JOINT 7538	11.600	18.867	35.500	2016858557
JOINT 7539	-11.600	-18.867	35.500	2017860574
JOINT 7549	-11.600	19.734	35.500	2018862592
JOINT 7551	-9.000	19.734	35.500	2019864611
JOINT 7555	-5.000	19.734	35.500	2020866631
JOINT 7560	0.000	19.734	35.500	2021868652
JOINT 7566	5.000	19.734	35.500	2022870674
JOINT 7570	9.000	19.734	35.500	2023872697
JOINT 7572	11.600	19.734	35.500	2024874721
JOINT 7573	15.376	-20.149	35.500	2025876746
JOINT 7574	11.121	-24.364	35.500	2026878772
JOINT 7575	11.203	-15.797	35.500	2027880799
JOINT 7576	6.878	-20.121	35.500	2028882827
JOINT 7651	-9.000	9.600	40.800	2029884856
JOINT 7652	-5.000	9.600	40.800	2030886886
JOINT 7653	0.000	9.600	40.800	2031888917
JOINT 7654	5.000	9.600	40.800	2032890949
JOINT 7655	-9.000	13.500	40.800	2033892982
JOINT 7656	5.000	13.500	40.800	2034895016
JOINT 7657	-9.000	18.000	40.800	2035897051
JOINT 7658	-5.000	18.000	40.800	2036899087
JOINT 7659	0.000	18.000	40.800	2037901124
JOINT 7660	5.000	18.000	40.800	2038903162
JOINT 7661	-5.000	13.500	40.800	2039905201
JOINT 7662	0.000	13.500	40.800	2040907241
JOINT 7663	-9.000	-12.000	35.500	2041909282
JOINT 7664	-6.000	-12.000	35.500	2042911324
JOINT 7665	-3.000	-12.000	35.500	2043913367
JOINT 7666	0.000	-12.000	35.500	2044915411
JOINT 7667	-9.000	-18.000	40.800	2045917456
JOINT 7668	-6.000	-18.000	40.800	2046919502
JOINT 7669	-3.000	-18.000	40.800	2047921549
JOINT 7670	0.000	-18.000	40.800	2048923597
JOINT 7671	-9.000	-12.000	40.800	2049925646
JOINT 7672	-6.000	-12.000	40.800	2050927696
JOINT 7673	-3.000	-12.000	40.800	2051929747

JOINT 7674	0.000-12.000	40.800	2052931799
JOINT 7675	-9.000-15.000	40.800	2053933852
JOINT 7676	-6.000-15.000	40.800	2054935906
JOINT 7677	-3.000-15.000	40.800	2055937961
JOINT 7678	0.000-15.000	40.800	2056940017
JOINT 7679	-9.000-15.000	35.500	2057942074
JOINT 7680	0.000-15.000	35.500	2058944132
JOINT 8101	28.445-37.445	83.131	2059946191
JOINT 8102	34.821-39.594	83.131	2060948251
JOINT 8103	30.566-43.809	83.131	2061950312
JOINT 8104	19.960-28.960	62.346	2062952374
JOINT 8105	22.081-35.324	62.346	2063954437
JOINT 8106	26.336-31.109	62.346	2064956501
JOINT 8107	9.353-18.353	36.365	2065958566
JOINT 8108	11.474-24.717	36.365	2066960632
JOINT 8109	15.729-20.502	36.365	2067962699
JOINT 8110	11.475-20.475	41.562	2068964767
JOINT 8111	13.596-22.596	46.758	2069966836
JOINT 8112	15.717-24.717	51.954	2070968906
JOINT 8113	17.839-26.839	57.150	2071970977
JOINT 8114	17.851-22.624	41.562	2072973049
JOINT 8115	19.972-24.745	46.758	2073975122
JOINT 8116	22.093-26.866	51.954	2074977196
JOINT 8117	24.215-28.988	57.150	2075979271
JOINT 8118	13.596-26.839	41.562	2076981347
JOINT 8119	15.717-28.960	46.758	2077983424
JOINT 8120	17.838-31.081	51.954	2078985502
JOINT 8121	19.960-33.203	57.150	2079987581
JOINT 8122	22.081-31.081	67.542	2080989661
JOINT 8123	24.202-33.202	72.739	2081991742
JOINT 8124	26.324-35.324	77.935	2082993824
JOINT 8125	28.457-33.230	67.542	2083995907
JOINT 8126	30.578-35.351	72.739	2084997991
JOINT 8127	32.700-37.473	77.935	2085 76
JOINT 8128	24.202-37.445	67.542	2086 2162
JOINT 8129	26.323-39.566	72.739	2087 4249
JOINT 8130	28.445-41.688	77.935	2088 6337
JOINT 8131	15.723-24.731	41.562	2089 8426
JOINT 8132	14.871-25.576	41.562	2090 10516
JOINT 8133	16.576-23.887	41.562	2091 12607
JOINT 8134	12.970-23.658	41.562	2092 14699
JOINT 8135	14.676-21.968	41.562	2093 16792
JOINT 8136	12.644-23.981	41.562	2094 18886
JOINT 8137	14.988-21.659	41.562	2095 20981
JOINT 8138	13.815-24.510	41.562	2096 23077
JOINT 8139	15.520-22.821	41.562	2097 25174
JOINT 8140	17.828-26.869	46.758	2098 27272
JOINT 8141	18.681-26.024	46.758	2099 29371
JOINT 8142	16.976-27.713	46.758	2100 31471

JOINT 8143	15.076-25.795	46.758	2101	33572
JOINT 8145	16.781-24.106	46.758	2102	35674
JOINT 8146	14.765-26.103	46.758	2103	37777
JOINT 8147	17.109-23.780	46.758	2104	39881
JOINT 8148	15.920-26.647	46.758	2105	41986
JOINT 8149	17.625-24.958	46.758	2106	44092
JOINT 8150	19.949-28.990	51.954	2107	46199
JOINT 8151	20.802-28.145	51.954	2108	48307
JOINT 8152	19.097-29.834	51.954	2109	50416
JOINT 8153	17.197-27.916	51.954	2110	52526
JOINT 8154	18.902-26.227	51.954	2111	54637
JOINT 8155	16.886-28.224	51.954	2112	56749
JOINT 8156	19.230-25.901	51.954	2113	58862
JOINT 8157	18.041-28.768	51.954	2114	60976
JOINT 8158	19.746-27.079	51.954	2115	63091
JOINT 8159	22.071-31.112	57.150	2116	65207
JOINT 8160	22.924-30.267	57.150	2117	67324
JOINT 8161	21.219-31.956	57.150	2118	69442
JOINT 8162	19.319-30.038	57.150	2119	71561
JOINT 8163	21.024-28.349	57.150	2120	73681
JOINT 8164	19.008-30.346	57.150	2121	75802
JOINT 8165	21.352-28.023	57.150	2122	77924
JOINT 8166	20.163-30.890	57.150	2123	80047
JOINT 8167	21.868-29.201	57.150	2124	82171
JOINT 8168	24.192-33.233	62.346	2125	84296
JOINT 8169	25.045-32.388	62.346	2126	86422
JOINT 8170	23.340-34.077	62.346	2127	88549
JOINT 8171	21.440-32.159	62.346	2128	90677
JOINT 8172	23.145-30.470	62.346	2129	92806
JOINT 8173	21.129-32.467	62.346	2130	94936
JOINT 8174	23.473-30.144	62.346	2131	97067
JOINT 8175	22.284-33.011	62.346	2132	99199
JOINT 8176	23.989-31.322	62.346	2133	101332
JOINT 8177	26.313-35.354	67.542	2134	103466
JOINT 8178	27.166-34.509	67.542	2135	105601
JOINT 8179	25.461-36.198	67.542	2136	107737
JOINT 8180	23.561-34.280	67.542	2137	109874
JOINT 8183	25.266-32.591	67.542	2138	112012
JOINT 8184	23.250-34.588	67.542	2139	114151
JOINT 8185	25.594-32.265	67.542	2140	116291
JOINT 8186	24.405-35.132	67.542	2141	118432
JOINT 8187	26.110-33.443	67.542	2142	120574
JOINT 8188	28.434-37.475	72.739	2143	122717
JOINT 8189	29.287-36.630	72.739	2144	124861
JOINT 8190	27.582-38.319	72.739	2145	127006
JOINT 8191	25.682-36.401	72.739	2146	129152
JOINT 8192	27.387-34.712	72.739	2147	131299
JOINT 8193	25.371-36.709	72.739	2148	133447
JOINT 8194	27.715-34.386	72.739	2149	135596



JOINT 8195	26.526-37.253	72.739	2150137746
JOINT 8196	28.231-35.564	72.739	2151139897
JOINT 8199	9.177-18.177	35.932	2152142049
JOINT 8209	30.556-39.597	77.935	2153144202
JOINT 8210	29.704-40.441	77.935	2154146356
JOINT 8211	31.409-38.752	77.935	2155148511
JOINT 8212	27.804-38.523	77.935	2156150667
JOINT 8213	29.509-36.834	77.935	2157152824
JOINT 8214	27.493-38.831	77.935	2158154982
JOINT 8215	29.837-36.508	77.935	2159157141
JOINT 8216	28.648-39.375	77.935	2160159301
JOINT 8217	30.353-37.686	77.935	2161161462
JOINT 8218	35.549-40.322	84.914	2162163624
JOINT 8221	31.294-44.537	84.914	2163165787
JOINT 8222	29.173-38.173	84.914	2164167951
JOINT 8223	34.486-39.964	84.914	2165170116
JOINT 8224	33.423-39.605	84.914	2166172282
JOINT 8225	32.361-39.247	84.914	2167174449
JOINT 8226	31.298-38.889	84.914	2168176617
JOINT 8227	30.235-38.531	84.914	2169178786
JOINT 8228	30.940-43.476	84.914	2170180956
JOINT 8229	30.587-42.415	84.914	2171183127
JOINT 8230	30.233-41.355	84.914	2172185299
JOINT 8231	29.880-40.294	84.914	2173187472
JOINT 8232	29.526-39.233	84.914	2174189646
JOINT 8233	32.003-43.834	84.914	2175191821
JOINT 8234	32.712-43.132	84.914	2176193997
JOINT 8235	33.421-42.429	84.914	2177196174
JOINT 8236	34.130-41.727	84.914	2178198352
JOINT 8237	34.840-41.024	84.914	2179200531
JOINT 8238	32.710-44.541	84.914	2180202711
JOINT 8239	33.419-43.839	84.914	2181204892
JOINT 8240	34.128-43.136	84.914	2182207074
JOINT 8241	34.837-42.434	84.914	2183209257
JOINT 8242	35.547-41.731	84.914	2184211441
JOINT 8243	31.646-45.595	84.914	2185213626
JOINT 8244	36.609-40.679	84.914	2186215812
JOINT 8245	30.150-44.267	84.914	2187217999
JOINT 8246	28.736-40.024	84.914	2188220187
JOINT 8247	29.796-43.206	84.914	2189222376
JOINT 8248	29.443-42.145	84.914	2190224566
JOINT 8249	29.089-41.085	84.914	2191226757
JOINT 8250	30.501-45.322	84.914	2192228949
JOINT 8251	28.382-38.963	84.914	2193231142
JOINT 8252	29.966-37.385	84.914	2194233336
JOINT 8253	35.279-39.176	84.914	2195235531
JOINT 8254	34.217-38.818	84.914	2196237727
JOINT 8255	33.154-38.459	84.914	2197239924
JOINT 8256	32.091-38.101	84.914	2198242122

JOINT 8257	31.029-37.743	84.914		2199244321
JOINT 8258	36.344-39.534	84.914		2200246521
JOINT 8259	27.985-37.773	84.914		2201248722
JOINT 8260	28.777-36.984	84.914		2202250924
JOINT 8261	31.109-36.937	77.935		2203253127
JOINT 8265	27.181-37.894	77.935		2204255331
JOINT 8266	28.372-37.960	77.935		2205257536
JOINT 8267	29.216-38.812	77.935		2206259742
JOINT 8268	26.609-36.180	77.935		2207261949
JOINT 8269	27.749-37.331	77.935		2208264157
JOINT 8272	26.038-36.752	77.935		2209266366
JOINT 8273	13.601-22.610	36.365		2210268576
JOINT 8274	32.694-41.701	83.131		2211270787
JOINT 8275	13.297-22.301	36.615		2212272999
JOINT 8276	32.387-41.396	83.381		2213275212
JOINT 8277	15.418-24.423	41.811		2214277426
JOINT 8278	17.539-26.545	47.007		2215279641
JOINT 8279	19.660-28.666	52.204		2216281857
JOINT 8280	21.782-30.788	57.400		2217284074
JOINT 8281	23.903-32.909	62.596		2218286292
JOINT 8282	26.024-35.031	67.792		2219288511
JOINT 8283	28.145-37.153	72.989		2220290731
JOINT 8284	30.266-39.274	78.185		2221292952
JOINT 8285	30.943-40.651	84.914		2222295174
JOINT 8286	31.654-39.947	84.914		2223297397
JOINT 8287	31.653-41.359	84.914		2224299621
JOINT 8288	32.363-40.655	84.914		2225301846
JOINT 8289	-16.473-18.000	-52.482	111111	2226304072
JOINT 8290	16.473-18.000	-52.482	111111	2227306299
JOINT 8291	-16.473	18.000-52.482	111111	2228308527
JOINT 8292	16.474	18.000-52.482	111111	2229310756
JOINT 8293	-8.250	18.000	5.000	2230312986
JOINT 8294	-3.850	18.000	5.000	2231315217
JOINT 8295	-1.450	18.000	5.000	2232317449
JOINT 8296	5.800	18.000	5.000	2233319682
JOINT 8297	-8.350	18.000	-9.000	2234321916
JOINT 8298	-1.450	18.000	-9.000	2235324151
JOINT 8300	-3.850	18.000	-9.000	2236326387
JOINT 8303	-8.350	18.000-25.300		2237328624
JOINT 8304	-3.850	18.000-25.300		2238330862
JOINT 8305	-1.450	18.000-25.300		2239333101
JOINT 8306	11.888	18.000	1.000	2240335341
JOINT 8307	11.888	23.843	1.000	2241337582
END				

## A.2 Fatigue

SPECTRAL ANALYSIS

```

FTOPTG7  50.          1.0TTSMTTP SK      NE EX 6  0.5  18.  7.5  TLPEFT
FTOPT2   PTVC                      -0.81  4.71DE -41.60  42.72TI
SCF      1.6  3.0  3.0  3.0  1.6  1.6  1.6  1.6  1.6  1.6  1.0  1.0  1.0  1.0
JSLC    101 103 119 117 122 118 121 181 104 199 111 112 113 114 115 116 105 106
JSLC    201 203 219 205 206 281 299 301 303 319 305 306 381 304 399 401 419 481
JSLC    49910121007101510131022102510261027102810291023102183068307
JSLC    10301031103210331034102410021005100110111017101010161006

SEAS
FTLOAD   1      0.494          SPC
SCATD D          JS
SCWAV          0.25  0.75  1.25  1.75  2.25  2.75  3.25  3.75  4.25
SCPER     1.50.0002
SCPER     2.50.0231
SCPER     3.50.29160.16290.0002
SCPER     4.50.03860.26360.05680.0002
SCPER     5.5      0.01250.09100.03810.0014
SCPER     6.5          0.00020.00900.00790.00120.0002
SCPER     7.5          0.0002      0.00020.00020.00020.0002
FTLOAD   2      0.128          SPC
SCATD D          JS
SCWAV          0.25  0.75  1.25  1.75  2.25  2.75  3.25  3.75  4.25
SCPER     1.50.0009
SCPER     2.50.07450.0018
SCPER     3.50.51300.14030.0027
SCPER     4.50.04200.15190.0223
SCPER     5.5      0.00450.03130.00710.0018
SCPER     6.5          0.00270.0036
FTLOAD   3      0.035          SPC
SCATD D          JS
SCWAV          0.25  0.75  1.25  1.75  2.25  2.75  3.25  3.75  4.25
SCPER     1.5
SCPER     2.50.0888
SCPER     3.50.66120.0724
SCPER     4.50.09540.06580.0033
SCPER     5.5      0.00660.0033
SCPER     6.5          0.0033
FTLOAD   4      0.034          SPC
SCATD D          JS
SCWAV          0.25  0.75  1.25  1.75  2.25  2.75  3.25  3.75  4.25
SCPER     1.50.0033
SCPER     2.50.0861
SCPER     3.50.64240.0563
SCPER     4.50.10260.0728
SCPER     5.5      0.01990.0132
SCPER     6.5
SCPER     7.5          0.0033
FTLOAD   5      0.140          SPC
SCATD D          JS
    
```

```

SCWAV      0.25  0.75  1.25  1.75  2.25  2.75  3.25  3.75  4.25
SCPER      1.50.0024
SCPER      2.50.06260.0008
SCPER      3.50.36340.0870
SCPER      4.50.11220.17320.02030.0008
SCPER      5.50.00240.03900.05200.01140.0008
SCPER      6.50.00080.00650.00980.02030.00410.0024
SCPER      7.5          0.00240.00330.00240.00410.00330.0016
SCPER      8.5          0.00160.0016          0.00330.0008
SCPER      9.5          0.00080.00160.0008
FTLOAD     6    0.050          SPC
SCATD D          JS
SCWAV      0.25  0.75  1.25  1.75  2.25  2.75  3.25  3.75  4.25
SCPER      1.50.0069
SCPER      2.50.1304
SCPER      3.50.51030.0755
SCPER      4.50.08470.11210.0229
SCPER      5.5          0.02290.01140.0023
SCPER      6.50.00460.00460.00460.00230.0023
SCPER      7.5          0.0023
FTLOAD     7    0.031          SPC
SCATD D          JS
SCWAV      0.25  0.75  1.25  1.75  2.25  2.75  3.25  3.75  4.25
SCPER      1.5
SCPER      2.50.1606
SCPER      3.50.59850.0620
SCPER      4.50.09120.05110.0146
SCPER      5.5          0.00360.0073
SCPER      6.5          0.0073
SCPER      7.5          0.0036
FTLOAD     8    0.088          SPC
SCATD D          JS
SCWAV      0.25  0.75  1.25  1.75  2.25  2.75  3.25  3.75  4.25
SCPER      1.50.0069
SCPER      2.50.1304
SCPER      3.50.51030.0755
SCPER      4.50.08470.11210.0229
SCPER      5.5          0.02290.01140.0023
SCPER      6.50.00460.00460.00460.00230.0023
SCPER      7.5          0.0023
END
    
```

## A.3 Wave response

```

WROPT  MNPSL  ALL  ES      0.100    0.100   10  -1
PSEL                      BS                      27.9421.590.254 1
PLTTF                      BS                      FQ
TFLCAS   1  38
DAMP      2.0
END

LDOPT      NF+Z   1.03   7.85  -41.60  42.72GLOBMN DYN      NP      K
      SEASTATE FILE FOR WAVE RESPONSE
      FILE S
      CDM
      CDM      1.00 0.821      2.736      0.957      2.736
      CDM  200.00 0.821      2.736      0.957      2.736
      MGROV
      MGROV      0.000 39.100   1.250 -41.600      1.400
      MGROV      39.100 44.600   2.500      1.400
      MGROV      44.600 80.000   0.000
      GRPOV
      GRPOV      B0A                      1.121.122.912.91
      GRPOV      B0B                      1.121.122.142.14
      GRPOV      B0C                      1.161.162.952.95
      GRPOV      B1A                      1.121.122.932.93
      GRPOV      B1D                      1.121.122.932.93
      GRPOV      B1B                      1.181.182.972.97
      GRPOV      B1C                      1.181.182.972.97
      GRPOV      B2A                      1.111.112.902.90
      GRPOV      B2B                      1.141.142.912.91
      GRPOV      B2C                      1.071.072.892.89
      GRPOV      RAA                      1.201.202.972.97
      GRPOV      RBA                      1.201.202.972.97
      GRPOV      RAB                      1.101.102.912.91
      GRPOV      RAM                      1.101.102.912.91
      GRPOV      RAL                      1.101.102.912.91
      GRPOV      RAC                      1.101.102.912.91
      GRPOV      RBB                      1.101.102.912.91
      GRPOV      RBL                      1.101.102.912.91
      GRPOV      RBM                      1.101.102.912.91
      GRPOV      RBC                      1.101.102.912.91
      GRPOV      RAD                      1.121.122.932.93
      GRPOV      RAE                      1.121.122.932.93
      GRPOV      RBD                      1.121.122.932.93
      GRPOV      RBE                      1.121.122.932.93
      GRPOV      RAJ                      1.151.152.962.96
      GRPOV      RAH                      1.151.152.962.96
      GRPOV      RBH                      1.151.152.962.96
      GRPOV      RBJ                      1.151.152.962.96
      GRPOV      R1E                      1.121.122.912.91
      GRPOV      R1F                      1.121.122.912.91
      GRPOV      R1C                      1.121.122.912.91
    
```

GRPOV	R1D	1.121.122.912.91
GRPOV	R2E	1.121.122.912.91
GRPOV	R2F	1.121.122.912.91
GRPOV	R2C	1.121.122.912.91
GRPOV	R2D	1.121.122.912.91
GRPOV	R1A	1.141.142.962.96
GRPOV	R1B	1.141.142.962.96
GRPOV	R2A	1.141.142.962.96
GRPOV	R2B	1.141.142.962.96
GRPOV	LG2	1.081.082.872.87
GRPOV	LG2	1.081.082.872.87
GRPOV	LG2	1.081.082.872.87
GRPOV	LG3	1.081.082.872.87
GRPOV	LG3	1.081.082.872.87
GRPOV	LG3	1.081.082.872.87
GRPOV	LG4	1.051.052.862.86
GRPOV	LG4	1.051.052.862.86
GRPOV	LG4	1.051.052.862.86
GRPOV	L42	1.081.082.872.87
GRPOV	L42	1.081.082.872.87
GRPOV	BLH	2.742.743.943.94
GRPOV	BLI	2.162.163.583.58
GRPOV	BLJ	2.012.013.553.55
MEMOV		
MEMOV	10301031	1.501.503.023.02
MEMOV	10311032	1.501.503.023.02
MEMOV	10321033	1.501.503.023.02
MEMOV	10331034	1.501.503.023.02
MEMOV	10341024	1.501.503.023.02
MEMOV	10211022	1.841.843.583.58
MEMOV	10181021	1.841.843.583.58
MEMOV	10231024	1.841.843.583.58
MEMOV	10241016	1.841.843.583.58
LOAD		
LOADCN		
GNTRF	BS 10 0.0625 10.0 0.50	0.00 20AIRCPF
GNTRF	BS 4 0.0625 5.0 0.25	0.00 20AIRCPF
GNTRF	BS 20 0.0625 4.0 0.05	0.00 20AIRCPF
GNTRF	BS 21 0.0625 3.0 0.10	0.00 20AIRCPF
END		



## A.4 Transfer function

LDOPT            NF+Z    1.03    7.85   -41.60   42.72GLOBMN DYN            NP    K

SEA STATE FILE FOR TRANSFER FUNCTION GENERATION ALONG 0,45 AND 90 DEG.,  
 FOR 1:25 WAVE STEEPNESS

FILE S

CDM

CDM	1.00	0.600	2.000	0.700	2.000
CDM	200.00	0.600	2.000	0.700	2.000

MGROV

MGROV	0.000	39.100	1.250	-41.600	1.400
MGROV	39.100	44.600	2.500		1.400
MGROV	44.600	80.000	0.000		

GRPOV

GRPOV	B0A	0.820.822.072.07
GRPOV	B0B	0.920.922.142.14
GRPOV	B0C	0.860.862.102.10
GRPOV	B1A	0.830.832.082.08
GRPOV	B1D	0.830.832.082.08
GRPOV	B1B	0.890.892.122.12
GRPOV	B1C	0.890.892.122.12
GRPOV	B2A	0.810.812.062.06
GRPOV	B2B	0.840.842.072.07
GRPOV	B2C	0.770.772.042.04
GRPOV	RAA	0.900.902.132.13
GRPOV	RBA	0.900.902.132.13
GRPOV	RAB	0.800.802.062.06
GRPOV	RAM	0.800.802.062.06
GRPOV	RAL	0.800.802.062.06
GRPOV	RAC	0.800.802.062.06
GRPOV	RBB	0.800.802.062.06
GRPOV	RBL	0.800.802.062.06
GRPOV	RBM	0.800.802.062.06
GRPOV	RBC	0.800.802.062.06
GRPOV	RAD	0.830.832.082.08
GRPOV	RAE	0.830.832.082.08
GRPOV	RBD	0.830.832.082.08
GRPOV	RBE	0.830.832.082.08
GRPOV	RAJ	0.850.852.122.12
GRPOV	RAH	0.850.852.122.12
GRPOV	RBH	0.850.852.122.12
GRPOV	RBJ	0.850.852.122.12
GRPOV	R1E	0.820.822.072.07
GRPOV	R1F	0.820.822.072.07
GRPOV	R1C	0.820.822.072.07
GRPOV	R1D	0.820.822.072.07
GRPOV	R2E	0.820.822.072.07
GRPOV	R2F	0.820.822.072.07
GRPOV	R2C	0.820.822.072.07
GRPOV	R2D	0.820.822.072.07
GRPOV	R1A	0.840.842.122.12

GRPOV	R1B				0.840.842.122.12
GRPOV	R2A				0.840.842.122.12
GRPOV	R2B				0.840.842.122.12
GRPOV	LG2				0.780.782.022.02
GRPOV	LG2				0.780.782.022.02
GRPOV	LG2				0.780.782.022.02
GRPOV	LG3				0.780.782.022.02
GRPOV	LG4				0.750.752.012.01
GRPOV	LG4				0.750.752.012.01
GRPOV	LG4				0.750.752.012.01
GRPOV	L42				0.780.782.022.02
GRPOV	L42				0.780.782.022.02
GRPOV	BLH				2.442.443.093.09
GRPOV	BLI				1.871.872.732.73
GRPOV	BLJ				1.611.612.672.67
MEMOV					
MEMOV	10301031				1.151.152.172.17
MEMOV	10311032				1.151.152.172.17
MEMOV	10321033				1.151.152.172.17
MEMOV	10331034				1.151.152.172.17
MEMOV	10341024				1.151.152.172.17
MEMOV	10211022				1.551.552.742.74
MEMOV	10181021				1.551.552.742.74
MEMOV	10231024				1.551.552.742.74
MEMOV	10241016				1.551.552.742.74
LOAD					
LOADCN					
GNTRF	BS 10	0.040	10.00	0.500	0.00 20AIRCPF
GNTRF	BS 10	0.040	5.000	0.250	0.00 20AIRCPF
GNTRF	BS 16	0.040	2.500	0.100	0.00 20AIRCPF
LOADCN					
GNTRF	BS 10	0.040	10.00	0.500	45.00 20AIRCPF
GNTRF	BS 10	0.040	5.000	0.250	45.00 20AIRCPF
GNTRF	BS 16	0.040	2.500	0.100	45.00 20AIRCPF
LOADCN					
GNTRF	BS 10	0.040	10.00	0.500	90.00 20AIRCPF
GNTRF	BS 10	0.040	5.000	0.250	90.00 20AIRCPF
GNTRF	BS 16	0.040	2.500	0.100	90.00 20AIRCPF
END					

## A.5 Response function

LDOPT	NF+Z	1.030	7.85	0.00	0.00	GLOBMN	DYN	NP	K
RESPONSE FUNCTION (RMS) DETERMINATION									
OPTIONS	MN	DY	SDUC	3	3		PT		
SECT									
*									
GRUP									
GRUP B0A	61.000	1.905	20.50	8.0034.50	1	.800.800		0.50N0.0001	
GRUP B0A	61.000	2.540	20.50	8.0034.50	1	.800.800		0.50N0.00011.25	
GRUP B0B	61.000	1.905	20.50	8.0034.50	1	.800.800		0.50N0.0001	
GRUP B0B	61.000	2.540	20.50	8.0034.50	1	.800.800		0.50N0.00011.06	
GRUP B0C	61.000	1.270	20.50	8.0035.50	1	.800.800		0.50N0.0001	
GRUP B0D	61.000	2.540	20.50	8.0034.50	1	.800.800		0.50N0.0001	
GRUP B1A	61.000	1.270	20.50	8.0035.50	1	.800.800		0.50N0.0001	
GRUP B1A	61.000	2.060	20.50	8.0034.50	1	.800.800		0.50N0.00011.25	
GRUP B1B	101.60	4.500	20.50	8.0035.50	1	.800.800		0.50N0.00011.75	
GRUP B1B CONB0B			20.50	8.0035.50	1	.800.800		0.50N0.00010.81	
GRUP B1B	61.000	1.270	20.50	8.0035.50	1	.800.800		0.50N0.0001	
GRUP B1C	50.800	1.270	20.50	8.0035.50	1	.800.800		0.50N0.0001	
GRUP B1D	61.000	1.270	20.50	8.0035.50	1	.800.800		0.50N0.0001	
GRUP B2A	81.300	2.000	20.50	8.0034.50	1	.800.800		0.50N0.0001	
GRUP B2A	81.300	2.540	20.50	8.0034.50	1	.800.800		0.50N0.00011.25	
GRUP B2B	81.300	2.200	20.50	8.0034.50	1	.800.800		0.50N0.0001	
GRUP B2B	81.300	2.540	20.50	8.0034.50	1	.800.800		0.50N0.00011.75	
GRUP B2C	66.000	1.750	20.50	8.0034.50	1	.800.800		0.50N0.0001	
GRUP B2D	81.300	2.000	20.50	8.0034.50	1	.800.800		0.50N0.0001	
GRUP B3A	50.800	1.270	20.50	8.0035.50	1	.800.800		0.50N0.0001	
GRUP BLA	66.000	2.540	20.50	8.0034.50	1	1.001.00		0.50N0.0001	
GRUP BLB	86.400	2.540	20.50	8.0034.50	1	1.001.00		0.50N0.0001	
GRUP BLC	66.000	2.540	20.50	8.0034.50	1	1.001.00		0.50N0.0001	
GRUP BLD	86.400	2.540	20.50	8.0034.50	1	1.001.00		0.50N0.0001	
GRUP BLE	86.400	3.000	20.50	8.0034.50	1	1.001.00		0.50N0.0001	
GRUP BLF	86.400	2.540	20.50	8.0034.50	1	1.001.00		0.50N0.0001	
GRUP BLG	86.400	2.540	20.50	8.0034.50	1	1.001.00		0.50N0.0001	
GRUP BLH	45.720	1.905	20.50	8.0034.50	1	1.001.00		0.50N0.0001	
GRUP BLI	45.720	1.905	20.50	8.0034.50	1	1.001.00		0.50N0.0001	
GRUP BLJ	45.720	1.905	20.50	8.0034.50	1	1.001.00		0.50N0.0001	
GRUP CS1	50.800	1.270	20.50	8.0035.50	1	1.001.00		0.50N0.0001	
GRUP CSA	90.000	2.540	20.50	8.0034.50	1	1.001.00		0.50F0.0001	
GRUP CSB	90.000	2.540	20.50	8.0034.50	1	1.001.00		0.50F0.0001	
GRUP CSC	90.000	2.540	20.50	8.0034.50	1	1.001.00		0.50F0.0001	
GRUP CSZ	90.000	2.540	20.50	8.0024.80	1	1.001.00		0.50N0.0001	
GRUP DB1	50.800	1.270	20.50	8.0035.50	1	1.001.00		0.50N0.0001	
GRUP DB2	61.000	2.540	20.50	8.0034.50	1	1.001.00		0.50N0.0001	
GRUP DB3	81.300	2.500	20.50	8.0034.50	1	1.001.00		0.50N0.0001	
GRUP DB4	81.300	2.000	20.50	8.0034.50	1	1.001.00		0.50N0.0001	

GRUP DB5	40.600	1.900	20.50	8.0034.50	1	1.001.00	0.50N0.0001
GRUP DB6	35.600	1.270	20.50	8.0027.50	1	1.001.00	0.50N0.0001
GRUP DB7	27.300	1.270	20.50	8.0027.50	1	1.001.00	0.50N0.0001
GRUP DB8	16.800	0.950	20.50	8.0027.50	1	1.001.00	0.50N0.0001
GRUP DC0 DJPG10			20.50	8.0034.00	1	1.001.00	0.50N0.0001
GRUP DC1 DPG7			20.50	8.0034.50	1	1.001.00	0.50N0.0001
GRUP DC2 DPG5			20.50	8.0034.50	1	1.001.00	0.50N0.0001
GRUP DC3 DPG4			20.50	8.0034.50	1	1.001.00	0.50N0.0001
GRUP DC4 IPE270			20.50	8.0027.50	1	1.001.00	1.00 0.50N0.0001
GRUP DC5 DJPG3			20.50	8.0034.50	1	1.001.00	0.50N0.0001
GRUP DC6 DJPG4			20.50	8.0034.00	1	1.001.00	0.50N0.0001
GRUP DC7 DJPG5			20.50	8.0034.00	1	1.001.00	0.50N0.0001
GRUP DC8 IPE600			20.50	8.0034.50	1	1.001.00	0.50N0.0001
GRUP DC9 DPG1			20.50	8.0034.00	1	1.001.00	0.50N0.0001
GRUP DCE HEB600			20.50	8.0034.50	1	1.001.00	0.50N0.0001
GRUP DCQ DEQ			20.50	8.0024.80	1	1.001.00	0.50N0.0001
GRUP DCW HEB600			20.50	8.0034.50	1	1.001.00	0.50N0.0001
GRUP DF1	45.720	1.270	20.50	8.0034.50	1	1.001.00	0.50N0.0001
GRUP DF2	40.640	1.270	20.50	8.0034.50	1	1.001.00	0.50N0.0001
GRUP DF3	27.300	0.927	20.50	8.0027.50	1	1.001.00	0.50N0.0001
GRUP DF4	21.910	0.953	20.50	8.0027.50	1	1.001.00	0.50N0.0001
GRUP DFB	27.300	1.270	20.50	8.0027.50	1	1.001.00	0.50N0.0001
GRUP DFC UPN220			20.50	8.0024.80	1	1.001.00	0.50N0.0001
GRUP DFG IPE220			20.50	8.0035.50	1	2.001.00	0.50N0.0001
GRUP DFH UPN220			20.50	8.0027.50	1	1.001.00	0.50N0.0001
GRUP DFK IPE220			20.50	8.0035.50	1	1.001.00	0.50N0.0001
GRUP DFL HEB300			20.50	8.0035.50	1	1.001.00	0.50N0.0001
GRUP DFP	40.600	1.270	20.50	8.0024.80	1	1.001.00	0.50N0.0001
GRUP DL1	137.10	6.500	20.50	8.0034.00	1	1.201.20	1.00 0.50N0.0001
GRUP DL2	152.40	2.500	20.50	8.0034.50	1	1.001.00	0.50N0.0001
GRUP DL3	152.40	2.500	20.50	8.0034.50	1	1.001.00	1.00 0.50N0.0001
GRUP DL4	152.40	2.500	20.50	8.0034.50	1	1.001.00	1.00 0.50N0.0001
GRUP DL5	152.40	2.500	20.50	8.0034.50	1	1.001.00	0.50N0.0001
GRUP DL5	152.40	4.000	20.50	8.0034.50	1	1.001.00	0.50N0.00011.0
GRUP DL6	152.40	4.000	20.50	8.0034.50	1	1.001.00	0.50N0.0001
GRUP DLC DLCON			20.50	8.0034.50	1	1.001.00	0.50N0.0001
GRUP DLG	137.10	6.500	20.50	8.0034.00	1	1.201.20	1.00 0.50N0.0001
GRUP DM0 DJPG0			20.50	8.0034.50	1	1.001.00	0.50N0.0001
GRUP DM1 DPG12			20.50	8.0034.50	1	1.001.00	0.50N0.0001
GRUP DM2 DPG5			20.50	8.0034.50	1	1.001.00	0.50N0.0001
GRUP DM3 DPG10			20.50	8.0034.50	1	1.001.00	0.50N0.0001
GRUP DM4 DPG4			20.50	8.0034.50	1	1.001.00	0.50N0.0001
GRUP DM5 IPE270			20.50	8.0027.50	1	1.001.00	1.00 0.50N0.0001
GRUP DM6 DJPG2			20.50	8.0034.50	1	1.001.00	0.50N0.0001
GRUP DM7 IPE600			20.50	8.0034.50	1	1.001.00	0.50N0.0001

GRUP DM8 HEB600			20.50	8.0034.50	1	1.001.00	0.50N0.0001
GRUP DM9 DPG3			20.50	8.0034.50	1	1.001.00	0.50N0.0001
GRUP DME HEB600			20.50	8.0034.50	1	1.001.00	0.50N0.0001
GRUP DMQ DEQ			20.50	8.0024.80	1	1.001.00	0.50N 0.001
GRUP DS1	32.380	1.270	20.50	8.0027.50	1	1.001.00	0.50N0.0001
GRUP DS2 HEB300			20.50	8.0034.50	1	1.001.00	0.50N0.0001
GRUP DS3	27.300	1.270	20.50	8.0027.50	1	1.001.00	0.50N0.0001
GRUP DS4	16.800	1.097	20.50	8.0027.50	1	1.001.00	0.50N0.0001
GRUP DV1	121.90	3.000	20.50	8.0034.50	1	1.001.00	0.50N0.0001
GRUP DV2	61.000	3.000	20.50	8.0034.50	1	1.001.00	0.50N0.0001
GRUP DV3	50.800	1.430	20.50	8.0035.50	1	1.001.00	0.50N0.0001
GRUP DV4	50.800	1.270	20.50	8.0035.50	1	1.001.00	0.50N0.0001
GRUP DW0 DPG7			20.50	8.0034.50	1	1.001.00	0.50N0.0001
GRUP DW1 DPG12			20.50	8.0034.50	1	1.001.00	0.50N0.0001
GRUP DW2 DPG5			20.50	8.0034.50	1	1.001.00	0.50N0.0001
GRUP DW3 DPG9			20.50	8.0034.50	1	1.001.00	0.50N0.0001
GRUP DW4 IPE270			20.50	8.0027.50	1	1.001.00	1.00 0.50N0.0001
GRUP DW6 DJPG6			20.50	8.0034.50	1	1.001.00	0.50N0.0001
GRUP DW7 DJPG7			20.50	8.0034.50	1	1.001.00	0.50N0.0001
GRUP DW8 IPE600			20.50	8.0034.50	1	1.001.00	0.50N0.0001
GRUP DW9 DJPG8			20.50	8.0034.50	1	1.001.00	0.50N0.0001
GRUP DWB HEB300			20.50	8.0024.80	1	1.001.00	0.50N 0.001
GRUP DWC HEB300			20.50	8.0024.80	1	1.001.00	0.50N 0.001
GRUP DWD IPE270			20.50	8.0027.50	1	1.001.00	0.50N 0.010
GRUP DWN DPG2			20.50	8.0034.50	1	1.001.00	0.50N0.0001
GRUP DWS DJPG11			20.50	8.0034.50	1	1.001.00	0.50N0.0001
GRUP DWT	27.300	1.270	20.50	8.0024.80	1	1.001.00	0.50N 0.001
GRUP DWW HEB600			20.50	8.0034.50	1	1.001.00	0.50N0.0001
GRUP DZ0 DJPG9			20.50	8.0034.50	1	1.001.00	0.50N0.0001
GRUP DZ1 DPG7			20.50	8.0034.50	1	1.001.00	0.50N0.0001
GRUP DZ2 DPG5			20.50	8.0034.50	1	1.001.00	0.50N0.0001
GRUP DZ3 DPG4			20.50	8.0034.50	1	1.001.00	0.50N0.0001
GRUP DZ4 DPG13			20.50	8.0034.00	1	1.001.00	0.50N0.0001
GRUP DZ5 DPG9			20.50	8.0034.50	1	1.001.00	0.50N0.0001
GRUP DZ6 IPE270			20.50	8.0027.50	1	1.001.00	1.00 0.50N0.0001
GRUP DZ7 DJPG1			20.50	8.0034.50	1	1.001.00	0.50N0.0001
GRUP DZ8 IPE600			20.50	8.0034.50	1	1.001.00	0.50N0.0001
GRUP DZ9 HEB300			20.50	8.0027.50	1	1.001.00	0.50N0.0001
GRUP DZB HEB300			20.50	8.0035.50	1	1.001.00	0.50N0.0001
GRUP DZC DPB			20.50	8.0034.50	1	1.001.00	0.50N0.0001
GRUP DZE HEB600			20.50	8.0034.50	1	1.001.00	0.50N0.0001
GRUP DZQ DEQ			20.50	8.0024.80	1	1.001.00	0.50N 0.001
GRUP DZW HEB600			20.50	8.0034.50	1	1.001.00	0.50N0.0001
GRUP L31 CON7			20.50	8.0034.50	1	1.001.00	0.50F0.0001
GRUP L32 CON2			20.50	8.0034.00	1	1.001.00	0.50F0.0001

GRUP L33 CON4			20.50	8.0034.00	1	1.001.00	0.50F0.0001
GRUP L34 CON2			20.50	8.0034.00	1	1.001.00	0.50F0.0001
GRUP L35 CON2			20.50	8.0034.00	1	1.001.00	0.50F0.0001
GRUP L41 CON4			20.50	8.0034.00	1	1.001.00	0.50F0.0001
GRUP L42 CON3			20.50	8.0034.50	1	1.001.00	0.50F0.0001
GRUP L42 CON5			20.50	8.0034.50	1	1.001.00	0.50F0.00012.02
GRUP L43 CON5			20.50	8.0034.50	1	1.001.00	0.50F0.0001
GRUP L43 CON6			20.50	8.0034.00	1	1.001.00	0.50F0.00012.0
GRUP L44 CON4			20.50	8.0034.00	1	1.001.00	0.50F0.0001
GRUP L45 CON2			20.50	8.0034.00	1	1.001.00	0.50F0.0001
GRUP LG2 CON2			20.50	8.0034.00	1	1.001.00	0.50F0.00013.0
GRUP LG2 CON3			20.50	8.0034.50	1	1.001.00	0.50F0.0001
GRUP LG2 CON2			20.50	8.0034.00	1	1.001.00	0.50F0.00011.35
GRUP LG3 CON7			20.50	8.0034.50	1	1.001.00	0.50F0.0001
GRUP LG4 CON3			20.50	8.0034.50	1	1.001.00	0.50F0.0001
GRUP LG4 CON5			20.50	8.0034.50	1	1.001.00	0.50F0.00014.06
GRUP LG4 CON6			20.50	8.0034.00	1	1.001.00	0.50F0.00012.00
GRUP LG5 CON2			20.50	8.0034.00	1	1.001.00	0.50F0.0001
GRUP LG6	137.20	5.000	20.50	8.0034.50	1	1.001.00	0.50F0.0001
GRUP PL1 CON1			20.50	8.0034.00	1	1.001.00	0.50F0.0001
GRUP R1A	45.700	1.270	20.50	8.0035.50	1	.800.800	0.50N0.0001
GRUP R1B	45.700	1.270	20.50	8.0035.50	1	.800.800	0.50N0.0001
GRUP R1C	71.100	1.900	20.50	8.0034.50	1	.800.800	0.50N0.0001
GRUP R1D	71.100	1.900	20.50	8.0034.50	1	.800.800	0.50N0.0001
GRUP R1E	71.100	1.430	20.50	8.0035.50	1	.800.800	0.50N0.0001
GRUP R1F	71.100	1.430	20.50	8.0035.50	1	.800.800	0.50N0.0001
GRUP R2A	45.700	1.270	20.50	8.0035.50	1	.800.800	0.50N0.0001
GRUP R2B	45.700	1.270	20.50	8.0035.50	1	.800.800	0.50N0.0001
GRUP R2C	71.100	1.900	20.50	8.0034.50	1	.800.800	0.50N0.0001
GRUP R2D	71.100	1.900	20.50	8.0034.50	1	.800.800	0.50N0.0001
GRUP R2E	71.100	1.430	20.50	8.0035.50	1	.800.800	0.50N0.0001
GRUP R2F	71.100	1.430	20.50	8.0035.50	1	.800.800	0.50N0.0001
GRUP RAA	61.000	1.590	20.50	8.0035.50	1	.800.800	0.50N0.0001
GRUP RAB	66.000	1.430	20.50	8.0035.50	1	.900.900	0.50N0.0001
GRUP RAB	66.000	2.060	20.50	8.0034.50	1	.900.900	0.50N0.00011.0
GRUP RAC	66.000	1.430	20.50	8.0035.50	1	.900.900	0.50N0.0001
GRUP RAD	61.000	1.270	20.50	8.0035.50	1	.900.900	0.50N0.0001
GRUP RAD	61.000	2.060	20.50	8.0034.50	1	.900.900	0.50N0.00011.0
GRUP RAE	61.000	1.270	20.50	8.0035.50	1	.900.900	0.50N0.0001
GRUP RAF	50.800	1.905	20.50	8.0034.50	1	.900.900	0.50N0.0001
GRUP RAG	49.600	1.305	20.50	8.0035.50	1	.900.900	0.50N0.0001
GRUP RAH	50.800	1.905	20.50	8.0034.50	1	.900.900	0.50N0.0001
GRUP RAJ	50.800	1.905	20.50	8.0034.50	1	.900.900	0.50N0.0001
GRUP RAJ	50.800	2.540	20.50	8.0034.50	1	.900.900	0.50N0.00010.75
GRUP RAK	50.800	1.905	20.50	8.0034.50	1	.900.900	0.50N0.0001



GRUP RAK	50.800	2.540	20.50	8.0034.50	1	.900.900	0.50N0.00010.75
GRUP RAL	66.000	1.270	20.50	8.0035.50	1	.900.900	0.50N0.0001
GRUP RAL	66.000	2.062	20.50	8.0035.50	1	.900.900	0.50N0.00011.0
GRUP RAM	66.000	1.270	20.50	8.0035.50	1	.900.900	0.50N0.0001
GRUP RBA	61.000	1.590	20.50	8.0035.50	1	.800.800	0.50N0.0001
GRUP RBB	66.000	1.430	20.50	8.0035.50	1	.900.900	0.50N0.0001
GRUP RBB	66.000	2.060	20.50	8.0034.50	1	.900.900	0.50N0.00011.0
GRUP RBC	66.000	1.430	20.50	8.0035.50	1	.900.900	0.50N0.0001
GRUP RBD	61.000	1.270	20.50	8.0035.50	1	.900.900	0.50N0.0001
GRUP RBD	61.000	2.060	20.50	8.0034.50	1	.900.900	0.50N0.00011.0
GRUP RBE	61.000	1.270	20.50	8.0035.50	1	.900.900	0.50N0.0001
GRUP RBF	49.600	1.305	20.50	8.0034.50	1	.900.900	0.50N0.0001
GRUP RBG	50.800	1.905	20.50	8.0034.50	1	.900.900	0.50N0.0001
GRUP RBH	50.800	1.905	20.50	8.0034.50	1	.900.900	0.50N0.0001
GRUP RBH	50.800	2.540	20.50	8.0034.50	1	.900.900	0.50N0.00010.75
GRUP RBJ	50.800	1.905	20.50	8.0034.50	1	.900.900	0.50N0.0001
GRUP RBK	50.800	1.905	20.50	8.0034.50	1	.900.900	0.50N0.0001
GRUP RBK	50.800	2.540	20.50	8.0034.50	1	.900.900	0.50N0.00010.75
GRUP RBL	66.000	1.270	20.50	8.0035.50	1	.900.900	0.50N0.0001
GRUP RBM	66.000	1.270	20.50	8.0035.50	1	.900.900	0.50N0.0001
GRUP RBM	66.000	2.062	20.50	8.0034.50	1	.900.900	0.50N0.00011.0
GRUP RIA	58.500	2.540	20.50	8.0035.50	1	1.001.00	0.50F 0.001
GRUP RS1	25.400	1.270	20.50	8.0035.50	1	1.001.00	0.50N0.0001
GRUP SEA	27.300	1.270	20.50	8.0034.00	1	1.001.00	0.50N0.0001
GRUP SEB	50.000	1.270	20.50	8.0024.80	1	1.001.00	0.50N0.0001
GRUP SEC	50.000	1.270	20.50	8.0024.80	1	1.001.00	0.50N0.0001
GRUP STB PILSTUB			20.50	8.0034.50	9	1.001.00	0.50F0.0001

MEMBER

\*

PGRUP

PGRUP DP0	1.0000	20.000	0.250	24.800			0.001
PGRUP DP1	0.8000	20.000	0.250	27.500			0.001
PGRUP DP2	0.8000	20.000	0.250	27.500			0.001
PGRUP DP3	0.8000	20.000	0.250	27.500			0.001
PGRUP DP4	0.8000	20.000	0.250	27.500			0.001

PLATE

\*

JOINT

\*

CDM

CDM	1.00	0.853	0.001	0.995	0.001		
CDM	200.00	0.853	0.001	0.995	0.001		

MGROV

\*

GRPOV

\*

MEMOV

MEMOV	10301031	1.501.503.023.02
MEMOV	10311032	1.501.503.023.02
MEMOV	10321033	1.501.503.023.02
MEMOV	10331034	1.501.503.023.02
MEMOV	10341024	1.501.503.023.02
MEMOV	10211022	1.841.843.583.58
MEMOV	10181021	1.841.843.583.58
MEMOV	10231024	1.841.843.583.58
MEMOV	10241016	1.841.843.583.58

\*

LOAD

END

WROPT	MNPSL	MAXS	10	-1
PLTTF		BSB		PF
DAMP	100.			
WSPEC	JS	0.737	3.750	1 36
WSPEC	JS	1.311	5.000	37 72
WSPEC	JS	1.311	5.000	73 108
END				

## A.6 Deterministic base shear range

```

LDOPT      NF+Z    1.03    7.85   -41.60   42.72GLOBMN      NP      K
      SEA STATE FOR SINGLE WAVE CORRESPONDING TO CENTER OF FATIGUE
LCSEL ST      SW1  SW2  SW3
FILE S
CDM
CDM      1.00 0.600      2.000      0.700      2.000
CDM     200.00 0.600      2.000      0.700      2.000
MGROV
MGROV      0.000 39.100  1.250 -41.600      1.400
MGROV     39.100 44.600  2.500      1.400
MGROV     44.600 80.000  0.000
GRPOV
GRPOV      B0A      0.820.822.072.07
GRPOV      B0B      0.920.922.142.14
GRPOV      B0C      0.860.862.102.10
GRPOV      B1A      0.830.832.082.08
GRPOV      B1D      0.830.832.082.08
GRPOV      B1B      0.890.892.122.12
GRPOV      B1C      0.890.892.122.12
GRPOV      B2A      0.810.812.062.06
GRPOV      B2B      0.840.842.072.07
GRPOV      B2C      0.770.772.042.04
GRPOV      RAA      0.900.902.132.13
GRPOV      RBA      0.900.902.132.13
GRPOV      RAB      0.800.802.062.06
GRPOV      RAM      0.800.802.062.06
GRPOV      RAL      0.800.802.062.06
GRPOV      RAC      0.800.802.062.06
GRPOV      RBB      0.800.802.062.06
GRPOV      RBL      0.800.802.062.06
GRPOV      RBM      0.800.802.062.06
GRPOV      RBC      0.800.802.062.06
GRPOV      RAD      0.830.832.082.08
GRPOV      RAE      0.830.832.082.08
GRPOV      RBD      0.830.832.082.08
GRPOV      RBE      0.830.832.082.08
GRPOV      RAJ      0.850.852.122.12
GRPOV      RAH      0.850.852.122.12
GRPOV      RBH      0.850.852.122.12
GRPOV      RBJ      0.850.852.122.12
GRPOV      R1E      0.820.822.072.07
GRPOV      R1F      0.820.822.072.07
GRPOV      R1C      0.820.822.072.07
GRPOV      R1D      0.820.822.072.07
GRPOV      R2E      0.820.822.072.07
GRPOV      R2F      0.820.822.072.07
GRPOV      R2C      0.820.822.072.07
GRPOV      R2D      0.820.822.072.07
GRPOV      R1A      0.840.842.122.12
    
```

```

GRPOV      R1B      0.840.842.122.12
GRPOV      R2A      0.840.842.122.12
GRPOV      R2B      0.840.842.122.12
GRPOV      LG2      0.780.782.022.02
GRPOV      LG2      0.780.782.022.02
GRPOV      LG2      0.780.782.022.02
GRPOV      LG3      0.780.782.022.02
GRPOV      LG3      0.780.782.022.02
GRPOV      LG3      0.780.782.022.02
GRPOV      LG4      0.750.752.012.01
GRPOV      LG4      0.750.752.012.01
GRPOV      LG4      0.750.752.012.01
GRPOV      L42      0.780.782.022.02
GRPOV      L42      0.780.782.022.02
GRPOV      BLH      2.442.443.093.09
GRPOV      BLI      1.871.872.732.73
GRPOV      BLJ      1.611.612.672.67
MEMOV
MEMOV 10301031      1.151.152.172.17
MEMOV 10311032      1.151.152.172.17
MEMOV 10321033      1.151.152.172.17
MEMOV 10331034      1.151.152.172.17
MEMOV 10341024      1.151.152.172.17
MEMOV 10211022      1.551.552.742.74
MEMOV 10181021      1.551.552.742.74
MEMOV 10231024      1.551.552.742.74
MEMOV 10241016      1.551.552.742.74
DUMMY RISER
KEEP      101 201 301 501
DELETE 1101 1102 1103 1104
LOAD
LOADCN SW1
WAVE
WAVE 1.0AIRC 1.371      3.750      0.000      D      10. 36MS10 1 0
LOADCN SW2
WAVE
WAVE 1.0AIRC 2.438      5.000      45.000      D      10. 36MS10 1 0
LOADCN SW3
WAVE
WAVE 1.0AIRC 2.438      5.000      90.000      D      10. 36MS10 1 0
END
    
```

## A.7 Pile-stub generation

```

LDOPT      NF+Z   1.030   7.85  -41.60  42.720GLOBMN      NP      K
      INPLACCE ANALYSIS FOR PILESTUB GENERATION
OPTIONS      MN  PI  SDUC   3 3      PT
LCSEL ST      CSW1 CSW2 CSW3
UCPART      0.00 0.80 0.80 1.00 1.001000.
SECT
*
GRUP
*
MEMBER
*
PGRUP
*
PLATE
*
JOINT
*
CDM
CDM      1.00 0.600      2.000      0.700      2.000
CDM 200.00 0.600      2.000      0.700      2.000
MGROV
*
GRPOV
*
MEMOV
*
LOAD
*
LOADCN SW1
WAVE
WAVE 1.0AIRC 1.371      3.750      0.000      D      10. 36MS10 1 0
LOADCN SW2
WAVE
WAVE 1.0AIRC 2.438      5.000      45.000      D      10. 36MS10 1 0
LOADCN SW3
WAVE
WAVE 1.0AIRC 2.438      5.000      90.000      D      10. 36MS10 1 0
LCOB
*
LCOB CSW1 C005 1.000 SW1 1.000
LCOB CSW2 C005 1.000 SW2 1.000
LCOB CSW3 C005 1.000 SW3 1.000
*
END

PSIOPT +ZMN      SM0.00254 0.0001 200      PT      100      7.849047
PLTRQ SD      DL      AL      UC
PLGRUP
PLGRUP PL1      137.16 5.00 20. 8. 34.0 67.5      1.0 1.477
    
```

```

PILE
PILE      2 101 PL1                                SOL1 SOL1
PILE     20 119 PL1                                SOL1 SOL1
PILE     82 181 PL1                                SOL1 SOL1
PILE    100 199 PL1                                SOL1 SOL1

SOIL
SOIL
SOIL TZAXIAL HEAD 22                                0.1SOL1
SOIL      SLOCSM  7  0.00          0.0209          CLAY
SOIL      T-Z  0.000  0.00  .002  2.4  .003  4.7  0.005  8.7  0.006  12.2
SOIL      T-Z  0.006  15.2  0.004  30.5
SOIL      SLOCSM  7  1.00          0.0209          CLAY
SOIL      T-Z  0.000  0.00  .006  2.4  .011  4.7  0.016  8.7  0.019  12.2
SOIL      T-Z  0.021  15.2  0.015  30.5
SOIL      SLOCSM  7  1.01          0.0209          CLAY
SOIL      T-Z  0.000  0.00  .026  2.4  .043  4.7  0.064  8.7  0.077  12.2
SOIL      T-Z  0.085  15.2  0.060  30.5
SOIL      SLOCSM  7  5.50          0.0209          CLAY
SOIL      T-Z  0.000  0.00  .041  2.4  .069  4.7  0.104  8.7  0.124  12.2
SOIL      T-Z  0.138  15.2  0.097  30.5
SOIL      SLOCSM  7  5.51          0.0209          CLAY
SOIL      T-Z  0.000  0.00  .088  2.4  .147  4.7  0.220  8.7  0.264  12.2
SOIL      T-Z  0.294  15.2  0.206  30.5
SOIL      SLOCSM  7  11.40         0.0209          CLAY
SOIL      T-Z  0.000  0.00  .177  2.4  .295  4.7  0.443  8.7  0.532  12.2
SOIL      T-Z  0.591  15.2  0.413  30.5
SOIL      SLOCSM  7  11.41         0.0209          SAND
SOIL      T-Z  0.000  0.00  .024  .5  .049  1.0  0.073  1.5  0.098  2.0
SOIL      T-Z  0.122  2.5  0.122  5.1
SOIL      SLOCSM  7  20.00         0.0209          SAND
SOIL      T-Z  0.000  0.00  .046  .5  .091  1.0  0.137  1.5  0.182  2.0
SOIL      T-Z  0.228  2.5  0.228  5.1
SOIL      SLOCSM  7  20.01         0.0209          CLAY
SOIL      T-Z  0.000  0.00  .162  2.4  .270  4.7  0.406  8.7  0.487  12.2
SOIL      T-Z  0.541  15.2  0.379  30.5
SOIL      SLOCSM  7  36.00         0.0209          CLAY
SOIL      T-Z  0.000  0.00  .271  2.4  .451  4.7  0.677  8.7  0.812  12.2
SOIL      T-Z  0.903  15.2  0.632  30.5
SOIL      SLOCSM  7  36.01         0.0209          CLAY
SOIL      T-Z  0.000  0.00  .271  2.4  .452  4.7  0.678  8.7  0.814  12.2
SOIL      T-Z  0.904  15.2  0.633  30.5
SOIL      SLOCSM  7  40.10         0.0209          CLAY
SOIL      T-Z  0.000  0.00  .279  2.4  .465  4.7  0.697  8.7  0.837  12.2
SOIL      T-Z  0.930  15.2  0.651  30.5
SOIL      SLOCSM  7  40.11         0.0209          SAND
SOIL      T-Z  0.000  0.00  .091  .5  .182  1.0  0.273  1.5  0.364  2.0
SOIL      T-Z  0.455  2.5  0.455  5.1
SOIL      SLOCSM  7  63.00         0.0209          SAND
SOIL      T-Z  0.000  0.00  .091  .5  .182  1.0  0.273  1.5  0.364  2.0
    
```



SOIL	T-Z	0.455	2.5	0.455	5.1															
SOIL	SLOCSM	7	63.01		0.0209					CLAY										
SOIL	T-Z	0.000	0.00	.385	2.4	.641	4.7	0.962	8.7	1.155	12.2									
SOIL	T-Z	1.283	15.2	0.898	30.5															
SOIL	SLOCSM	7	75.00		0.0209					CLAY										
SOIL	T-Z	0.000	0.00	.421	2.4	.702	4.7	1.053	8.7	1.263	12.2									
SOIL	T-Z	1.403	15.2	0.982	30.5															
SOIL	SLOCSM	7	75.01		0.0209					SAND										
SOIL	T-Z	0.000	0.00	.091	.5	.182	1.0	0.273	1.5	0.364	2.0									
SOIL	T-Z	0.455	2.5	0.455	5.1															
SOIL	SLOCSM	7	81.00		0.0209					SAND										
SOIL	T-Z	0.000	0.00	.091	.5	.182	1.0	0.273	1.5	0.364	2.0									
SOIL	T-Z	0.455	2.5	0.455	5.1															
SOIL	SLOCSM	7	81.01		0.0209					CLAY										
SOIL	T-Z	0.000	0.00	.392	2.4	.654	4.7	0.980	8.7	1.176	12.2									
SOIL	T-Z	1.307	15.2	0.915	30.5															
SOIL	SLOCSM	7	88.00		0.0209					CLAY										
SOIL	T-Z	0.000	0.00	.409	2.4	.682	4.7	1.023	8.7	1.227	12.2									
SOIL	T-Z	1.363	15.2	0.954	30.5															
SOIL	SLOCSM	7	88.01		0.0209					CLAY										
SOIL	T-Z	0.000	0.00	.436	2.4	.726	4.7	1.089	8.7	1.307	12.2									
SOIL	T-Z	1.452	15.2	1.017	30.5															
SOIL	SLOCSM	7	91.00		0.0209					CLAY										
SOIL	T-Z	0.000	0.00	.529	2.4	.882	4.7	1.323	8.7	1.587	12.2									
SOIL	T-Z	1.764	15.2	1.235	30.5															
SOIL BEARING HEAD	20				0.1	SOLL														
SOIL	SLOC	6	55.0		0.0548	SAND														
SOIL	T-Z	0.0	0.0	2.96	3.00	5.93	19.80	8.89	64.00	10.67	111.3									
SOIL	T-Z	11.86	152.4																	
SOIL	SLOC	6	57.0		0.0548	SAND														
SOIL	T-Z	0.0	0.0	2.96	3.00	5.93	19.80	8.89	64.00	10.67	111.3									
SOIL	T-Z	11.86	152.4																	
SOIL	SLOC	6	59.0		0.0548	SAND														
SOIL	T-Z	0.0	0.0	2.85	3.00	5.70	19.80	8.55	64.00	10.26	111.3									
SOIL	T-Z	11.40	152.4																	
SOIL	SLOC	6	61.0		0.0548	SAND														
SOIL	T-Z	0.0	0.0	2.45	3.00	4.90	19.80	7.35	64.00	8.82	111.3									
SOIL	T-Z	9.80	152.4																	
SOIL	SLOC	6	63.0		0.0548	CLAY														
SOIL	T-Z	0.0	0.0	2.05	3.00	4.10	19.80	6.16	64.00	7.39	111.3									
SOIL	T-Z	8.21	152.4																	
SOIL	SLOC	6	65.0		0.0548	CLAY														
SOIL	T-Z	0.0	0.0	2.05	3.00	4.10	19.80	6.16	64.00	7.39	111.3									
SOIL	T-Z	8.21	152.4																	
SOIL	SLOC	6	67.0		0.0548	CLAY														
SOIL	T-Z	0.0	0.0	2.05	3.00	4.10	19.80	6.16	64.00	7.39	111.3									
SOIL	T-Z	8.21	152.4																	
SOIL	SLOC	6	69.0		0.0548	CLAY														
SOIL	T-Z	0.0	0.0	2.05	3.00	4.10	19.80	6.16	64.00	7.39	111.3									

SOIL	T-Z	8.21	152.4								
SOIL	SLOC	6	71.0			0.0548	CLAY				
SOIL	T-Z	0.0	0.0	2.05	3.00	4.10	19.80	6.16	64.00	7.39	111.3
SOIL	T-Z	8.21	152.4								
SOIL	SLOC	6	73.0			0.0548	CLAY				
SOIL	T-Z	0.0	0.0	2.05	3.00	4.10	19.80	6.16	64.00	7.39	111.3
SOIL	T-Z	8.21	152.4								
SOIL	SLOC	6	75.0			0.0548	SAND				
SOIL	T-Z	0.0	0.0	3.31	3.00	6.61	19.80	9.92	64.00	11.90	111.3
SOIL	T-Z	13.23	152.4								
SOIL	SLOC	6	77.0			0.0548	SAND				
SOIL	T-Z	0.0	0.0	3.82	3.00	7.64	19.80	11.45	64.00	13.74	111.3
SOIL	T-Z	15.27	152.4								
SOIL	SLOC	6	79.0			0.0548	SAND				
SOIL	T-Z	0.0	0.0	2.92	3.00	5.84	19.80	8.76	64.00	10.51	111.3
SOIL	T-Z	11.67	152.4								
SOIL	SLOC	6	81.0			0.0548	CLAY				
SOIL	T-Z	0.0	0.0	1.64	3.00	3.28	19.80	4.93	64.00	5.91	111.3
SOIL	T-Z	6.57	152.4								
SOIL	SLOC	6	83.0			0.0548	CLAY				
SOIL	T-Z	0.0	0.0	1.64	3.00	3.28	19.80	4.93	64.00	5.91	111.3
SOIL	T-Z	6.57	152.4								
SOIL	SLOC	6	85.0			0.0548	CLAY				
SOIL	T-Z	0.0	0.0	1.64	3.00	3.28	19.80	4.93	64.00	5.91	111.3
SOIL	T-Z	6.57	152.4								
SOIL	SLOC	6	87.0			0.0548	CLAY				
SOIL	T-Z	0.0	0.0	1.64	3.00	3.28	19.80	4.93	64.00	5.91	111.3
SOIL	T-Z	6.57	152.4								
SOIL	SLOC	6	88.0			0.0548	CLAY				
SOIL	T-Z	0.0	0.0	1.74	3.00	3.49	19.80	5.23	64.00	6.28	111.3
SOIL	T-Z	6.98	152.4								
SOIL	SLOC	6	89.0			0.0548	CLAY				
SOIL	T-Z	0.0	0.0	1.96	3.00	3.92	19.80	5.88	64.00	7.05	111.3
SOIL	T-Z	7.84	152.4								
SOIL	SLOC	6	91.0			0.0548	CLAY				
SOIL	T-Z	0.0	0.0	2.67	3.00	5.34	19.80	8.00	64.00	9.60	111.3
SOIL	T-Z	10.67	152.4								
SOIL	LATERAL HEAD	28	152.4			0.1	SOL1 CYCLIC P-Y DATA				
SOIL	SLOC	SM	5	0.00	10.0		CLAY				
SOIL	P-Y	0.0	0.0	0.007	12.6	0.011	57.1	0.016	171.4	0.000	857.2
SOIL	SLOC	SM	5	1.30	10.0		CLAY				
SOIL	P-Y	0.0	0.0	0.093	8.4	0.155	38.1	0.223	114.3	0.014	571.5
SOIL	SLOC	SM	5	2.00	10.0		CLAY				
SOIL	P-Y	0.0	0.0	0.100	8.4	0.166	38.1	0.239	114.3	0.023	571.5
SOIL	SLOC	SM	5	3.00	10.0		CLAY				
SOIL	P-Y	0.0	0.0	0.110	8.4	0.182	38.1	0.263	114.3	0.037	571.5
SOIL	SLOC	SM	5	4.00	10.0		CLAY				
SOIL	P-Y	0.0	0.0	0.120	8.4	0.199	38.1	0.287	114.3	0.054	571.5
SOIL	SLOC	SM	5	5.00	10.0		CLAY				

SOIL	P-Y	0.0	0.0	0.130	8.4	0.216	38.1	0.311	114.3	0.072	571.5
SOIL	SLOCSM	5	6.20	10.0					CLAY		
SOIL	P-Y	0.0	0.0	0.383	8.4	0.635	38.1	0.915	114.3	0.191	571.5
SOIL	SLOCSM	5	7.50	10.0					CLAY		
SOIL	P-Y	0.0	0.0	0.482	8.4	0.799	38.1	1.152	114.3	0.283	571.5
SOIL	SLOCSM	5	8.50	10.0					CLAY		
SOIL	P-Y	0.0	0.0	0.563	8.4	0.933	38.1	1.346	114.3	0.368	571.5
SOIL	SLOCSM	5	10.00	10.0					CLAY		
SOIL	P-Y	0.0	0.0	0.694	8.4	1.149	38.1	1.657	114.3	0.522	571.5
SOIL	SLOCSM	5	11.00	10.0					CLAY		
SOIL	P-Y	0.0	0.0	0.786	8.4	1.302	38.1	1.878	114.3	0.643	571.5
SOIL	SLOCSM	5	12.50	10.0					SAND		
SOIL	P-Y	0.0	0.0	1.401	3.4	3.048	14.4	3.048	25.4	3.048	57.1
SOIL	SLOCSM	5	15.00	10.0					SAND		
SOIL	P-Y	0.0	0.0	2.025	4.1	3.048	14.7	3.048	25.4	3.048	57.1
SOIL	SLOCSM	5	16.50	10.0					SAND		
SOIL	P-Y	0.0	0.0	2.454	4.5	3.048	15.0	3.048	25.4	3.048	57.1
SOIL	SLOCSM	5	18.00	10.0					SAND		
SOIL	P-Y	0.0	0.0	2.923	4.9	3.048	15.2	3.048	25.4	3.048	57.1
SOIL	SLOCSM	5	20.00	10.0					SAND		
SOIL	P-Y	0.0	0.0	3.048	4.4	3.048	15.4	3.048	25.4	3.048	57.1
SOIL	SLOCSM	5	20.01	10.0					CLAY		
SOIL	P-Y	0.0	0.0	0.798	8.4	1.323	38.1	1.907	114.3	1.253	571.5
SOIL	SLOCSM	5	22.50	10.0					CLAY		
SOIL	P-Y	0.0	0.0	0.928	8.4	1.538	38.1	2.218	114.3	1.620	571.5
SOIL	SLOCSM	5	25.00	10.0					CLAY		
SOIL	P-Y	0.0	0.0	1.068	8.4	1.769	38.1	2.551	114.3	2.048	571.5
SOIL	SLOCSM	5	27.50	10.0					CLAY		
SOIL	P-Y	0.0	0.0	1.215	8.4	2.014	38.1	2.904	114.3	2.541	571.5
SOIL	SLOCSM	5	29.00	10.0					CLAY		
SOIL	P-Y	0.0	0.0	1.308	8.4	2.168	38.1	3.126	114.3	2.870	571.5
SOIL	SLOCSM	5	31.50	10.0					CLAY		
SOIL	P-Y	0.0	0.0	1.470	8.4	2.436	38.1	3.513	114.3	3.475	571.5
SOIL	SLOCSM	5	33.00	10.0					CLAY		
SOIL	P-Y	0.0	0.0	1.539	8.4	2.550	38.1	3.678	114.3	3.678	571.5
SOIL	SLOCSM	5	37.00	10.0					CLAY		
SOIL	P-Y	0.0	0.0	1.656	8.4	2.743	38.1	3.956	114.3	3.956	571.5
SOIL	SLOCSM	5	39.00	10.0					CLAY		
SOIL	P-Y	0.0	0.0	1.656	8.4	2.743	38.1	3.956	114.3	3.956	571.5
SOIL	SLOCSM	5	42.00	10.0					SAND		
SOIL	P-Y	0.0	0.0	8.906	6.3	9.906	12.7	9.906	25.4	9.906	57.1
SOIL	SLOCSM	5	45.00	10.0					SAND		
SOIL	P-Y	0.0	0.0	9.545	6.3	9.906	12.7	9.906	25.4	9.906	57.1
SOIL	SLOCSM	5	50.00	10.0					SAND		
SOIL	P-Y	0.0	0.0	9.906	5.7	9.906	12.7	9.906	25.4	9.906	57.1
END											

PLOPT MN 100 100 0.00254 7.850 PT

PLTRQ SD DL AL UC

```
PLGRUP
PLGRUP PL1          137.16  5.00  20.   8.   34.0   67.5          1.0 1.477
PILE
PILE      2 101 PL1          SOL1 SOL1
SOIL
*
PLSTUB  F  51          212.29   565.00 18339.14   1.66
END
```

```

PLOPT MN      100 100 0.00254      7.850 PT
PLTRQ SD      DL      AL      UC
PLGRUP
PLGRUP PL1      137.16 5.00 20. 8. 34.0 67.5      1.0 1.477
PILE
PILE 2 101 PL1      SOL1 SOL1
SOIL
*
PLSTUB F 51      212.29 565.00 18339.14 1.66
END
    
```

\*\*\*\*\* SACS SAMPLE CARD IMAGES \*\*\*\*\*

```

          1          2          3          4          5          6          7          8
1234567890123456789012345678901234567890123456789012345678901234567890
    
```

```

SECT PILSTUB  PRI620.196503500.6503500.6503500. 10.000 10.000
    
```

```

GRUP STB PILSTUB
    
```

```

MEMBER2 51 2 STBSK
    
```

```

MEMBER OFFSETS      154.0
    
```

```

JOINT 2 0.0 0.0 0.0 0.0 0.0 0.0
    
```

```

JOINT 51      -996.8 111111
    
```

```

          1          2          3          4          5          6          7          8
1234567890123456789012345678901234567890123456789012345678901234567890
    
```

## A.8 Dynamic characteristics

DYNPAC INPUT

DYNOPT +ZMN 10CONS7.84905 1.025 1.0 SA-Z  
 END

LDOPT NF+Z1.0300007.850000 -41.600 42.720GLOBMN DYN CMB NP K

DYNAMIC CHARECTERISTICS OF PLATFORM

OPTIONS MN SDUC 3 3 PT

LCSEL ST C005

SECT

\*

SECT P1LSTUB PRI630.296508500.6508500.6508500. 10.0 10.0

GRUP

\*

GRUP STB P1LSTUB 20.508.00034.50 9 1.001.00 0.500F7.8490

MEMBER

\*

PGRUP

\*

PLATE

\*

JOINT

\*

JOINT 101	-15.073-18.000-41.285	222000
JOINT 103	0.000-18.000-41.285	222000
JOINT 104	0.000 18.000-41.285	222000
JOINT 111	0.000-18.000-32.861	222000
JOINT 112	0.000-18.000-16.566	222000
JOINT 113	0.000-18.000 -1.397	222000
JOINT 114	0.000 18.000-32.861	222000
JOINT 115	-0.001 18.000-16.565	222000
JOINT 116	0.000 18.000 -1.397	222000
JOINT 119	15.073-18.000-41.285	222000
JOINT 181	-15.073 18.000-41.285	222000
JOINT 199	15.073 18.000-41.285	222000
JOINT 201	-13.075-18.000-25.300	222000
JOINT 219	13.075-18.000-25.300	222000
JOINT 281	-13.075 18.000-25.300	222000
JOINT 299	13.075 18.000-25.300	222000
JOINT 301	-11.038-18.000 -9.000	222000
JOINT 319	11.038-18.000 -9.000	222000
JOINT 381	-11.038 18.000 -9.000	222000
JOINT 399	11.038 18.000 -9.000	222000
JOINT 401	-9.288-18.000 5.000	222000
JOINT 419	9.288-18.000 5.000	222000
JOINT 481	-9.288 18.000 5.000	222000
JOINT 499	9.288 18.000 5.000	222000
JOINT 4101	-9.000-18.000 13.300	222000
JOINT 4120	9.000-18.000 13.300	222000
JOINT 4501	-9.000 18.000 13.300	222000

```

JOINT 4510  0.000 18.000 13.300                222000
JOINT 4520  9.000 18.000 13.300                222000
JOINT 5101 -9.000-18.000 19.900                222000
JOINT 5110  0.000-18.000 19.900                222000
JOINT 5120  9.000-18.000 19.900                222000
JOINT 5501 -9.000 18.000 19.900                222000
JOINT 5520  9.000 18.000 19.900                222000
JOINT 6101 -9.000-18.000 27.900                222000
JOINT 6110  0.000-18.000 27.900                222000
JOINT 6120  9.000-18.000 27.900                222000
JOINT 6501 -9.000 18.000 27.900                222000
JOINT 6510  0.000 18.000 27.900                222000
JOINT 6520  9.000 18.000 27.900                222000
JOINT 7101 -9.000-18.000 35.500                222000
JOINT 7110  0.000-18.000 35.500                222000
JOINT 7120  9.000-18.000 35.500                222000
JOINT 7501 -9.000 18.000 35.500                222000
JOINT 7510  0.000 18.000 35.500                222000
JOINT 7520  9.000 18.000 35.500                222000
JOINT 8289 -16.473-18.000-52.482                111111
JOINT 8290  16.473-18.000-52.482                111111
JOINT 8291 -16.473 18.000-52.482                111111
JOINT 8292  16.474 18.000-52.482                111111

CDM
CDM    1.00 0.600      2.000      0.700      2.000
CDM   200.00 0.600      2.000      0.700      2.000

MGROV
MGROV  0.000      39.100      1.250 -41.6002.5400-4      1.400
MGROV  39.100      44.600      2.500 -41.6002.5400-4      1.400
MGROV  44.600      80.000              -41.6002.5400-4

GRPOV
*
MEMOV
*
LOAD
*
LCOVB
*
LCOVB C005 C0011.1500C0021.2000C0031.2000C0040.3500D0882.0000
END
    
```



## Appendix B Fatigue analysis results

JOINT	MEMBER	GRUP	TYPE	ORIGINAL		JNT	MEM	CHORD	GAP * STRESS CONC. FACTORS *			FATIGUE RESULTS				
				OD	WT				(CM)	AX-CR	AX-SD	IN-PL	OU-PL	DAMAGE	LOC	SVC
ID	ID	ID	ID	(CM)	(CM)	TYP	TYP	(M)	(CM)	(CM)	(CM)	(CM)				
8306	8306-8307	BLA	TUB	66.00	2.540	T	BRC	2.13	2.01	3.26	2.48	3.57	.0208066	R	2403.083	
8306	1004-8306	BLA	TUB	66.00	2.540	T	CHD	2.13	4.70	5.15	3.29	6.77	.4704556	R	106.2799	
-----																
1012	1012-1015	BLC	TUB	66.00	2.540	T	BRC	4.09	2.27	7.38	2.77	6.95	.0449812	L	1111.574	
1012	1009-1012	BLB	TUB	86.40	3.000	T	CHD	4.09	4.12	11.13	3.46	11.04	.4361105	L	114.6498	
-----																
399	399-306	B2B	TUB	81.30	2.200	K	BRC	3.77	7.50	2.65	3.42	1.99	2.72	.0148306	T	3371.396
399	222-399	L33	TUB	155.80	9.625	K	CHD	3.77	1.78	2.89	1.34	2.45	.0320710	R	1559.040	
399	399-1211	B2D	TUB	81.30	2.000	TK	BRC	3.77	15.00	2.70	3.03	1.96	2.57	.0898829	R	556.2796
399	399-1009	L41	TUB	155.80	9.625	TK	CHD	3.77	2.04	2.53	1.23	2.20	.1755284	R	284.8542	
399	399-206	R2F	TUB	71.10	1.905	K	BRC	3.77	7.50	2.48	2.21	2.12	1.68	.1201366	T	416.1929
399	222-399	L33	TUB	155.80	9.625	K	CHD	3.77	1.41	1.57	0.92	1.35	.0174618	TL	2863.395	
399	399-115	RBD	TUB	61.00	1.270	TK	BRC	3.77	15.00	2.49	2.44	1.79	1.72	.83188-2	TL	6010.515
399	222-399	L33	TUB	155.80	9.625	TK	CHD	3.77	1.27	1.46	0.70	1.07	.33628-2	L	14868.40	
399	399-116	RBJ	TUB	50.80	1.905	TK	BRC	3.77	15.00	2.53	2.38	1.97	1.46	.64214-3	TL	77864.59
399	399-1009	L41	TUB	155.80	9.625	TK	CHD	3.77	1.81	1.79	0.80	1.09	.72245-3	L	69208.94	

JOINT	MEMBER	GRUP	TYPE	ORIGINAL		JNT	MEM	CHORD	GAP * STRESS CONC. FACTORS *				FATIGUE RESULTS				
				OD	WT				TYP	TYP	LEN.	AX-CR	AX-SD	IN-PL	OU-PL	DAMAGE	LOC
	ID	ID	ID	(CM)	(CM)			(M)	(CM)								
499	1203-	499	B3A	TUB	50.80	1.588	K	BRC	5.04	7.50	2.79	3.57	1.84	2.14	.0200030	R	2499.626
499	499-	599	LG5	TUB	154.78	8.750	K	CHD	5.04	1.49	2.60	0.97	1.54		.0225423	R	2218.048
499	499-1001	BLA	TUB	66.00	2.540	Y	BRC	5.04	2.68	5.04	2.12	2.96		.83279-2	L	6003.931	
499	499-	599	LG5	TUB	154.78	8.750	Y	CHD	5.04	1.85	5.42	1.63	2.89		.0227458	L	2198.208
499	499-1010	BLA	TUB	66.00	2.540	T	BRC	5.04	2.65	4.61	2.11	3.10		.0528508	L	946.0603	
499	499-	599	LG5	TUB	154.78	8.750	T	CHD	5.04	2.12	4.50	1.63	3.03		.1251028	L	399.6713
499	499-	125	RBF	TUB	50.20	2.240	K	BRC	5.04	7.50	2.82	3.43	2.03	2.05	.87041-2	R	5744.405
499	499-	599	LG5	TUB	154.78	8.750	K	CHD	5.04	2.06	3.09	1.20	1.76		.0161727	R	3091.624
-----																	
319	319-	303	B2A	TUB	81.30	2.000	TK	BRC	3.31	15.00	2.83	3.15	2.06	2.80	.12377-2	BL	40396.76
319	319-	323	L45	TUB	154.78	8.750	TK	CHD	3.31	2.35	2.84	1.41	2.54		.15364-2	L	32544.56
319	319-	306	B2B	TUB	81.30	2.200	K	BRC	3.31	7.50	2.82	3.34	2.10	2.96	.0162211	B	3082.403
319	225-	319	L35	TUB	154.78	8.750	K	CHD	3.31	2.32	3.12	1.54	2.83		.0129603	B	3857.950
319	319-	206	R2E	TUB	71.10	1.905	K	BRC	3.31	7.50	2.40	2.21	2.22	2.00	.0951410	T	525.5360
319	225-	319	L35	TUB	154.78	8.750	K	CHD	3.31	1.63	1.80	1.06	1.71		.0268792	TL	1860.173

JOINT	MEMBER	GRUP	TYPE	ORIGINAL		JNT	MEM	CHORD	GAP * STRESS CONC. FACTORS *			FATIGUE RESULTS				
				OD	WT				(CM)	AX-CR	AX-SD	IN-PL	OU-PL	DAMAGE	LOC	SVC
	ID	ID	ID	(CM)	(CM)	TYP	TYP	(M)	(CM)	(CM)	(CM)	(CM)				
319	319-112	RAD	TUB	61.00	1.270	TK	BRC	3.31	15.00	2.52	2.50	1.88	1.99	.58810-3	TL	85019.62
319	225-319	L35	TUB	154.78	8.750	TK	CHD	3.31		1.55	1.70	0.82	1.31	.29537-3	L	169281.7
319	319-113	RAH	TUB	50.80	1.905	TK	BRC	3.31	15.00	2.65	2.52	2.07	1.63	.83888-3	L	59603.21
319	319-323	L45	TUB	154.78	8.750	TK	CHD	3.31		2.07	2.07	0.94	1.29	.11558-2	L	43260.02
-----																
381	381-305	B2B	TUB	81.30	2.200	K	BRC	3.31	7.50	2.76	3.42	2.10	2.97	.0123889	B	4035.880
381	224-381	L35	TUB	154.78	8.750	K	CHD	3.31		2.18	3.18	1.54	2.84	.92203-2	B	5422.842
381	381-8297	B2D	TUB	81.30	2.000	TK	BRC	3.31	15.00	2.88	3.06	2.06	2.78	.15081-2	BL	33153.56
381	381-322	L45	TUB	154.78	8.750	TK	CHD	3.31		2.51	2.79	1.41	2.53	.18488-2	BL	27044.39
381	381-205	R1F	TUB	71.10	1.905	K	BRC	3.31	7.50	2.44	2.22	2.22	1.92	.0949951	T	526.3430
381	224-381	L35	TUB	154.78	8.750	K	CHD	3.31		1.60	1.79	1.06	1.64	.0242147	TR	2064.861
381	381-115	RBE	TUB	61.00	1.270	TK	BRC	3.31	15.00	2.50	2.49	1.88	1.99	.29831-2	TR	16760.92
381	224-381	L35	TUB	154.78	8.750	TK	CHD	3.31		1.62	1.73	0.82	1.32	.24669-2	R	20268.18
381	381-116	RBH	TUB	50.80	1.905	TK	BRC	3.31	15.00	2.65	2.52	2.07	1.58	.10121-2	TR	49401.12
381	381-322	L45	TUB	154.78	8.750	TK	CHD	3.31		2.06	2.06	0.94	1.25	.14808-2	R	33766.02

JOINT	MEMBER	GRUP	TYPE	ORIGINAL		JNT	MEM	CHORD	GAP * STRESS CONC. FACTORS *			FATIGUE RESULTS					
				OD	WT				(CM)	(CM)	AX-CR	AX-SD	IN-PL	OU-PL	DAMAGE	LOC	SVC
301	301-	303	B2A	TUB	81.30	2.000	TK	BRC	3.31	15.00	2.82	3.18	2.06	2.79	.15296-2	BR	32688.79
301	301-	324	L45	TUB	154.78	8.750	TK	CHD	3.31		2.31	2.86	1.41	2.53	.17659-2	BR	28313.94
301	301-	305	B2B	TUB	81.30	2.200	K	BRC	3.31	7.50	2.79	3.38	2.10	2.97	.0145335	B	3440.331
301	223-	301	L35	TUB	154.78	8.750	K	CHD	3.31		2.25	3.15	1.54	2.83	.0112494	B	4444.666
301	301-	205	R1E	TUB	71.10	1.905	K	BRC	3.31	7.50	2.42	2.21	2.22	1.97	.0922385	T	542.0732
301	223-	301	L35	TUB	154.78	8.750	K	CHD	3.31		1.62	1.79	1.06	1.68	.0249314	TR	2005.501
301	301-	112	RAE	TUB	61.00	1.270	TK	BRC	3.31	15.00	2.54	2.52	1.88	1.97	.63102-3	TR	79236.22
301	223-	301	L35	TUB	154.78	8.750	TK	CHD	3.31		1.52	1.70	0.82	1.30	.31682-3	R	157820.5
301	301-	113	RAJ	TUB	50.80	1.905	TK	BRC	3.31	15.00	2.62	2.49	2.08	1.61	.46924-3	R	106556.4
301	301-	324	L45	TUB	154.78	8.750	TK	CHD	3.31		2.04	2.04	0.93	1.28	.65498-3	R	76337.95
301	301-1103	RS1	TUB	25.40	1.270	T	BRC	3.31		3.21	2.85	1.58	1.26	.20858-2	R	23971.83	
301	301-	324	L45	TUB	154.78	8.750	T	CHD	3.31		1.44	1.47	0.59	0.75	.79782-3	R	62671.01
-----																	
304	305-	304	B2C	TUB	66.00	1.750	K	BRC	7.25	7.50	2.86	4.28	2.70	6.07	.57433-2	L	8705.756
304	8298-	304	B2A	TUB	81.30	2.540	K	CHD	7.25		4.63	6.28	2.66	8.86	.0659401	L	758.2636

JOINT	MEMBER	GRUP	TYPE	ORIGINAL		JNT	MEM	CHORD	GAP * STRESS CONC. FACTORS *			FATIGUE RESULTS					
				OD	WT				TYP	TYP	LEN.	AX-CR	AX-SD	IN-PL	OU-PL	DAMAGE	LOC
ID	ID	ID	ID	(CM)	(CM)			(M)	(CM)								
304	306-	304	B2C	TUB	66.00	1.750	K	BRC	7.25	7.50	2.88	4.10	2.70	6.18	.56167-2	R	8901.995
304	1212-	304	B2A	TUB	81.30	2.540	K	CHD	7.25	4.59	6.01	2.66	9.03	.0646530	R	773.3595	
-----																	
206	203-	206	B1C	TUB	50.80	1.270	K	BRC	37.55	54.19	2.65	2.17	2.40	1.50	.80494-4	T	621165.6
206	206-	219	B1B	TUB	101.60	4.500	K	CHD	37.55	2.15	1.85	0.84	1.12	.16086-4	T	3108244.	
206	204-	206	B1C	TUB	50.80	1.270	K	BRC	37.55	54.19	2.72	2.20	2.40	1.49	.46520-4	T	1074816.
206	206-	299	B1B	TUB	101.60	4.500	K	CHD	37.55	2.21	1.89	0.84	1.12	.14903-4	R	3354921.	
206	106-	206	R2A	TUB	45.70	1.270	TK	BRC	37.55	15.00	3.03	3.29	2.07	3.92	.14914-2	T	33526.58
206	206-	219	B1B	TUB	101.60	4.500	TK	CHD	37.55	2.40	2.73	1.20	2.86	.45604-3	T	109639.7	
206	206-	306	R2B	TUB	45.70	1.270	TK	BRC	37.55	15.00	3.02	3.33	2.07	3.92	.55331-2	B	9036.481
206	206-	219	B1B	TUB	101.60	4.500	TK	CHD	37.55	2.37	2.76	1.20	2.86	.17380-2	B	28768.48	
206	119-	206	R2C	TUB	71.10	1.900	TK	BRC	37.55	15.00	2.13	2.25	2.49	2.45	.0231812	T	2156.919
206	206-	219	B1B	TUB	101.60	4.500	TK	CHD	37.55	1.99	2.59	1.31	2.56	.0302683	T	1651.892	
206	199-	206	R2D	TUB	71.10	1.900	TK	BRC	37.55	15.00	2.09	2.16	2.49	2.50	.0217892	T	2294.715
206	206-	299	B1B	TUB	101.60	4.500	TK	CHD	37.55	2.05	2.45	1.31	2.60	.0291524	T	1715.124	

JOINT	MEMBER	GRP	TYPE	ORIGINAL		JNT	MEM	CHORD	GAP * STRESS CONC. FACTORS *			FATIGUE RESULTS					
				OD	WT				(CM)	AX-CR	AX-SD	IN-PL	OU-PL	DAMAGE	LOC	SVC	LIFE
	ID	ID	ID	(CM)	(CM)	TYP	TYP	LEN.	(CM)								
206	319-	206	R2E	TUB	71.10	1.905	TK	BRC	37.55	15.00	2.08	2.16	2.48	2.59	.0234044	T	2136.349
206	206-	219	B1B	TUB	101.60	4.500	TK	CHD	37.55	2.08	2.44	1.32	2.70	.0612509	T	816.3148	
206	399-	206	R2F	TUB	71.10	1.905	TK	BRC	37.55	15.00	2.13	2.24	2.48	2.55	.0222274	T	2249.475
206	206-	299	B1B	TUB	101.60	4.500	TK	CHD	37.55	2.05	2.57	1.32	2.66	.0612970	TL	815.7002	
-----																	
205	203-	205	B1C	TUB	50.80	1.270	K	BRC	37.55	54.19	2.59	2.14	2.40	1.50	.48340-4	T	1034344.
205	205-	201	B1B	TUB	101.60	4.500	K	CHD	37.55	2.10	1.82	0.84	1.13	.13454-4	L	3716419.	
205	204-	205	B1C	TUB	50.80	1.270	K	BRC	37.55	54.19	2.69	2.19	2.40	1.50	.26742-4	BR	1869704.
205	205-	281	B1B	TUB	101.60	4.500	K	CHD	37.55	2.19	1.88	0.84	1.12	.15920-4	L	3140753.	
205	105-	205	R1A	TUB	45.70	1.270	TK	BRC	37.55	15.00	3.04	3.27	2.07	3.93	.13200-2	T	37877.48
205	205-	201	B1B	TUB	101.60	4.500	TK	CHD	37.55	2.42	2.71	1.20	2.87	.40362-3	T	123878.2	
205	205-	305	R1B	TUB	45.70	1.270	TK	BRC	37.55	15.00	3.02	3.30	2.07	3.93	.47135-2	B	10607.80
205	205-	201	B1B	TUB	101.60	4.500	TK	CHD	37.55	2.39	2.74	1.20	2.87	.14628-2	B	34180.78	
205	101-	205	R1C	TUB	71.10	1.900	TK	BRC	37.55	15.00	2.10	2.20	2.49	2.48	.0201546	T	2480.821
205	205-	201	B1B	TUB	101.60	4.500	TK	CHD	37.55	2.02	2.50	1.31	2.58	.0271262	T	1843.238	



JOINT	MEMBER	GRUP	TYPE	ORIGINAL		JNT	MEM	CHORD	GAP * STRESS CONC. FACTORS *			FATIGUE RESULTS					
				OD	WT				AX-CR	AX-SD	IN-PL	OU-PL	DAMAGE	LOC	SVC	LIFE	
	ID	ID	ID	(CM)	(CM)	TYP	TYP	LEN.	(CM)								
205	181-	205	R1D	TUB	71.10	1.900	TK	BRC	37.55	15.00	2.11	2.18	2.49	2.49	.0199224	T	2509.740
205	205-	281	B1B	TUB	101.60	4.500	TK	CHD	37.55	2.08	2.48	1.31	2.60		.0269833	T	1853.000
205	301-	205	R1E	TUB	71.10	1.905	TK	BRC	37.55	15.00	2.09	2.16	2.48	2.59	.0203653	T	2455.161
205	205-	201	B1B	TUB	101.60	4.500	TK	CHD	37.55	2.09	2.45	1.32	2.71		.0551021	TR	907.4071
205	381-	205	R1F	TUB	71.10	1.905	TK	BRC	37.55	15.00	2.11	2.20	2.48	2.58	.0212644	T	2351.344
205	205-	281	B1B	TUB	101.60	4.500	TK	CHD	37.55	2.10	2.51	1.32	2.69		.0578244	TR	864.6873
-----																	
305	305-	303	B2C	TUB	66.00	1.750	K	BRC	34.45	7.50	3.39	2.20	2.88	2.95	.10647-2	T	46961.89
305	301-	305	B2B	TUB	81.30	2.540	K	CHD	34.45	4.72	4.03	1.87	4.30		.45722-2	TR	10935.55
305	305-	304	B2C	TUB	66.00	1.750	K	BRC	34.45	7.50	4.10	2.37	2.88	2.87	.58705-3	BR	85171.09
305	381-	305	B2B	TUB	81.30	2.540	K	CHD	34.45	5.68	4.68	1.87	4.19		.35547-2	R	14065.94
305	205-	305	R1B	TUB	45.70	1.270	T	BRC	34.45	5.19	9.15	2.71	6.32		.0216032	L	2314.475
305	301-	305	B2B	TUB	81.30	2.540	T	CHD	34.45	9.84	8.25	2.51	6.81		.0394538	L	1267.307
-----																	
306	306-	303	B2C	TUB	66.00	1.750	K	BRC	34.45	7.50	4.02	2.36	2.88	2.88	.18127-2	T	27583.33
306	319-	306	B2B	TUB	81.30	2.540	K	CHD	34.45	5.58	4.61	1.87	4.20		.40627-2	TL	12307.23



JOINT	MEMBER	GRUP	TYPE	ORIGINAL		JNT	MEM	CHORD	GAP * STRESS CONC. FACTORS *			FATIGUE RESULTS					
				OD	WT				AX-CR	AX-SD	IN-PL	OU-PL	DAMAGE	LOC	SVC	LIFE	
	ID	ID	ID	(CM)	(CM)	TYP	TYP	(M)	(CM)								
306	306-	304	B2C	TUB	66.00	1.750	K	BRC	34.45	7.50	4.35	2.43	2.88	2.84	.11660-2	T	42881.60
306	399-	306	B2B	TUB	81.30	2.540	K	CHD	34.45	6.02	4.90	1.87	4.15	.19790-2	R	25264.93	
306	206-	306	R2B	TUB	45.70	1.270	T	BRC	34.45	5.19	9.15	2.71	6.32	.0209017	R	2392.153	
306	319-	306	B2B	TUB	81.30	2.540	T	CHD	34.45	9.83	8.25	2.51	6.81	.0382428	R	1307.435	
-----																	
303	305-	303	B2C	TUB	66.00	1.750	K	BRC	20.51	7.50	3.95	4.19	2.70	6.30	.26420-2	R	18924.75
303	301-	303	B2A	TUB	81.30	2.540	K	CHD	20.51	6.81	6.63	2.66	9.20	.0323021	R	1547.888	
303	306-	303	B2C	TUB	66.00	1.750	K	BRC	20.51	7.50	3.86	4.08	2.70	6.35	.22967-2	L	21770.54
303	319-	303	B2A	TUB	81.30	2.540	K	CHD	20.51	6.59	6.43	2.66	9.28	.0277261	L	1803.357	
-----																	
116	381-	116	RBH	TUB	50.80	2.540	Y	BRC	12.73	3.64	2.58	2.41	1.47	.52264-3	B	95667.95	
116	126-	116	RBG	TUB	50.80	2.540	Y	CHD	12.73	5.59	3.55	2.90	2.75	.16636-2	R	30055.62	
116	125-	116	RBK	TUB	50.80	2.540	Y	BRC	12.73	3.64	3.44	2.70	2.17	.21938-2	T	22791.79	
116	399-	116	RBJ	TUB	50.80	1.905	Y	CHD	12.73	7.37	6.43	4.08	4.82	.0229614	R	2177.566	
-----																	
199	199-	104	B0A	TUB	61.00	1.905	K	BRC	17.43	7.50	3.01	3.94	1.97	2.71	.44435-4	T	1125230.

JOINT	MEMBER	GRUP	TYPE	ORIGINAL		JNT MEM	CHORD	GAP * STRESS CONC. FACTORS *				FATIGUE RESULTS					
				OD	WT			AX-CR	AX-SD	IN-PL	OU-PL	DAMAGE	LOC	SVC	LIFE		
ID	ID	ID	ID	(CM)	(CM)	TYP	(M)	(CM)	(CM)	(PL)	(PL)						
199	199-	299	LG2	TUB	154.78	8.750	K	CHD	17.43	2.43	2.92	1.23	2.23	.19485-4	T	25666049.	
199	199-	121	B0B	TUB	61.00	1.905	K	BRC	17.43	7.50	3.05	3.99	1.97	2.79	.57105-4	T	8755577.8
199	199-	299	LG2	TUB	154.78	8.750	K	CHD	17.43	2.49	2.97	1.24	2.29	.25556-4	T	19566452.	
199	199-	206	R2D	TUB	71.10	1.900	K	BRC	17.43	7.50	2.93	2.81	2.22	1.88	.79537-2	BL	6286.364
199	199-	299	LG2	TUB	154.78	8.750	K	CHD	17.43	2.25	2.37	1.06	1.60	.0128249	L	3898.656	
199	199-	114	RBC	TUB	66.00	1.430	K	BRC	17.43	7.50	2.88	2.92	2.01	1.82	.0223676	T	2235.375
199	199-	299	LG2	TUB	154.78	8.750	K	CHD	17.43	1.75	1.91	0.87	1.30	.73348-2	T	6816.807	
-----																	
181	181-	104	B0A	TUB	61.00	1.905	K	BRC	17.43	7.50	3.00	3.87	1.97	2.72	.42020-4	T	1189896.
181	181-	281	LG2	TUB	154.78	8.750	K	CHD	17.43	2.43	2.88	1.23	2.24	.18016-4	T	2775348.	
181	181-	118	B0B	TUB	61.00	1.905	K	BRC	17.43	7.50	3.05	3.89	1.97	2.82	.49268-4	T	1014856.
181	181-	281	LG2	TUB	154.78	8.750	K	CHD	17.43	2.49	2.92	1.24	2.31	.21918-4	T	2281185.	
181	181-	205	R1D	TUB	71.10	1.900	K	BRC	17.43	7.50	2.93	2.81	2.22	1.88	.76306-2	BR	6552.528
181	181-	281	LG2	TUB	154.78	8.750	K	CHD	17.43	2.25	2.36	1.06	1.60	.0123770	R	4039.740	
181	181-	114	RBB	TUB	66.00	1.430	K	BRC	17.43	7.50	2.85	2.90	2.01	1.84	.0221876	T	2253.511

JOINT	MEMBER	GRP	TYPE	ORIGINAL		JNT	MEM	CHORD	GAP * STRESS CONC. FACTORS *			FATIGUE RESULTS					
				OD	WT				(CM)	AX-CR	AX-SD	IN-PL	OU-PL	DAMAGE	LOC	SVC	LIFE
ID	ID	ID	ID	(CM)	(CM)	TYP	TYP	(M)									
181	181-	281	LG2	TUB	154.78	8.750	K	CHD	17.43	1.74	1.89	0.87	1.32	.72550-2	T	6891.843	
-----																	
1001	499-	1001	BLA	TUB	66.00	2.540	T	BRC	2.40	1.92	6.02	2.77	5.85	.23914-2	BL	20908.38	
1001	1005-	1001	BLD	TUB	86.40	3.000	T	CHD	2.40	3.24	9.49	3.46	9.28	.0192633	BL	2595.608	
-----																	
299	206-	299	B1B	TUB	61.00	1.270	T	BRC	17.76	2.95	3.92	1.82	2.20	.83176-2	B	6011.331	
299	299-	221	L32	TUB	154.78	8.750	T	CHD	17.76	1.67	2.08	0.88	1.45	.18322-2	B	27289.81	
299	299-	1223	B1D	TUB	61.00	1.270	TK	BRC	17.76	15.00	2.40	2.43	1.83	2.58	.10782-2	R	46375.08
299	299-	221	L32	TUB	154.78	8.750	TK	CHD	17.76	1.59	1.60	0.87	1.70	.73968-3	R	67596.82	
299	299-	115	RBE	TUB	61.00	1.270	TK	BRC	17.76	15.00	2.13	2.12	1.98	1.63	.11782-2	BL	42438.84
299	299-	221	L32	TUB	154.78	8.750	TK	CHD	17.76	1.51	1.51	0.73	1.07	.11454-2	BL	43651.30	
299	299-	114	RBM	TUB	66.00	1.270	TK	BRC	17.76	15.00	2.58	2.74	1.88	2.16	.0165567	L	3019.929
299	199-	299	LG2	TUB	154.78	8.750	TK	CHD	17.76	1.76	1.85	0.86	1.45	.0123757	L	4040.191	
-----																	
481	481-	8293	B3A	TUB	50.80	1.588	K	BRC	13.56	7.50	2.81	3.24	1.84	2.40	.0160864	R	3108.210
481	481-	581	LG5	TUB	154.78	8.750	K	CHD	13.56	1.86	2.13	0.97	1.72	.0161236	R	3101.044	

JOINT	MEMBER	GRUP	TYPE	ORIGINAL		JNT	MEM	CHORD	GAP * STRESS CONC. FACTORS *			FATIGUE RESULTS				
				OD	WT				(CM)	AX-CR	AX-SD	IN-PL	OU-PL	DAMAGE	LOC	SVC
	ID	ID	ID	(CM)	(CM)	TYP	TYP	(M)	(CM)	(CM)	(CM)	(CM)				
481	481-126	RBF	TUB	50.20	2.240	K	BRC	13.56	7.50	2.96	3.40	2.03	2.19	.20275-2	BL	24661.19
481	481-581	LG5	TUB	154.78	8.750	K	CHD	13.56	2.48	2.81	1.20	1.89		.26644-2	L	18765.99
-----																
8307	8306-8307	BLA	TUB	66.00	2.540	Y	BRC	7.76	4.40	1.47	3.23	0.80		.0160111	T	3122.836
8307	1004-8307	BLA	TUB	66.00	2.540	Y	CHD	7.76	7.24	1.01	1.55	1.52		.91980-2	T	5435.961
-----																
113	301-113	RAJ	TUB	50.80	2.540	Y	BRC	13.28	4.28	2.65	2.41	1.67		.15048-3	B	332279.5
113	124-113	RAF	TUB	50.80	2.540	Y	CHD	13.28	7.36	3.61	2.90	3.13		.66908-3	L	74729.17
113	123-113	RAK	TUB	50.80	2.540	Y	BRC	13.28	4.58	3.52	2.70	2.51		.70473-3	T	70949.45
113	319-113	RAH	TUB	50.80	1.905	Y	CHD	13.28	10.01	6.51	4.08	5.56		.0148695	L	3362.586
-----																
119	119-103	B0A	TUB	61.00	1.905	K	BRC	17.43	7.50	3.01	4.02	1.97	2.70	.10428-4	T	4794796.
119	119-219	LG2	TUB	154.78	8.750	K	CHD	17.43	2.44	2.97	1.23	2.21		.46939-5	T	10652.+3
119	119-122	B0B	TUB	61.00	1.905	K	BRC	17.43	7.50	3.06	3.57	1.97	2.90	.50279-4	T	994445.1
119	119-219	LG2	TUB	154.78	8.750	K	CHD	17.43	2.49	2.75	1.24	2.38		.21455-4	T	2330420.
119	119-206	R2C	TUB	71.10	1.900	K	BRC	17.43	7.50	2.91	2.79	2.22	1.90	.89042-2	BL	5615.345

JOINT	MEMBER	GRUP	TYPE	ORIGINAL			JNT	MEM	CHORD	GAP * STRESS CONC. FACTORS *			FATIGUE RESULTS				
				OD	WT	LEN.				(CM)	AX-CR	AX-SD	IN-PL	OU-PL	DAMAGE	LOC	SVC LIFE
119	119-	219	LG2	TUB	154.78	8.750	K	CHD	17.43	2.24	2.35	1.06	1.62	.0144984	L	3448.651	
119	119-	111	RAC	TUB	66.00	1.430	K	BRC	17.43	7.50	2.86	2.90	2.01	1.84	.49510-2	T	10098.92
119	119-	219	LG2	TUB	154.78	8.750	K	CHD	17.43	1.74	1.90	0.87	1.32	.15547-2	T	32160.24	
-----																	
101	101-	103	B0A	TUB	61.00	1.905	K	BRC	17.43	7.50	3.00	3.86	1.97	2.73	.97178-5	T	5145214.
101	101-	201	LG2	TUB	154.78	8.750	K	CHD	17.43	2.43	2.87	1.23	2.24	.42176-5	T	11855.+3	
101	101-	117	B0B	TUB	61.00	1.905	K	BRC	17.43	7.50	3.06	3.69	1.97	2.87	.44778-4	T	1116613.
101	101-	201	LG2	TUB	154.78	8.750	K	CHD	17.43	2.49	2.82	1.24	2.36	.19296-4	T	2591183.	
101	101-	205	R1C	TUB	71.10	1.900	K	BRC	17.43	7.50	2.92	2.81	2.22	1.89	.79993-2	BR	6250.553
101	101-	201	LG2	TUB	154.78	8.750	K	CHD	17.43	2.25	2.36	1.06	1.60	.0131641	R	3798.205	
101	101-	111	RAB	TUB	66.00	1.430	K	BRC	17.43	7.50	2.84	2.88	2.01	1.86	.48039-2	T	10408.13
101	101-	201	LG2	TUB	154.78	8.750	K	CHD	17.43	1.73	1.88	0.87	1.33	.15020-2	T	33288.79	
101	101-	1101	RS1	TUB	25.40	1.270	T	BRC	17.43	3.32	3.36	1.58	1.28	.30897-8	R	16183.+6	
101	101-	201	LG2	TUB	154.78	8.750	T	CHD	17.43	1.71	1.57	0.59	0.76	.11146-8	R	44859.+6	
-----																	
1010	499-	1010	BLA	TUB	66.00	2.540	T	BRC	2.40	1.92	6.02	2.77	5.85	.17493-2	BR	28582.51	

JOINT ID	MEMBER ID	GRUP ID	TYPE	ORIGINAL			JNT TYP	MEM TYP	CHORD LEN. (M)	GAP * STRESS CONC. FACTORS *			FATIGUE RESULTS			
				OD (CM)	WT (CM)	OD				AX-CR (CM)	AX-SD (CM)	IN-PL (CM)	OU-PL (CM)	DAMAGE	LOC	SVC LIFE
1010	1017-1010	BLD	TUB	86.40	3.000	T	CHD	2.40	3.24	9.49	3.46	9.28	.0117399	BR	4258.981	
-----																
281	205-	281	B1B	TUB	61.00	1.270	T	BRC	17.76	2.95	3.92	1.82	2.20	.55426-2	B	9020.958
281	281-	227	L34	TUB	154.78	8.750	T	CHD	17.76	1.67	2.08	0.88	1.45	.12045-2	BR	41510.59
281	281-	8303	B1D	TUB	61.00	1.270	TK	BRC	17.76	2.42	2.45	1.83	2.53	.55821-3	L	89571.61
281	281-	227	L34	TUB	154.78	8.750	TK	CHD	17.76	1.60	1.61	0.87	1.67	.38501-3	L	129865.3
281	281-	115	RBD	TUB	61.00	1.270	TK	BRC	17.76	2.11	2.10	1.98	1.65	.14967-2	BR	33407.66
281	281-	227	L34	TUB	154.78	8.750	TK	CHD	17.76	1.49	1.49	0.73	1.09	.14577-2	BR	34300.44
281	281-	114	RBL	TUB	66.00	1.270	TK	BRC	17.76	2.60	2.75	1.88	2.14	.0105997	R	4717.104
281	181-	281	LG2	TUB	154.78	8.750	TK	CHD	17.76	1.78	1.87	0.86	1.44	.80290-2	R	6227.449
-----																
115	299-	115	RBE	TUB	61.00	1.270	Y	BRC	26.95	2.39	2.62	2.30	1.26	.29219-2	R	17111.87
115	399-	115	RBD	TUB	61.00	2.060	Y	CHD	26.95	2.26	3.06	2.14	1.85	.97900-2	R	5107.261
115	381-	115	RBE	TUB	61.00	1.270	Y	BRC	26.95	2.47	2.63	2.30	1.29	.28671-2	R	17439.04
115	281-	115	RBD	TUB	61.00	2.060	Y	CHD	26.95	2.46	3.06	2.14	1.89	.98463-2	R	5078.053
-----																
1002	8306-1002	BLA	TUB	66.00	2.540	T	BRC	5.60	2.59	7.60	2.77	7.23	.69400-3	L	72046.55	



JOINT ID	MEMBER ID	GRUP ID	TYPE	ORIGINAL		JNT TYP	MEM TYP	CHORD LEN. (M)	GAP * STRESS CONC. FACTORS *			FATIGUE RESULTS					
				OD (CM)	WT (CM)				AX-CR (CM)	AX-SD (CM)	IN-PL	OU-PL	DAMAGE	LOC	SVC	LIFE	
1002	1002-1005	BLD	TUB	86.40	3.000	T	CHD	5.60	4.91	11.17	3.46	11.47	.88748-2	I	5633.905		
-----																	
1006	1006-1018	BLE	TUB	86.40	3.200	T	BRC	6.00	3.02	3.71	2.49	4.62	.83134-3	BL	60143.58		
1006	1005-1006	BLE	TUB	86.40	3.200	T	CHD	6.00	7.35	5.66	3.34	8.78	.87556-2	BL	5710.624		
-----																	
114	104-	114	RBA	TUB	45.72	1.588	K	BRC	30.29	7.50	2.95	4.57	2.63	5.04	.24657-3	T	202782.5
114	181-	114	RBB	TUB	66.00	2.540	K	CHD	30.29	3.40	6.60	2.39	6.51	.50220-3	R	99561.42	
114	199-	114	RBC	TUB	66.00	1.430	K	BRC	30.29	7.50	2.37	2.08	2.26	0.91	.50674-2	B	9867.066
114	299-	114	RBM	TUB	66.00	2.540	K	CHD	30.29	1.81	2.10	1.78	1.27	.29928-2	BR	16706.71	
114	281-	114	RBL	TUB	66.00	1.270	Y	BRC	30.29	2.49	2.05	2.20	0.88	.59882-2	T	8349.772	
114	181-	114	RBB	TUB	66.00	2.540	Y	CHD	30.29	1.88	1.89	1.62	1.15	.30347-2	R	16475.83	
-----																	
1015	1012-1015	BLC	TUB	66.00	2.540	Y	BRC	8.59	3.22	2.58	3.15	2.54	.56179-2	T	8900.059		
1015	1009-1015	BLB	TUB	86.40	3.000	Y	CHD	8.59	5.25	4.93	2.19	4.03	.35757-2	T	13983.33		
-----																	
201	201-	203	B1A	TUB	61.00	1.270	TK	BRC	17.76	15.00	2.42	2.46	1.83	2.56	.21005-3	BR	238033.2

JOINT	MEMBER	GRUP	TYPE	ORIGINAL			JNT	MEM	CHORD	GAP * STRESS CONC. FACTORS *			FATIGUE RESULTS				
				OD	WT	LEN.				(CM)	AX-CR	AX-SD	IN-PL	OU-PL	DAMAGE	LOC	SVC
201	201-	228	L34	TUB	154.78	8.750	TK	CHD	17.76	1.59	1.61	0.87	1.69	.88035-4	R	567953.8	
201	205-	201	B1B	TUB	61.00	1.270	T	BRC	17.76	2.95	3.92	1.82	2.20	.51150-2	BR	9775.189	
201	201-	228	L34	TUB	154.78	8.750	T	CHD	17.76	1.67	2.08	0.88	1.45	.11902-2	BR	42009.35	
201	201-	112	RAD	TUB	61.00	1.270	TK	BRC	17.76	15.00	2.13	2.11	1.98	.21129-3	B	236637.1	
201	201-	228	L34	TUB	154.78	8.750	TK	CHD	17.76	1.50	1.49	0.73	1.08	.17980-3	B	278084.8	
201	201-	111	RAM	TUB	66.00	1.270	TK	BRC	17.76	15.00	2.59	2.74	1.88	.27309-2	R	18309.04	
201	101-	201	L62	TUB	154.78	8.750	TK	CHD	17.76	1.77	1.86	0.86	1.46	.18498-2	R	27029.68	
201	201-	1102	RS1	TUB	25.40	1.270	T	BRC	17.76	3.32	3.36	1.58	1.28	.24159-5	R	20696.+3	
201	201-	228	L34	TUB	154.78	8.750	T	CHD	17.76	1.71	1.57	0.59	0.76	.86986-6	R	57481.+3	
-----																	
1011	8307-	1011	BLA	TUB	66.00	2.540	T	BRC	5.60	2.59	7.60	2.77	7.23	.43292-3	BL	115494.2	
1011	1011-	1017	BLD	TUB	86.40	3.000	T	CHD	5.60	4.91	11.17	3.46	11.47	.48779-2	L	10250.24	
-----																	
219	219-	203	B1A	TUB	61.00	1.270	TK	BRC	17.76	15.00	2.41	2.44	1.83	2.57	.24208-3	BL	206542.7
219	219-	226	L34	TUB	154.78	8.750	TK	CHD	17.76	1.59	1.61	0.87	1.70	.11539-3	L	433327.9	
219	206-	219	B1B	TUB	61.00	1.270	T	BRC	17.76	2.95	3.92	1.82	2.20	.48501-2	B	10309.01	



JOINT	MEMBER	GRP	TYPE	ORIGINAL			JNT	MEM	CHORD	GAP * STRESS CONC. FACTORS *			FATIGUE RESULTS				
				OD	WT	(CM)				TYP	TYP	LEN.	(CM)	AX-CR	AX-SD	IN-PL	OU-PL
219	219-	226	L34	TUB	154.78	8.750	T	CHD	17.76	1.67	2.08	0.88	1.45	.10938-2	BL	45712.18	
219	219-	112	RAE	TUB	61.00	1.270	TK	BRC	17.76	15.00	2.13	2.11	1.98	1.66	.24057-3	B	207836.8
219	219-	226	L34	TUB	154.78	8.750	TK	CHD	17.76	1.51	1.50	0.73	1.09	.20214-3	B	247351.9	
219	219-	111	RAL	TUB	66.00	1.270	TK	BRC	17.76	15.00	2.59	2.76	1.88	2.16	.22981-2	L	21757.49
219	119-	219	LG2	TUB	154.78	8.750	TK	CHD	17.76	1.76	1.86	0.86	1.45	.16186-2	L	30890.21	
-----																	
1029	1029-	1034	BLH	TUB	45.72	1.905	T	BRC	2.67	2.21	6.80	2.77	5.75	.58445-3	L	85550.56	
1029	1028-	1029	BLF	TUB	86.40	3.000	T	CHD	2.67	2.67	8.80	2.88	6.87	.28716-2	L	17412.04	
-----																	
1025	1025-	1030	BLH	TUB	45.72	1.905	T	BRC	2.67	2.21	6.80	2.77	5.75	.53669-3	L	93163.30	
1025	1022-	1025	BLF	TUB	86.40	3.000	T	CHD	2.67	2.67	8.80	2.88	6.87	.26873-2	L	18606.03	
-----																	
401	401-	419	B3A	TUB	50.80	1.588	K	BRC	13.56	7.50	2.88	3.55	1.84	2.28	.18807-5	T	26586.+3
401	401-	501	LG5	TUB	154.78	8.750	K	CHD	13.56	1.87	2.27	0.97	1.63	.87351-6	L	57240.+3	
401	401-	124	RAG	TUB	50.20	2.240	K	BRC	13.56	7.50	3.00	3.56	2.03	2.13	.15264-2	BR	32757.76
401	401-	501	LG5	TUB	154.78	8.750	K	CHD	13.56	2.55	2.96	1.20	1.84	.21690-2	R	23051.76	

JOINT ID	MEMBER ID	GRUP TYPE	ORIGINAL		JNT TYP	MEM TYP	CHORD LEN. (M )	GAP * STRESS CONC. FACTORS *		FATIGUE RESULTS						
			OD (CM)	WT (CM)				AX-CR (CM)	IN-PL (CM)	OU-PL (CM)	DAMAGE	LOC	SVC LIFE			
1024	1034-1024	BLG	TUB	86.40	3.000	T	BRC	5.30	2.76	3.60	2.46	4.49	.87198-4	L	573406.4	
1024	1023-1024	BLE	TUB	86.40	3.200	T	CHD	5.30	6.36	5.27	3.16	8.23	.18879-2	L	26484.88	
-----																
419	401- 419	B3A	TUB	50.80	1.588	K	BRC	13.56	7.50	2.86	3.45	1.84	2.32	.22790-5	R	21940.+3
419	419- 519	LG5	TUB	154.78	8.750	K	CHD	13.56	1.87	2.22	0.97	1.66	.15304-5	R	32671.+3	
419	419- 123	RAG	TUB	50.20	2.240	K	BRC	13.56	7.50	2.99	3.54	2.03	2.14	.11591-2	R	43136.05
419	419- 519	LG5	TUB	154.78	8.750	K	CHD	13.56	2.54	2.94	1.20	1.84	.17242-2	R	28998.54	
419	1224- 419	SEA	TUB	27.30	1.270	Y	BRC	13.56	3.26	3.29	1.58	1.27	.92485-9	B	54063.+6	
419	419- 519	LG5	TUB	154.78	8.750	Y	CHD	13.56	1.62	1.56	0.59	0.76	.4036-10	B	12388.+8	
-----																
1016	1024-1016	BLE	TUB	86.40	3.200	T	BRC	6.00	3.02	3.71	2.49	4.62	.14348-3	BR	348484.2	
1016	1016-1017	BLE	TUB	86.40	3.200	T	CHD	6.00	7.35	5.66	3.34	8.78	.16735-2	BR	29877.12	
-----																
111	103- 111	RAA	TUB	45.72	1.588	K	BRC	30.29	7.50	2.85	4.86	2.63	4.95	.62624-4	L	798417.3
111	101- 111	RAB	TUB	66.00	2.540	K	CHD	30.29	3.14	7.11	2.39	6.40	.45082-3	L	110909.4	
111	119- 111	RAC	TUB	66.00	1.430	K	BRC	30.29	7.50	2.43	2.08	2.26	0.94	.11429-2	B	43746.46

JOINT	MEMBER	GROUP	TYPE	ORIGINAL		JNT	MEM	CHORD	GAP * STRESS CONC. FACTORS *			FATIGUE RESULTS				
				OD	WT				(CM)	(M )	(CM)	AX-CR	AX-SD	IN-PL	OU-PL	DAMAGE
111	219-	111	RAL	TUB	66.00	2.540	K	CHD	30.29	1.95	2.11	1.78	1.30	.64669-3	BL	77316.82
111	201-	111	RAM	TUB	66.00	1.270	Y	BRC	30.29	2.49	2.05	2.20	0.88	.13756-2	T	36348.18
111	101-	111	RAB	TUB	66.00	2.540	Y	CHD	30.29	1.88	1.89	1.62	1.15	.57091-3	L	87578.98
-----																
112	219-	112	RAE	TUB	61.00	1.270	Y	BRC	26.95	2.56	2.64	2.30	1.32	.42217-3	L	118434.6
112	319-	112	RAD	TUB	61.00	2.060	Y	CHD	26.95	2.69	3.06	2.14	1.93	.13652-2	L	36623.84
112	301-	112	RAE	TUB	61.00	1.270	Y	BRC	26.95	2.51	2.64	2.30	1.30	.45769-3	TL	109244.2
112	201-	112	RAD	TUB	61.00	2.060	Y	CHD	26.95	2.56	3.06	2.14	1.91	.13279-2	L	37652.21
-----																
1007	1012-	1007	BLB	TUB	86.40	3.000	T	BRC	11.00	4.49	3.77	2.46	4.49	.61586-4	R	811870.0
1007	1022-	1007	BLE	TUB	86.40	3.200	T	CHD	11.00	10.69	5.27	3.16	8.23	.12130-2	R	41219.38
-----																
1026	1026-	1031	BLH	TUB	45.72	1.905	T	BRC	2.67	2.21	6.80	2.77	5.75	.24317-3	L	205613.8
1026	1025-	1026	BLF	TUB	86.40	3.000	T	CHD	2.67	2.67	8.80	2.88	6.87	.12079-2	L	41394.72
-----																
1034	1029-	1034	BLH	TUB	45.72	1.905	T	BRC	2.67	2.21	6.80	2.77	5.75	.22084-3	R	226408.1

JOINT ID	MEMBER ID	GRP	TYPE	ORIGINAL		JNT TYP	MEM TYP	CHORD LEN. (M)	GAP * STRESS CONC. FACTORS *			FATIGUE RESULTS				
				OD (CM)	WT (CM)				AX-CR (CM)	AX-SD (CM)	IN-PL	OU-PL	DAMAGE	LOC	SVC LIFE	
1034	1033-1034	BLG	TUB	86.40	3.000	T	CHD	2.67	2.67	8.80	2.88	6.87	.10901-2	R	458866.20	
-----																
1028	1028-1033	BLH	TUB	45.72	1.905	T	BRC	2.67	2.21	6.80	2.77	5.75	.20273-3	L	246637.2	
1028	1027-1028	BLF	TUB	86.40	3.000	T	CHD	2.67	2.67	8.80	2.88	6.87	.98998-3	L	50506.13	
-----																
203	203-205	B1C	TUB	50.80	1.270	K	BRC	24.59	7.50	3.88	3.27	2.58	5.15	.44429-3	T	112538.3
203	201-203	B1A	TUB	61.00	2.060	K	CHD	24.59	6.32	5.38	2.23	7.12	.93598-3	T	53419.96	
203	203-206	B1C	TUB	50.80	1.270	K	BRC	24.59	7.50	3.93	3.29	2.58	5.14	.37318-3	T	133982.4
203	219-203	B1A	TUB	61.00	2.060	K	CHD	24.59	6.43	5.44	2.23	7.10	.76504-3	T	65356.07	
-----																
1027	1027-1032	BLH	TUB	45.72	1.905	T	BRC	2.67	2.21	6.80	2.77	5.75	.16317-3	L	306435.5	
1027	1026-1027	BLF	TUB	86.40	3.000	T	CHD	2.67	2.67	8.79	2.88	6.87	.79840-3	L	62624.95	
-----																
106	106-206	R2A	TUB	45.70	1.270	T	BRC	6.18	2.96	5.59	2.32	4.82	.48049-3	T	104060.4	
106	121-106	B0D	TUB	61.00	2.540	T	CHD	6.18	3.75	5.34	2.04	5.66	.79554-3	L	62850.07	
-----																
104	118-104	B0C	TUB	61.00	1.270	K	BRC	28.58	7.50	5.21	2.01	2.27	1.99	.17640-5	T	28345.43

JOINT	MEMBER	GRUP	TYPE	ORIGINAL		JNT	MEM	CHORD	GAP * STRESS CONC. FACTORS *			FATIGUE RESULTS					
				OD	WT				TYP	TYP	LEN.	(CM)	AX-CR	AX-SD	IN-PL	OU-PL	DAMAGE
104	181-	104	B0A	TUB	61.00	2.540	K	CHD	28.58	7.95	1.77	1.40	2.58	.10206-5	T	48989.43	
104	121-	104	B0C	TUB	61.00	1.270	K	BRC	28.58	7.50	5.61	2.04	2.27	1.96	.14247-5	T	35095.43
104	199-	104	B0A	TUB	61.00	2.540	K	CHD	28.58	8.62	1.74	1.40	2.54	.96922-6	T	51588.43	
104	104-	114	RBA	TUB	45.72	1.588	T	BRC	28.58	7.94	6.91	2.44	5.34	.33541-3	B	149069.9	
104	181-	104	B0A	TUB	61.00	2.540	T	CHD	28.58	16.74	6.82	2.47	7.08	.70577-3	B	70844.47	
-----																	
105	105-	205	R1A	TUB	45.70	1.270	T	BRC	6.18	2.96	5.59	2.32	4.82	.42697-3	B	117103.4	
105	117-	105	B0D	TUB	61.00	2.540	T	CHD	6.18	3.75	5.34	2.04	5.66	.63455-3	L	78796.57	
-----																	
1030	1025-	1030	BLH	TUB	45.72	1.905	T	BRC	2.67	2.25	7.46	2.77	5.63	.13262-4	R	3770172.	
1030	1021-	1030	BLG	TUB	86.40	3.000	T	CHD	2.67	2.41	10.07	2.88	6.73	.74361-4	R	672396.2	
1030	1030-	1035	BLI	TUB	45.72	1.905	T	BRC	2.67	2.31	8.40	2.77	5.46	.11764-3	L	425036.9	
1030	1021-	1030	BLG	TUB	86.40	3.000	T	CHD	2.67	2.03	11.90	2.88	6.53	.60320-3	L	82891.88	
-----																	
1033	1028-	1033	BLH	TUB	45.72	1.905	T	BRC	2.67	2.21	6.80	2.77	5.75	.73350-4	R	681666.9	
1033	1032-	1033	BLG	TUB	86.40	3.000	T	CHD	2.67	2.67	8.80	2.88	6.87	.36033-3	R	138759.8	

JOINT ID	MEMBER ID	GRUP ID	TYPE	ORIGINAL		JNT TYP	MEM TYP	CHORD LEN. (M)	GAP * STRESS CONC. FACTORS *			FATIGUE RESULTS				
				OD (CM)	WT (CM)				AX-CR (CM)	AX-SD (CM)	IN-PL	OU-PL	DAMAGE	LOC	SVC LIFE	
1021	1021-1030	BLG	TUB	86.40	3.000	T	BRC	4.63	2.56	3.57	2.46	4.37	.15501-4	R	32255520.	
1021	1018-1021	BLE	TUB	86.40	3.200	T	CHD	4.63	5.85	5.27	3.16	8.01	.35041-3	R	142689.2	
-----																
103	117-103	B0C	TUB	61.00	1.270	K	BRC	28.58	7.50	4.82	1.97	2.27	2.02	.17370-5	T	28786.43
103	101-103	B0A	TUB	61.00	2.540	K	CHD	28.58	7.29	1.80	1.40	2.63	.11624-5	T	43016.43	
103	122-103	B0C	TUB	61.00	1.270	K	BRC	28.58	7.50	5.42	2.03	2.27	1.97	.19881-5	T	25150.43
103	119-103	B0A	TUB	61.00	2.540	K	CHD	28.58	8.31	1.76	1.40	2.56	.11028-5	T	45339.43	
103	103-111	RAA	TUB	45.72	1.588	T	BRC	28.58	7.94	6.91	2.44	5.34	.83980-4	B	595382.6	
103	101-103	B0A	TUB	61.00	2.540	T	CHD	28.58	16.74	6.82	2.47	7.08	.17559-3	T	284756.1	
-----																
1022	1022-1025	BLF	TUB	86.40	3.000	T	BRC	8.40	3.70	3.71	2.46	4.49	.19597-4	TR	2551431.	
1022	1021-1022	BLE	TUB	86.40	3.200	T	CHD	8.40	8.71	5.27	3.16	8.23	.16425-3	TR	304419.8	
-----																
1031	1026-1031	BLH	TUB	45.72	1.905	T	BRC	2.67	2.27	7.76	2.77	5.57	.19061-4	R	2623122.	
1031	1030-1031	BLG	TUB	86.40	3.000	T	CHD	2.67	2.29	10.66	2.88	6.67	.10171-3	R	491575.3	
1031	1031-1036	BLI	TUB	45.72	1.905	T	BRC	2.67	2.30	8.14	2.77	5.51	.29764-4	R	1679857.	

JOINT ID	MEMBER ID	GRUP TYPE	ORIGINAL			JNT MEM TYP	CHORD LEN. (M )	GAP * STRESS CONC. FACTORS *			FATIGUE RESULTS			
			OD (CM)	WT (CM)	WT (M )			AX-CR	AX-SD	IN-PL	OU-PL	DAMAGE	LOC	SVC LIFE
1031	1030-1031	BLG TUB	86.40	3.000	T	CHD	2.67	2.14	11.39	2.88	6.59	.15153-3	R	329975.2
-----														
1032	1027-1032	BLH TUB	45.72	1.905	T	BRC	2.67	2.21	6.80	2.77	5.75	.26967-4	R	1854094.
1032	1031-1032	BLG TUB	86.40	3.000	T	CHD	2.67	2.67	8.79	2.88	6.87	.13348-3	R	374587.8
-----														
1013	1015-1013	BLB TUB	86.40	3.000	T	BRC	11.00	4.49	3.77	2.46	4.49	.39509-5	L	12655.+3
1013	1013-1023	BLE TUB	86.40	3.200	T	CHD	11.00	10.69	5.27	3.16	8.23	.78912-4	L	633617.9
-----														
1023	1029-1023	BLF TUB	86.40	3.000	T	BRC	8.40	3.70	3.71	2.46	4.49	.45161-5	B	11071.+3
1023	1013-1023	BLE TUB	86.40	3.200	T	CHD	8.40	8.71	5.27	3.16	8.23	.40406-4	BL	1237429.
-----														
1005	1005-1006	BLE TUB	86.40	3.200	T	BRC	4.00	2.32	3.83	2.57	4.72	.12380-6	L	40387.+4
1005	1005-1001	BLD TUB	86.40	3.000	T	CHD	4.00	6.19	6.45	3.60	9.30	.15144-5	L	33016.+3
-----														
121	121- 104	B0C TUB	61.00	1.270	Y	BRC	17.22	5.73	2.12	2.27	1.73	.37459-6	T	13348.+4
121	199- 121	B0B TUB	61.00	2.540	Y	CHD	17.22	8.61	1.46	1.40	2.24	.20583-6	T	24291.+4
-----														
1017	1016-1017	BLE TUB	86.40	3.200	T	BRC	4.00	2.32	3.83	2.57	4.72	.17587-7	L	28431.+5



JOINT ID	MEMBER ID	GRUP ID	TYPE	ORIGINAL		JNT TYP	MEM TYP	CHORD LEN. (M)	GAP * STRESS CONC. FACTORS *			FATIGUE RESULTS			
				OD (CM)	WT (CM)				AX-CR (CM)	AX-SD (CM)	IN-PL	OU-PL	DAMAGE	LOC	SVC LIFE
1017	1017-1010	BLD	TUB	86.40	3.000	T	CHD	4.00	6.19	6.45	3.60	9.30	.21513-6	L	23241.+4
-----															
117	117-103	B0C	TUB	61.00	1.270	Y	BRC	17.22	5.73	2.12	2.27	1.73	.13604-6	T	36755.+4
117	101-117	B0B	TUB	61.00	2.540	Y	CHD	17.22	8.61	1.46	1.40	2.24	.20486-6	TL	24407.+4
-----															
122	122-103	B0C	TUB	61.00	1.270	Y	BRC	17.22	5.73	2.12	2.27	1.73	.88097-7	T	56756.+4
122	119-122	B0B	TUB	61.00	2.540	Y	CHD	17.22	8.61	1.46	1.40	2.24	.15280-6	TR	32722.+4
-----															
118	118-104	B0C	TUB	61.00	1.270	Y	BRC	17.22	5.73	2.12	2.27	1.73	.59977-7	T	83366.+4
118	181-118	B0B	TUB	61.00	2.540	Y	CHD	17.22	8.61	1.46	1.40	2.24	.85696-7	TR	58346.+4